# Valorization of lignocellulosic biocrudes by supercritical carbon dioxide extraction

Montesantos, Nikos

*Publication date:*
2020

*Document Version*
Publisher's PDF, also known as Version of record

# VALORIZATION OF LIGNOCELLULOSIC BIOCRUDES BY CSUPERCRITICAL CARBON DIOXIDE EXTRACTION

**BY**
**NIKOLAOS MONTESANTOS**

DISSERTATION SUBMITTED 2020

AALBORG UNIVERSITY
DENMARK

# Valorization of lignocellulosic biocrudes by supercritical carbon dioxide extraction

PhD Dissertation

by

Nikolaos Montesantos

AALBORG UNIVERSITY
DENMARK

Dissertation submitted July 2020

| | |
|---|---|
| Dissertation submitted: | July 2020 |
| PhD supervisor: | Associate Professor Marco Maschietti,<br>Aalborg University, Denmark |
| Assistant PhD supervisor: | Associate Professor Rudi Pankratz Nielsen,<br>Aalborg University, Denmark |
| PhD committee: | Associate Professor Saqib Sohail Toor<br>Aalborg University |
| | Professor Maria Jose Cocero Alonso<br>Valladolid University |
| | Associate Professor Marcos L. Corazza<br>Federal University of Paraná |
| PhD Series: | Faculty of Engineering and Science, Aalborg University |
| Department: | Department of Chemistry and Bioscience |

ISSN (online): 2446-1636
ISBN (online): 978-87-7210-670-0

Published by:
Aalborg University Press
Kroghstræde 3
DK – 9220 Aalborg Ø
Phone: +45 99407140
aauf@forlag.aau.dk
forlag.aau.dk



Printed in Denmark by Rosendahls, 2020

# Abstract

Crude bio-oils (biocrudes) produced via thermochemical processing of low value lignocellulosic biomass, such as byproducts of forestry, agriculture and industry, are an attractive alternative to liquid fossil fuels. Unlike their petroleum equivalents, biocrudes have high oxygen and water content, high acidity, polarity and average molecular weight and impurities such as alkali and earth metals. In addition, they have high density and viscosity. Due to these properties, biocrudes cannot directly replace or be mixed with conventional fuel. One of the major improvements that is required for this purpose is the removal of organic oxygen by catalytic hydrotreatment (HDO). As a consequence of HDO, acidity, polarity, molecular weight as well as the higher heating value (HHV) of the biocrude is improved. However, the high water and metal content of biocrudes can significantly reduce the lifecycle of the hydrotreatment catalysts by inducing irreversible deactivation. In addition, the high molecular weight fraction of biocrudes is resistant to HDO and can accelerate coking. This PhD thesis focuses on the fractionation of lignocellulosic biocrudes by supercritical carbon dioxide ($sCO_2$) extraction to produce an extracted fraction with improved properties. As such, an extract with lower molecular weight, acidity, polarity and oxygen content as well as dewatered and demetallized is better suited for direct hydrotreatment than the whole biocrude.

Two biocrudes produced by hydrothermal liquefaction (HTL) of woody biomass were selected as feeds for the $sCO_2$ extractions. One feed was dewatered and demetallized prior the extractions, while the other did not undergo any further processing after the HTL. For this thesis, novel work on $sCO_2$ fractionation of biocrudes was performed by utilizing a semi-continuous extraction apparatus under different pressure temperature conditions. The operability of the single stage batch extractor was improved significantly at temperatures above 80 °C. Parametric investigation revealed that high extraction yields are achieved at high pressure and temperature (e.g. >300 bar and >100 °C), with values exceeding 50 wt% for extractions at 450 bar and 100-150 °C. The high yield was the result of a considerable increase of the vapor phase loading (VPL) that reached and, in many cases, exceeded 100 g of biocrude per kg of $CO_2$. The high VPL resulted in a lower solvent-to-feed ratio (e.g. 30 g/g), both of which indicate the potential of industrial scale application.

A range of analytical methods was developed for the detailed characterization of the biocrudes and their $sCO_2$ extracts. Most of the physicochemical properties of the extracted fractions were improved compared to the feed biocrudes. The density of the extracts was found consistently lower with an average reduction of 5%. At the same time, the extracts were richer in low molecular weight components. Especially, aromatic hydrocarbons and fatty acids were concentrated up to 24 wt% and 14 wt%, respectively. The acidity (i.e. total acid number) was in many cases reduced, and it

was revealed that the reduction was mainly due to the phenolic rather than the carboxylic acid number. The phenolic acid number was reduced in all extracts, while increased in the heavy residue indicating that high molecular weight lignin-derived phenolics (i.e. oligomers) are not extracted by $sCO_2$.

The $sCO_2$ extracts were significantly dewatered, reaching up to 91% water content reduction. In addition, it was observed that the higher initial water content (i.e. 5.7 wt%) increased the VPL of aromatic hydrocarbons, which was beneficial to the fuel quality of the extracts in terms of reduced oxygen-to-carbon (O/C) ratio and increased HHV. The $sCO_2$ extracts were also found almost free of metals, with the values reducing from 8500 mg/kg in the biocrude down to an average of 170 mg/kg. The very low water and metal content result in a much lower rate of irreversible deactivation for hydrotreatment catalysts. Regarding the specific chemical classes extracted, the concentrated fatty acids are relatively easy to convert to alkanes via hydrotreatment and the high mass fraction of aromatic hydrocarbons results in lower oxygen that needs to be removed. This PhD thesis proves that $sCO_2$ can be successfully utilized as a green solvent to extract a large fraction of lignocellulosic biocrudes, with the extracted fraction improved as a hydrotreatment feed and overall fuel precursor.

# Dansk Résumé

Rå Bio-olier (bioråolie) produceret via termokemisk omdannelse af lav-værdi lignocellulosisk biomasse, så som biprodukter fra skovhugst, landbrug og industri, er et attraktivt alternativ til flydende fossile brændstoffer. I modsætning til deres fossile ækvivalenter har bioråolier høje indhold af ilt og vand, højt syretal og gennemsnitlig molekylvægt, er mere polære og indeholder urenheder som alkali og jordmetaller. Desuden har de høje densiteter og viskositeter. På grund af disse egenskaber kan bioråolie ikke direkte erstatte eller blandes med konventionelle brændstoffer. En af de store forbedringer der kræves for at kunne anvende bioråolien, er fjernelse af den organisk bundne ilt vha. katalytisk hydrogenbehandling (HDO). Konsekvensen af HDO er at syretal, polaritet, molekylvægt samt øvre brændværdi (HHV) forbedres. Dog kan det høje indhold af vand og metaller medføre signifikant reduktion af levetiden af hydrogenbehandlingskatalysatoren pga. irreversibel deaktivering af katalysatoren. Ydermere er den fraktion af bioråolien med høj molekylvægt resistent overfor HDO og kan medføre accelereret koksdannelse. Denne Ph.d.-afhandling fokuserer på fraktionering af lignocellulosisk bioråolie vha. superkritisk kuldioxid (sCO2) ekstraktion for at fremstille et ekstrakt med forbedrede egenskaber. Et sådant afvandet ekstrakt, uden metaller, med lavere molekylvægt, syretal, polaritet og iltindhold vil være bedre egnet til direkte hydrogenbehandling end bioråolien.

To bioråolier produceret ved hydrothermal liquefaction (HTL) af træ blev valgt som udgangsmateriale for $sCO_2$ ekstraktionerne. Den ene bioråolie var afvandet og renset for metaller inden ekstraktionerne, mens den anden ikke havde fået nogen efterbehandling efter HTL-processen. I forbindelse med denne afhandling er nyhedsskabende arbejde med sCO2 fraktionering udført på et halvkontinuert ekstraktionsapparat ved forskellige tryk- og temperaturforhold. Driften af et-trins batch-ekstraktoren forbedredes markant ved temperaturer over 80 °C. Parameterstudie viste at høje ekstraktionsudbytter kunne opnås ved høje tryk og temperaturer (f.eks. >300 bar og >100 °C), med over 50 vægtpct for ekstraktioner ved 450 bar og 100-150 °C. Det høje udbytte skyldtes en betragtelig forøgelse af vapor phase loading (VPL) som nåede og, i mange tilfælde, overgik 100 g bioråolie pr. kg $CO_2$. Den høje VPL resulterede i et lavere solvent-to-feed forhold (f.eks. 30 g/g), hvilket tilsammen indikerer et potentiale for applikation af teknologien i industriel skala.

En række analytiske metoder blev udviklet for at kunne udføre en detaljeret karakterisering af bioråolierne og deres $sCO_2$ ekstrakter. De fleste af de fysisk-kemiske egenskaber af ekstrakterne var forbedrede ift. den oprindelige bioråolie. Densiteten af ekstrakter var altid lavere med en gennemsnitlig reduktion på 5%. Ekstrakterne havde et større indhold af stoffer med lav molekylvægt, især var aromatiske kulbrinter og fedtsyrer koncentreret op til hhv. 24 og 14 vægtpct. Syretallet

(dvs. total acid number) var i mange tilfælde reduceret og det kunne identificeres at denne reduktion var primært pga. phenol-syretallet fremfor carboxylsyretallet. Phenol-syretallet var reduceret i alle ekstrakter men øget i den tungere remanens, hvilket indikerer at lignin-baserede phenoler med høj molekylvægt (dvs. oligomerer) ekstraheres ikke med $sCO_2$.

Vandindholdet i $sCO_2$ ekstrakterne var markant reduceret med op til 91% reduktion af vandindhold. Desuden blev der observeret at det højere vandindhold ved start (dvs. 5,7 vægtpct) øgede VPL for aromatiske kulbrinter, hvilket var fordelagtigt for brændstofkvaliteten for ekstrakterne pga. reduceret ilt-kulstof (O/C) forhold og øget HHV. Det fandtes også at $sCO_2$ ekstrakterne var næsten fri for metaller med reduktion af indholdet fra 8500 mg/kg til et gennemsnitligt indhold på 170 mg/kg. The meget lave vand- og metalindhold resulterer i en meget lavere rate for den irreversible deaktivering af hydrogenbehandlingskatalysatoren. Med hensyn til de specifikke kemiske stofgrupper som ekstraheres, så kan de koncentrerede fedtsyrer relativt let omdannes til alkaner vha. hydrogenbehandling og det højere indhold af aromatiske kulbrinter resulterer i et lavere indhold af ilt som efterfølgende skal fjernes. Denne Ph.d.-afhandling beviser at $sCO_2$ kan anvendes som et grønt opløsningsmiddel til ekstraktion af store fraktioner af lignocellulosisk bioråolie, hvor ekstraktet er mere velegnet til hydrogenbehandling og som udgangspunkt til brændstofproduktion.

# Preface

This thesis is submitted to the Doctoral School of Engineering and Science in partial fulfillment of the requirements for the PhD degree at the Department of Chemistry and Bioscience, Aalborg University, Denmark. The research was carried out from August 2017 to July 2020 at the Section of Chemical Engineering at Aalborg University in Esbjerg, Denmark.

*"There are many hypotheses in science that are wrong. That's perfectly alright; it's the aperture to finding out what's right. Science is a self-correcting process. To be accepted, new ideas must survive the most rigorous standards of evidence and scrutiny" Carl Sagan, Cosmos (Episode 4, 33 min 20 sec), 1980.*

The abovementioned quote serves two purposes. To eloquently summarize my own experience with the present research work, and at the same time highlight my motivation to initiate it and complete it. That said, this endeavor would not be possible without the support of some people, and in the following I would like to express my sincere gratitude to them.

First and foremost, to my principal supervisor Associate Professor Marco Maschietti for the opportunity given to pursue this PhD, and for his unwavering guidance, advice and patience as well as friendly interactions during the project duration. In addition, I am grateful to my co-supervisor Rudi Pankratz Nielsen for his invaluable contribution, especially in technical ideas and practical solutions.

I would also like to express my gratitude to Dorte Spangsmark, Linda Madsen, and Lisbeth Skou. Their help and guidance in the laboratory were indispensable during the long hours with the analytical instruments. Special thanks to the Section of Chemical Engineering senior researchers for constructive scientific discussions and critical questions about my research as well as Heidi Thomsen for her always topical help with administrative matters. I sincerely thank my fellow PhD students and especially Mahdi Nikbakht Fini and Jacqueline Cobos for our late afternoon discussions and wonderful time "in the same boat".

I was fortunate to spend some time abroad at the Illinois Sustainable Technology Center (ISTC) in the USA. I am grateful for meeting and collaborating with Senior Research Scientist Brajendra Kumar Sharma and Postdoctoral Researcher Kritika Kohli. They made my stay there highly educational and enjoyable and although the COVID-19 pandemic cut my stay in ISTC short by half, their contribution helped achieving the research goals of the stay.

Closing, I would like to express my heartfelt gratitude to my dear parents Eirini and Spiros for their lifelong encouragement and my sister Eleanna as well as my close friends Spiros, Mihalis and Stathis, that although in Greece always kept me company through this journey.

# Thesis Details

| | |
|---|---|
| Thesis title: | Valorization of lignocellulosic biocrudes by supercritical carbon dioxide extraction |
| PhD student: | Nikolaos Montesantos |
| Supervisors: | Marco Maschietti |
| | Rudi Pankratz Nielsen |

The main body of this PhD thesis consists of the following articles:

[A] N. Montesantos, T.H. Pedersen, R.P. Nielsen, L. Rosendahl, M. Maschietti, Supercritical carbon dioxide fractionation of bio-crude produced by hydrothermal liquefaction of pinewood, J. Supercrit. Fluids. 149 (2019) 97–109. doi:https://doi.org/10.1016/j.supflu.2019.04.001.

[B] N. Montesantos, T.H. Pedersen, R.P. Nielsen, L.A. Rosendahl, M. Maschietti, High-temperature extraction of lignocellulosic bio-crude by supercritical carbon dioxide, Chem. Eng. Trans. 74 (2019) 799–804. doi:10.3303/CET1974134.

[C] N. Montesantos, R.P. Nielsen, M. Maschietti, Upgrading of Nondewatered Nondemetallized Lignocellulosic Biocrude from Hydrothermal Liquefaction Using Supercritical Carbon Dioxide, Ind. Eng. Chem. Res. 59 (2020) 6141–6153. doi:10.1021/acs.iecr.9b06889.

[D] N. Montesantos, M. Maschietti, Supercritical Carbon Dioxide Extraction of Lignocellulosic Bio-Oils: The Potential of Fuel Upgrading and Chemical Recovery, Energies. 13 (2020) 1600. doi:10.3390/en13071600.

In addition to the main papers, the following contributions were made during the PhD:

Journal articles:

[E] N. Montesantos, M. Chirullo, M. Maschietti, Liquid-Liquid Equilibrium of Water + 2-Methoxyphenol + Methyl Isobutyl Ketone and Water + 1,2-Benzenediol + Methyl Isobutyl Ketone at 303.15 K and 328.15 K, J. Chem. Eng. Data. 63 (2018). doi:10.1021/acs.jced.7b00887.

Conference Proceedings:

[F] M.K. Jørgensen, N- Montesantos, M. Maschietti, Effect of Corrosion Inhibitors on Oil in Water Demulsification in Topside Separators, Poster presented at Danish Hydrocarbon Research and Technology Conference, 2017, Kolding, Denmark.

[G] T.H. Pedersen, K. Sharma, S. Toor, N. Montesantos, R.P. Nielsen, M. Maschietti, L. Rosendahl, Evaluation of bio-crude refinery value chains: experimental fractional distillation, supercritical $CO_2$ extraction, and hydrotreatment, in: EUBCE 2019, 27th European Biomass Conference and Exhibition, Book of abstracts summaries, 2019, p. 508.

This thesis has been submitted for assessment in partial fulfillment of the PhD degree. The thesis is based on the published scientific papers, which are listed above. Parts of the papers are used directly or indirectly in the extended summary of the thesis. As part of the assessment, co-author statements have been made available to the assessment committee and are also available at the Faculty.

# Table of Contents

# Table of Figures

# Nomenclature

| | |
|---|---|
| HTL | Hydrothermal liquefaction |
| PYR | Pyrolysis |
| $CO_2$ | Carbon dioxide |
| $sCO_2$ | Supercritical carbon dioxide |
| LLE | Liquid-liquid extraction |
| HT | Catalytic hydrotreatment |
| HDO | Hydrodeoxygenation |
| HHV | Higher heating value |
| GC-MS | Gas chromatography-mass spectrometry |
| ICP-OES | Inductively coupled plasma - optical emission spectrometry |
| TAN | Total acid number |
| CAN | Carboxylic acid number |
| PhAN | Phenolic acid number |
| BTL | Biomass-to-liquid |
| LC | Lignocellulosic |
| MW | Molecular weight |
| BP | Boiling point |
| VPL | Vapor phase loading |
| KF | Karl Fischer titration |
| S/F | Solvent-to-feed ratio |
| Y | Extraction yield |
| H/C | Hydrogen-to-carbon ratio |
| O/C | Oxygen-to-carbon ratio |
| RT | Retention time |
| Bio-oil | Organic rich liquid product of hydrothermal liquefaction or pyrolysis of biomass |
| TRL | Technology readiness level |
| FT-ICR-MS | Fourier transform-ion cyclotron resonance-mass spectrometry |

# I. EXTENDED SUMMARY

# Chapter 1. Introduction

The human society is heavily dependent on fossil resources to cover the demand in energy as well as commodity chemicals and materials. As it is shown in Figure 1.1, the majority of the global energy in 2017 was produced from fossil fuel, with crude oil covering 32%, coal 27% and natural gas 22% of the total production worldwide [1]. This translates to the consumption of about 50 Mt/day of fossil fuels globally [2].

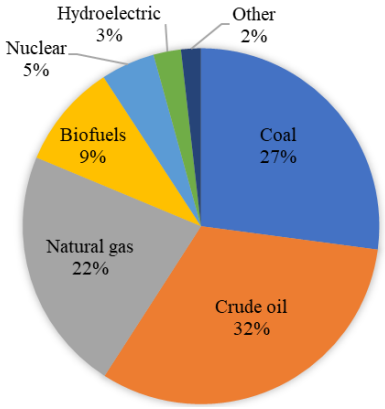


Figure 1.1: Global energy production in 2017 by source. “Other” sources include geothermal, solar, wind and tidal energy [1].

About one third of this energy corresponds to transportation fuels, with crude oil utilized for the majority of their production. Approximately 65% out of 11 Mt/d of crude oil is consumed to produce transportation fuel (Figure 1.2). The second largest share of transport fuel (i.e. 20%) corresponds to long haul road transportation (i.e. diesel), while 7% and 8% to aviation (i.e. jet fuel) and navigation (i.e. marine fuel), respectively.

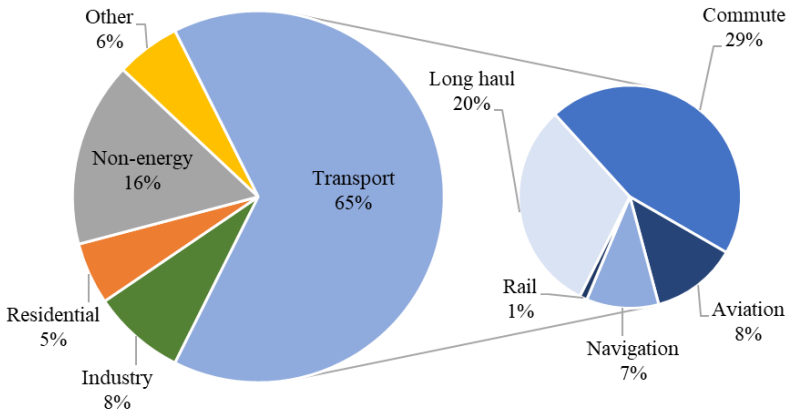


Figure 1.2: Distribution of crude oil utilization between different sectors in 2017-2018 [1].

The use of fossils to produce chemicals and materials is relatively small compared to energy generation but significant. It corresponds to around 14% of the crude oil, 7% of the natural gas and 12% of the coal [3]. The importance of petrochemicals (e.g. polyethylene) for the multimillion oil and gas industry should not be underestimated since it provides an almost twice as high gross margin compared to gasoline and diesel [3]. The continuous increase in demand for energy, liquid fuels and commodity chemicals result in current scenarios predicting a significant increase in the consumption of fossil fuel for the next decades (i.e. 10-30%) [2]. The production and utilization of fossil fuel is well known to be associated with environmental impact. One of the most recognizable indexes of the extent of this impact are the greenhouse gas emissions. Indicatively, the anthropogenic $CO_2$ emitted in the atmosphere in 2017 was approximately 90 Mt/d, while oil and gas related methane emissions were estimated to more than 0.2 Mt/d in 2019 [4,5].

There is no doubt that considering environmental issues as well as geopolitical powerplay the societal dependency in fossils has to be reduced. A major prospect to mitigate the abovementioned environmental footprint of human activities is the shift from fossil fuels to renewable resources for the production of energy and commercial chemicals. Renewable technologies like wind and solar energy are expected to play a large role in production of electricity in the future, which will also improve the potential of commuting in electric vehicles. However, regarding the fueling of the long-distance transportation sector (i.e. trucking, navigation and aviation), there is no clear alternative to liquid fuels at the moment.

In that regard, the only well identified renewable raw material to produce liquid fuel and chemicals is biomass. First-generation biomass is edible biomass that is cultivated exclusively for the production of fuel [6]. Examples that are characterized by mature industrial applications are the production of ethanol from sugarcane in Brazil and from corn in the US as well as the production of biodiesel from rapeseed oil in Germany and from palm oil in Malaysia [7]. However, factors such as water utilization, deforestation and the inherent competition with food production are major pitfalls in the sustainability of first-generation biomass.

On the other hand, second-generation biomass is defined as materials with lignocellulosic structure [7]. The byproducts of forestry (e.g. thinning branches and leaves, sawdust), agriculture (e.g. corn stover, sugarcane bagasse), industry (e.g. paper pulp lignin) and the organic fraction of municipal waste (e.g. sewage sludge) are considered relevant second generation biomasses [8]. In addition, energy crops (e.g. perennial grasses) cultivated in marginal and abandoned or underutilized land as well as short rotation tree plantations (e.g. hybrid poplar) can complement to increase the available lignocellulosic biomass [9]. These types of biomass are currently considered as a good option to address a lot of the issues associated with the first-generation biomass.

In Figure 1.1, the fraction of energy corresponding to biofuel is considerable (i.e. 9%) but reflects mainly the extended use of lignocellulosic biomass as a low value direct combustion fuel in forms such as pellets (e.g. home heating) or on-site burning (e.g. lignin for energy in pulp mills). On the other hand, its conversion to high value liquid fuel and chemicals remains very limited. In fact, according to the International Energy Agency (IEA), biofuels including first generation and lignocellulosics only correspond to about 3% of the global production of transportation fuel [10]. Nevertheless, a large scientific effort was directed towards developing conversion technologies of lignocellulosic biomass to bio-oils in the last few decades. In that respect, pyrolysis (mainly fast pyrolysis) and hydrothermal liquefaction (HTL) have been at the frontline of research as the most promising biomass-to-liquid (BTL) technologies. Some industrial scale pyrolysis plants are in operation around the globe, while several pilot units utilize HTL, with some demonstration plants planned to start operating in the near future [11,12].

The bio-oils produced by BTL technologies have the potential to be upgraded to biofuel or to be used as precursors for the synthesis of green chemicals and biomaterials. This can be achieved by processing them up to specifications after which they can be introduced as blendstock in conventional refineries, thus introducing a renewable feedstock into a multi-trillion worth infrastructure [13]. Otherwise, smaller scale localized and stand-alone biorefineries have to be developed, which produce finished products by achieving both the fuel and chemical/biomaterial specifications, while remaining financially competitive.

Bio-oils own some detrimental properties that have to be improved to follow any of the abovementioned valorization pathways. Bio-oils cannot be used directly in engines and they cannot be readily co-processed in existing refinery units (i.e. blended with conventional fuel). They have high oxygen and water content, high molecular weight (MW) and high acidity. On a physical standpoint they own high density and viscosity [11,14]. For these reasons, downstream upgrading processes are required that aim to improve these bulk properties. Most importantly, the oxygen has to be removed by catalytic hydrotreating (HT) resulting to a liquid that resembles conventional petroleum products (i.e. hydrocarbons). Since the HT process and catalysts are developed for fossil fuel, to some extent the properties of bio-oils such as the high oxygen content, the presence of water and other impurities (e.g. metals) make the process challenging [15,16].

Many of the abovementioned detrimental properties are related to the overwhelming number of chemical species that result in a largely variable molecular weight distribution and polarity. The majority of these compounds are oxygenated and can include a wide array of ketones, phenolics and organic acids [11,14]. This complex chemistry makes well designed separation processes very important. Similarly to their fossil counterparts, bio-oils have to be fractionated both regarding bulk fractionation to narrow MW and boiling point (BP) equivalents (i.e. gasoline, jet, diesel, marine) as well as selective separation of high-value chemical species. It is important to note that

separation processes, such as distillation and liquid-liquid extraction (LLE), account for up to 50% of the total cost of a conventional oil refinery [17]. However, these processes that have been developed for crude oil are not directly applicable to bio-oils. The progress made in BTL technologies in conjunction with the less studied downstream valorization (i.e. upgrading and separations) gradually increases the research interest in the latter. Therefore, it is relevant to study separations of lignocellulosic bio-oils both to optimize process parameters and to produce data that can be used for validation of thermodynamic models.

With regard to separation technologies, one alternative process is supercritical carbon dioxide ($sCO_2$) extraction. It is a process that works particularly well when the feed is thermally labile, since it is typically operated at temperature lower than other competitor processes like distillation. Considering lignocellulosic bio-oils, distillation temperatures above 100 °C can lead to polymerization reactions in the distillation column [11,18]. In addition, $sCO_2$ can be considered a better alternative than distillation for high water content mixtures. This is due to the almost twice as high energy requirement for evaporation of water per kg, compared to the equivalent energy required to recompress $CO_2$ [17]. It is a good option for the separation of high MW and low volatility oils [19,20], while the absence of a dipole but presence of a large quadrupole moment make $sCO_2$ a good solvent for apolar and low polarity components [21,22]. Non-toxicity, non-flammability, availability and low cost make it a good solvent for environmentally friendly separations. Comparing with LLE, the use of $sCO_2$ instead of petroleum derived and toxic solvents (e.g. toluene, methyl ethyl ketone) is clearly advantageous in an environmental point of view. In addition, the separation of the $CO_2$ solvent for recirculation is performed simply by pressure reduction, without the additional process step required for liquid solvents. The use of a green solvent is consistent with the larger perspective of reducing the dependency on petroleum and design industrial operations that have small to none environmental footprint. In addition, $CO_2$ is co-produced in BTL processes and especially in HTL at high pressure and considerable quantity making it available on site [11,12].

The advantages of $sCO_2$ extraction have been exploited in a few industrial processes such as decaffeination of coffee and tea [21]. Another niche industrial application is the production of lubricants by fractionation of perfluoropolyether mixtures [23]. In addition, separation of organic mixtures and extraction of value added chemical classes has been demonstrated on research level for oils such as citrus, vegetable and frying oils [24–30]. A few patents have also shown interesting results on heavy oil, tar sand and bitumen, with $sCO_2$ extracting a lighter fraction and leaving a heavy asphaltenic residue that can be efficiently refined separately [31,32]. Regarding bio-oils, a few literature works on lignocellulosic pyrolysis oils indicate the utility of $sCO_2$ for producing extracts with improved properties like lower water content, viscosity and higher heating values compared to the feed bio-oils [33–36].

## 1.1. Thesis objectives

The initiating problem of this PhD thesis was defined as follows:

*"Can supercritical carbon dioxide be used as a solvent for the valorization of lignocellulosic bio-oils to liquid biofuel and green chemicals?"*

To investigate the abovementioned problem, the following specific tasks were addressed and literature contributions were made:

- Review of the state of the art for the $sCO_2$ fractionation of lignocellulosic bio-oils. The potential of $sCO_2$ extraction to be part of the valorization of such matrices is suggested in the literature review Paper D. In addition, the article serves as a comprehensive starting point for future research initialization.

- Finalization of a lab scale extraction setup and the experimental procedure based on a newly acquired supercritical extractor system. The apparatus is described in detail in Paper A, while some minor modifications are reported in Paper C.

- Evaluation of the extraction performance regarding operating conditions, for different HTL biocrude feeds, and with respect to extraction yield, vapor phase loading and solvent-to-feed ratio. The effect of temperature and pressure is analyzed in Papers A, B, C and optimal values are suggested in Paper C.

- Development of an analytical characterization protocol regarding physical and chemical bulk properties of the HTL biocrudes and their supercritical extracts. Methodologies are described in Papers A, B, C. In addition, the necessity for standardization of such analytical tools to the particularities of bio-oils is highlighted in Paper D.

- Development of a methodology for detailed compositional characterization of the volatile fraction of HTL biocrudes and their $sCO_2$ extracts. Quantitative compositional data are reported and experimental distribution factors pertaining to the selective separation of specific chemical classes are analyzed in Papers A, B, C.

## 1.2. Thesis outline

The thesis is divided in two parts. Part I consists of the extended summary, which sets the background and summarizes the main experimental findings of the PhD work, as well as provides conclusions and perspectives for future work. Part 0 consists of the outcome of the PhD with respect to scientific publications.

Part I is outlined in 6 chapters that are described as follows:

**Chapter 1** introduces the context on which the initiating problem of the PhD project was defined.

**Chapter 2** describes the properties of lignocellulosic bio-oils and how these need to be improved.

**Chapter 3** provides an overview of the $sCO_2$ separations of oils and reviews the state of the art of $sCO_2$ extraction of lignocellulosic pyrolysis oils. The chapter closes with analyzing the potential of $sCO_2$ extraction as a part of the valorization of lignocellulosic HTL biocrudes in terms of fuel upgrading and highlights the technology gaps that are investigated in this PhD thesis.

**Chapter 4** serves as a materials and methods section by reporting the detailed characteristics of the feed HTL biocrudes studied in this work as well as describing the supercritical extraction apparatus.

**Chapter 5** analyzes the major experimental findings and their significance. The chapter is divided in three parts. The first analyzes technical aspects of the extraction efficiency in connection to the operation parameters (pressure, temperature, feed). The second analyzes the effect of $sCO_2$ on the bulk physicochemical properties of the extracted fractions. In addition, the specific chemistry of the volatile fraction of the extracts is reported and analyzed in terms of separation factors. The third suggests two potential applications for the heavy $sCO_2$ residue that are hypothesized, based on its analytical characterization during this work.

**Chapter 6** summarizes the most important conclusions and provides perspectives for future work.

# Chapter 2. Lignocellulosic bio-oils

## 2.1. Lignocellulosic biomass

Lignocellulosic (LC) biomass attributes its name to the three macromolecules that it consists of. Figure 2.1 shows the general structure of lignocellulose as it is found in the cell wall of plants. The figure represents the way the three macromolecules coexist, with cellulose (yellow) embedded in a matrix of hemicellulose (blue) and lignin (red). In addition, representative chemical structures of the macromolecules are shown. Cellulose and hemicellulose are polysaccharides, whereas lignin is a complex aromatic polymer. A typically small mass fraction of inorganics is present (i.e. alkali and earth metals) in LC biomass, which is reported as ash.

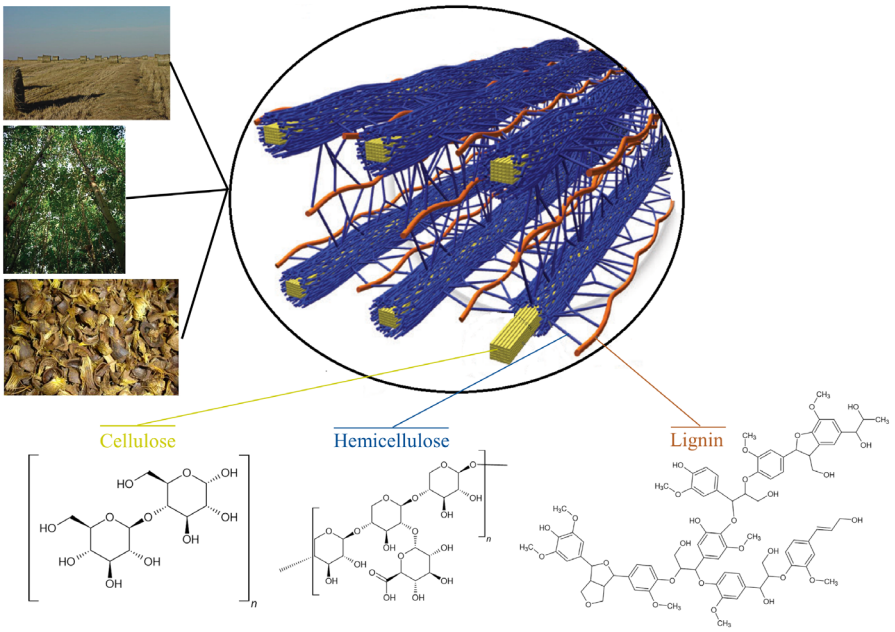


Figure 2.1 Structure of lignocellulose. (Images taken from the public image library of the US Office of Biological and Environmental Research [37])

In agriculture LC biomass is available in the form of byproducts such as wheat straw and sugarcane bagasse [9]. With regard to forestry, thinning (e.g. branches, leaves) and sawmill byproducts (e.g. sawdust) are relevant LC biomasses [9]. Examples of industrial byproduct LC feedstocks are lignin from the paper pulp industry [38], enzymatic lignin residues from bioethanol production [39], as well as residues from the production of vegetable oils (e.g. palm kernel shell) [40]. Availability of such LC biomasses varies for the different feedstocks [41]. An estimation of the availability for relevant types of LC biomasses is reported in Table 2.1.

Table 2.1 Lignocellulosic biomass availability as byproducts

| Biomass type | Availability | Area | Year | Ref. |
|---|---|---|---|---|
| Agricultural residue | 11-47 Mt/day | World | 2017 | [9] |
| Forestry residue | 2.1 Mt/day | World | 2017 | [9] |
| Sewage sludge | 25 kt/day | Europe | 2010 | [42] |
| Paper pulp lignin | 0.19 Mt/day | World | 2020 | [43] |
| Enzymatic lignin | 0.7-2.2 kt/day | World | 2020 | [44] |
| Palm oil residue | 0.14 Mt/day | Malaysia | 2006 | [40] |

The LC biomass that is estimated to have the largest available amounts globally are agricultural residues, followed by forestry residues. In total the potential of only byproduct LC biomass is significant, although it is still underutilized due to technological gaps in pretreatment, conversion and valorization processes [10].

## 2.2. Characteristics of lignocellulosic bio-oils

Among thermochemical technologies, pyrolysis and hydrothermal liquefaction (HTL) are the most prominent processes to produce bio-oils from LC biomass. Via different conversion pathways the two processes result in a product that can be further processed to fuel and chemicals [45]. Pyrolysis is typically performed at 500-600 °C in an oxygen-free environment. At these conditions the macromolecules constituting the dry biomass thermally break down to simpler compounds, which vaporize and consequently condense to an organic-rich and an aqueous phase. The organic-rich liquid after gravity separation is typically denoted bio-oil [11]. HTL utilizes water at high pressure (i.e. 100-350 bar) and temperature (i.e. 250-450 °C) to break down cellulose, hemicellulose and lignin to an array of chemical species that constitute an organic-rich phase, while some are dissolved in the co-produced aqueous phase. The organic-rich phase that separates freely from the aqueous phase is typically denoted biocrude [12]. In both processes, a $CO_2$ rich gas mixture and solids (e.g. biochar) are produced as byproducts. Especially for HTL the $CO_2$ can reach as high as 90 wt% of the total gas product, which is comparable in mass basis to the biocrude product [46]. In addition, HTL operates at high pressure and temperature, which results to that $CO_2$ stream being at supercritical conditions. Another important difference between the two processes is that HTL can handle both dry and wet biomass, while drying is required prior to pyrolysis.

In this thesis, the word bio-oil is used when referring to pyrolysis and HTL oils collectively, while pyrolysis oil and biocrude are the terms used for addressing individually the products of pyrolysis and HTL, respectively. The bio-oil yields

typically reported on a dry-biomass basis are between 30-60 wt%, although values up to 75 wt% have been achieved in certain literature studies for both processes [11,12].

Several pyrolysis plants on demonstration and commercial level were started up in the past years, utilizing proprietary fast pyrolysis technologies. The few of them that are operational at the moment (i.e. 2020) are reported in Table 2.2 [47]. On the other hand, HTL is still at a lower technology readiness level (TRL) with several pilot units around the globe and a few announced demonstration plants [12,48]. The latter are reported in Table 2.2.

Table 2.2: Commercial pyrolysis plants in operation and announced HTL demonstration plants [12,47,48].

| **Conversion** | **Technology proprietor** | **Operator** | **Location** | **Output (t/day)** |
|---|---|---|---|---|
| PYR | BTG-BTL | BTG-BLT (Empyro) | Netherlands | 77 |
| PYR | BTG-BTL | Twence (Hengelo) | Netherlands | 66 |
| PYR | Ensyn | Ensyn (Côte-Nord) | Canada | 41 |
| PYR | Ensyn | Ensyn | Canada | 130 |
| PYR | Ensyn | Red Arrow | USA | NA |
| PYR | VTT | Fortum | Finland | 152 |
| HTL | Steeper Energy | Silva Green Fuel | Norway | 4[1] |
| HTL | Altaca Energy | Gönen Energy | Turkey | 124[1] |
| HTL | Licella | Licella | Australia | 27[1,2] |
| HTL | Genifuel | Metro Vancouver | Canada | 10[1,2] |

PYR: Fast pyrolysis; HTL: Hydrothermal liquefaction; NA: No data reported; [1]Announced values; [2]Slurry throughput (no yield data for estimating output are reported).

LC bio-oils produced by pyrolysis and HTL are viscous dark colored water-in-oil emulsions (Figure 2.2). Water content has been reported to range from 20 to 30 wt% and 4 to 15 wt% for pyrolysis and HTL oils, respectively [49–54]. As it can be seen in Table 2.3, the water content of bio-oils is very high compared to typical refinery feedstocks. This means that it has to be reduced significantly, before it is blended with other refinery streams. In addition, catalytic hydrotreatment processes have low tolerance to water, which makes its reduction prior to hydrotreatment a necessity [16].

Typical viscosity values for HTL biocrudes and pyrolysis oils are reported in Table 2.3. The viscosity of pyrolysis oils strongly depends on its water content, with kinematic viscosities reported to range from 10 to 50 cSt at 40 °C and water content

17 wt% to 48% [49,55]. HTL biocrude dynamic viscosities have been reported in a wide range with values between 1700 and 67000 cP and corresponding water content of 5 and 1 wt% for the minimum and maximum value, respectively [56,57].

(a) (b)

Figure 2.2: (a) HTL biocrude and (b) Pyrolysis oil from pinewood (Paper D).

These values are comparable to heavy fossil resources that can range between 10000 cP for heavy oil and higher than 50000 cP for bitumen [58]. Considering the viscosities of petroleum derived fuel, bio-oils are typically at much higher levels, apart from residual marine fuel. Given the relation between water content and viscosity as well as the necessity to remove it, the viscosity is expected to increase even for the seemingly low viscosity pyrolysis oils.

Table 2.3: Comparison of water content and physical properties between pyrolysis oil, HTL biocrude and typical fossil fuel and their fractions.

| | **Water (wt%)** | **Density (kg/m$^3$)** | **Viscosity (cP)** | **Ref.** |
|---|---|---|---|---|
| PYR oil | 20-30 | 1000-1200 | 10-50[1] | [49] |
| HTL biocrude | 4-15 | 970-1100 | 1700-67000 | [50–54] |
| Conventional crude | 0-0.5 | 800-930 | 10-100 | [58,59] |
| Heavy crude | 0-0.5 | 960-1000 | 1000-10000 | [58,59] |
| Bitumen | 8-30 | >1000 | >50000 | [60] |
| Kerosene (Jet A-1) | 0 | 775-840 | <8 (at -20 °C) | [61] |
| Diesel | <0.0005 | 820-845 | 2-4 | [62] |
| Marine fuel | 0.3-0.5 | 890-1010 | 5-700[1] | [63] |

[1]Estimated from kinematic viscosity; PYR: pyrolysis; HTL: Hydrothermal liquefaction.

The density of bio-oils is typically higher than 1000 kg/m$^3$ (Table 2.3), with HTL values ranging between 970 and 1100 kg/m$^3$ [64–66], while somewhat higher for pyrolysis oils, reaching up to 1200 kg/m$^3$ [67]. This density is higher than conventional crude oil (i.e. 800-930 kg/m$^3$) and similar to that of tar sand bitumen [58,60]. Density is very important for the economy of a refinery. Simply put, lower density means higher volume per unit mass of liquid product [13]. Regarding typical density of refinery finished products, they all have lower densities except for the residual marine fuel (i.e. 920-1010 kg/m$^3$).

The oxygenated organic components, in which the bio-oils are rich, introduce a polarity that make them only miscible with polar organic solvents like dichloromethane (DCM) and tetrahydrofuran (THF) [13,68]. On the other hand, bio-oils are only partially miscible with hydrocarbon solvents. This poor miscibility results in direct blending with conventional hydrocarbon fuel (i.e. petroleum fractions) being unfeasible [13,68]. In addition, the abundance of oxygenated components results in one of the major differences of bio-oils and fossil fuel, which is their oxygen content that can range between 10 and 50 wt%. The elemental composition (CHNSO) and the HHV of a few representative examples of pyrolysis oils and HTL biocrudes from different biomasses are reported in Table 2.4 and compared with corresponding ranges of fossil fuels.

Table 2.4. Elemental composition and higher heating value (HHV), on a water-free basis, of bio-oils from different biomass feedstocks and conversion process.

| **Biomass Type** | **Industrial Residue** | | **Hardwood** | | **Agricultural Residue** | | **Typical fossil fuel range** |
|---|---|---|---|---|---|---|---|
| | Kraft Lignin | Palm shell | Aspen | Eucalyptus | Wheat straw | Sugarcane bagasse | |
| Process | HTL | PYR | HTL | PYR | PYR | HTL | - |
| Carbon (wt%) | 70.0 | 58.3 | 78.4 | 69.5 | 53.8 | 55.8 | 83-87 |
| Hydrogen (wt%) | 6.5 | 8.5 | 8.1 | 6.3 | 6.1 | 7.7 | 10-14 |
| Nitrogen (wt%) | - | - | 0.5 | 0.3 | 0.1 | 0.1 | 0.1-2 |
| Sulfur (wt%) | 0.4 | 0.1 | 0.3 | - | - | 0.1 | 0.05-6 |
| Oxygen (wt%) | 21.0 | 33.0 | 13 | 23.8 | 40.0 | 36.3 | 0.05-1.5 |
| HHV (MJ/kg) | 32 | 27 | 36[1] | 29 | 22 | 25[1] | 42-47 |
| Reference | [69] | [70] | [71] | [72] | [73] | [74] | [75] |

PYR: Pyrolysis;; HTL: hydrothermal liquefaction; [1]Calculated as reported in the literature [76]

Even though these oxygen ranges are in all cases lower than those in the corresponding biomasses, they are still at least one order of magnitude higher than typical petroleum values that do not exceed 1.5 wt% [75]. Bio-oils derived from agricultural residues own the highest oxygen contents for both pyrolysis and HTL, when compared to woody biomass and industrial residues. Lignin and woody biomass have carbon content that is closer to fossil values, while they are almost free of sulfur and nitrogen. Especially for HTL of woody biomass, there are several literature examples in which the oxygen content is low (e.g. 10-15 wt%), relatively to typical pyrolysis oil values [46,51,71]. The elemental characteristics of the bio-oils in Table 2.4 show cumulatively that the bio-oils have a high potential fuel value with HHVs higher than the original biomasses (i.e. 16-28 MJ/kg). Although, in order to reach HHVs comparable to conventional fuel, bio-oils have to be almost completely deoxygenated. Research on the hydrotreatment of bio-oils has shown promising hydrodeoxygenation (HDO) levels reaching 98% removal of oxygen. Nevertheless, in order to achieve that deep level of HDO the required hydrogen was as high as that for high-sulfur heavy crude oil fractions such as the vacuum distillation residual oil (e.g. 300 – 600 $Nm^3/m^3$) [64,77,78].

Depending on the biomass and the process, bio-oils end up with various amounts of alkali and earth metals, such as sodium, potassium and iron (i.e. ash) [79]. Pyrolysis oils typically have low ash content (i.e. lower than 0.2 wt%) [67,80], since the majority of metals are not in volatile organometallic compounds and in the case of entrainment, filters block their transfer to the pyrolytic condensate. On the other hand, metals present during the HTL process are dissolved in the process water and transferred to the biocrude in the emulsified water droplets [46]. In addition to the metals present in biomass, HTL often utilizes homogeneous catalysts (e.g. potassium carbonate) or pH regulators (e.g. sodium hydroxide). These process additives result in biocrudes with high ash content (e.g. 5 wt%) [46,65,71]. The presence of metals is a well-recognized problem in petroleum refining, due to the irreversible deactivation they induce to commercial catalysts such as cobalt-molybdenum (CoMo) and nickel molybdenum (NiMo) [15]. Even amounts as low as 0.5 wt% of metals can be problematic for hydrotreatment units, since catalytic beds have to be replaced if the accumulated metal content exceeds 3-4 wt% [71,81].

Acidity is a relevant bulk characteristic for bio-oils since their high values can lead to corrosion in process equipment. Acidity is typically quantified by the total acid number (TAN). Values of TAN between 9 and 200 mg KOH/g have been reported in literature [46,56,80,82–84]. TAN is the cumulative effect of carboxylic acids and weakly acidic phenolic compounds. However, measurement methods were developed for petroleum liquids, which mainly contain a small amount of naphthenic acids resulting to low TAN (e.g. maximum 4 mg KOH/g) [85]. On the other hand, bio-oils contain an abundance of carboxylic acids (e.g. fatty acids) and phenolic components, both contributing to the value of TAN. Phenolic acidity cannot always be determined by standard TAN measurements and thus the reported values range widely.

Bio-oils are a mixture of an overwhelming number of oxygenated compounds and some aromatic hydrocarbons. The average molecular weight of bio-oils typically ranges from 300 to 500 g/mol [86,87], although the range for individual components is much larger and can be lower than 100 g/mol up to several thousand g/mol [86,88–90]. Most information on the specific chemical composition of bio-oils refers to the volatile fraction, that is typically investigated by gas chromatography coupled with mass spectrometry (GC-MS). This volatile fraction of bio-oils rarely accounts for more than 50 wt%. The specific chemistry of the nonvolatile fraction remains mostly uncharacterized, with only a few works in literature reporting analytical data [84,88–90].

In general, it is reported that the nonvolatile fraction of pyrolysis oils contains both carbonyl and phenolic groups originating from the decomposition of all three macromolecules (i.e. cellulose, hemicellulose, lignin) [84,89]. The oxygenated part of this fraction is mostly of phenolic nature, since the majority (e.g. 70%) of phenolics in LC pyrolysis oils exist as oligomers (i.e. 3-5 monomeric units) with carbon number up to 29 and oxygen up to 16 [13,89]. Stankovikj et al. [89] reported average MW of a non GC-MS detectable heavy fraction of a pyrolysis oil between 350-400 g/mol, comprised of a very large number of single components (i.e. 440-740 single chromatographic peaks identified by FT-ICR-MS). Individual oligomers can reach up to 2500 g/mol [13,89]. Even though the analytical characterization of LC pyrolysis oils has advanced significantly in the past two decades, roughly 20% of the oil is still not characterized, which highlights the complexity of the mixture [13].

Regarding HTL biocrudes, the analytical characterization of the non-volatile fraction is at a somewhat earlier stage. Phenolic dimers and oligomers derived from lignin have been reported in the nonvolatile fraction [69,90]. The average MW was reported similar to that of the pyrolysis oil heavy fraction (i.e. up to 300 g/mol) [88]. Dimers reached MW of 250 g/mol while oligomers ranged 2500-17000 g/mol [90]. Functional groups that are identified in the nonvolatile fraction of HTL biocrudes include alcohol, methylene and dibenzene moieties, while they are low in aliphatic functionalities [88,90]. Interestingly, recent research has proven that phenolic dimers and oligomers found in bio-oils have antioxidant activity, which in some cases was higher than that of commercial petroleum derived antioxidants (e.g. butylated hydroxytoluene) [91,92]. On the other hand, HT catalysts deactivate due to coking and high boiling fractions are prone to coking, thus resulting to lower operational time before regeneration in needed [15].

The volatile fraction of both HTL and pyrolysis oils consist of ketones, phenols, aromatic hydrocarbons and organic acids. In addition, aldehydes, esters, furans and sugars are reported in pyrolysis oils [14,93]. Typical examples of the abovementioned chemical classes are reported in Table 2.5, together with MW and carbon number ranges. A marked difference between pyrolysis oils and HTL biocrudes is that the former typically contains some components at high mass fractions. Such are acetol,

acetic acid, glycoladehyde and levoglucosan that have been reported to individually reach up to 10 wt% of the bio-oil. This results to the total mass fraction characterized by GC-MS reaching up to 50 wt% [70,94–98]. These compounds are important intermediates for chemical synthesis in applications such as the production of medicine, adhesives and dyes [99,100]. In addition, the sugar levoglucosan has been considered as a potential precursor for the production of pharmaceuticals [101,102].

Table 2.5: Typical chemical classes in bio-oils and examples of specific components [33,71,96,99,103–106].

| **Chemical class** | **MW** | **Carbon number** | **Examples** |
|---|---|---|---|
| Ketones | 74–124 | C3–C10 | Hydroxyacetone<br>Cyclopenten-1-one, 2-<br>Cyclopentanone, 2,5-dimethyl |
| Phenols | 94–122 | C6–C8 | Phenol<br>o-Cresol<br>4-Ethylphenol |
| Guaiacols | 124–178 | C7–C10 | Guaiacol<br>Eugenol<br>Creosol |
| Benzenediols | 110–124 | C6–C8 | Catechol<br>4-Ethylcatechol |
| Short chain fatty acids[1] | 60–144 | C2–C8 | Acetic acid<br>Octanoic acid |
| Long chain fatty acids | 172–284 | C10–C19 | Decanoic acid<br>Octadecanoic acid |
| Aromatic acids | 152–300 | C8–C20 | Benzeneacetic acid, 3-hydroxy |
| Furans | 84–132 | C4–C8 | Furfural<br>Furanone, 2(5H)- |
| Aldehydes | 60–152 | C2–C8 | Glycolaldehyde<br>Benzaldehyde, 3-hydroxy-4-methyl- |
| Esters | 130–296 | C6–C19 | Benzoic acid, 4-methoxy-, methyl ester<br>Furoic acid methylester |
| Sugars | 132–144 | C5–C6 | Levoglucosan<br>2,3-Anhydro-d-galactosan |
| Benzenes | 92–124 | C7–C10 | Toluene<br>1-Methylcyclooctene |
| Polyaromatic hydrocarbons | 174–234 | C10–C18 | Naphthalene, 1,2,3,4-tetrahydro-1,5,7-trimethyl-<br>Retene |

[1] For simplicity, small carboxylic acids (e.g. acetic) are included in this class

On the other hand, quantitative data on HTL biocrudes are sparse, most of which refer specifically to the conversion of paper pulp lignin. Single components at high mass

fractions are not reported in biocrudes, resulting to total mass fractions characterized by GC-MS that are lower than those for pyrolysis oils (i.e. up to 30 wt%) [52,69,96,107,108]. Regarding the chemical species that comprise the volatile fraction of bio-oils the "easiness of hydrodeoxygenation" as it is suggested in literature is as follows: Alcohols > Ketones > Carboxylic acids > Phenols > Guaiacols > Benzenediols [16,109]. An important conclusion of this hierarchy of deoxygenation is that carboxylic acids are relatively easy to hydrotreat, compared to other chemical classes such as phenolics derived from the lignin fraction of biomass [15]. The chemical composition of pyrolysis oils makes the production of chemicals an interesting perspective. On the other hand, HTL biocrudes are more suitable for fuel production due to properties such as lower water and oxygen content and their consistent abundance of aromatic hydrocarbons as well as components that are easily hydrodeoxygenated (e.g. fatty acids).

# Chapter 3. $sCO_2$ fractionation of oils

## 3.1. Continuous countercurrent fractionation

$sCO_2$ extraction is an established industrial technology for separation from solid matter, whereas only a few applications have been developed so far for the fractionation of liquids. One example of the latter is the niche application of $sCO_2$ for fractionation of perfluoropolyether mixtures according to narrow MW ranges for lubricant production [23]. On the other hand, several literature studies have demonstrated the potential of the process for the fractionation of organic liquid mixtures (e.g. essential oils). Brunner [19] and Reverchon and De Marco [20] have published comprehensive reviews of the literature up to 2008 in the subject of fractionating liquid mixtures. In the following, the principles of $sCO_2$ extraction with focus on continuous countercurrent fractionation are discussed, together with some applications reported in literature that are relevant to the separation of oils.

At its supercritical state (i.e. at and above 73.8 bar and 31 °C), carbon dioxide is an interesting solvent due to some unique properties. It can exhibit density similar to that of liquid organic solvents that are used in industrial separations. At the same time, it maintains favorable transport properties such as high diffusivity and low viscosity [110]. In addition, for continuous treatment of highly viscous organic mixtures it can decrease viscosity by dissolving in the liquid and expanding it, something that has been exploited by the oil industry for decades during $CO_2$ injection (i.e. enhanced oil recovery) [111]. The $CO_2$ phase diagram reported in Figure 3.1 shows that the supercritical range that can be exploited for separations is rather large.

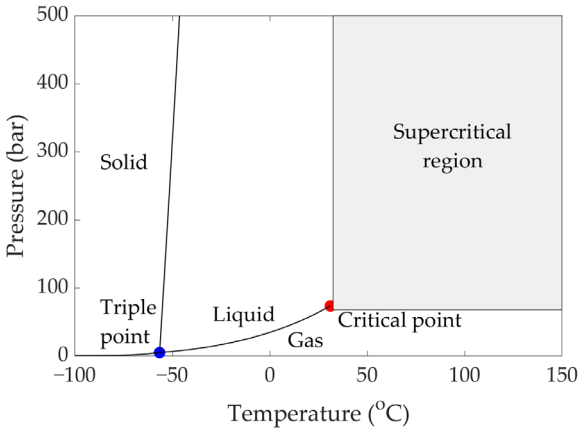


Figure 3.1: $CO_2$ phase diagram (Paper D)

This range offers wide tunability of the solvent density (i.e. solvent power) according to the process requirements by altering two major extraction parameters, temperature and pressure. As an example, considering a pressure range of 75 to 400 bar and

temperature of 35 to 150 °C the $CO_2$ density can vary from 105 to 973 kg/m$^3$. Comparing with a typical hydrocarbon solvent such as n-hexane, which has a density of 655 kg/m$^3$, $sCO_2$ at similar density exhibits viscosity approximately four times lower [112].

During continuous countercurrent operation the feed enters from the top or mid-section of a fractionation column while the compressed $CO_2$ flows from the bottom and comes in contact with the downward flowing liquid (Figure 3.2a). Typically, the extraction column is packed with an inert packing material or trays to increase the contact area between the two fluids. In order to achieve better separation a reflux loop is utilized. In this case (Figure 3.2b), the feed is introduced at an intermediate point of the column. The reflux can be achieved by partially recirculating extract to the top of the column (external reflux). Alternatively, a temperature gradient across the height of the column induces a drop in solubility (i.e. solute in $CO_2$) at the top section thus resulting to internal reflux [19]. The unextracted material (i.e. raffinate) typically exits continuously from the bottom of the column.

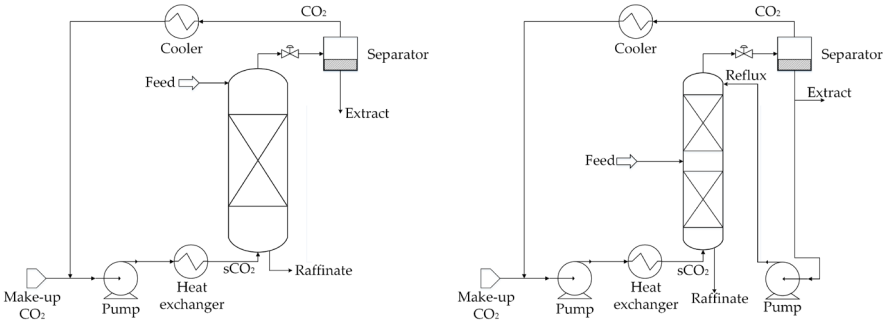


Figure 3.2: Flow diagram of continuous countercurrent extraction. (a) Without reflux; (b) With reflux (Paper D)

The operating parameters for continuous countercurrent separations include the pressure and temperature of the extraction column, the solvent-to-feed ratio (S/F), the reflux ratio, the height of the column (or number of stages) and the pressure and temperature of the top separator. The selection of the extraction temperature and pressure is based on the solubilities of the mixture components in $sCO_2$. The parameters can be optimized to maximize the bulk solubility of the mixture (i.e. all soluble components) in the solvent or to maximize the difference between the solubility of the components to be extracted and the ones to remain in the raffinate. Except for the solubility consideration (thermodynamics) the mass transfer (kinetics) between the two phases is also affected by extraction conditions and is taken into account [19,20]. The two phenomena cumulatively drive the vapor phase loading (VPL) of different chemical species in the $sCO_2$ stream. VPL is typically expressed in g/kg and is a useful technical parameter defined as the bulk of solute dissolved in $sCO_2$ at any given stage of the separation column.

The selective separation is generally driven by MW and polarity of the compounds in the oil. $sCO_2$ has an affinity towards the lower MW and less polar components. This characteristic of separation has been demonstrated in many studies for different liquid mixtures. Among others, the removal of hydrocarbon solvent (e.g. n-hexane) from soybean oil [113], the fractionation of fish oil ethyl esters [26–28] and deterpenation of citrus oils have been demonstrated [24,25]. In another interesting liquid extraction (aqueous feed) proposed by Persson et al. [114], a hydrolysate (i.e. acid hydrolysis) was extracted with $sCO_2$ to remove organic components like acetic acid, furfural and phenol, that are well-known fermentation inhibitors in first generation ethanol biorefineries [115,116].

A well-studied $sCO_2$ countercurrent separation is the removal of fatty acids from different oil types by concentrating them in the extract [29,117–120]. This is an interesting example since bio-oils contain various fatty acids. Regarding the operation conditions for these separations, at a constant temperature the increase of pressure (i.e. increase of solvent density) leads to larger mass fraction of fatty acids in the extract. For example, at 60 °C the increase of pressure during the extraction of rapeseed oil from 200 to 250 bar significantly increased the bulk solubility of the oil, which consequently led to the depletion of the fatty acids (e.g. oleic acid) in the raffinate [117]. In another work the importance of temperature was highlighted by observing the lowest fatty acid content in the extracts of rice bran oil at the highest solvent density tested (i.e. 275 bar and 45 °C). On the contrary the highest mass fraction of fatty acids was found at a relatively low pressure and high temperature (i.e. 138 bar and 80 °C) [118]. This was attributed to an increased selectivity of $CO_2$ towards fatty acids compared to other chemical classes in the oils (e.g. ferulic acid esters of phytosterols, triolein) [118,119]. The combination of relatively low pressure and high temperature (i.e. 150-200 bar and 55-80 °C) was observed to be beneficial for the extraction of fatty acids from used cooking oil as well [29,120]. From the above it can be derived that the increase of temperature benefits the extraction of the relatively polar fatty acids, while the heavier components remain in the raffinate. In all these studies the total extracted mass exceeded 50 wt% and reached up to 90 wt%. The abovementioned $sCO_2$ extraction studies indicate the feasibility of countercurrent separations for low volatility oils and mixtures with chemical components relevant to lignocellulosic bio-oils.

## 3.2. Supercritical carbon dioxide extraction of bio-oils

Supercritical carbon dioxide ($sCO_2$) extraction has in the last decade become recognized as a promising separation process for the fractionation of LC bio-oils [121,122]. In this context, some research works have started appearing in the scientific literature, regarding the $sCO_2$ extractions of LC pyrolysis oils. On the other hand, no studies regarding HTL biocrudes were published prior to this PhD project. Most of these exploratory works were centered on $CO_2$ extraction without focusing on the

industrial feasibility of the process, leading to either very low VPLs (i.e. 0.03-12 g/kg) or high S/F ratios (up to 288 g/g). Nevertheless, they provide insight regarding the process parameters and the selective extraction of bio-oil chemical species.

In all cases except for one, the experimental system utilized was a semi-continuous single stage apparatus. Mudraboyina et al. [123] included a rectification column, enabling an internal reflux by a temperature gradient along the column (i.e. multi-stage semi-continuous extraction). The lab scale systems used included the following main elements. 1) $CO_2$ cylinder; 2) Heat exchanger; 3) $CO_2$ pump; 4) Extraction vessel (i.e. extractor); 5) Extractor heating; 6) Control valve; 7) Extract trapping system. A generalized diagram of the extraction system is shown in Figure 3.3. The extractor is typically packed with an inert material (e.g. glass beads) to increase the contact area of $sCO_2$ with the bio-oil.

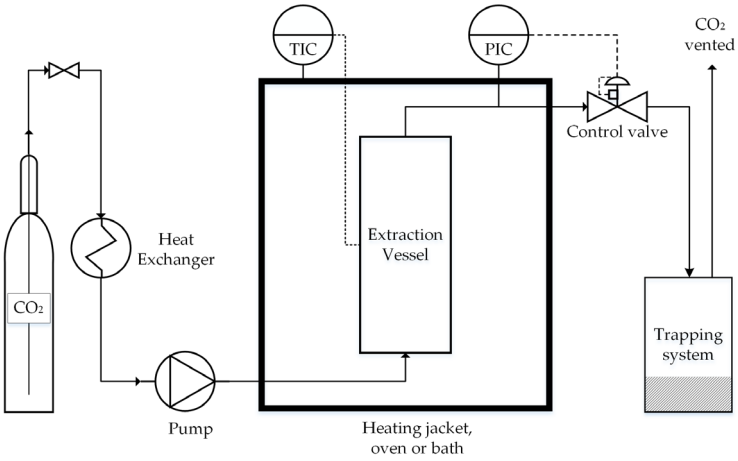


Figure 3.3: Semi-continuous $sCO_2$ extraction system (Paper D).

As it is reported in Table 3.1, the extraction pressures and temperatures investigated in literature were 80-400 bar and 35-80 °C, respectively, resulting to a range of $CO_2$ density of 380-961 kg/m$^3$. At these conditions, extraction yields between 0.1 and 45 wt% were achieved using pure $CO_2$, while in one case a yield of 71 wt% was achieved using up to 25 vol% of methanol as co-solvent [124]. In general, pressure increase at given temperature increases the total extraction yield due to improving the solvent power. On the other hand, the effect of temperature increase at constant pressure is not that clear due to two competing effects. The decrease of solvent density, which negatively affects the extraction efficiency, and the improvement of mass transfer that acts inversely. For example, at high pressures (e.g. 300 bar) the increase of temperature from 60 to 80 °C was beneficial to the overall extraction yield despite the decrease of solvent power [33].

Table 3.1: Published literature studies on $sCO_2$ extraction of bio-oils. Biomass type, conversion process, extraction system size (volume), year of publication and operating pressure (P), temperature (T) and $CO_2$ density (ρ) range.

| **Biomass type** | **Conversion process** | **Extractor volume ($cm^3$)** | **Year** | **P (bar)** | **T (°C)** | **ρ ($kg/m^3$)** | **Ref.** |
|---|---|---|---|---|---|---|---|
| Palm kernel shell | Slow pyrolysis | 50 | 2018 | 300-400 | 50-70 | 788-923 | [125] |
| Pine | Fast pyrolysis | 640 | 2017 | 100-300 | 60-80 | 221-830 | [33] |
| Palm kernel shell | Slow pyrolysis | 50 | 2017 | 150-400 | 33-66 | 691-961 | [126] |
| Beech | Slow pyrolysis | 640 | 2016 | 200 | 60 | 723 | [127] |
| Red pine | Fast pyrolysis | 25 | 2016 | 100-300 | 50 | 384-870 | [124] |
| Kraft lignin | Microwave pyrolysis | 160 | 2015 | 80-100 | 35 (45-95)[1] | 490-700 | [123] |
| Beech | Slow and fast pyrolysis | 600 | 2015 | 150-250 | 60 | 603-786 | [99] |
| Sugarcane bagasse and cashew shells | Pyrolysis | - | 2011 | 120-300 | 50 | 510-870 | [36] |
| Wheat-hemlock | Fast pyrolysis | - | 2010 | 100-300 | 40 | 628-910 | [35] |
| Wheat-sawdust | Fast pyrolysis | - | 2009 | 250-300 | 45 | 857-890 | [34] |

[1] Rectification column temperatures in parentheses

The physical properties (i.e. viscosity and density) of $sCO_2$ extracts were improved when compared to the feed bio-oils. The kinematic viscosity of the extract of a sugarcane bagasse pyrolysis oil was found lower than that of the feed bio-oil. The value decreased from 28 cSt for the feed to 18 cSt for the extract. The same work reported that the extract was more stable with regard to viscosity after a 60 days aging test. During that period the viscosity was increased by only 4 cSt for the extract as opposed to the bio-oil that increased by 22 cSt [36]. The viscosity instability of bio-oils is often associated with phase separation and polymerization or condensation reactions occurring in the heavy fraction [49,80,90,107]. In another work, the density of a corn stalk pyrolysis oil was reported to reduce from 1150 $kg/m^3$ in the feed to 952-1017 $kg/m^3$ in the $sCO_2$ extract [128].

Considering the elemental composition of $sCO_2$ extracts, literature data do not show a clear trend. In most cases the oxygen content in the extracts was found comparable to that of the corresponding feeds. The data in Figure 3.4 refer to LC pyrolysis oils for which only relatively low MW oxygenated components have been identified in the volatile fraction. These components are typically extracted preferentially by $sCO_2$, and result to extracts with an oxygen content comparable to that of the feed bio-oils.

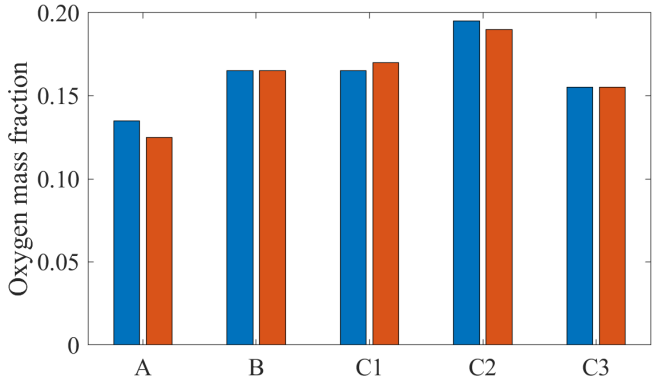


Figure 3.4: Oxygen content of different lignocellulosic pyrolysis oils and their $sCO_2$ extracts (adapted from Paper D). A: [126]; B: [127]; C1-C3: [99].

Regarding the presence of water in LC bio-oils, Feng and Meyer [33] reported a reduction in the $sCO_2$ extracts as well as the residues of a fast pyrolysis oil from pinewood. In other cases, the pyrolysis oil extracts were reported dewatered as well [34,35]. These literature findings clearly indicate that water is co-extracted with the bio-oil, although it highlights the importance of a well-designed downstream separation system to efficiently collect water in a lab scale semi-continuous system.

The chemical classes that have been identified in the volatile fraction of the $sCO_2$ extracts correspond to some of those reported in Table 2.5 for the bio-oils. 1) ketones; 2) phenols; 3) guaiacols; 4) benzenediols; 5) aldehydes; 6) esters; 7) furans; 8) syringols; 9) short chain fatty acids (SFAs). Long chain fatty acids, aromatic acids and single- and multiple-ring aromatic hydrocarbons are not reported in these pyrolysis oils. Even though most of the data in literature is qualitative (i.e. chromatographic areas), in a few cases mass fractions are reported. These were used to estimate distribution factors (i.e. K-values), which are reported in a box-plot in Figure 3.5. The K-values were evaluated using the mass fraction of a given chemical class in the extract, and an average value for the mass fraction in the liquid phase (i.e. bio-oil in the extractor). The calculation was performed on a $CO_2$ free basis.

Most of the compounds constituting these chemical classes are low MW components resulting to their K-values being above 1. Ketones and furans that are of similar MW ranges exhibit comparable K-values, which average between 2 and 3. Regarding the phenolic components they are extracted preferentially in the order guaiacols > phenols > syringols > benzenediols. This trend corresponds to the solubility of major compounds included in these classes (i.e. guaiacol > phenol > syringol > catechol) [121]. The esters that were reported by a single work were low MW as well (e.g. 130 g/mol), and as expected own relatively high K-values. It should be noted that the sugar levoglucosan that is typically present in LC pyrolysis oils is not extracted by $sCO_2$ and remains in the extraction residue [33].

Even though the quantitative data on separation of chemical classes are scarce in literature, the fact that that K-values in most cases are between 1.5 and 10 indicates that the application of a continuous countercurrent extraction scheme is technically feasible [19].

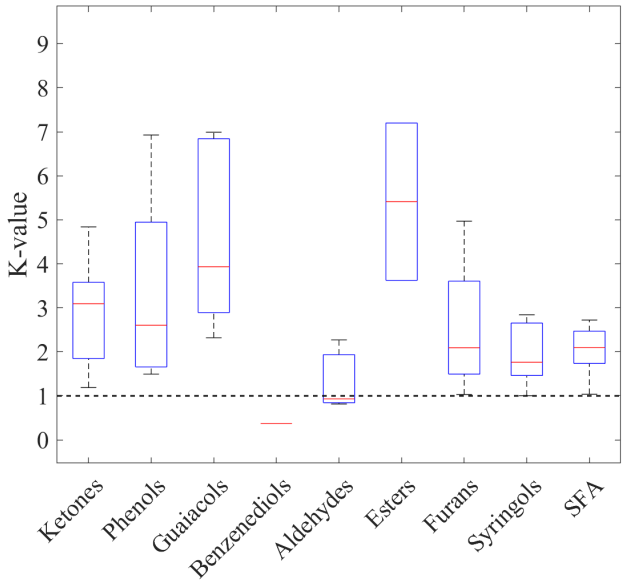


Figure 3.5: Distribution factors (K-values) of extracted bio-oil components. SFA: Short chain fatty acids. Data taken from literature [99,123,125,127]. (Adapted from Paper D).

## 3.3. Potential $sCO_2$ interface

The characteristics of HTL biocrudes such as relatively low water and oxygen content as well as the consistent presence of aromatic hydrocarbons and easily hydrotreated chemical classes (e.g. fatty acids) make them a promising feedstock to produce fuel. For this purpose, catalytic hydrotreatment (HT) of the biocrudes is required for the removal of organic oxygen (HDO), reduction of the average molecular weight and increase of the H/C ratio. However, the process encounters some obstacles due to the physicochemical nature of biocrudes, which necessitates a level of pretreatment. The excess water has to be removed because it can alter the structure of the catalyst and obstruct the HDO reactions [16]. In addition, the high metal content that some HTL biocrudes own due to the use of chemical additives (e.g. $K_2CO_3$) accelerates the irreversible deactivation of the catalysts both during the HDO process and by sintering the catalyst surface during regeneration [16]. Especially the heavy fraction of the biocrudes is resistant to HDO and can intensify coking during the HT process due to its phenolic nature and high MW [84,88]. Literature examples for the vacuum distillate and n-pentane extract of dewatered LC biocrudes resulted to HT products

with low oxygen and high HHVs. In addition, the upgraded oil had a narrowed down composition closer to gasoline and jet fuel fractions, which have the highest fuel value [88,103]. Interestingly, vacuum distillation leaves the long chain fatty acids in the residue thus preventing one of the easiest hydrotreated chemical classes (as well as relatively large in mass fraction) to reach the hydrotreater and be converted to alkanes [103].

The $sCO_2$ separation of oils, including LC pyrolysis oils, highlighted the applicability of the process on such mixtures. Importantly, $CO_2$ is co-produced at high pressure and temperature during the HTL process. With this in mind, a $sCO_2$ fractionation unit is hypothesized as a part of the overall scheme of biocrude valorization. Therefore, the interface of a $sCO_2$ extraction unit downstream the HTL and upstream the HT reactors is discussed below as it is shown in Figure 3.6. The supercritical extraction yields two biocrude fractions, one lighter fuel precursor (i.e. extract) and a heavier fraction (i.e. residue). The routing of only the lighter fraction for hydrotreating is expected to be beneficial regarding HT process requirements.

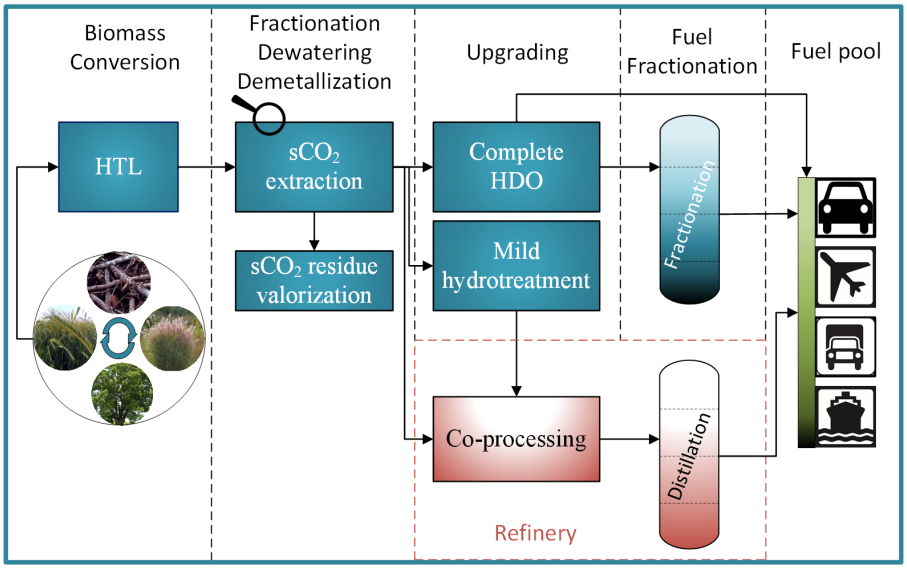


Figure 3.6: Potential interface of $sCO_2$ extraction process in the biomass to finished fuel overall scheme.

There are two major potential pathways for the valorization of biocrudes as they are suggested in Figure 3.6. One is the development of a complete fuel upgrading scheme that leads to finished fuel, and the second mildly upgrading the $sCO_2$ extract to specifications that are acceptable from petroleum refinery operators. Refineries have a number of different catalytic hydrotreatment units such as the distillate and naphtha hydrotreatment units and the fluid catalytic cracker (FCC), where a slightly hydrotreated $sCO_2$ extract can be blended with the regular feed stream. Blending the

$sCO_2$ extract to the heavy hydroprocessing units (e.g. gas oil and resid) can be an option as well. Such processes are operated at severe enough conditions (e.g. 400 °C, 165 bar) but this option is expected to reduce the value of the $sCO_2$ extract.

On the other hand, the complete valorization of the $sCO_2$ extract is expected to require milder hydrotreatment conditions than the biocrude since its free of the HDO resistant heavy fraction. This pathway can lead directly to blending of the hydrotreated extract with one of the conventional fuel fractions if the boiling point distribution is narrow enough. Although it is more probable that a fractionation prior to blending is a better option since it would maximize the value of the upgraded extract. In this way the input in higher value fractions (e.g. gasoline and jet fuel) will be optimized as opposed to blending the whole fraction with, for example, marine fuel. Finally, the $sCO_2$ residue fraction can be combusted for energy or further processed for production of chemicals or materials.

The major focus of this PhD thesis is the investigation of $sCO_2$ as a solvent to fractionate LC HTL biocrudes directly after the HTL reactor in order to prepare a hydrotreatment-ready fraction. More specifically, the aspects that are in focus include improvements of the physicochemical properties (i.e. density, viscosity, TAN). HT specific aspects are the water and metal removal as well as reduction of the high-boiling fraction in the $sCO_2$ extracts. In addition, the chemical classes that $sCO_2$ extracts is relevant since different classes will affect differently the HDO. The effect of the extraction to the elemental composition with most importantly the O/C and H/C ratio of the extract as compared to the biocrude extracted is important as well. Finally, the technical aspects of the extraction (i.e. yield, VPL and S/F) are on focus. High yield and a high VPL are very important regarding the process economics and potential for industrial application. The following sections analyze the experimental findings that support the abovementioned working hypothesis.

# Chapter 4. Materials and methods

## 4.1. Feed biocrudes

Two feed biocrudes were used in this work that were produced at a continuous flow pilot HTL unit located at Aalborg university. The HTL unit processes biomass slurry with partial recirculation of process water and biocrude [46,71]. The HTL was performed at supercritical water conditions (i.e. 400 °C and 300 bar). A pinewood sawdust slurry (17-18 wt% biomass) was processed, with potassium carbonate ($K_2CO_3$) as catalyst and sodium hydroxide (NaOH) for pH adjustment. The biocrude used in Papers A and B underwent demetallization and dewatering after gravity separation from the co-produced aqueous phase. Henceforth, this feed is denoted BCR-DM (Figure 4.1a). The dewatering-demetallization process that is described in detail elsewhere [129], involves dilution of the biocrude in methyl ethyl ketone, washing with a citric acid aqueous solution and removal of the solvent and water by vacuum evaporation. The biocrude used in Paper C did not undergo any further processing after the gravity separation. Henceforth, it is denoted BCR-RAW (Figure 4.1b). The $sCO_2$ separations of BCR-RAW served to test the pretreatment hypothesis prior to hydrotreatment (e.g. fractionation, dewatering, demetallization), while BCR-DM provided a baseline of hydrotreatment feedstock.

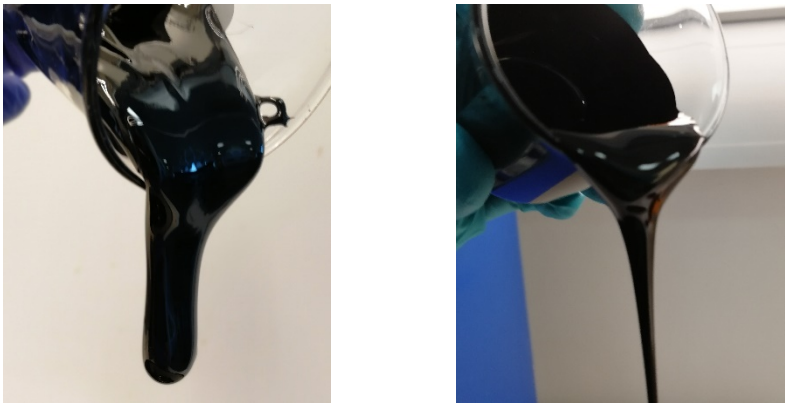

(a) (b)

Figure 4.1: Biocrude feed. (a) BCR-DM; (b) BCR-RAW

Both biocrudes were viscous water-in-oil emulsions of black color with BCR-RAW relatively less viscous than the dewatered BCR-DM. The water content, density and acid numbers of the feed biocrudes are reported in Table 4.1. One of the major differences between the two biocrudes was the water content, which was measured by Karl Fischer titration (KF) as it is described in Papers A and C. The dewatered BCR-DM contains about half of the water compared to the raw BCR-RAW. This is also the reason why the viscosity of BCR-RAW is lower than that of BCR-DM, having a similar inverse correlation to the water content as is observed for pyrolysis oils. The dynamic viscosity of BCR-RAW is reported in Table 4.1 as well, measured at 22 °C

utilizing a Fann 35FA viscometer. The viscosity of BCR-RAW (i.e. 7700 cP at 22 °C) is in the lower range of typical values reported in literature for LC biocrudes (see Table 2.3). The viscosity of BCR-DM was not determined due to exceeding instrument limitations. The density measurement method is described in Papers A, B, C. The density of the two feeds is comparable (i.e. 1051 and 1030 kg/m$^3$) since the two biocrudes were produced at the same HTL conditions and from the same biomass.

Table 4.1: Bulk physicochemical properties of the feed biocrudes

| | **$H_2O$** | **Density** | **Viscosity** | **CAN** | **PhAN** | **TAN** |
|---|---|---|---|---|---|---|
| | wt% | kg/m$^3$ | cP | | mg KOH/g | |
| BCR-DM | 2.7 ± 0.1 | 1051 ± 3 | >30000[1] | 43 ± 1 | 86 ± 6 | 129 ± 6 |
| BCR-RAW | 5.7 ± 0.4 | 1030 ± 9 | 7700 ± 130 | 42 ± 1 | 56 ± 2 | 97 ± 2 |

[1] Maximum measuring limit of the instrument; All measurements were performed at least in triplicate.

Three acid numbers are reported as they have been defined in detail in Paper A. The acid number measurement that was developed in Paper A is based on a modification to the ASTM D664 [130] standard, suggested by NREL for measuring acid numbers in phenolic-rich LC pyrolysis oils [84,131]. According to this method two acid numbers can be determined, namely the carboxylic acid number (CAN) and the phenolic acid number (PhAN). The summation of CAN and PhAN constitutes the TAN. The procedure was developed to avoid underestimating the TAN as standard procedures developed for fossil fuel can be inadequate for the determination of PhAN. In the case of CAN both biocrudes have the same values, although the PhAN is higher in the dewatered BCR-DM, which in turn increases the TAN. Higher TAN on a biocrude dewatered and demetallized by the same procedure was reported by Jensen [129], which indicates that the acid washing results to acidity increase. The reason has not been investigated, although Jensen [129] suggested that it is not due to residual citric acid. This is also supported by the fact that BCR-DM and BCR-RAW have approximately the same CAN.

The elemental composition of carbon (C), hydrogen (H), nitrogen (N) and sulfur (S) was measured as described in Papers A, B and C. Oxygen (O) was calculated by difference. It should be noted that sulfur was always lower than the detection limit of the elemental analyzer, which is in line with the fact that woody lignocellulosic biomass typically has very low sulfur content [132]. This is a major advantage for the production of low-sulfur fuel compared to fossil heavy oils in which the sulfur has been consistently rising in the past years (e.g. 1.34 wt% for an average US refinery input in 2020) [133]. The water free elemental composition values in Table 4.2 show a slight difference in the carbon content that is translated to oxygen, since the latter is calculated by difference. The elemental composition of these biocrudes result in some of the highest HHV values reported for LC biocrudes (see Table 2.4), which further strengthens their potential fuel upgrading.

Table 4.2: Elemental carbon (C), hydrogen (H), nitrogen (N) and oxygen (O) and higher heating value (HHV) on a water free basis for the feed biocrudes

| | C | H | N | O[1] | HHV[2] |
|---|---|---|---|---|---|
| | | | wt% | | MJ/kg |
| BCR-DM | 83 ± 1 | 8.5 ± 0.4 | 0.5 ± 0.02 | 8 ± 1 | 38 ± 1 |
| BCR-RAW | 80 ± 1 | 8.3 ± 0.9 | 1.3 ± 0.8 | 10 ± 1 | 37 ± 2 |

[1]Calculated by difference; [2]Calculated as reported in literature [76];
All measurements were performed at least in triplicate.

The metal content of the biocrudes was measured by inductively coupled plasma optical emission spectrometry (ICP-OES) as it is described in Paper C. The individual metal content as well as the total for each biocrude are reported in Table 4.3. BCR-RAW had an order of magnitude higher metal content than the demetallized BCR-DM. The values for BCR-RAW show that the majority of the metals (i.e. 90%) correspond to potassium (K) and sodium (Na), which are introduced as additives (i.e. NaOH and $K_2CO_3$) during the HTL process. The remaining metals (i.e. Al, Fe, Mg and Ti) are in similar amounts in both biocrudes and are present due to their natural occurrence in the pinewood biomass or are introduced during harvest and processing of the biomass [79,132].

Table 4.3: Metal content of biocrudes used in this work.

| | Al | Fe | K | Mg | Na | Ti | Total metals |
|---|---|---|---|---|---|---|---|
| | | | | mg/kg | | | |
| BCR-DM | 12 | 262 | 91 | 61 | 74 | 87 | 587 |
| BCR-RAW | 40 | 190 | 3400 | 96 | 3800 | 40 | 8500 |

With regard to the chemical composition of the biocrudes, the volatile fraction was investigated by GC-MS in Papers A, B and C. The method adopted in this work allowed a semi-quantitative characterization of the biocrudes by using internal standards. Neat samples as well as derivatized samples were analyzed. The derivatization was performed using a silylation agent (i.e. BSTFA) in order to quantitate the numerous organic acids, present in the biocrudes. The chemical classes were the same for both biocrudes. An example of the chromatograms of neat and derivatized BCR-RAW is shown in Figure 4.2, indicating the retention time or retention time ranges of the identified chemical classes as they were lumped in Paper C.

The identified components were lumped in ten chemical classes according to their functionalities. Specifically: 1) Cyclic aliphatic C6 – C9 ketones, saturated or monounsaturated (Ketones, K); 2) Alkylbenzenes (AB); 3) Phenol and alkylphenols (Phenols, P); 4) Guaiacol and alkylguaiacols (Guaiacols, G); 5) Benzenediols and acetyl derivatives of benzenediols (BD); 6) 2- and 3-ring aromatic hydrocarbons (PAH); 7) Dehydroabeityl alcohol (ArAl); 8) Short chain fatty acids, in the range C2 – C8 (SFA); 9) Long chain fatty acids, in the range C16 – C18 (LFA); 10) Dehydroabietic acid (ArAcid). A detailed list of specific components that are included

in these chemical classes is published along with Paper C as supplementary information.

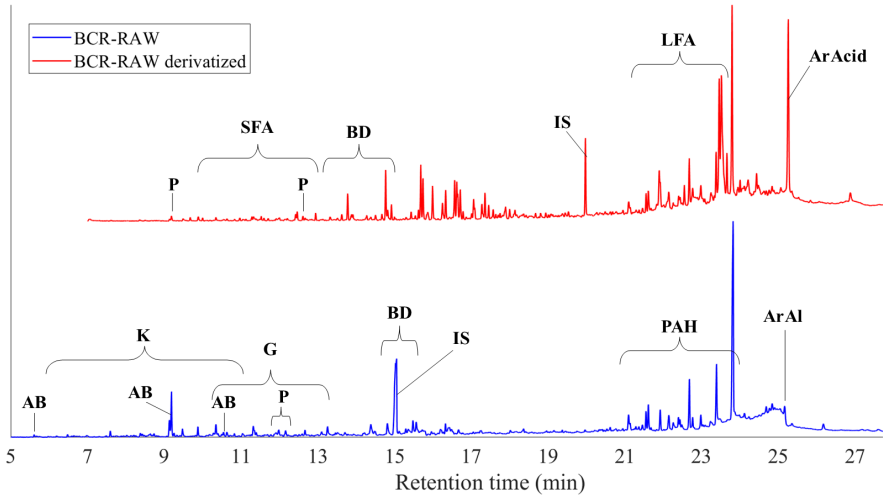


Figure 4.2: Chromatogram of BCR-RAW with retention time ranges of identified chemical classes in the neat and derivatized samples. (IS, internal standard).

Figure 4.3 provides an overview of the relative amount (i.e. mass fraction) of each chemical class with respect to the total GC-MS quantified fraction. The total quantified fraction was approximately 9 wt% for BCR-DM and 19 wt% for BCR-RAW. The difference is partly due to the larger number of compounds identified in Paper C and partly to the GC-MS methodology and IS used.

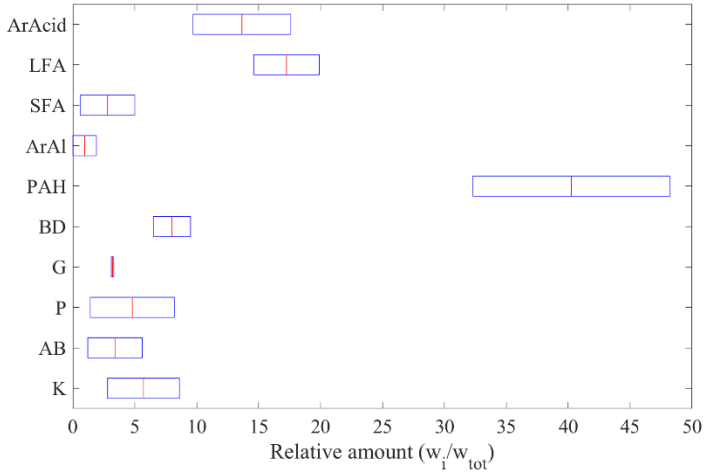


Figure 4.3: Relative amount of chemical classes quantitated in BCR-DM and BCR-RAW. Data taken from Papers B and C.

The most abundant chemical class was the PAH, which include two and three ring aromatic hydrocarbons with a MW range of 156-238 g/mol. Components include phenanthrene, anthracene and naphthalene isomers. Retene is a representative of these components since it represents approximately 56% of the PAH fraction. Such components are typically produced by high temperature decomposition of abietane skeleton diterpenoids, such as dehydroabietic acid [134]. PAH have been reported in literature for lignocellulosic biocrudes, although typically not quantified [103,135]. LFA is another class with a relatively high mass fraction that are typically found in lignocellulosic biocrudes [136]. Dehydroabietic acid (i.e. ArAcid) is found in pinewood, although its presence in the biocrude indicates that it is partly not converted by the HTL process [137].

Even though the majority of GC-MS identified components are single-ring phenolics and ketones they constitute only a small fraction (i.e. 2.6 and 0.5 wt%, respectively). Single ring phenolics are some of the less susceptible components to catalytic HDO, although their presence in small amounts (e.g. up to 2 vol%) can be viable for utilization as diesel fuel [138,139]. On the other hand, they are important in the perspective of chemical production, since many of them are commercial chemicals (e.g. phenol, guaiacol) or can be used as intermediates for synthesis (e.g. catechol). In fact, from all single-ring phenolics the benzenediols fraction was approximately 65%. The alkylbenzenes are the only low boiling hydrocarbons in the biocrudes, with a small mass fraction (i.e. 1 wt%). The single alcohol identified (i.e. dehydroabeityl alcohol) was also found at a low mass fraction of approximately 0.4 wt%.

## 4.2. $sCO_2$ extraction apparatus

The semicontinuous supercritical extractor (single-stage) apparatus used in this work is depicted in Figure 4.4.

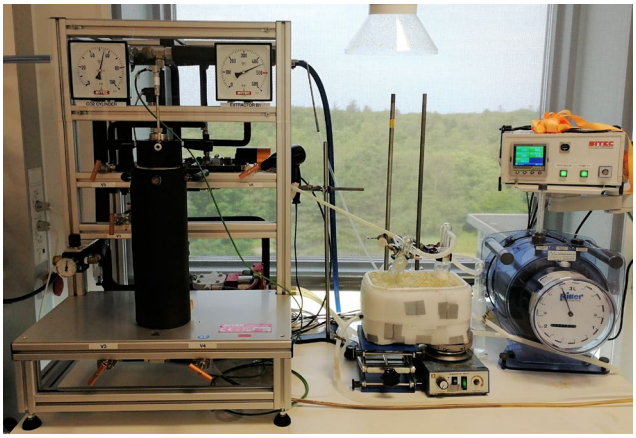

Figure 4.4: Supercritical extractor system

The configuration was custom ordered and delivered in December 2017. The detailed diagram of the apparatus is reported in Figure 4.5. The system is described in detail in Paper A, thus only a short description of the experimental procedure follows. Before the experimental work was initiated the apparatus was tested with pure $CO_2$, n-decane and crude oil, and a few modifications were deemed necessary. The most important modification was the bypass of the automatic pressure valve (C1) that was originally designed to lead to the sampling line. The reason was that the automatic valve is designed for higher gas flow rates than those used in the planned $sCO_2$ extraction experiments. A new sampling line was mounted, downstream of a micrometering valve (V6). The new sampling line was connected downstream with a cold trapping system that led to a drum type gas meter (G).

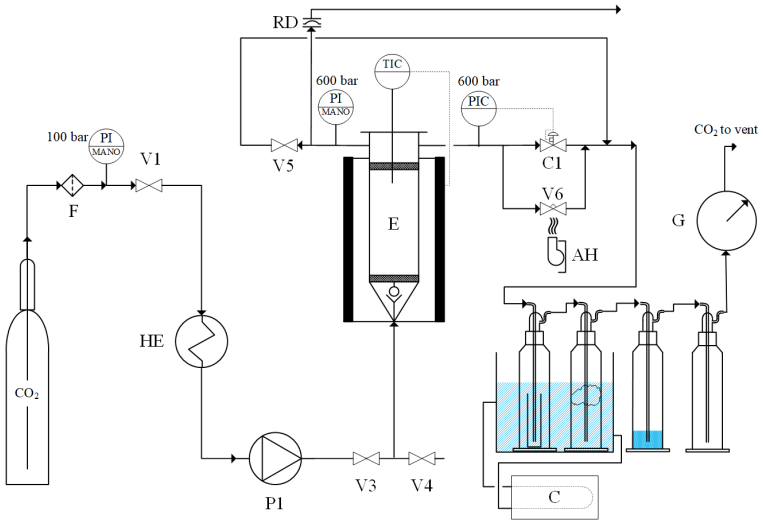


Figure 4.5: Diagram of the finalized supercritical extractor apparatus as used in Paper C. (Adapted from Paper A). F: filter; HE: heat exchanger: P1: pneumatic pump; E: extractor vessel; AH: air heater; C: refrigerating circulator; G: gas meter; V1-V5: on-off valves; V6: micrometering valve; C1: pneumatic control valve; RD: rupture disk.

Prior to an extraction an amount of biocrude was charged in a basket insert, which was packed with glass beads. The basket was then inserted in the extractor (E), which was sealed tight and the extraction temperature was set. When the temperature was reached, $CO_2$ from a dip-tube cylinder was subcooled (approximately 5 °C) in a heat exchanger (HE) and the liquid $CO_2$ was fed to a pneumatic pump (P1), which pressurized the extractor to the set pressure. The pressure was controlled manually by the air supplied to the pump. The extraction initiated by opening the micrometering valve, which was used to regulate the flow rate manually. The micrometering valve was heated by air (AH), to avoid its freezing due to the rapid gas expansion (i.e. Joule-Thomson effect), while in parallel the heat decreased the viscosity of the extracts so they flowed easier towards the following cold trap.

The extracts were released from the $CO_2$ after expansion downstream the micrometering valve and were collected in a preweighed vial that was inserted in the first of a series of gas washing bottles immersed in the cold trap. The extract collection was performed at approximately 5 °C for the extractions in Papers A and B, while a refrigerating circulator (C) was added for the experiments in Paper C. The addition of the refrigerating circulator achieved a temperature approximately -10 °C, which improved the condensing of the lighter extracted fractions. For each extraction, several extracts (i.e. E1-E5) were collected, which enabled the analysis of the results in terms of extraction progression (i.e. variable feed composition), as well as helped avoiding sample evaporation due to the long gas flow duration. The $CO_2$ volume was accurately measured by the gas-meter before it was vented in a fumehood. The temperature of the gas flowing though the gas meter was measured as well to accurately calculate the corresponding mass of the $CO_2$.

# Chapter 5. Results and discussion

## 5.1. Technical data of $sCO_2$ extraction

The biocrudes (i.e. BCR-DM and BCR-RAW) were fractionated by $sCO_2$ extraction over a wide range of pressure and temperature, covering several isothermal, isobaric and isodensity conditions. The experimental pressure and temperature combinations covered in this work are reported in Figure 5.1, together with the corresponding $CO_2$ density range.

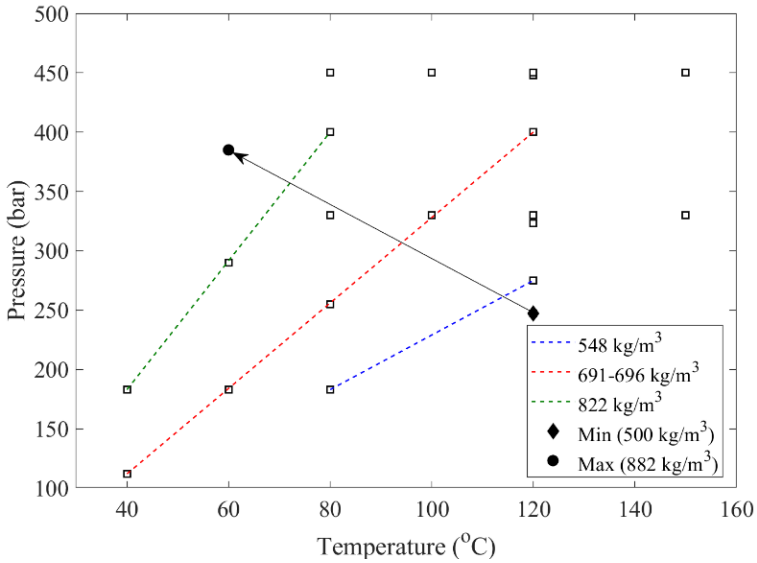


Figure 5.1: Pressure, temperature combinations and $sCO_2$ density covered in this work

During preliminary extraction tests it was observed that the solvent density has to be relatively high (i.e. above 500 kg/m$^3$) in order to obtain high total extraction yield (Y above 30 wt%), vapor phase loading (VPL above 10 g/kg) and solvent-to-feed ratio (S/F under 100 g/g). Such data provided a meaningful interpretation regarding the potential of the process as it was hypothesized in Figure 3.6. For each extract Y, VPL and S/F were calculated as follows:

$$Y = \frac{m_{ext}}{m_{feed}} \ (wt\%) \tag{1}$$

$$VPL = \frac{m_{ext}}{m_{CO_2}} \cdot 1000 \left(\frac{g}{kg}\right) \tag{2}$$

$$S/F = \frac{m_{co_2}}{m_{feed}} \left(\frac{g}{g}\right) \tag{3}$$

Where $m_{feed}$ is the mass of biocrude originally charged in the extractor (i.e. feed), while $m_{co_2}$ and $m_{ext}$ is the mass of $CO_2$ flowed and extract collected over a specific time interval, respectively. The range of solvent density that was investigated was 500-822 kg/m$^3$, which was achieved at pressures 112-450 bar and temperatures 40-150 °C. It is noted that the VPL was used to evaluate the reproducibility of the extraction experiments by calculating the relative standard deviation (RSD) for extractions of BCR-RAW at 450 bar, 150 °C and 60 g initial feed. The extraction was repeated six times and the RSD for four consecutive extracts (i.e. E1-E4) was 7%, 12%, 14% and 11%, respectively.

In the following the effect of extraction parameters (i.e. pressure, temperature and feed type) is analyzed in terms of efficiency using the progressive extraction yield (i.e. cumulative), vapor phase loading and solvent-to-feed ratio.

### 5.1.1. Effect of pressure

Pressure increase at a given temperature increases the supercritical solvent density, which results in higher solvent power. This translates to higher mass extracted for a given mass of $CO_2$ (i.e. higher VPL). The driving phenomenon is the increase of solubility of biocrude compounds in the $sCO_2$. This effect can be observed in Figure 5.2, where the cumulative extraction yield of extractions at 120 °C is plotted against the S/F at different $sCO_2$ densities (i.e. different pressures) for BCR-DM and BCR-RAW.

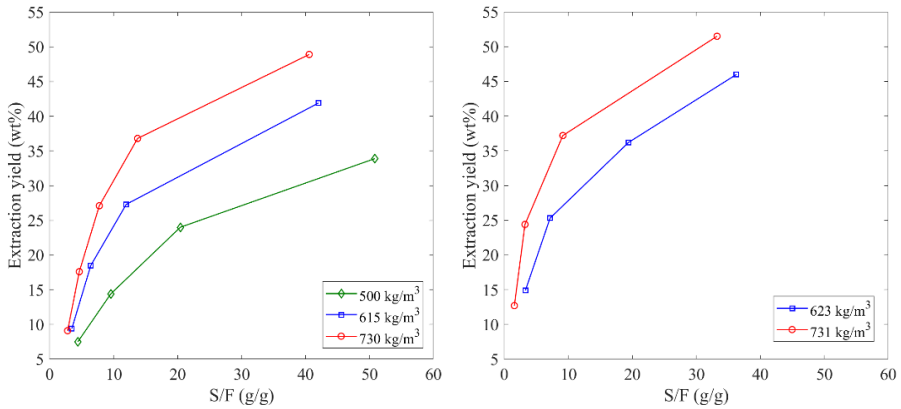


Figure 5.2: Extraction yield vs solvent-to-feed ratio (S/F) at 120 °C and different solvent densities. (a) BCR-DM (Paper B); (b) BCR-RAW (Paper C)

The positive effect of the increase of solvent density is clear for both biocrudes. The effect is more pronounced during the early stages of the extraction, while the rate of increase (i.e. slope) is decreasing as the extraction progresses. Qualitatively this slope

represents the VPL, which typically decreases with extraction progression since the feed remaining in the extractor becomes heavier (i.e. less soluble in $sCO_2$).

### 5.1.2. Effect of temperature

The effect of temperature on the extraction of biocrudes is discussed under two separate considerations. Firstly, considering a given solvent density, increasing the temperature significantly improves the extraction efficiency. This is clearly observed in Figure 5.3a, where the cumulative extraction yield for BCR-DM is plotted against the S/F at a given solvent density (i.e. 691-693 kg/m$^3$) and different temperatures. Secondly, considering the effect of temperature increase at a given pressure (Figure 5.3b) the significant decrease of solvent density does not significantly reduce the extraction efficiency. Especially at the early stages of the extraction (up to about 15 wt%), the slope of the curve is practically the same for 40, 60 and 80 °C.

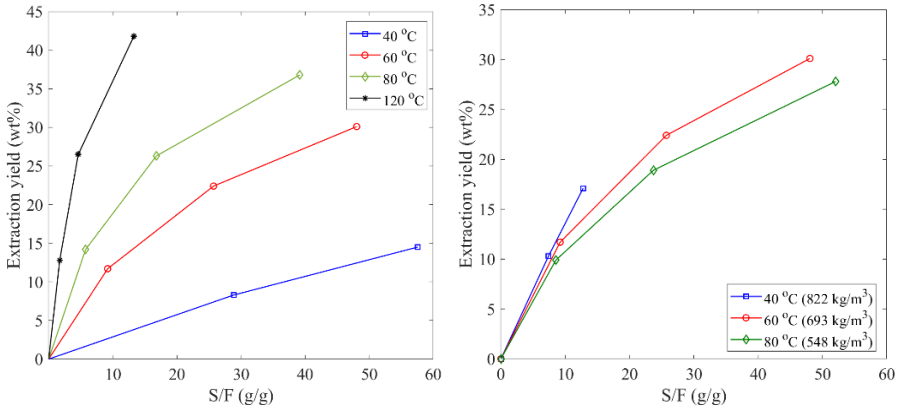


Figure 5.3: Extraction yield of BCR-DM vs solvent-to-feed ratio (S/F) at: (a) 691-693 kg/m$^3$ and different temperatures (Paper A); (b) 183 bar and different temperatures.

This effect is even more pronounced at more severe conditions (i.e. higher pressure and temperature) as it can be observed in Figure 5.4. Perusing Figure 5.4a, it is observed that a temperature increase from 80 to 150 °C, clearly increases the extraction yield for a fixed S/F. The VPL is also plotted against extraction yield in Figure 5.4b, which further demonstrates that at this pressure the extraction becomes more efficient with increasing temperature, even though the solvent power reduces. These observations are the result of the competing effect of solvent density decrease and mass transfer improvement when increasing temperature at given pressure [140].

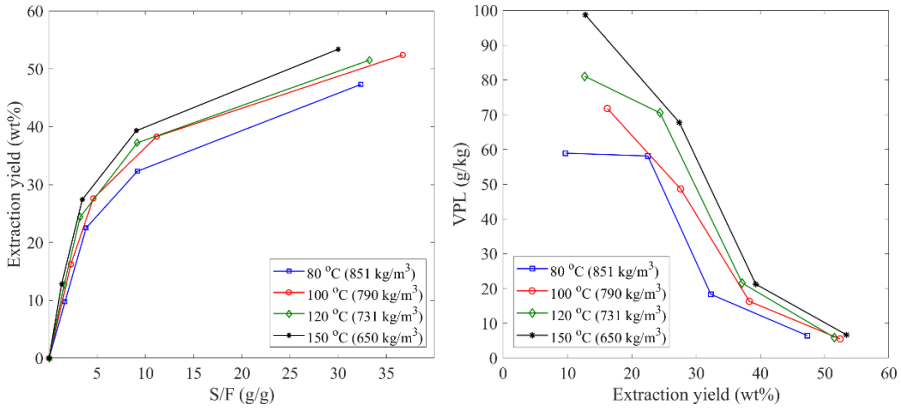


Figure 5.4: (a) Extraction yield of BCR-RAW vs solvent-to-feed ratio (S/F) at 450 bar and different temperatures; (b) Vapor phase loading (VPL) vs extraction yield for BCR-RAW at 450 bar and different temperatures (Paper C).

In fact, Figure 5.4 indicates that at a given high pressure (i.e. 450 bar) and temperatures (80-150 °C), the increase of temperature increases the mass extracted at a given S/F. This indicates that the mass transfer improvement at high pressure and temperature conditions is high enough to overcome the reduction of solubility of the biocrude in the $sCO_2$. The highest possible VPL is equal to the thermodynamic solubility of the biocrude components in $sCO_2$, that can be attained under equilibrium conditions. During semi-continuous extraction the two phases are not typically in equilibrium and if the VPL at a given pressure and temperature is far lower than the thermodynamic solubility a mass transfer improvement due to a temperature increase (at the same pressure) can increase the VPL, despite the solubility reduction. Alternatively, this could be due to a crossover pressure, resulting to the solubility of the biocrude increasing with temperature, although this would require phase equilibrium measurements to be proven.

### 5.1.3. Effect of feed

Comparing extractions at similar conditions, it was observed that BCR-RAW is extracted more efficiently than BCR-DM, especially in the early stages of the extraction. For example, perusing the curves for the extractions at 120 °C and 730-731 kg/m$^3$ (i.e. 448 and 450 bar) in Figure 5.2, approximately 37 wt% is extracted, utilizing approximately 9 g/g and 14 g/g $CO_2$ for BCR-RAW and BCR-DM, respectively. The reason for this observation was analyzed in detail in Paper C as it is shown in Figure 5.5. The extractions at the same conditions (i.e. 120 °C and 448-450 bar) were compared in terms of cumulative extract vs S/F (Figure 5.5a).

As it was mentioned in Section 4.1, one of the major differences between BCR-DM and BCR-RAW was the water content, which was found to be at least partly

responsible for the difference in the extraction efficiency. The improvement was mostly connected to the increased VPL for some of the extracted chemical classes, thus the VPL variation was plotted for the identified chemical classes for different S/F values in Figure 5.5b. As it is observed, the VPL of multiple ring aromatic hydrocarbons (PAH) was significantly higher for BCR-RAW at given S/F. Especially, during the early stages of the extraction, while this effect diminished at the later stages consequently to the drying of the feed remaining in the extractor.

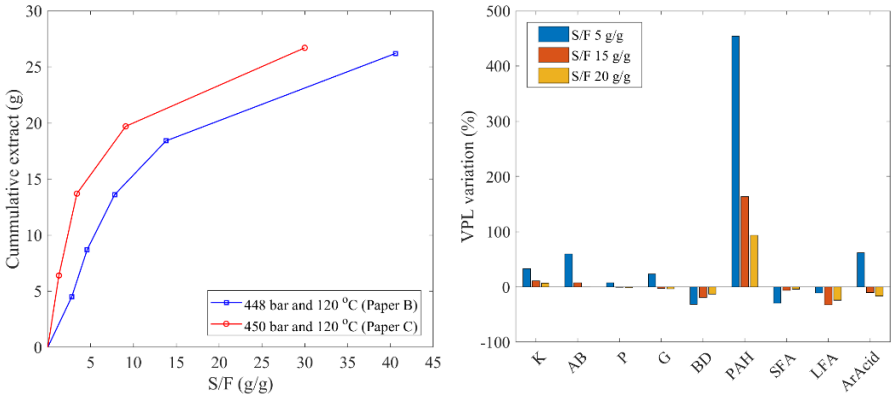


(a) (b)

Figure 5.5: (a) Extract vs S/F and (b) Chemical class VPL variation at different S/F. Comparison of BCR-DM and BCR-RAW. (Paper C)

For example, for S/F 15 g/g the VPL of PAH was about 150 times higher for BCR-RAW extraction, when compared to BCR-DM. This observation, suggests that the $sCO_2$ extraction can be more efficient for a raw biocrude, while at the same time it can serve for dewatering the extract and the residue by an optimized downstream separation system. This is a key finding of Paper C and is in line with the hypothesis of using the $sCO_2$ extraction directly after the HTL reactor for an efficient (i.e. high yield) separation and dewatering of the extract.

With regard to process performance the results of this work indicate that for semi continuous extractions of lignocellulosic biocrudes temperatures above 80 °C are required if a relatively high extraction yield is to be achieved (above 30 wt%). In addition, extraction yields above 50 wt% were only achieved at the highest pressure tested (i.e. 450 bar), in combination with temperatures above 100 °C. The highest conditions tested, resulted to the highest extraction yield (i.e. 53 wt%) by utilizing 30 g/g $sCO_2$, which is also the lowest S/F for extractions with high yield. During the semicontinuous extraction regime it was observed that the later stage extracts become viscous enough to make flow towards the trapping system very slow. The atmospheric pressure part of the pipeline (downstream the expansion valve) would benefit by being heated, thus enabling the viscous late extracts to flow freely and possibly reduce the S/F ratio. It is clear that maximum extraction yield is the objective of the separation of an extract directed to hydrotreating for fuel upgrading. Therefore, the optimal

conditions among the ones tested in this work are 150 °C and 450 bar. Considering the main competitor separation process, vacuum distillation, the $sCO_2$ extraction yield is in par with the maximum distillation yield reported in literature for similar LC biocrudes (i.e. 47-53 wt%) [77,103]. Although, it is noted that in these cases the biocrude was dewatered prior to distillation due to water reducing the efficiency of the process and leading to unsteady boiling as well as process control issues.

## 5.2. The $sCO_2$ extract properties

### 5.2.1. Density, TAN and water content

Figure 5.6 depicts $sCO_2$ extracts produced from BCR-DM at 80 °C and 183 bar (Figure 5.6a), and at 448 bar and 120 °C (Figure 5.6b). It was observed that the more severe the conditions the darker the color was, ranging from amber to black. In addition, the color progressively turned darker with extraction progression.

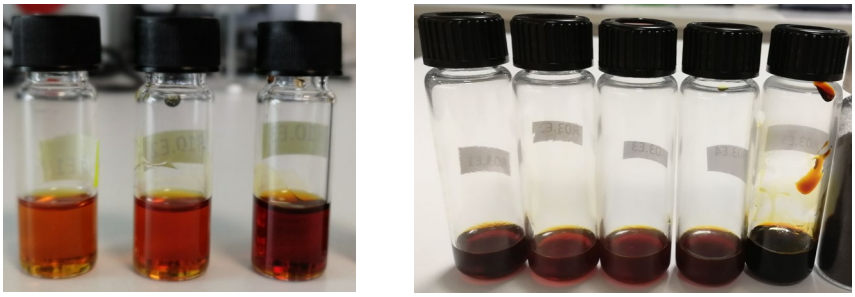

(a) (b)

Figure 5.6: $sCO_2$ extracts of BCR-DM. (a) Extraction at 80 °C and 183 bar; (b) Extraction at 120 °C and 448 bar.

On the other hand, the extracts of BCR-RAW were in all cases black colored. An example is shown in Figure 5.7. Visually all extracts (i.e. for both biocrudes) appeared less viscous than the biocrudes, although their actual viscosity was not measured due to sample size limitations.

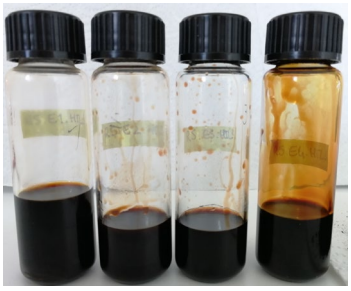

Figure 5.7: $sCO_2$ extracts of BCR-RAW at 100 °C and 450 bar.

The density of $sCO_2$ extracts was measured by weighing the volume displaced by a precision pipette at ambient temperature (i.e. 23-25 °C), as it is described in Papers A, B and C. The density of the extracts was found in most cases lower than that of the feeds. The values ranged between 941-1044 kg/m$^3$ for BCR-DM extracts and 913-1034 kg/m$^3$ for BCR-RAW. The lowest density was measured for the extracts collected earlier during the extraction (i.e. lower yield), while it was consistently increasing as the extraction was progressing. In order to visualize the increase of density with extraction progression, the distribution of the percentile reduction of density is plotted in Figure 5.8 for three increasing ranges of extraction yield.

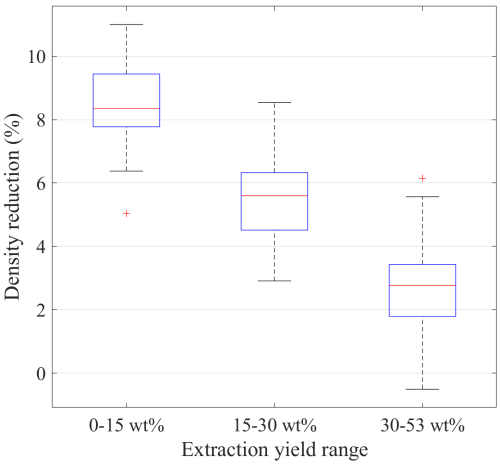


Figure 5.8: Percentile density reduction of the $sCO_2$ extracts with respect to the biocrude feeds.

In addition, it can be observed that only in a couple of cases for the latest stages of extraction (i.e. yield of 30-53 wt%) the density of the extracts reached values comparable to the feed biocrudes. The extraction conditions show negligible effect on the density reduction, even though the lower density values were measured for the early extracts at 150 °C (e.g. 912 kg/m$^3$), which is the highest temperature tested in this work. Density is an important bulk property in the fuel perspective of biocrudes, thus the extract has to be compared as a whole to the feed. Calculating the weighted average of density for each extraction performed in this work, it has been found that the overall density reduction of the extract is approximately 5%. Even though this is a relatively small reduction, it translates to a density range of 977-997 kg/m$^3$, which is in the middle range of residual marine fuel (i.e. 920-1010 kg/m$^3$) [63]. In addition, the intended hydrodeoxygenation will reduce the density further, thus the $sCO_2$ extract is at a better starting point than the biocrude feed with respect to the density of the final product.

Regarding the acid numbers of the $sCO_2$ extracts, lower values of CAN, PhAN and TAN were observed for the earlier extracts. In fact, extracts that correspond to

approximately 70% of the total extracted mass owned TAN lower than that of the feed. The three acid numbers were increasing with extraction progression, which can be seen in the examples for CAN vs cumulative extraction yield in Figure 5.9. Only in a few cases the TAN of the latest extracts was found somewhat higher than that of their respective feed. The range of TAN for the extracts of BCR-DM was 61-120 mg KOH/g, while those for the extracts of BCR-RAW was in the range 44-124 mg KOH/g. It is reminded that the BCR-DM and BCR-RAW owned TAN of 129 and 97 mg KOH/g, respectively. As in the case of density, the extraction conditions did not affect the acid numbers significantly.

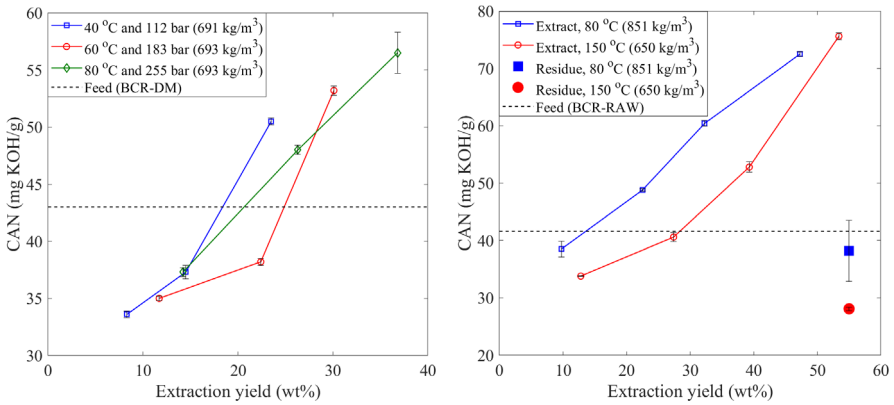


Figure 5.9: Carboxylic acid number (CAN) vs extraction yield for (a) BCR-DM extracts at 691-693 kg/m$^3$ and 40, 60 and 80 °C; (b) BCR-RAW extracts at 450 bar and 80 and 150 °C. Error bars correspond to standard deviation of at least triplicate measurements.

In terms of $sCO_2$ extracts being an improved hydrotreatment feed, the CAN and PhAN provide more relevant information than TAN. As it can be observed in Figure 5.9, earlier extracts have lower CAN than the feed, while at later stages the values for the extracts surpass the feed. This is a clear indication that the numerous fatty acids that are present in the biocrudes are not extracted preferentially in the early extraction stages, while they are concentrated in the later extracts. In addition, in Figure 5.9b the CAN of the residue for the corresponding extraction experiments are shown to own lower values than both the feed and the extracts. This indicates than while the carboxylic acids are depleted from the residue, its acidity is shifting towards phenolic. This is in line with the observed PhAN values, which were always lower in the extracts than the biocrudes (i.e. 22-62 mg KOH/g and 14-48 mg KOH/g for BCR-DM and BCR-RAW, respectively).

Clearly the type of acidic components that were mostly affecting TAN of the extracts were of carboxylic nature. This was verified by the values of PhAN for the same extractions, an example of which is reported in Figure 5.10, for extractions of BCR-RAW at 450 bar and 80 °C and 150 °C. These observations show that carboxylic acids

are concentrated in the $sCO_2$ extract, while the phenolic fraction is reduced, making them a better feed for the downstream hydrotreating. Literature on hydrotreatment of bio-oils indicates that CAN is effectively eliminated by the HT process, which supports the fact that the fatty acids are some of the easiest chemical classes to HDO [84,135].

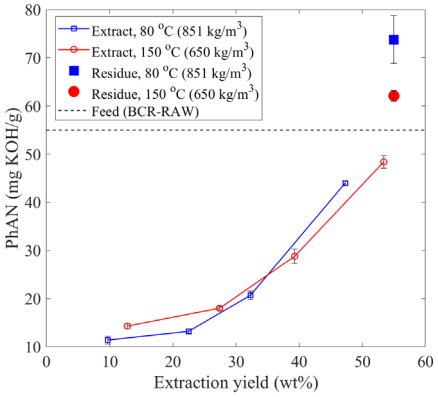


Figure 5.10: Phenolic acid number PhAN vs extraction yield for BCR-RAW and its $sCO_2$ extracts at 450 bar and 80 and 150 °C (Adapted from Paper C). Error bars correspond to standard deviation of at least triplicate measurements.

Regarding the effect that $sCO_2$ extraction has on the water content of the biocrudes, the comparison of BCR-DM (i.e. dewatered) and BCR-RAW (i.e. non-dewatered) leads to some interesting observations. The extracts of BCR-DM were moderately dewatered from 2.7 ± 0.1 wt% to a range of 1.3-1.9 wt% ± 0.2 wt%. The BCR-RAW was dewatered from 5.7 ± 0.3 wt% to a range of 0.5-2.0 wt% ± 0.1 wt%. This clearly indicates that water is co-extracted in parallel with biocrude compounds. Interestingly, the dewatering of BCR-RAW (i.e. 64%-91%) by $sCO_2$ achieved water content values in the extracts that are even lower that of the BCR-DM, which was already dewatered by vacuum evaporation. Therefore, it is important to note that $sCO_2$ extraction produces a hydrotreatment ready extract with respect to water content.

As it was reported in Paper C, the early extracts (i.e. 22-28 wt%), which accounts for 46% to 59% of the total mass extracted, exhibited water separating freely at the bottom of the sampling vials. This was not observed in later extracts. The freely separated water was only quantitated in a single case and was found to be approximately 6% of the original water in the feed. In addition, the range of water content in the extracts was relatively narrow (i.e. 1.3-1.8 wt%). These observations in conjunction with the fact that residues were found dewatered as well (i.e. 0.9-1.6 wt% ± 0.1 wt%), point out that most of the water is extracted in the early stages of the semicontinuous extraction. At the same time, calculation of the mass balance showed that about 50% of the water in the original feed was not recovered during sampling, which verified the intrinsic difficulty of capturing water in the cold trap. Nevertheless, an optimized

separation system following the extractor would provide the means to achieve at least this level of dewatering of the $sCO_2$ extract. For example, by stepwise decreasing the pressure in a series of separators the water can be separated from the extract in one separator, while the majority of the extracted biocrude components are condensed in a following unit at ambient pressure.

### 5.2.2. Elemental composition and HHV

The range of elemental carbon, hydrogen, nitrogen and oxygen for the $sCO_2$ extracts for the two biocrudes (i.e. BCR-DM, BCR-RAW) is reported in Table 5.1. Sulfur was also measured, although it was always below the detection limit of the elemental analyzer. The first interesting observation is that the ranges for C, H are wider for extracts of BCR-DM compared to those of BCR-RAW, which results in a very wide range of the calculated by difference O.

Table 5.1: Elemental composition ranges for the $sCO_2$ extracts of BCR-DM and BCR-RAW, on water free basis and average standard deviation values for at least triplicate measurements.

| | C (wt%) | H (wt%) | N (wt%) | O (wt%) | HHV (MJ/kg)[1] |
|---|---|---|---|---|---|
| BCR-DM extract | 75-83 ± 1 | 6-10 ± 1 | 0.4-1.2 ± 0.2 | 6-18 ± 2 | 32-40 ± 2 |
| BCR-RAW extract | 82-84 ± 0.4 | 9-11 ± 1 | 0.7-1.3 ± 0.1 | 5-8 ± 2 | 38-43 ± 2 |

[1]Calculated as reported in literature [76]; All measurements were performed at least in triplicates.

In majority, the BCR-DM extracts ended up with higher oxygen content than the BCR-DM feed, without showing a clear trend with extraction conditions. This has been observed also in the case of vacuum distillation for lignocellulosic biocrude as well as pyrolysis oils [103,141]. The only case where extracts of BCR-DM were found with oxygen lower than the feed was for the extraction at 400 bar and 120 °C (i.e. oxygen 5.9-7.1 wt%). This indicates that severe extraction conditions (i.e. high pressure and temperature) lead to a level of deoxygenation. This observation, together with the improvement in process efficiency discussed in Section 5.1, led to the focus of Paper C at high pressure and temperature conditions (i.e. 80-150 °C and 330 and 450 bar). In fact, the lowest oxygen content between all the extracts of BCR-RAW was found for the extraction at 150 °C and 450 bar (4.6 wt%). All extracts of BCR-RAW exhibited an oxygen reduction as it can be seen in Table 5.1.

The effect of the elemental composition to the fuel potential of the $sCO_2$ extracts can be qualitatively appreciated in the Van Krevelen diagram. In Figure 5.11, the H/C ratio is plotted against O/C ratio for the two biocrudes and their extracts. In general, the closer the point in the Van Krevelen diagram is to the y-axis the closer the fluid is to hydrocarbon mixtures (e.g. crude oil). In addition, higher H/C indicates higher fuel value.

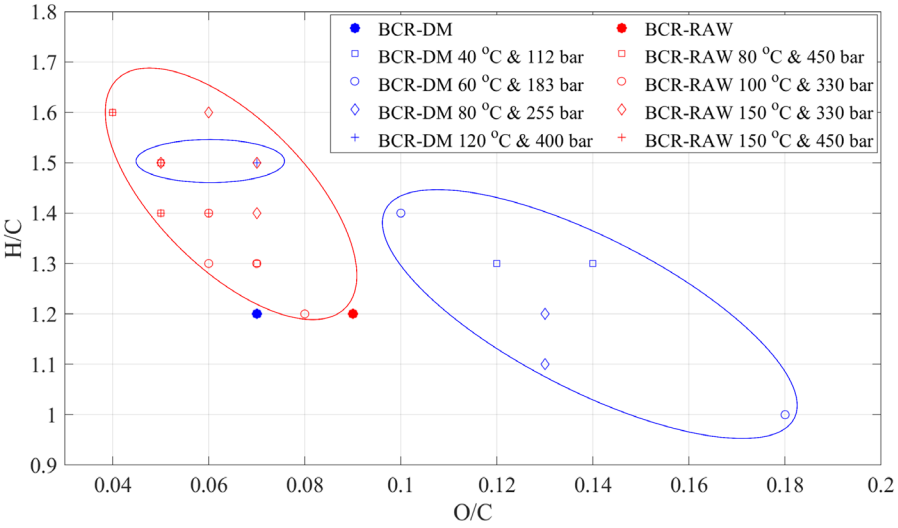


Figure 5.11: Van Krevelen diagram of the biocrudes and their $sCO_2$ extracts

The diagram shows that for BCR-DM, only the extracts at 120 °C and 400 bar (i.e. smaller blue ellipse) are improved. On the other hand, all extracts of BCR-RAW (i.e. red ellipse) are improved compared to the feed. This is the result of increase of the H/C and reduction of O/C ratios for the BCR-RAW extracts. The consistent improvement of the BCR-RAW extracts is attributed to the largely improved VPL values for the polyaromatic hydrocarbons (see Figure 5.5). Figure 5.11, indicates that the $sCO_2$ extraction process placed directly after the HTL reactor produces an extract that is slightly upgraded in terms of fuel value. This improvement can be quantitatively translated to the HHV values (up to 43 MJ/kg) that are closer to conventional fuels (e.g. 45 MJ/kg for diesel) than those of the whole biocrude (i.e. 37-38 MJ/kg).

The effect of $sCO_2$ extraction on the metal content of LC biocrudes was studied in Paper C. The extracts were found almost free of metals with the reduction ranging from 95.9% to 99.5%. The range of metal content was between 40-310 mg/kg with an average of 170 mg/kg, whereas the initial BCR-RAW value was 8500 mg/kg. These numbers are even lower than the metal content of BCR-DM (i.e. 587 mg/kg), which was demetallized by acid washing. It should be noted that the acid washing process requires a petroleum derived organic diluent (e.g. methyl ethyl ketone) [129]. The removal of metals was verified by their concentration in the residue, in which the metal content was measured between 13800 and 20100 mg/kg. As an example, the metal content of BCR-RAW, its $sCO_2$ extracts (indicated by increasing cumulative extraction yield) and the residue are reported in Figure 5.12.

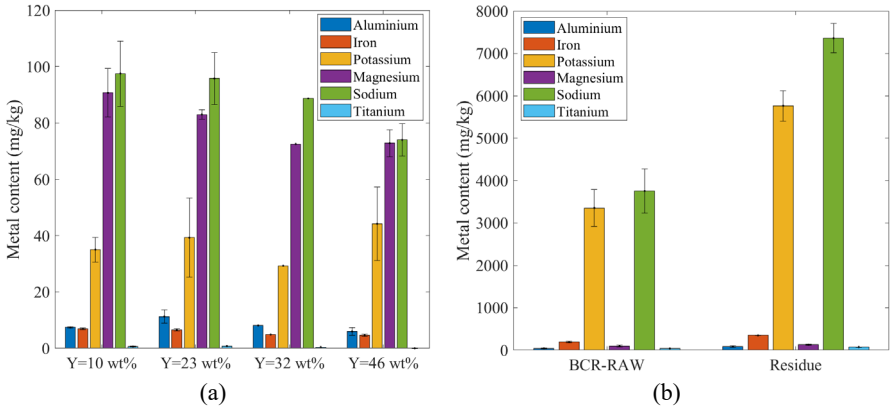


Figure 5.12: Metal content of (a) BCR-RAW extracts and (b) BCR-RAW feed and residue at 150 °C and 330 bar (adapted from Paper C). Y: cumulative extraction yield. The error bars indicate the standard deviation of at least triplicate measurements.

Even though K and Na constitute 90% of the metal content in BCR-RAW, their values drop to 100 mg/kg and lower in the extracts. The extracts do not show any significant difference between each other, and there in no clear effect of the extraction conditions tested (i.e. 80-150 °C and 330, 450 bar). The presence of the metals indicate that they are either dissolved in the emulsified water droplets or organometallic components that are soluble in $CO_2$ are present in the biocrude. It should be noted that a 10 μm filter is present at the top of the extractor, which is expected to at least partly reduce entrainment of water droplets. The direct hydrotreatment of the demetallized extracts can clearly provide a much longer operational time of the catalytic bed, considering the values at which catalyst replacement is typically considered (i.e. 30000-40000 mg/kg). In conjunction with the dewatering discussed in Section 5.2.1, the extracts are ready to be hydrotreated.

### 5.2.3. Detailed composition of volatile fraction

GC-MS analysis of consecutive $sCO_2$ extracts was performed in order to elucidate aspects of selective extraction of biocrude components and chemical classes. Qualitatively, the extraction trend can be observed in the example of Figure 5.13, where the chromatograms of BCR-RAW and three consecutive extracts (i.e. extraction yield 10, 32 and 46 wt%) are plotted against the retention time. Figure 5.13a corresponds to neat samples (i.e. non derivatized), while Figure 5.13b to samples after silylation (i.e. derivatized). The lighter and less polar components (RT up to 20 min) are abundant in the early extracts and are gradually depleted. On the other hand, the heavier and more polar components (RT above 20 min) are increasing considerably for the latest extracts (i.e. yield of 32-46 wt%).

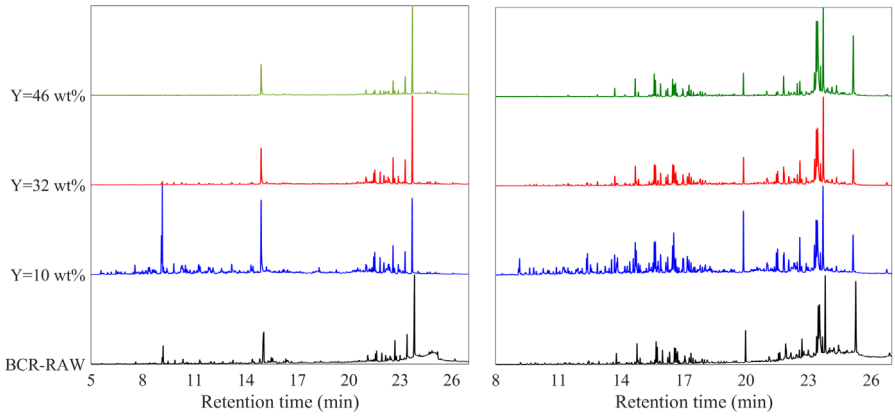


Figure 5.13: Chromatogram of BCR-RAW and its consecutive extracts at 330 bar and 150 °C. (a) Neat samples; (b) Silylated (derivatized) samples (Adapted from Paper C).

All chemical classes that were identified in the feed biocrudes (See Section 4.1) were found in the extracts as well. In most cases the components that were found in the $sCO_2$ extracts were concentrated compared to the feed and thus the volatile fraction of the extracts was much higher than that of the feed biocrude. It is noted that the GC-MS characterization of BCR-RAW performed for Paper C was the most extensive in number of single components that were identified and quantitated (i.e. 46 components). The volatile fraction of BCR-RAW was 19 wt%, while the values ranged between 25 and 40 wt% for its $sCO_2$ extracts. The extraction of BCR-RAW with the highest extraction yield (i.e. 150 °C and 450 bar) is used in Figure 5.14 as an example. The height of each bar corresponds to the total mass fraction identified for each sample, while the colors correspond to the mass fraction of each chemical class.

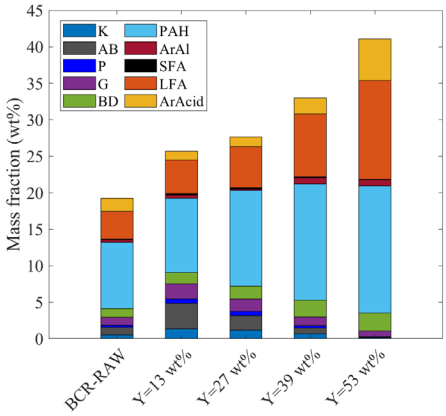


Figure 5.14: GC-MS quantified mass fraction of BCR-RAW and its extracts at 150 °C and 450 bar. Colors correspond to the individual mass fractions of chemical classes as they were defined in Section 4.1 (Paper C).

Since most of the components identified by GC-MS own relatively low MW and polarity, they end up having high extraction yields. In the specific example of Figure 5.14, the extraction yield range was from 77 wt% to 100 wt% for the ten chemical classes. The chemical class with the highest mass fraction in the extracts is the multiple ring aromatic hydrocarbons (PAH) with values ranging 9.1-17.4 wt% and increasing with the extraction progression. Similar trend was observed for the benzenediols (BD), long chain fatty acids (LFA) and dehydroabietic acid (ArAcid), which ranged 1.2-2.5 wt%, 3.7-13.5 wt% and 1.8-5.7 wt%, respectively. On the other hand, ketones (K), alkylbenzenes (AB), phenols (P) and guaiacols (G) were found decreasing with extraction progression. Their mass fractions ranged 1.4-0.1 wt%, 3.5-0.1 wt%, 0.6-0.1 wt% and 2.1-0.8 wt%, respectively. Dehydroabeityl alcohol (ArAl) and short chain fatty acids (SFA) were found having relatively stable mass fractions across the extracts ranging 0.1-0.2 and 0.4-0.8 wt%, respectively.

The abovementioned observations result to two major qualitative conclusions. Firstly, the vast majority of the volatile fraction of the lignocellulosic biocrudes studied in this work consists of PAH, LFA and ArAcid. Cumulatively they constitute 76% of the characterized volatile fraction of the biocrude feed and between 55% and 89% of the extracts. Secondly, preferential extraction is very much dependent on the composition of the feed remaining in the extractor, with lighter less polar components (i.e. K, AB, P, G) extracted at the early stage of the extraction. When these components are depleted, the heavier and more polar (i.e. BD, PAH, LFA, ArAcid) are extracted preferentially. In order to quantitatively investigate preferential extraction, the distribution factors (K-values) of each chemical class, calculated as it was described in Paper A are discussed below for consecutive extracts.

In Figure 5.15, the K-values of each chemical class in BCR-DM is plotted against cumulative extraction yield that corresponds to the consecutive $sCO_2$ extract samples at 120 °C and 247 bar and 448 bar. A notable difference is that at 448 bar PAH and LFA have K-values higher than 1 from very early extraction stages. Particularly the LFA achieve much higher K-values, by the later stage of the extraction (i.e. Y=49 wt%), reaching almost 8. In addition, the ArAcid reaches a high K-value at the latest stage of the extraction at 448 bar. On the contrary, lower MW components (i.e. K, AB and SFA) are generally extracted with higher K-values in the early stages of the extraction at 247 bar. Regardless, the extraction at 448 bar ended up to higher total extraction yield (i.e. 64-97%) for all classes, compared to the extraction at 247 bar (i.e. 10-93%). This is especially true for LFA and ArAcid that ended up extracted 97% and 64% at 448 bar, as opposed to 67% and 10% at 247 bar. The higher extraction yield is also reflected to the total extraction yield of the two experiments that were 34 wt% and 49 wt% at 247 and 448 bar, respectively.

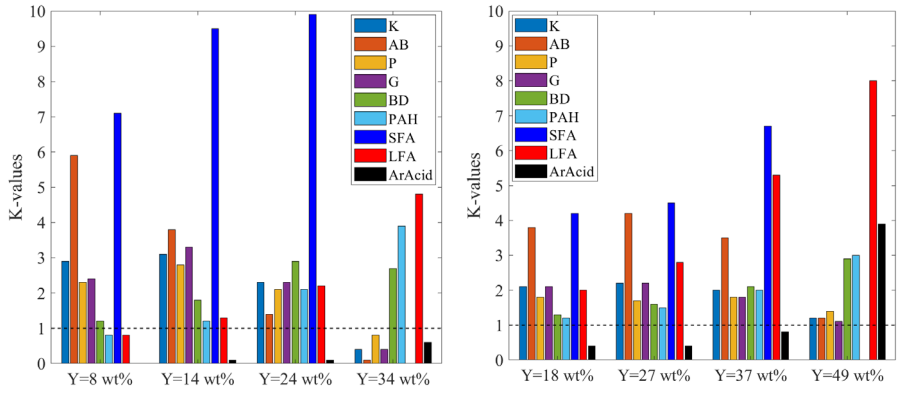


Figure 5.15: Distribution factors (K-values) of BCR-DM extracts at 120 °C and (a) 247 bar; (b) 448 bar

In Figure 5.16, the K-values of each chemical class found in consecutive $sCO_2$ extracts of BCR-RAW are shown at 450 bar and 80 °C and 150 °C. In this case, one of the most notable differences is the K-values of BD and ArAcid chemical classes. The extraction at 150 °C is improving the separation of these two classes and increases their extraction yield from 64% to 89% for BD and from 33% to 77% for ArAcid. On the other hand, the light and less polar components such AB and G are extracted better at 80 °C. It is noted that the solvent density at 80 °C is 850 kg/m$^3$ and at 150 °C it is 650 kg/m$^3$, which translates to a higher solvent power and typically higher solubility of individual components in the supercritical phase. However, as it was discussed in Section 5.1, the temperature enhances the overall extraction yield (in this case 47 to 53 wt%).

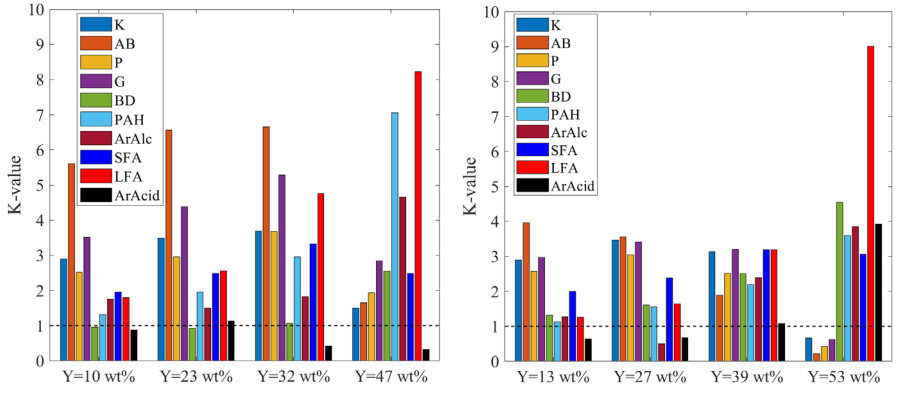


Figure 5.16: Distribution factors (K-values) of BCR-RAW extracts at 450 bar and (a) 80 °C; (b) 150 °C.

The observations of this section corroborate one of the important results of this work, which is that the high extraction pressure and temperature combination can produce a hydrotreatment-ready fraction. The maximum K-values for LFA are achieved at such conditions, and in combination with maximizing the total extraction yield, the extract ends up containing a large mass fraction of hydrocarbons and fatty acids. For example, for the extraction at 450 bar and 150 °C the hydrocarbons (AB and PAH) were 16 wt% and the fatty acids (SFA and LFA) 3 wt% of the total extract, respectively. In addition, the high temperature (i.e. 150 °C) reduces the K-values of guaiacols that are known coke precursors and difficult to hydrodeoxygenate.

## 5.3. Potential applications for the $sCO_2$ residue

The $sCO_2$ extract is suggested in the previous sections as a good feed for the production of liquid fuel via hydrotreating. On the other hand, it leaves approximately half of the biocrude as residue. The residue in this work was retrieved as described in Paper C, by washing the extraction vessel with THF. The THF was evaporated by rotary vacuum evaporation and the residue collected for analysis. An example of the residue after vacuum evaporation is shown in Figure 5.17.

Figure 5.17: Example of $sCO_2$ residue. Extraction of BCR-DM at 120 °C and 248 bar.

In this work, the potential of the residue was not investigated experimentally, although some of its properties indicate possible utilizations that would require further investigation. One of the lignocellulosic biomass macromolecules, lignin, is interesting due to its phenolic moieties. The decomposition of lignin by thermochemical processes such as HTL and pyrolysis results to many phenolic monomers as well as dimers and oligomers. One property that has been attributed to phenolic hydroxyl groups derived from lignin is their antioxidant activity [142]. In general, phenolic hydroxyl groups increase the antioxidant activity, while the opposite is true for aliphatic hydroxyl groups. Recently, several publications demonstrated the antioxidant potential of lignocellulosic pyrolysis oils as well as for HTL biocrudes.

More specifically, the antioxidant activity of pyrolysis product of lignin and wood was attributed to phenolic dimers or oligomers with MW 270-340 g/mol, while phenolic monomers show insignificant antioxidant activity [92,143]. Similar were the observations for a HTL biocrude from woody biomass, where the phenolic concentration was corelated positively with antioxidant activity [91]. In addition, the carboxylic acids were indicated to be detrimental on the antioxidant activity. Considering that the $sCO_2$ extraction depletes the phenolic monomers as well as the fatty acids from the residue, while its acidity shifts to phenolic, it is suggested that the residue contains compounds with antioxidant activity (e.g. phenolic dimers and oligomers). These compounds can be extracted to be used as antioxidants in fuel such as biodiesel.

Another potential for the $sCO_2$ residue of lignocellulosic biocrudes is the production of solid carbon materials like adsorbents or renewable coke. The $sCO_2$ residue is expected to be a good candidate for the production renewable coke, due to its relatively high molecular weight and its phenolic nature [144]. The residue of the biocrudes studied in this work have elemental carbon and HHV values close to that of petroleum coke (i.e. C:78-79 wt% and HHV: 35 MJ/kg). Much like petroleum coke, instead of used as low value combustion fuel, it can be potentially valorized by calcination in the same manner as low sulfur and metals petroleum coke. Calcined petroleum coke is used for the production of electrodes for the steel and aluminium industry [145]. As an example, the distillation residue of lignocellulosic pyrolysis oils have been suggested in literature as a feedstock for the production of bio-coke by calcination [146]. The high MW aromatic structure of this distillation residue is expected to have similarities with the $sCO_2$ residue of biocrudes. However, it should be noted that in the case of the biocrudes studied in this work (e.g. BCR-RAW), demetallization of the residue would have to be performed prior calcination, since the presence of alkali and earth metals in coke can considerably reduce the quality of the produced electrode [147,148]. The metal content of the $sCO_2$ residue in this work ranged 1.5-2.0 wt%, while typical petroleum coke values are lower than 1 wt% [145]. Nevertheless, since the vast majority of these metals are not bonded to biocrude components, they are relatively easy to remove.

# Chapter 6. Conclusion and perspectives

## 6.1. Conclusion

This work focuses on the fractionation of lignocellulosic biocrudes, produced by hydrothermal liquefaction (HTL), using supercritical carbon dioxide ($sCO_2$). The work suggests a $sCO_2$ unit as a part of the valorization of said organic mixtures to liquid fuel. Currently the biocrudes are obstructed from commercial utilization due to their detrimental physicochemical properties. The high molecular weight, acidity, aromaticity, polarity and presence of impurities (i.e. oxygen, water, metals) require well developed processing trains that include upgrading and separations. The current state of the art for upgrading crude oils with high oxygen content to fuel is hydrodeoxygenation (HDO) by catalytic hydrotreatment. However, some of the biocrude properties (i.e. water and metal content, large high molecular weight fraction) are associated with HDO process operation issues. This PhD thesis suggests supercritical $CO_2$ extraction prior to hydrotreatment as a processing step that provides a feed to the hydrotreater with minimized catalyst deactivation rate and is easier to HDO than the whole biocrude.

The benefits of the addition of a $sCO_2$ unit were studied by analyzing the effect of a large supercritical region through a wide range of extraction pressure and temperature combinations. High solvent density achieved at high pressures is crucial to attain high extraction yields and produce a large liquid fuel precursor fraction (e.g. >50%). In addition, relatively high temperature (e.g. 100-150 °C) is beneficial for the overall process efficiency due to its large positive effect on the overall vapor phase loading (VPL). The severe conditions are in fact increasing the extraction of the multiple ring aromatic hydrocarbons (PAH) and the long chain fatty acids in the biocrude. The natural presence of water in biocrudes was found to enhance the VPL of the PAH as well. The result of these observations is a large extract fraction that is produced by a combination of high pressure and temperature and is partially deoxygenated, with lower O/C than the biocrude feed.

The $sCO_2$ process is able to produce an extract with reduced water content (i.e. up to 91% reduction) and almost free of metals (i.e. 95%-99% reduction). This improvement is beneficial to upgrading via catalytic hydrotreatment since it would prolong the lifecycle of the catalyst by reducing its irreversible deactivation rate. In fact, the average metal content in the $sCO_2$ extracts was lower than that of the biocrude that was demetallized by acid washing. Importantly, an environmentally benign solvent was used for the demetallization as opposed to the organic solvents required for the conventional washing method. With regard to the oxygenated chemical classes that are concentrated in the $sCO_2$ extracts, the by far largest fraction is owned by the fatty acids that reach up to 14 wt%. Despite the fact that such high mass fraction increases the carboxylic acidity (i.e. CAN), hydrotreatment effectively converts this chemical class to alkanes. This compositional aspect in addition to the $sCO_2$ concentrating the hydrocarbons (i.e. alkylbenzenes and polyaromatics) in the extracts

leads to a hydrotreating feed with higher H/C and lower O/C that possibly requires less severe hydrotreating conditions (e.g. hydrogen pressure and retention time). In addition, the heavy phenolic fraction is left in the residue, which is beneficial since high molecular weight phenolic fractions are resistant to hydrodeoxygenation. On the other hand, their concentration in the residue may increase the potential for the production of antioxidants.

To sum up to a single conclusion, the $sCO_2$ extracts of lignocellulosic biocrudes are hydrotreatment ready and show favorable characteristics as a hydrotreatment feedstock than the whole biocrude.

## 6.2. Perspectives

The natural continuation of this PhD project is studying the hydrotreatment of $sCO_2$ extracts of lignocellulosic biocrudes. Experimental works dedicated in the comparison of hydrotreating the raw biocrudes and its $sCO_2$ extract are essential in this context. Except for the product yields and properties, attention should be given to the deactivation of the HT catalysts (i.e. irreversible and coking), as well as to the hydrogen and reaction time required for the considerable hydrodeoxygenation of the two matrices.

The biocrude as a whole is difficult to utilize for a single purpose, so it makes sense to study potential applications for different fractions. Since characterization data for the heavy fraction of biocrudes (i.e. $sCO_2$ residue) is scarce, studies dedicated on this fraction can provide new knowledge and serve to investigate potential value-added applications, including the ones hypothesized in this PhD thesis (i.e. production of antioxidants and renewable coke).

Vacuum distillation is naturally a competitor separation process and it has similar yields to those achieved in this work by $sCO_2$ extraction. Experimental works comparing the two processes by assessing yields, selectivity, product quality and energy requirements would be relevant.

Regarding scaling up to a pilot continuous countercurrent operation, the downstream separation as well as the application of a multistage separation (i.e. internal or external reflux) are interesting perspectives. A series of separators can be optimized to condense most of the organic extract in the first, while the water condenses in the following separator, together with some of the lighter organics. The separators would be essential for the design of a continuous system, since their optimization could effectively dewater the extract and provide a high purity $CO_2$ for recirculation, thus reducing the make-up requirement. The reflux loop can enhance the separation of specific chemical species as it is indicated by the K-value data acquired in this work from the semi-continuous single stage extractor.

One major benefit of the versatility of the $sCO_2$ process is that small amounts of co-solvents can be added to the supercritical stream. Biomass based co-solvents such as ethanol, methanol and butanol can work both for increasing the total extraction yield, or can be used to alter the selectivity towards specific chemical classes. The implementation of a co-solvent would benefit both lab-scale and pilot units, since it can additionally be used for cleaning the pipelines without dismantling them. The latter is very important for rapidly testing different feedstocks and avoiding cross-contamination of the samples. In addition, it would provide a means to reduce downtime due to fouling of the high-pressure lines.

# BIBLIOGRAPHY


[1] IEA, World Energy Statistics 2019, Paris. https://www.iea.org/reports/world-energy-statistics-2019, (2019).

[2] U.S. Energy Information Administration (EIA), International Energy Outlook, (2019). https://www.eia.gov/outlooks/ieo/ (accessed December 17, 2019).

[3] IEA, The future of petrochemicals towards more sustainable plastics and fertilisers, (2018). https://www.iea.org/reports/the-future-of-petrochemicals.

[4] IEA, Global methane emissions from oil and gas, (2020). https://www.iea.org/articles/global-methane-emissions-from-oil-and-gas (accessed June 22, 2020).

[5] IEA, $CO_2$ emissions statistics, (2020). https://www.iea.org/subscribe-to-data-services/co2-emissions-statistics (accessed June 22, 2020).

[6] US Environmental Protection Agency, Biofuels and the Environment: Second Triennial Report to Congress, EPA/600/R-10/183F, Washington DC, 2018.

[7] R. Sims, M. Taylor, J.N. Saddler, W. Mabee, From 1st- to 2nd-Generation Biofuel Technologies, Paris, 2008.

[8] S. V. Hanssen, V. Daioglou, Z.J.N. Steinmann, S. Frank, A. Popp, T. Brunelle, P. Lauri, T. Hasegawa, M.A.J. Huijbregts, D.P. Van Vuuren, Biomass residues as twenty-first century bioenergy feedstock—a comparison of eight integrated assessment models, Clim. Change. (2019). doi:10.1007/s10584-019-02539-x.

[9] WBA, Global bioenergy statistics, World Bioenergy Association, Stockholm, Sweden, 2019. https://worldbioenergy.org/global-bioenergy-statistics.

[10] IEA, Renewables, (2019). https://www.iea.org/reports/renewables-2019 (accessed December 17, 2019).

[11] A. V. Bridgwater, Review of fast pyrolysis of biomass and product upgrading, Biomass and Bioenergy. 38 (2012) 68–94. doi:10.1016/j.biombioe.2011.01.048.

[12] D. Castello, T. Pedersen, L. Rosendahl, Continuous hydrothermal

liquefaction of biomass: A critical review, Energies. 11 (2018) 3165. doi:10.3390/en11113165.

[13] M.S. Talmadge, R.M. Baldwin, M.J. Biddy, R.L. McCormick, G.T. Beckham, G.A. Ferguson, S. Czernik, K.A. Magrini-Bair, T.D. Foust, P.D. Metelski, C. Hetrick, M.R. Nimlos, A perspective on oxygenated species in the refinery integration of pyrolysis oil, Green Chem. 16 (2014) 407–453. doi:10.1039/c3gc41951g.

[14] J.A. Ramirez, R.J. Brown, T.J. Rainey, A review of hydrothermal liquefaction bio-crude properties and prospects for upgrading to transportation fuels, Energies. 8 (2015) 6765–6794. doi:10.3390/en8076765.

[15] P. Kokayeff, S. Zink, P. Roxas, Hydrotreating in petroleum processing, in: S.A. Treese, P.R. Pujadó, D.S.J. Jones (Eds.), Handb. Pet. Process., 2nd ed., Springer International Publishing, 1995: pp. 363–434.

[16] E. Furimsky, F.E. Massoth, Deactivation of hydroprocessing catalysts, Catal. Today. 52 (1999) 381–495. doi:10.1016/S0920-5861(99)00096-6.

[17] A.A. Kiss, J.P. Lange, B. Schuur, D.W.F. Brilman, A.G.J. van der Ham, S.R.A. Kersten, Separation technology–Making a difference in biorefineries, Biomass and Bioenergy. 95 (2016) 296–309. doi:10.1016/j.biombioe.2016.05.021.

[18] A. Taghipour, J.A. Ramirez, R.J. Brown, T.J. Rainey, A review of fractional distillation to improve hydrothermal liquefaction biocrude characteristics; future outlook and prospects, Renew. Sustain. Energy Rev. 115 (2019) 109355. doi:10.1016/j.rser.2019.109355.

[19] G. Brunner, Counter-current separations, J. Supercrit. Fluids. 47 (2009) 574–582. doi:10.1016/j.supflu.2008.09.022.

[20] E. Reverchon, I. De Marco, Supercritical fluid extraction and fractionation of natural matter, J. Supercrit. Fluids. 38 (2006) 146–166. doi:10.1016/j.supflu.2006.03.020.

[21] M.A. McHugh, V.J. Krukonis, Supercritical Fluid Extraction, Second, Elsevier, 1994. doi:10.1016/C2009-0-26919-4.

[22] R.B. Gupta, J.-J. Shim, Solubility in Supercritical Carbon Dioxide, CRC Press, Boca Raton, 2006. doi:10.1201/9781420005998.

[23] R.P. Nielsen, R. Valsecchi, M. Strandgaard, M. Maschietti, Experimental

study on fluid phase equilibria of hydroxyl-terminated perfluoropolyether oligomers and supercritical carbon dioxide, J. Supercrit. Fluids. 101 (2015) 124–130. doi:10.1016/j.supflu.2015.03.011.

[24] F. Gironi, M. Maschietti, Supercritical carbon dioxide fractionation of lemon oil by means of a batch process with an external reflux, J. Supercrit. Fluids. 35 (2005) 227–234. doi:10.1016/j.supflu.2005.01.007.

[25] F. Gironi, M. Maschietti, Continuous countercurrent deterpenation of lemon essential oil by means of supercritical carbon dioxide: Experimental data and process modelling, Chem. Eng. Sci. 63 (2008) 651–661. doi:10.1016/j.ces.2007.10.008.

[26] M. Maschietti, A. Pedacchia, Supercritical carbon dioxide separation of fish oil ethyl esters by means of a continuous countercurrent process with an internal reflux, J. Supercrit. Fluids. 86 (2014) 76–84. doi:10.1016/j.supflu.2013.12.003.

[27] F. Gironi, M. Maschietti, Separation of fish oils ethyl esters by means of supercritical carbon dioxide: Thermodynamic analysis and process modelling, Chem. Eng. Sci. 61 (2006) 5114–5126. doi:10.1016/j.ces.2006.03.041.

[28] V. Riha, G. Brunner, Separation of fish oil ethyl esters with supercritical carbon dioxide, J. Supercrit. Fluids. 17 (2000) 55–64. doi:10.1016/S0896-8446(99)00038-8.

[29] L.S. Osséo, G. Caputo, I. Gracia, E. Reverchon, Continuous fractionation of used frying oil by supercritical $CO_2$, JAOCS, J. Am. Oil Chem. Soc. 81 (2004) 879–885. doi:10.1007/s11746-004-0995-3.

[30] S.K. Kim, J.Y. Han, S.A. Hong, Y.W. Lee, J. Kim, Supercritical $CO_2$-purification of waste cooking oil for high-yield diesel-like hydrocarbons via catalytic hydrodeoxygenation, Fuel. 111 (2013) 510–518. doi:10.1016/j.fuel.2013.03.080.

[31] T. Meyer, Extracting and upgrading heavy hydrocarbons using supercritical carbon dioxide, (2011) UK Patent GB 2471862 A.

[32] A. Subramanian, R. Floyd, Residuum oil supercritical extraction process, (2011) US Patent 2011/0094937 A1.

[33] Y. Feng, D. Meier, Supercritical carbon dioxide extraction of fast pyrolysis oil from softwood, J. Supercrit. Fluids. 128 (2017) 6–17.

doi:10.1016/j.supflu.2017.04.010.

[34] P.K. Rout, M.K. Naik, S.N. Naik, V. V. Goud, L.M. Das, A.K. Dalai, Supercritical $CO_2$ fractionation of bio-oil produced from mixed biomass of wheat and wood sawdust, Energy and Fuels. 23 (2009) 6181–6188. doi:10.1021/ef900663a.

[35] S. Naik, V. V. Goud, P.K. Rout, A.K. Dalai, Supercritical $CO_2$ fractionation of bio-oil produced from wheat-hemlock biomass, Bioresour. Technol. 101 (2010) 7605–7613. doi:10.1016/j.biortech.2010.04.024.

[36] R.N. Patel, S. Bandyopadhyay, A. Ganesh, Extraction of cardanol and phenol from bio-oils obtained through vacuum pyrolysis of biomass using supercritical fluid extraction, Energy. 36 (2011) 1535–1542. doi:10.1016/j.energy.2011.01.009.

[37] U.S. Department of Energy (Bioenergy), Research Centers: 2020 Program Update, DOE/SC–0201, U.S. Department of Energy Office of Science, 2020. genomicscience.energy.gov/centers/ BRC2020programupdate.pdf.

[38] J. Zakzeski, P.C.A. Bruijnincx, A.L. Jongerius, B.M. Weckhuysen, The catalytic valorization of lignin for the production of renewable chemicals, Chem. Rev. 110 (2010) 3552–3599. doi:10.1021/cr900354u.

[39] E. Miliotti, S. Dell'Orco, G. Lotti, A.M. Rizzo, L. Rosi, D. Chiaramonti, Lignocellulosic ethanol biorefinery: Valorization of lignin-rich stream through hydrothermal liquefaction, Energies. 12 (2019) 723. doi:10.3390/en12040723.

[40] S. Sumathi, S.P. Chai, A.R. Mohamed, Utilization of oil palm as a source of renewable energy in Malaysia, Renew. Sustain. Energy Rev. 12 (2008) 2404–2421. doi:10.1016/j.rser.2007.06.006.

[41] J. Kosinkova, A. Doshi, J. Maire, Z. Ristovski, R. Brown, T.J. Rainey, Measuring the regional availability of biomass for biofuels and the potential for microalgae, Renew. Sustain. Energy Rev. 49 (2015) 1271–1285. doi:10.1016/j.rser.2015.04.084.

[42] J. Mateo-Sagasta, L. Raschid-Sally, A. Thebo, Global Wastewater and Sludge Production, Treatment and Use, in: P. Drechsel, M. Qadir, D. Wichelns (Eds.), Wastewater Econ. Asset an Urban. World, Springer Netherlands, Dordrecht, 2015: pp. 15–38. doi:10.1007/978-94-017-9545-6_2.

[43] Lignin Products Global Market Size, Sales Data 2017-2022 & Applications

in Animal Feed Industry., Orb. Res. (2017). https://www.orbisresearch.com/contacts/request-sample/218258 (accessed May 13, 2019).

[44] X. Tian, Z. Fang, R.L. Smith, Z. Wu, M. Liu, Properties, chemical characteristics and application of lignin and its derivatives, in: Z. Fang, R.L. Smith Jr. (Eds.), Prod. Biofuels Chem. from Lignin, Springer Singapore, Singapore, 2016: pp. 3–33. doi:10.1007/978-981-10-1965-4_1.

[45] H.A. Baloch, S. Nizamuddin, M.T.H. Siddiqui, S. Riaz, A.S. Jatoi, D.K. Dumbre, N.M. Mubarak, M.P. Srinivasan, G.J. Griffin, Recent advances in production and upgrading of bio-oil from biomass: A critical overview, J. Environ. Chem. Eng. 6 (2018) 5101–5118. doi:10.1016/j.jece.2018.07.050.

[46] C.U. Jensen, J.K. Rodriguez Guerrero, S. Karatzos, G. Olofsson, S.B. Iversen, Fundamentals of Hydrofaction™: Renewable crude oil from woody biomass, Biomass Convers. Biorefinery. 7 (2017) 495–509. doi:10.1007/s13399-017-0248-8.

[47] IEA Bioenergy, Facilities, (2020). https://www.ieabioenergy.com/installations/ (accessed May 28, 2020).

[48] Silva Green Fuel., Statkraft. (2019). https://www.statkraft.com/about-statkraft/Projects/norway/value-creation-tofte/silva-green-fuel/ (accessed October 22, 2019).

[49] D.C. Elliott, A. Oasmaa, D. Meier, F. Preto, A. V. Bridgwater, Results of the IEA round robin on viscosity and aging of fast pyrolysis bio-oils: Long-Term tests and repeatability, Energy and Fuels. 26 (2012) 7362–7366. doi:10.1021/ef301607v.

[50] B.H.Y. Ong, T.G. Walmsley, M.J. Atkins, M.R.W. Walmsley, Hydrothermal liquefaction of Radiata Pine with Kraft black liquor for integrated biofuel production, J. Clean. Prod. 199 (2018) 737–750. doi:10.1016/j.jclepro.2018.07.218.

[51] J.M. Jarvis, K.O. Albrecht, J.M. Billing, A.J. Schmidt, R.T. Hallen, T.M. Schaub, Assessment of hydrotreatment for hydrothermal liquefaction biocrudes from sewage sludge, microalgae, and pine feedstocks, Energy and Fuels. 32 (2018) 8483–8493. doi:10.1021/acs.energyfuels.8b01445.

[52] T. Belkheiri, S.I. Andersson, C. Mattsson, L. Olausson, H. Theliander, L. Vamling, Hydrothermal liquefaction of kraft lignin in sub-critical water: the influence of the sodium and potassium fraction, Biomass Convers.

Biorefinery. 8 (2018) 585–595. doi:10.1007/s13399-018-0307-9.

[53] K. Anastasakis, P. Biller, R.B. Madsen, M. Glasius, I. Johannsen, Continuous hydrothermal liquefaction of biomass in a novel pilot plant with heat recovery and hydraulic oscillation, Energies. 11 (2018) 1–23. doi:10.3390/en11102695.

[54] A.R.K. Gollakota, N. Kishore, S. Gu, A review on hydrothermal liquefaction of biomass, Renew. Sustain. Energy Rev. 81 (2018) 1378–1392. doi:10.1016/j.rser.2017.05.178.

[55] R. Fahmi, A. V. Bridgwater, I. Donnison, N. Yates, J.M. Jones, The effect of lignin and inorganic species in biomass on pyrolysis oil yields, quality and stability, Fuel. 87 (2008) 1230–1240. doi:10.1016/j.fuel.2007.07.026.

[56] G. Haarlemmer, C. Guizani, S. Anouti, M. Déniel, A. Roubaud, S. Valin, Analysis and comparison of bio-oils obtained by hydrothermal liquefaction and fast pyrolysis of beech wood, Fuel. 174 (2016) 180–188. doi:10.1016/j.fuel.2016.01.082.

[57] M. Déniel, G. Haarlemmer, A. Roubaud, E. Weiss-Hortala, J. Fages, Optimisation of bio-oil production by hydrothermal liquefaction of agro-industrial residues: Blackcurrant pomace (Ribes nigrum L.) as an example, Biomass and Bioenergy. 95 (2016) 273–285. doi:10.1016/j.biombioe.2016.10.012.

[58] J.G. Speight, Classification, in: Chem. Technol. Pet., 5th ed., CRC Press, Boca Raton, FL, 2014: pp. 31–44. doi:10.1201/9781420008388.

[59] J.G. Speight, Instability and Incompatibility, in: Chem. Technol. Pet., 5th ed., CRC Press, Boca Raton, FL, 2014: pp. 371–387. doi:10.1201/9781420008388.

[60] Y. Long, T. Dabros, H. Hamza, Selective solvent deashphalting for heavy oil emultion treatment, in: O.C. Mullins, E.Y. SheU, A. Hammami, A.G. Marshall (Eds.), Asph. Heavy Oils, Pet., 1st ed., Springer Science+Business Media, LLC, New York, 2007: pp. 511–545.

[61] Shell, Jet A-1 safety data sheet, Shell Prod. Cat. (2018). https://www.epc.shell.com/ (accessed June 3, 2020).

[62] Shell, Diesel 10 ppm, Shell Prod. Cat. (2017). https://www.epc.shell.com/ (accessed June 3, 2020).

[63] ISO 8217:2017, Petroleum products — Fuels (class F) — Specifications of marine fuels, (2017).

[64] C.U. Jensen, J. Hoffmann, L.A. Rosendahl, Co-processing potential of HTL bio-crude at petroleum refineries. Part 2: A parametric hydrotreating study, Fuel. 165 (2016) 536–543. doi:10.1016/j.fuel.2015.08.047.

[65] I.M. Sintamarean, I.F. Grigoras, C.U. Jensen, S.S. Toor, T.H. Pedersen, L.A. Rosendahl, Two-stage alkaline hydrothermal liquefaction of wood to biocrude in a continuous bench-scale system, Biomass Convers. Biorefinery. 7 (2017) 425–435. doi:10.1007/s13399-017-0247-9.

[66] J. Kosinkova, J.A. Ramirez, Z.D. Ristovski, R. Brown, T.J. Rainey, Physical and chemical stability of bagasse biocrude from liquefaction stored in real conditions, Energy and Fuels. 30 (2016) 10499–10504. doi:10.1021/acs.energyfuels.6b02115.

[67] D.C. Elliott, D. Meier, A. Oasmaa, B. Van De Beld, A. V. Bridgwater, M. Marklund, Results of the international energy agency round robin on fast pyrolysis bio-oil production, Energy and Fuels. 31 (2017) 5111–5119. doi:10.1021/acs.energyfuels.6b03502.

[68] J.A. Ramirez, R.J. Brown, T.J. Rainey, Liquefaction biocrudes and their petroleum crude blends for processing in conventional distillation units, Fuel Process. Technol. 167 (2017) 674–683. doi:10.1016/j.fuproc.2017.08.022.

[69] T.D.H. Nguyen, M. Maschietti, L.E. Åmand, L. Vamling, L. Olausson, S.I. Andersson, H. Theliander, The effect of temperature on the catalytic conversion of Kraft lignin using near-critical water, Bioresour. Technol. 170 (2014) 196–203. doi:10.1016/j.biortech.2014.06.051.

[70] P. Ghorbannezhad, F. Kool, H. Rudi, S. Ceylan, Sustainable production of value-added products from fast pyrolysis of palm shell residue in tandem micro-reactor and pilot plant, Renew. Energy. 145 (2020) 663–670. doi:10.1016/j.renene.2019.06.063.

[71] T.H. Pedersen, I.F. Grigoras, J. Hoffmann, S.S. Toor, I.M. Daraban, C.U. Jensen, S.B. Iversen, R.B. Madsen, M. Glasius, K.R. Arturi, R.P. Nielsen, E.G. Søgaard, L.A. Rosendahl, Continuous hydrothermal co-liquefaction of aspen wood and glycerol with water phase recirculation, Appl. Energy. 162 (2016) 1034–1041. doi:10.1016/j.apenergy.2015.10.165.

[72] B. Gómez-Monedero, F. Bimbela, J. Arauzo, J. Faria, M.P. Ruiz, Pyrolysis of red eucalyptus, camelina straw, and wheat straw in an ablative reactor, Energy

and Fuels. 29 (2015) 1766–1775. doi:10.1021/ef5026054.

[73] H. Hernando, S. Jiménez-Sánchez, J. Fermoso, P. Pizarro, J.M. Coronado, D.P. Serrano, Assessing biomass catalytic pyrolysis in terms of deoxygenation pathways and energy yields for the efficient production of advanced biofuels, Catal. Sci. Technol. 6 (2016) 2829–2843. doi:10.1039/c6cy00522e.

[74] H.A. Baloch, S. Nizamuddin, M.T.H. Siddiqui, N.M. Mubarak, D.K. Dumbre, M.P. Srinivasan, G.J. Griffin, Sub-supercritical liquefaction of sugarcane bagasse for production of bio-oil and char: Effect of two solvents, J. Environ. Chem. Eng. 6 (2018) 6589–6601. doi:10.1016/j.jece.2018.10.017.

[75] J.G. Speight, Chemical Composition, in: Chem. Technol. Pet., 5th ed., CRC Press, Boca Raton, FL, 2014.

[76] A. Oasmaa, B. Van De Beld, P. Saari, D.C. Elliott, Y. Solantausta, Norms, standards, and legislation for fast pyrolysis bio-oils from lignocellulosic biomass, Energy and Fuels. 29 (2015) 2471–2484. doi:10.1021/acs.energyfuels.5b00026.

[77] J. Hoffmann, C.U. Jensen, L.A. Rosendahl, Co-processing potential of HTL bio-crude at petroleum refineries – Part 1: Fractional distillation and characterization, Fuel. 165 (2016) 526–535. doi:10.1016/j.fuel.2015.10.094.

[78] D. Castello, M.S. Haider, L.A. Rosendahl, Catalytic upgrading of hydrothermal liquefaction biocrudes: Different challenges for different feedstocks, Renew. Energy. 141 (2019) 420–430. doi:10.1016/j.renene.2019.04.003.

[79] E.J. Leijenhorst, W. Wolters, L. Van De Beld, W. Prins, Inorganic element transfer from biomass to fast pyrolysis oil: Review and experiments, Fuel Process. Technol. 149 (2016) 96–111. doi:10.1016/j.fuproc.2016.03.026.

[80] D.C. Elliott, A. Oasmaa, F. Preto, D. Meier, A. V. Bridgwater, Results of the IEA round robin on viscosity and stability of fast pyrolysis bio-oils, Energy and Fuels. 26 (2012) 3769–3776. doi:10.1021/ef300384t.

[81] S. Eijsbouts, A.A. Battiston, G.C. van Leerdam, Life cycle of hydroprocessing catalysts and total catalyst management, Catal. Today. 130 (2008) 361–373. doi:10.1016/j.cattod.2007.10.112.

[82] J.M. Jarvis, J.M. Billing, R.T. Hallen, A.J. Schmidt, T.M. Schaub, Hydrothermal liquefaction biocrude compositions compared to petroleum

crude and shale oil, Energy and Fuels. 31 (2017) 2896–2906. doi:10.1021/acs.energyfuels.6b03022.

[83] R.B. Madsen, R.Z.K. Bernberg, P. Biller, J. Becker, B.B. Iversen, M. Glasius, Hydrothermal co-liquefaction of biomasses – quantitative analysis of bio-crude and aqueous phase composition, Sustain. Energy Fuels. 1 (2017) 789–805. doi:10.1039/C7SE00104E.

[84] E.D. Christensen, G.M. Chupka, J. Luecke, T. Smurthwaite, T.L. Alleman, K. Iisa, J.A. Franz, D.C. Elliott, R.L. McCormick, Analysis of oxygenated compounds in hydrotreated biomass fast pyrolysis oil distillate fractions, Energy and Fuels. 25 (2011) 5462–5471. doi:10.1021/ef201357h.

[85] J.G. Speight, Chapter 1 - Naphthenic Acids in Petroleum, in: J.G. Speight (Ed.), High Acid Crudes, Gulf Professional Publishing, Boston, 2014: pp. 1–29. doi:https://doi.org/10.1016/B978-0-12-800630-6.00001-0.

[86] A.E. Harman-Ware, J.R. Ferrell, Methods and challenges in the determination of molecular weight metrics of bio-oils, Energy and Fuels. 32 (2018) 8905–8920. doi:10.1021/acs.energyfuels.8b02113.

[87] H. Hwang, J.H. Lee, I.G. Choi, J.W. Choi, Comprehensive characterization of hydrothermal liquefaction products obtained from woody biomass under various alkali catalyst concentrations, Environ. Technol. (United Kingdom). 40 (2019) 1657–1667. doi:10.1080/09593330.2018.1427799.

[88] S. Bjelić, J. Yu, B.B. Iversen, M. Glasius, P. Biller, Detailed investigation into the asphaltene fraction of hydrothermal liquefaction derived bio-crude and hydrotreated bio-crudes, Energy and Fuels. 32 (2018) 3579–3587. doi:10.1021/acs.energyfuels.7b04119.

[89] F. Stankovikj, A.G. McDonald, G.L. Helms, M. Garcia-Perez, Quantification of bio-oil functional groups and evidences of the presence of pyrolytic humins, Energy and Fuels. 30 (2016) 6505–6524. doi:10.1021/acs.energyfuels.6b01242.

[90] H.N. Lyckeskog, C. Mattsson, L. Olausson, S.I. Andersson, L. Vamling, H. Theliander, Thermal stability of low and high Mw fractions of bio-oil derived from lignin conversion in subcritical water, Biomass Convers. Biorefinery. 7 (2017) 401–414. doi:10.1007/s13399-016-0228-4.

[91] X.F. Wu, Q. Zhou, M.F. Li, S.X. Li, J. Bian, F. Peng, Conversion of poplar into bio-oil via subcritical hydrothermal liquefaction: Structure and antioxidant capacity, Bioresour. Technol. 270 (2018) 216–222.

doi:10.1016/j.biortech.2018.09.032.

[92] R.A. Larson, B.K. Sharma, K.A. Marley, B. Kunwar, D. Murali, J. Scott, Potential antioxidants for biodiesel from a softwood lignin pyrolyzate, Ind. Crops Prod. 109 (2017) 476–482. doi:10.1016/j.indcrop.2017.08.053.

[93] K. Jacobson, K.C. Maheria, A. Kumar Dalai, Bio-oil valorization: A review, Renew. Sustain. Energy Rev. 23 (2013) 91–106. doi:10.1016/j.rser.2013.02.036.

[94] S. Conrad, C. Blajin, T. Schulzke, G. Deerberg, Comparison of fast pyrolysis bio-oils from straw and miscanthus, Environ. Prog. Sustain. Energy. (2019) 1–8. doi:10.1002/ep.13287.

[95] G. Yildiz, F. Ronsse, R. Venderbosch, R. van Duren, S.R.A. Kersten, W. Prins, Effect of biomass ash in catalytic fast pyrolysis of pine wood, Appl. Catal. B Environ. 168–169 (2015) 203–211. doi:10.1016/j.apcatb.2014.12.044.

[96] N. Doassans-Carrère, J.H. Ferrasse, O. Boutin, G. Mauviel, J. Lédé, Comparative study of biomass fast pyrolysis and direct liquefaction for bio-oils production: Products yield and characterizations, Energy and Fuels. 28 (2014) 5103–5111. doi:10.1021/ef500641c.

[97] R. Azargohar, K.L. Jacobson, E.E. Powell, A.K. Dalai, Evaluation of properties of fast pyrolysis products obtained, from Canadian waste biomass, J. Anal. Appl. Pyrolysis. 104 (2013) 330–340. doi:10.1016/j.jaap.2013.06.016.

[98] A. Undri, M. Abou-Zaid, C. Briens, F. Berruti, L. Rosi, M. Bartoli, M. Frediani, P. Frediani, A simple procedure for chromatographic analysis of bio-oils from pyrolysis, J. Anal. Appl. Pyrolysis. 114 (2015) 208–221. doi:10.1016/j.jaap.2015.05.019.

[99] Y. Feng, D. Meier, Extraction of value-added chemicals from pyrolysis liquids with supercritical carbon dioxide, J. Anal. Appl. Pyrolysis. 113 (2015) 174–185. doi:10.1016/j.jaap.2014.12.009.

[100] M.H. Mohamad, R. Awang, W.Z.W. Yunus, A Review of acetol: Application and production, Am. J. Appl. Sci. 8 (2011) 1135–1139. doi:10.3844/ajassp.2011.1135.1139.

[101] L. Chen, J. Zhao, S. Pradhan, B.E. Brinson, G.E. Scuseria, Z.C. Zhang, M.S. Wong, Ring-locking enables selective anhydrosugar synthesis from

carbohydrate pyrolysis, Green Chem. 18 (2016) 5438–5447. doi:10.1039/c6gc01600f.

[102] C.J. Longley, D.P.C. Fung, Potential Applications and Markets for Biomass-Derived Levoglucosan, in: Adv. Thermochem. Biomass Convers., Springer Netherlands, Dordrecht, 1993: pp. 1484–1494. doi:10.1007/978-94-011-1336-6_120.

[103] T.H. Pedersen, C.U. Jensen, L. Sandström, L.A. Rosendahl, Full characterization of compounds obtained from fractional distillation and upgrading of a HTL biocrude, Appl. Energy. 202 (2017) 408–419. doi:10.1016/j.apenergy.2017.05.167.

[104] B. Maddi, S. Viamajala, S. Varanasi, Comparative study of pyrolysis of algal biomass from natural lake blooms with lignocellulosic biomass, Bioresour. Technol. 102 (2011) 11018–11026. doi:10.1016/j.biortech.2011.09.055.

[105] A. Aqsha, M.M. Tijani, B. Moghtaderi, N. Mahinpey, Catalytic pyrolysis of straw biomasses (wheat, flax, oat and barley) and the comparison of their product yields, J. Anal. Appl. Pyrolysis. 125 (2017) 201–208. doi:10.1016/j.jaap.2017.03.022.

[106] Z. Zhu, L. Rosendahl, S.S. Toor, D. Yu, G. Chen, Hydrothermal liquefaction of barley straw to bio-crude oil: Effects of reaction temperature and aqueous phase recirculation, Appl. Energy. 137 (2015) 183–192. doi:10.1016/j.apenergy.2014.10.005.

[107] H. Nguyen Lyckeskog, C. Mattsson, L.E. Åmand, L. Olausson, S.I. Andersson, L. Vamling, H. Theliander, Storage stability of bio-oils derived from the catalytic conversion of softwood Kraft lignin in subcritical water, Energy and Fuels. 30 (2016) 3097–3106. doi:10.1021/acs.energyfuels.6b00087.

[108] T.D.H. Nguyen, M. Maschietti, T. Belkheiri, L.E. Åmand, H. Theliander, L. Vamling, L. Olausson, S.I. Andersson, Catalytic depolymerisation and conversion of Kraft lignin into liquid products using near-critical water, J. Supercrit. Fluids. 86 (2014) 67–75. doi:10.1016/j.supflu.2013.11.022.

[109] P.M. Mortensen, J.D. Grunwaldt, P.A. Jensen, K.G. Knudsen, A.D. Jensen, A review of catalytic upgrading of bio-oil to engine fuels, Appl. Catal. A Gen. 407 (2011) 1–19. doi:10.1016/j.apcata.2011.08.046.

[110] G. Brunner, Supercritical fluids: Technology and application to food processing, J. Food Eng. 67 (2005) 21–33.

doi:10.1016/j.jfoodeng.2004.05.060.

[111] L.W. Lake, R. Johns, B. Rossen, G. Pope, Fundamentals of enhanced oil recovery, 1st ed., Society of Petroleum Engineers, 2014.

[112] E.W. Lemmon, M.O. McLinden, D.G. Friend, Thermophysical Properties of Fluid Systems, in: P.J. Linstrom, W.G. Mallard (Eds.), NIST Chem. WebBook, NIST Stand. Ref. Database Number 69, National Institute of Standards and Technology, Gaithersburg MD, 20899. doi:https://doi.org/10.18434/T4D303.

[113] E. Reverchon, M. Poletto, L. Sesti Osséo, M. Somma, Hexane elimination from soybean oil by continuous packed tower processing with supercritical CO2, JAOCS, J. Am. Oil Chem. Soc. 77 (2000) 9–14. doi:10.1007/s11746-000-0002-z.

[114] P. Persson, S. Larsson, L.J. Jönsson, N.O. Nilvebrant, B. Sivik, F. Munteanu, L. Thörneby, L. Gorton, Supercritical fluid extraction of a lignocellulosic hydrolysate of spruce for detoxification and to facilitate analysis of inhibitors, Biotechnol. Bioeng. 79 (2002) 694–700. doi:10.1002/bit.10324.

[115] S.M. Bhatt, Shilpa, Lignocellulosic feedstock conversion, inhibitor detoxification and cellulosic hydrolysis - A review, Biofuels. 5 (2014) 633–649. doi:10.1080/17597269.2014.1003702.

[116] L.J. Jönsson, B. Alriksson, N.O. Nilvebrant, New Biotechnologies for Increased Energy Security, in: J.C. Serrano-Ruiz (Ed.), New Biotechnol. Increased Energy Secur., Apple Academic Press, Oakville, ON, 2015: pp. 41–64. doi:10.1201/b18537.

[117] P. Zacchi, S.C. Bastida, P. Jaeger, M.J. Cocero, R. Eggers, Countercurrent de-acidification of vegetable oils using supercritical $CO_2$: Holdup and RTD experiments, J. Supercrit. Fluids. 45 (2008) 238–244. doi:10.1016/j.supflu.2008.02.005.

[118] N.T. Dunford, J.A. Teel, J.W. King, A continuous countercurrent supercritical fluid deacidification process for phytosterol ester fortification in rice bran oil, Food Res. Int. 36 (2003) 175–181. doi:10.1016/S0963-9969(02)00134-5.

[119] L. Vázquez, A.M. Hurtado-Benavides, G. Reglero, T. Fornari, E. Ibáñez, F.J. Señoráns, Deacidification of olive oil by countercurrent supercritical carbon dioxide extraction: Experimental and thermodynamic modeling, J. Food Eng. 90 (2009) 463–470. doi:10.1016/j.jfoodeng.2008.07.012.

[120] S.A. Hong, J. Kim, J.D. Kim, J.W. Kang, Y.W. Lee, Purification of waste cooking oils via supercritical carbon dioxide extraction, Sep. Sci. Technol. 45 (2010) 1139–1146. doi:10.1080/01496391003688480.

[121] W. Maqbool, P. Hobson, K. Dunn, W. Doherty, Supercritical carbon dioxide separation of carboxylic scids and phenolics from bio-oil of lignocellulosic origin: Understanding bio-oil compositions, compound solubilities, and their fractionation, Ind. Eng. Chem. Res. 56 (2017) 3129–3144. doi:10.1021/acs.iecr.6b04111.

[122] Y.H. Chan, S.K. Loh, B.L. Fui Chin, C.L. Yiin, B.S. How, K.W. Cheah, M.K. Wong, A.C. Minh Loy, Y.L. Gwee, S.L. Yuen Lo, S. Yusup, S.S. Lam, Fractionation and extraction of bio-oil for production of greener fuel and value-added chemicals: Recent advances and future prospects, Chem. Eng. J. 397 (2020) 125406. doi:10.1016/j.cej.2020.125406.

[123] B.P. Mudraboyina, D. Fu, P.G. Jessop, Supercritical fluid rectification of lignin microwave-pyrolysis oil, Green Chem. 17 (2015) 169–172. doi:10.1039/c4gc01433b.

[124] T. Cheng, Y. Han, Y. Zhang, C. Xu, Molecular composition of oxygenated compounds in fast pyrolysis bio-oil and its supercritical fluid extracts, Fuel. 172 (2016) 49–57. doi:10.1016/j.fuel.2015.12.075.

[125] Y.H. Chan, S. Yusup, A.T. Quitain, Y.H. Chai, Y. Uemura, S.K. Loh, Extraction of palm kernel shell derived pyrolysis oil by supercritical carbon dioxide: Evaluation and modeling of phenol solubility, Biomass and Bioenergy. 116 (2018) 106–112. doi:10.1016/j.biombioe.2018.06.009.

[126] Y.H. Chan, S. Yusup, A.T. Quitain, Y. Uemura, S.K. Loh, Fractionation of pyrolysis oil via supercritical carbon dioxide extraction: Optimization study using response surface methodology (RSM), Biomass and Bioenergy. 107 (2017) 155–163. doi:10.1016/j.biombioe.2017.10.005.

[127] Y. Feng, D. Meier, Comparison of supercritical $CO_2$, liquid $CO_2$, and solvent extraction of chemicals from a commercial slow pyrolysis liquid of beech wood, Biomass and Bioenergy. 85 (2016) 346–354. doi:10.1016/j.biombioe.2015.12.027.

[128] J. Wang, H. Cui, S. Wei, S. Zhuo, L. Wang, Z. Li, W. Yi, Separation of biomass pyrolysis oil by supercritical $CO_2$ extraction, Smart Grid Renew. Energy. 01 (2010) 98–107. doi:10.4236/sgre.2010.12015.

[129] C.U. Jensen, PIUS – Hydrofaction$^{TM}$ Platform with Integrated Upgrading

Step, PhD Thesis, Aalborg University, 2018.

[130] ASTM International., ASTM D664-17a, Standard test method for Acid Number of petroleum products by potentiometric titration, West Conshohocken, PA, 2017, (n.d.). doi:10.1520/D0664-17A.

[131] E. Christensen, J. Ferrell, M. V Olarte, A.B. Padmaperuma, T. Lemmon, Acid number determination of pyrolysis bio-oils using potentiometric titration laboratory analytical procedure (LAP), Golden, CO, USA, 2016. doi:10.2172/1241091.

[132] R. Rowell, R. Pettersen, M. Tshabalala, Cell Wall Chemistry, in: R.M. Rowell (Ed.), Handb. Wood Chem. Wood Compos. Second Ed., Second, CRC Press, 2012: pp. 33–72. doi:10.1201/b12487-5.

[133] U.S. Energy Information Administration (EIA), Crude Oil Input Qualities, (2020). https://www.eia.gov/dnav/pet/PET_PNP_CRQ_A_EPC0_YCS_PCT_M.htm (accessed April 30, 2020).

[134] A. Carpy, N. Marchand-Geneste, Molecular characterization of retene derivatives obtained by thermal treatment of abietane skeleton diterpenoids, J. Mol. Struct. THEOCHEM. 635 (2003) 45–53. doi:10.1016/S0166-1280(03)00400-7.

[135] C.U. Jensen, L.A. Rosendahl, G. Olofsson, Impact of nitrogenous alkaline agent on continuous HTL of lignocellulosic biomass and biocrude upgrading, Fuel Process. Technol. 159 (2017) 376–385. doi:10.1016/j.fuproc.2016.12.022.

[136] R.B. Madsen, H. Zhang, P. Biller, A.H. Goldstein, M. Glasius, Characterizing Semivolatile Organic Compounds of Biocrude from Hydrothermal Liquefaction of Biomass, Energy and Fuels. 31 (2017) 4122–4134. doi:10.1021/acs.energyfuels.7b00160.

[137] L.J. Standley, B.R.T. Simoneit, Resin diterpenoids as tracers for biomass combustion aerosols, J. Atmos. Chem. 18 (1994) 1–15. doi:10.1007/BF00694371.

[138] M.E. Baumgardner, T.L. Vaughn, A. Lakshminarayanan, D. Olsen, M.A. Ratcliff, R.L. McCormick, A.J. Marchese, Combustion of Lignocellulosic Biomass Based Oxygenated Components in a Compression Ignition Engine, Energy and Fuels. 29 (2015) 7317–7326. doi:10.1021/acs.energyfuels.5b01595.

[139] R.L. McCormick, M.A. Ratcliff, E. Christensen, L. Fouts, J. Luecke, G.M. Chupka, J. Yanowitz, M. Tian, M. Boot, Properties of oxygenates found in upgraded biomass pyrolysis oil as components of spark and compression ignition engine fuels, Energy and Fuels. 29 (2015) 2453–2461. doi:10.1021/ef502893g.

[140] M.A. McHugh, V.J. Krukonis, Phase Diagrams for Supercritical Fluid–Solute Mixtures, in: H. Brenner (Ed.), Supercrit. Fluid Extr., 2nd ed., Elsevier, 1994: pp. 27–84. doi:10.1016/B978-0-08-051817-6.50006-0.

[141] J.A. Capunitan, S.C. Capareda, Characterization and separation of corn stover bio-oil by fractional distillation, Fuel. 112 (2013) 60–73. doi:10.1016/j.fuel.2013.04.079.

[142] X. Pan, J.F. Kadla, K. Ehara, N. Gilkes, J.N. Saddler, Organosolv ethanol lignin from hybrid poplar as a radical scavenger: Relationship between lignin structure, extraction conditions, and antioxidant activity, J. Agric. Food Chem. 54 (2006) 5806–5813. doi:10.1021/jf0605392.

[143] S.R. Chandrasekaran, D. Murali, K.A. Marley, R.A. Larson, K.M. Doll, B.R. Moser, J. Scott, B.K. Sharma, Antioxidants from slow pyrolysis bio-oil of birch wood: Application for biodiesel and biobased lubricants, ACS Sustain. Chem. Eng. 4 (2016) 1414–1421. doi:10.1021/acssuschemeng.5b01302.

[144] D.C. Elliott, G.G. Neuenschwander, T.R. Hart, Hydroprocessing bio-oil and products separation for coke production, ACS Sustain. Chem. Eng. 1 (2013) 389–392. doi:10.1021/sc300103y.

[145] D.S.J. Jones, S.A. Treese, Petroleum Products and a Refinery Configuration, in: Handb. Pet. Process., Springer International Publishing, Cham, 2015: pp. 53–124. doi:10.1007/978-3-319-14529-7_10.

[146] Y. Elkasabi, C.A. Mullen, A.A. Boateng, A. Brown, M.T. Timko, Flash Distillation of Bio-Oils for Simultaneous Production of Hydrocarbons and Green Coke, Ind. Eng. Chem. Res. 58 (2019) 1794–1802. doi:10.1021/acs.iecr.8b04556.

[147] Y. Elkasabi, H. Darmstadt, A.A. Boateng, Renewable Biomass-Derived Coke with Texture Suitable for Aluminum Smelting Anodes, ACS Sustain. Chem. Eng. 6 (2018) 13324–13331. doi:10.1021/acssuschemeng.8b02963.

[148] Y. Elkasabi, A.A. Boateng, M.A. Jackson, Upgrading of bio-oil distillation bottoms into biorenewable calcined coke, Biomass and Bioenergy. 81 (2015) 415–423. doi:10.1016/j.biombioe.2015.07.028.

# II. PUBLICATIONS

# Paper A

## Supercritical carbon dioxide fractionation of bio-crude produced by hydrothermal liquefaction of pinewood

Nikolaos Montesantos, Thomas Helmer Pedersen, Rudi Pankratz Nielsen, Lasse Rosendahl, Marco Maschietti

The manuscript has been published in the

*Journal of Supercritical Fluids*, Volume 149, Pages 97-109, 2019

J. of Supercritical Fluids 149 (2019) 97–109

Contents lists available at ScienceDirect

The Journal of Supercritical Fluids

journal homepage: www.elsevier.com/locate/supflu

# Supercritical carbon dioxide fractionation of bio-crude produced by hydrothermal liquefaction of pinewood

Nikolaos Montesantos[a], Thomas Helmer Pedersen[b], Rudi Pankratz Nielsen[a], Lasse Rosendahl[b], Marco Maschietti[a,*]

[a] Department of Chemistry and Bioscience, Aalborg University, Niels Bohrs Vej 8A, 6700, Esbjerg, Denmark
[b] Department of Energy Technology, Aalborg University, Pontoppidanstræde 111, 9220, Aalborg Øst, Denmark

## HIGHLIGHTS

- Extractions of lignocellulosic bio-crude were carried out up to 120 °C and 400 bar.
- The process operability and efficiency drastically increases with temperature.
- Extraction yields up to 42% were achieved.
- Density and TAN reduction in the extracts was 10% and 40% respectively.
- Ketones, 1-ring phenols and light fatty acids were preferentially extracted.

## GRAPHICAL ABSTRACT

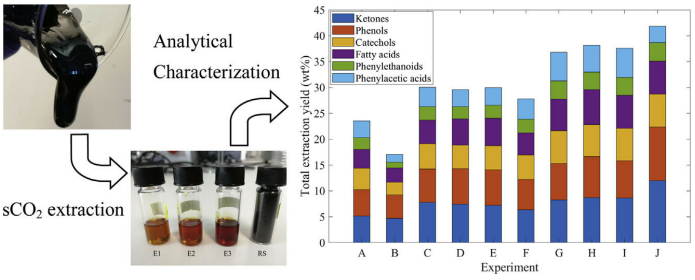


## ARTICLE INFO

*Article history:*
Received 11 December 2018
Received in revised form 3 April 2019
Accepted 4 April 2019
Available online 4 April 2019

*Keywords:*
Supercritical $CO_2$ extraction
Lignocellulosic
Bio-oil
Bio-crude valorization
Bio-crude upgrading

## ABSTRACT

The supercritical carbon dioxide extraction of bio-crude, produced by hydrothermal liquefaction of lignocellulosic biomass, was investigated for pressures and temperatures in the range 112–400 bar and 40–120 °C, corresponding to solvent densities in the range 548–882 kg/m$^3$. Total extraction yields ranged from 17 to 42%. For a given solvent density, temperature increase drastically improved both the process operability and efficiency. The extracts showed reduced density as well as 40% reduction of total acid number compared to the feed. The residue resulted to be partially deoxygenated. Ketones, 1-ring phenols and low molecular weight fatty acids were concentrated in the extract, with recoveries up to 80%, with ketones and phenols exhibiting the highest distribution factors. Observed selectivities suggest the feasibility of downstream separation of the key classes of extractives using supercritical carbon dioxide as a solvent.



## 1. Introduction

The diminishing availability of easily recoverable petroleum, together with the increasing environmental awareness and impulse to reduce utilization of fossil resources for fuel and commodity chemicals, has led to an increased research effort to find sustainable alternatives. One of the major candidates is advanced intermediate bio-fuels, namely bio-crudes or bio-oils, produced from so-called second-generation biomass, which encompasses low-cost material that is not competing with food production. Such examples are wood and crop residues, excess lignin from pulp mills, manure, sewage sludge, organic wastes [1–10]. Ther-

* Corresponding author.
*E-mail address:* marco@bio.aau.dk (M. Maschietti).

https://doi.org/10.1016/j.supflu.2019.04.001
0896-8446/

mochemical processes, such as hydrothermal liquefaction (HTL) and pyrolysis, have proven their ability to produce bio-crude from second-generation biomass in good yield [11,12]. In particular, HTL is a very versatile process, with the possibility of processing both dry and wet feedstock. Moreover, in comparison to pyrolysis, HTL produces more stable bio-crudes with lower water and oxygen content and higher heating values [13].

In the context of fuel production, and compared to fossil counterparts, HTL bio-crudes exhibit high heteroatom content, acidity, molecular weight and sometimes density [1,14]. For example, oxygen mass fractions have been reported for HTL bio-crudes in the range of 0.10–0.27 [14–17], total acid numbers in the range of 50–130 mg KOH/g [14–18] (measured by different methods; i.e. potentiometric, colorimetric, FTIR) and density above 1000 kg/m$^3$ [14]. The relatively high oxygen content necessitates significant hydrotreatment to upgrade the bio-crude to fuel grade and render it miscible with mineral oils. However, the heavier fraction of the bio-crude is expected to be difficult to hydrotreat [19]. Furthermore, cost intensive issues of the process, such as corrosion due to acidity and catalyst deactivation due to coking reactions of some of the components (e.g. guaiacols) [11] are also to be expected. Therefore, an effective separation process before hydrotreatment can be beneficial to produce a fraction with reduced acidity, molecular weight and oxygen content, which would lead to less problematic hydrotreatment. In contrast, the heavier residual fraction could be used as an activated carbon precursor (e.g. hydrochar) [20], or directed to robust refining processes (e.g. cracking) [17]. In addition, a separation process could serve to extract valuable chemicals from the high number of chemical species present in the bio-crude, such as phenols, fatty acids, ketones and alcohols [21].

Suitable separation technologies for the fractionation of HTL bio-crudes include distillation, liquid-liquid extraction (LLE), and supercritical fluid extraction (SFE). Distillation of heavy bio-crudes can be energy intensive requiring high temperatures even when operated in vacuum. For example, in order to reach a distillation yield of 53 wt% from a wood-derived HTL bio-crude, a final boiling temperature of 270 °C needed to be reached at a pressure of 0.1 torr (375 °C atmospheric pressure equivalent) [22]. LLE typically requires large amounts of organic solvents, which in majority originate from petroleum (e.g. pentane, dichloromethane) [23,24], can be toxic and require an additional process step for solvent recovery.

A possible alternative to distillation and LLE is represented by supercritical extraction using $CO_2$ as a solvent. The fractionation of bio-crudes with supercritical carbon dioxide ($sCO_2$) has recently attracted research attention, due to the possibility of carrying out an environmentally friendly separation process aimed at either upgrading the bio-crude or recovering valuable chemicals, with low operating temperatures and low operating cost [25]. In addition, $CO_2$ is co-produced in the HTL process and is available at elevated pressures and temperatures [2,12]; hence, the lack of need for an external supply can further motivate its usage.

Literature on $sCO_2$ fractionation of bio-crudes is scarce and the only available publications are on pyrolysis bio-oils with high water contents [26–35]. The operating conditions ranged between 40–80 °C and 100–300 bar, except for one publication where pressures in the range 300–400 bar were investigated [26]. Extraction yields varied around 30% with the exception of one case where a yield up to 71% was achieved due to the use of a substantial amount of methanol (25%) as co-solvent [30]. Extraction yields increased, as expected, with solvent density. Moreover, increasing temperature was observed to enhance the extraction efficiency, especially when increasing the pressure as well, due to the increase of solute solubility and improving mass transfer [27]. In general, the literature indicates that the extracts exhibit better properties in terms of lower water content, higher stability and higher heating values as compared with the feed bio-oil.

In a recent literature review, Maqbool et al. [25] highlighted that $sCO_2$ is selective towards low molecular weight, non-polar or slightly polar components, such as phenols, aldehydes and ketones, as opposed to strongly polar components such as acids, sugars and alcohols that remain in the residue. This is also in agreement with recent literature that was not included in the review. For example, phenol, which is often a major component in lignocellulosic bio-crudes, was found to be extracted preferentially and for all consecutive extracts [26,27,33]. $sCO_2$ extractions of pinewood pyrolysis oil showed selective separation of ketones, with their concentration progressively reduced in the extracts due to their depletion in the unextracted liquid phase [27]. Other important components that were preferentially extracted are guaiacols [20], esters and low molecular weight acids [28].

The aim of this work is to investigate the potential of $sCO_2$ extraction on a HTL bio-crude obtained from lignocellulosic biomass (pinewood). The study was carried out on a single-stage high-pressure extractor, analysing the effect of extraction temperature, pressure and solvent density over a wide range of operating conditions. The characterization of the feed and the extracts was carried out with the aim of highlighting the potential of improvement of fuel bulk properties (i.e. density, TAN, elemental composition), as well as the selective separation of the extracted chemical species in order to assess the feasibility of $sCO_2$ downstream separation for the production of chemicals.

## 2. Materials and methods

### 2.1. Materials

#### 2.1.1. Feed bio-crude

The bio-crude used in this work was produced by hydrothermal liquefaction (HTL) of pinewood in a continuous-flow unit, that is described elsewhere [2], located at Aalborg University. The pinewood was processed under supercritical water conditions (400 °C, 300 bar) in the presence of an alkali catalyst, feeding the reactor with a wood slurry (dry biomass content around 17–18% on mass basis) and with recycled aqueous phase and bio-crude produced by the reaction itself. Details on this mode of operation of the hydrothermal processing are provided elsewhere [36]. The HTL bio-crude was demineralized and dehydrated, according to the procedure reported by Jensen [37]. In brief, the procedure consists in diluting the bio-crude with methyl ethyl ketone (MEK), washing it with a citric acid aqueous solution and then removing both the solvent and water by evaporation under vacuum. The dehydrated and demineralized bio-crude used as feed in the $sCO_2$ extractions appears as a high-viscosity black liquid (Fig. 1) at ambient conditions.

#### 2.1.2. Chemicals

Carbon dioxide ($CO_2$, 99.8%) used for the extractions was purchased from AGA (Denmark). Tetrahydrofuran (THF, 99.9%), was purchased from VWR and used as solvent for the bio-crude. Diethyl ether (DEE, 99%), 4-bromophenol (99%) and pyridine (99%) were purchased from Merck and used as solvent, internal standard and derivatization agent, respectively, for the GC–MS analysis. Reagent Titrant 2 (VWR), KF solvent (VWR) and Aquastar 1% standard (Merck, water content: 10 g/kg ± 0.10 g/kg) were used for Karl Fischer (KF) titrations. Cystine 4G powder (Perkin Elmer) was used for elemental analysis calibration. 2-propanol (VWR, 99.8%), tetrabutyl-ammonium-hydroxide (TBAOH) 0.1 M in methanol (Sigma Aldrich), and tetraethyl ammonium bromide (TEABr) 0.4 M in ethyl glycol (Metrohm) were used for the Total Acid Number (TAN) titrations as solvent, titrant and electrode electrolyte solution, respectively. NIST traceable buffers pH 4, 7, 9 from

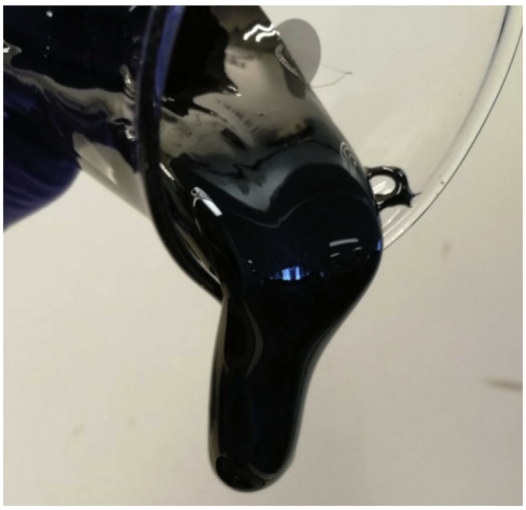

**Fig. 1.** Dehydrated and demineralized bio-crude (23 °C) used as feed in the $sCO_2$ extraction runs.

Reagecon were used for the calibration of the electrode whereas benzoic acid (99.5%) and phenol (99%) from Sigma Aldrich were used as standards for TAN. 2-pentanone (99%) and butanone (99%) from Merck, acetone (95%) from Cab Dan, as well as THF were used as solvents for the density measurements of the bio-crude.

### 2.2. Apparatus

Fig. 2 shows the diagram of the equipment used for the supercritical extractions. The apparatus consists of a heat exchanger (HE), a pneumatic pump (P1), an extractor vessel with a basket insert (E), temperature and pressure controls, and several valves, including a micrometering valve (V6) and an automatic pressure control valve (C1). $CO_2$ from a deep tube cylinder passes through a heat exchanger, which is connected to a cooling water supply that maintains a temperature between 1 °C and 5 °C and ensures that $CO_2$ is a subcooled liquid prior to entering the pump. The pump P1 (Maximator MSF72) is an air-driven pump with displacement volume of 1.5 $cm^3$ and maximum outlet pressure of 860 bar. The regulation of the pump outlet is attained by means of the air drive pressure, which can be varied in the range 1–10 bar. The extractor cylinder has a volume of 345 $cm^3$ with a basket insert of 178 $cm^3$ (i.d. 2.9 cm) and a length-to-diameter ratio of 9.3. The maximum operating pressure and temperature of the extractor are 500 bar and 200 °C, respectively. The extraction temperature is attained by a heating jacket and is controlled by a type-K (accuracy ±1.5 °C) thermocouple with the probe extended into the basket insert. The basket can be dismounted for charging the feed prior to an extraction and retrieving the residue after the end of the experiment. The top of the basket is equipped with a ring filter (porosity 10 μm) to prevent entrainment with the $CO_2$ flow. The bottom of the basket is equipped with a disk filter (porosity 10 μm) and a non-return valve to ensure that the feed cannot move downwards exiting the basket. The pressure gauges measure the pressure upstream the pump and the pressure of the extractor. V6 is used manually to regulate the flow rate of the extraction, whereas C1 acts automatically as a safety measure if the pressure in the extractor vessel exceeds a set value. In addition, V6 is heated by hot air (AH) to prevent clogging of the valve itself and the exit line, which may be caused by viscosity reduction and/or freezing of the extract due to the large temperature reduction induced by the depressurisation (Joule-Thomson effect). The extractor vessel is connected to a rupture disc (RD), which is activated at 550 bar (±5%). The $CO_2$ exits vessel E from the top and is led to a trapping system consisting of a series of four gas-washing bottles where the extracted components separate from the $CO_2$. The first three bottles are immersed in a cold bath maintained at around 5 °C to minimize off-gas losses due to evaporation. The extract is released in the first bottle in which a glass vial (the sampling vial) is inserted. The second bottle is meant to block fine droplet entrainment (if any) by being packed with approximately 3 g of cotton wool. The third bottle is filled with acidified water and it is meant to scrub the $CO_2$ flow from entrained components (if

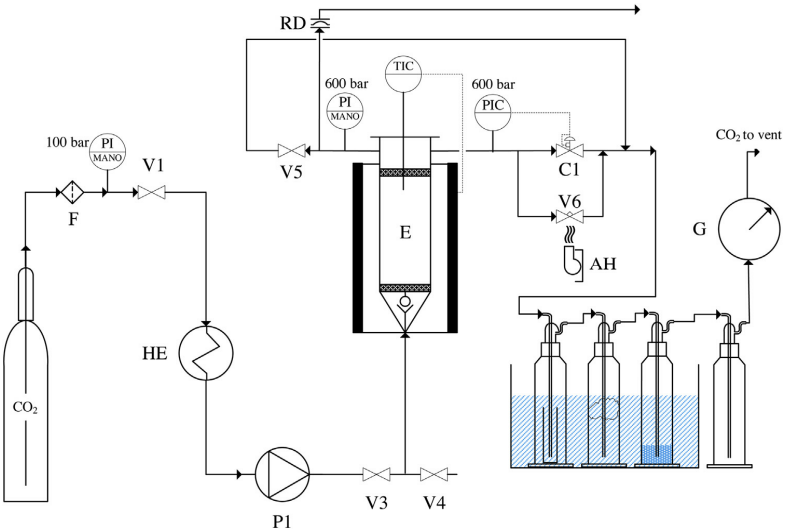


**Fig. 2.** Diagram of the supercritical extraction system. F: filter; HE: heat exchanger; P1: $CO_2$ pump; E: Extractor vessel; RD: Rupture disc; G: Gas meter, AH: Air heater; V1-V5: Shut off valves; V6: Micrometering valve; C1: Pneumatic valve.

any). The last bottle serves as a last measure to prevent contamination of the following drum-type gas meter (G), which is used to measure the $CO_2$ flow rate at ambient conditions. The gas meter (Ritter TG 3/5, max flow: 6 L/min; min flow: 0.1 L/min; accuracy 0.5% across full flow rate range) is equipped with a thermometer for the gas and it is packed with HCl 1% for accurate measurements of $CO_2$ flow [38]. The total length of the piping (i.d. 2.4 mm) for the whole system was estimated to 2200 mm. Out of this length, only 1380 mm are considered to contribute to a dead volume of 6.2 ml during normal operation.

### 2.3. Extraction

Before each extraction experiment the basket insert was packed with soda–lime glass beads (6 mm), up to a height of approximately 1/3 of the basket insert, and it was preheated to 60 °C in a heating cabinet. An amount of bio-crude feed was preheated in a beaker to 50 °C in order to reduce its viscosity and ensure dispersion between the glass beads. Approximately 50 g of the preheated feed were charged in the basket. After charging, the temperature of the extractor was set to the desired value of the extraction run. Once the operating temperature was reached, the pump was started in order to pressurize the vessel. When the desired extraction pressure was reached, the system was left static for 30 min and then the extraction began by opening the micrometering valve. The extraction pressure and the $CO_2$ flow rate were regulated by means of P1 and V6. The flow rate applied in the experiments was in the range 3.5–7.5 g/min. With the exception of sporadic clogging problems observed only at higher pressures, lower temperatures and higher extraction times, the $CO_2$ flow rate, as well as the extraction pressure and temperature, were stable. Average SD were 0.4 g/min, 3 bar, and 0.4 °C, respectively. The sampling vial was changed twice during the extraction, in order to collect three extract samples per each run. After the end of the extraction, the system was slowly depressurized. Subsequently, the basket was dismounted and washed with THF in order to collect the residue for mass balance closure. THF was used as the solvent of choice because the bio-crude feed appeared to be completely soluble in it for ratios above 1:1.

### 2.4. Analytical characterization

#### 2.4.1. Elemental analysis

A PerkinElmer 2400 Series II CHNS/O analyser coupled with a PerkinElmer AD-6 Autobalance was used to perform the elemental analysis (EA) of the bio-crude and its extract fractions. The instrument was set to measure carbon, hydrogen, nitrogen and sulphur, whereas oxygen was calculated by difference. Before each measurement, the cystine powder standard (mass fractions: C 0.2999; H 0.0503; N 0.1166; S 0.2669) was measured in triplicate to ensure accuracy and reproducibility. The average absolute deviation of the measurements on cystine with respect to the theoretical values was 0.0004, 0.0004, 0.0008, and 0.0230 for C, H, N, and S, respectively. Each sample was measured in triplicate as well.

#### 2.4.2. Water content

The water content of the bio-crude feed and the extracts was measured by means of Karl Fischer volumetric titration, utilizing a Metrohm 870KF Titrino Plus. The instrument was calibrated (single-point calibration) before each series of measurements using the Aquastar standard. The standard solution was also used to control the response stability in between measurements. With regard to the bio-crude feed, the sample preparation was inspired by a previous work [4]. A certain amount of bio-crude (approx. 0.3 g) was diluted in THF with a solvent to bio-crude mass ratio 20:1. Both the solution and pure THF were titrated in order to account for the water content of the THF. THF was consistently found to contain 0.5 g/kg water (SD 0 g/kg) and this value was taken into account when determining the water content of the bio-crude. Due to their low viscosity, the extracts did not require dilution in THF prior to the KF measurement. All KF measurements were performed at least in triplicates.

#### 2.4.3. TAN measurements

TAN of the bio-crude and its fractions was measured by potentiometric titration utilizing a Metrohm Titrando 888 equipped with a Metrohm Solvotrode (6.0229.010). The method applied in this work is based on a modification of ASTM D664 test method B [39], published by the National Renewable Energy Laboratory (NREL) [40], which was developed in a previous publication [41]. The modification mainly consists in the substitution of 0.1 M solution of KOH to 0.1 M solution of TBAOH as the titration agent. The results are reported as mg KOH per gram of oil, where the mass of KOH corresponds to the same equivalents of TBAOH used in the titration. The method demonstrates higher resolution of the titration curve by generating several endpoints, which can be referred to either carboxylic acids or phenolic components. Consequently, three acid numbers are reported in this work: the carboxylic acid number (CAN); the total acid number (TAN); and the phenolic acid number (PhAN), the latter being taken as the difference TAN-CAN.

A three point calibration (pH 4, 7, 9) was applied for the reading of the electrode, which resulted to the expected linearity ($R^2$ = 1) between pH and measured electric potential (u). In addition, control measurements were performed with two of the buffer solutions (pH 4 and 7) before each series of measurements, to ensure a correct response, as suggested by ASTM D664 test method B [39]. A determination of the range of electric potential corresponding to the neutralization of carboxylic acids and phenolics was carried out by using a standard solution containing benzoic acid and phenol. The titration showed a sharp inflection point at – 139 mV, and a subtle one at – 430 mV. The former represents benzoic acid while the latter represents phenol [40]. A number of titrations of the bio-crude feed generated the high inflection point at −150 mV and the low at −450 mV, which is in line to the standard solution. In addition, Christensen et al. [41] reports carboxylic acids and phenolics of pyrolysis oil generating inflection points at −100 and −420 mV, respectively, which is in fair agreement with the result in this work considering the differences in the feed material. All measurements were performed in triplicate, by diluting approx. 0.1 g of sample in 50 ml of 2-propanol and titrated with a solution of TBAOH in 2-propanol (0.1 M).

#### 2.4.4. Density

Density of the bio-crude was measured with an Anton Parr DMA 500 density meter and an Anton Parr DMA 35 Ex. Since the bio-crude is very viscous, it was diluted 1:1 by mass in four solvents (acetone, 2-pentanone, butanone, THF) prior to measurement. Both the density of the diluted samples and the density of the pure solvent were measured (single measurement for each sample, giving eight measurements in total). The density of the bio-crude was estimated assuming a linear relation between density and mass fraction of oil. According to this method, the density of the bio-crude resulted to be 1051 $kg/m^3 \pm 0.4$ $kg/m^3$. The density of the $sCO_2$ extracts was determined by weighing the mass of an accurately measured volume of sample. The weighing was carried out in triplicate on a precision balance (OHAUS PA224C). The volume of the sample was estimated using a positive displacement precision pipette (Gilson Microman M1000) fitted with a capillary piston. The volumetric response of the pipette, with the specific capillary piston, was calibrated by weighing the amount of distilled water supplied by the pipette and calculating the corresponding volume by using NIST [42] density values at the temperature of the labora-

**Table 1**
Operating conditions and experimental results of all extractions. Extraction temperature (T); extraction pressure (P); $CO_2$ density (ρ); average $CO_2$ flow rate (Q); mass of feed (F); mass of extract samples (E1, E2, E3); losses (L); solvent-to-feed ratio (S/F); yield (Y).

| Run | A | B | C | D | E | F | G | H | I | J |
|---|---|---|---|---|---|---|---|---|---|---|
| T (°C) | 40 | 40 | 60 | 60 | 60 | 80 | 80 | 80 | 120 | 120 |
| P (bar) | 112 | 183 | 183 | 290 | 385 | 183 | 255 | 400 | 275 | 400 |
| ρ (kg/m$^3$)[a] | 691 | 822 | 693 | 822 | 882 | 548 | 693 | 822 | 548 | 693 |
| Q (g/min) | 6.5 | 4.7 | 6.6 | 5.0 | 4.3 | 7.0 | 6.1 | 3.2 | 5.3 | 3.9 |
| F (g) | 40.9 | 50.2 | 47.9 | 50.5 | 47.1 | 50.9 | 47.4 | 48.9 | 51.1 | 45.6 |
| E1 (g) | 3.4 | 5.2 | 5.6 | 5.6 | 6.5 | 5.1 | 6.7 | 5.3 | 6.2 | 5.8 |
| E2 (g) | 2.5 | 3.4 | 5.3 | 6.2 | 4.9 | 4.6 | 5.8 | 5.7 | 5.6 | 6.2 |
| E3 (g) | 3.7[b] | – | 3.6 | 3.2 | 2.7 | 4.5 | 5.0 | 7.7 | 7.4 | 7.0 |
| L (%) | 9.7 | 14.5 | 9.7 | NA[c] | 15.4 | 9.7 | 7.8 | 6.0 | 6.6 | 9.1 |
| S/F (g/g) | 85.8 | 12.8 | 48.1 | 16.5 | 12.8 | 52.1 | 39.2 | 15.9 | 29.4 | 13.3 |
| $Y_T$ (%) | 23.5 | 17.1 | 30.1 | 29.6 | 30.0 | 27.8 | 36.8 | 38.2 | 37.6 | 41.8 |

NA: not applicable.
[a] Taken from NIST [42].
[b] Extracted at 350 bar (solvent density of 950 kg/m$^3$).
[c] Mass balance not possible due to severe clogging.

tory. All weighing and pipette volumetric readings were performed in triplicate.

*2.4.5. Functional group identification by ATR-FTIR*

Functional group identification was performed by Fourier-transform infrared spectroscopy (FTIR) utilizing a Thermo-Scientific Nicolet iS5 instrument coupled with an attenuated total reflectance (ATR) accessory iD7. The resolution was at 4 cm$^{-1}$ with a recording range 500–4000 cm$^{-1}$.

*2.4.6. Component identification by GC–MS*

Samples of bio-crude or extracts were dissolved in pyridine (1:1 ratio (w/w)) and derivatized (heat treatment 60 °C, 20 min) to trimethylsilyl derivatives. 4-bromophenol was added to the samples prior to derivatization to be used as an internal standard. The derivatized samples were diluted in diethyl ether (DEE) at a solvent-to-feed ratio 50:1. The derivatized bio-crude was partly soluble in DEE therefore the mixture was filtered through a 0.45 μm syringe filter and the insoluble fraction was weighed to 3 wt% of the initial bio-crude mass. The extracts appeared completely solubilized without any retained matter on the filter. 1 μL was injected into a Thermo Scientific Trace 1300 ISQ GC–MS system with a HP-5MS column (30 m, 0.25 mm, 0.25 μm). The oven temperature profile was as follows; 40 °C–120 °C at 10 °C /min, hold for 5 min, then heated to 300 °C at 5 °C /min, and hold for 4 min. Injector and ion source temperatures were maintained at 300 °C, split ratio was 1:20, and flow rate of the helium carrier gas was 1.0 mL/min. An approximate quantitation of the identified compounds was carried out assuming:

$$w_i = w_{IST} \cdot \frac{A_i}{A_{IST}}$$

where *w* and *A* indicate the mass fraction and the chromatographic peak area, respectively, while *i* and *IST* refer to species *i* and internal standard, respectively [4]. For each sample a single GC–MS injection was performed.

## 3. Results and discussion

### 3.1. Extraction yields and vapour phase loading (VPL)

Data pertaining the $sCO_2$ extraction experimental runs are reported in Table 1. The table includes the set values of the extraction pressure and temperature, together with the corresponding $CO_2$ density (NIST [42]). In addition, data on the average $CO_2$ flow rate, mass of different samples (feed, extracts, and residue), mass balance (losses), solvent-to-feed ratio and total yields are reported. The extraction temperature was varied in the range 40–120 °C (4 levels). At each temperature, the extraction pressure was selected in order to ensure the solvent density to be high enough, as needed for this heavy bio-crude. More specifically, the operating densities were varied in the range of 548–882 kg/m$^3$ (61% density variation). Overall, the experimental plan allowed for: two sets of isobaric runs (183 bar and 400 bar) at different temperatures and solvent densities; four sets of isothermal runs (40 °C, 60 °C, 80 °C, 120 °C) at different pressures and solvent densities; and three sets of isodensity runs (548 kg/m$^3$, 691–693 kg/m$^3$, and 822 kg/m$^3$) at different pressures and temperatures. Each run was executed at constant pressure and temperature, with the exception of Run A where the first two extracts were collected at 112 bar whereas the last extraction period, leading to the third extract, was carried out at 350 bar. Extractions B, D, E and J lasted under 3 h, G, H and I between 3 and 5 h, whereas A, C and F lasted over 6 h.

Three extracts were collected for each run, with the exception of Run B that was characterized by severe clogging and it was necessary to stop it after two extract samples. The mass of the extracts

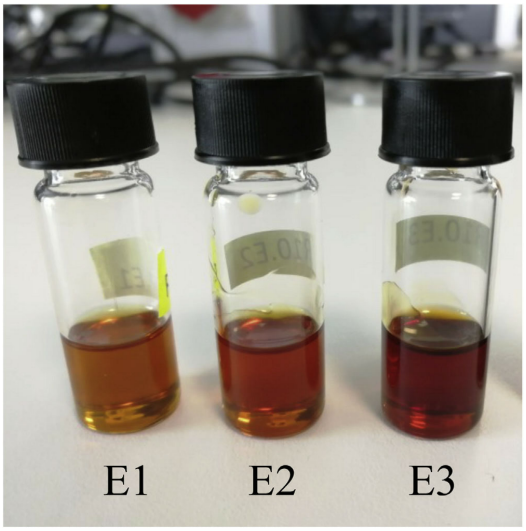


**Fig. 3.** Extracts of experimental Run F (T = 80 °C; P = 183 bar: $Y_T$ = 27.8%).

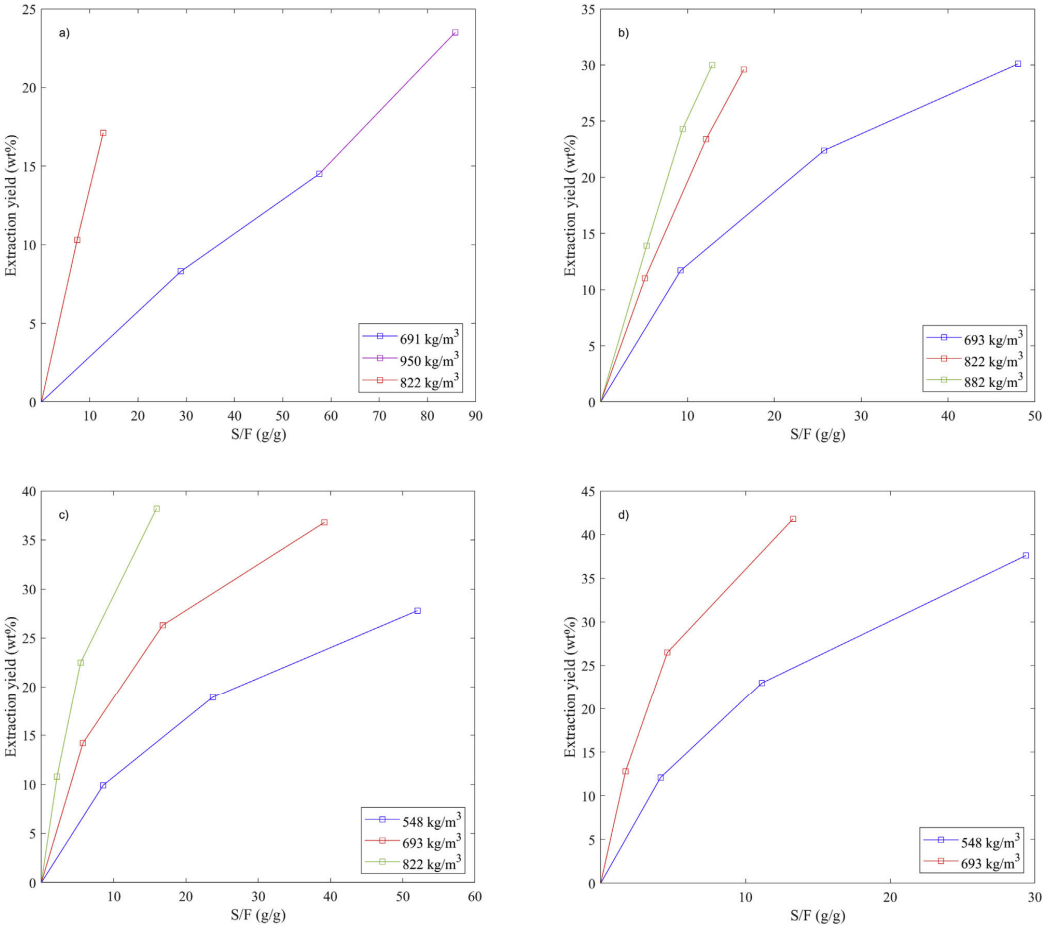


**Fig. 4.** Extraction yield vs. solvent to feed ratio (S/F) for different solvent densities. a) 40 °C; b) 60 °C; c) 80 °C; d) 120 °C.

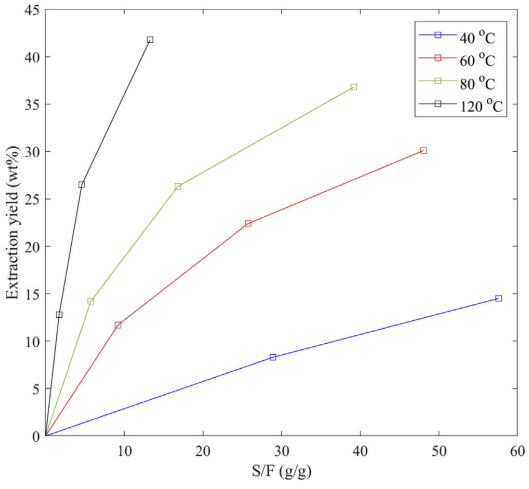


**Fig. 5.** Extraction yield vs. solvent to feed ratio (S/F) at different temperatures and for solvent density of 691–693 kg/m$^3$.

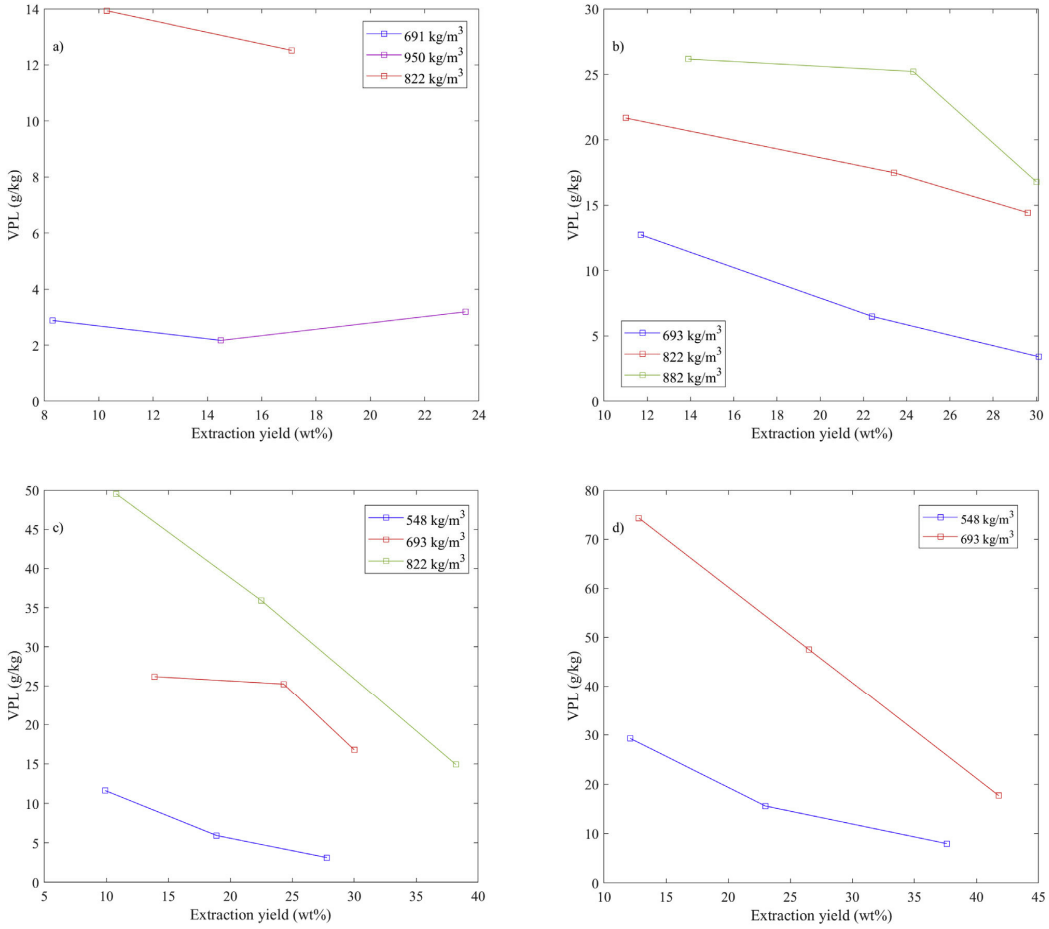


**Fig. 6.** Vapour phase loading (VPL) vs. extraction yield for given temperature and different solvent density. a) 40 °C; b) 60 °C; c) 80 °C; d) 120 °C.

ranged from 2.5 to 7.7 g. The extraction yield after collection of $N$ extracts ($Y_N$) was defined as:

$$Y_N = \frac{\sum_1^N E_k}{F} \cdot 100$$

where $N$ is the number of collected extracts, $E_k$ is the mass of the $k^{th}$ extract and $F$ is the mass of bio-crude fed to the extractor at the beginning of the run. When $N$ coincides with the last collection of extract during semi-continuous operation at the given extraction pressure and temperature (i.e. before depressurisation), then the total extraction yield is obtained ($Y_T$). At the operating conditions tested in this work, total extraction yields ranged from 17 to 42%. All extracts were liquid, showing a viscosity much lower than the feed and a colour ranging from amber to black. An example of the extracts obtained in an experimental run is shown in Fig. 3.

In Fig. 4, the extraction yield is plotted against the solvent to feed ratio, at given temperatures and for different solvent densities. As can be seen, and in line with typical findings in $sCO_2$ extraction experiments, at a given temperature extraction yield for a given S/F increases with the solvent density. The perusal of Fig. 4 also shows that at higher operating temperatures it is possible to obtain higher yields using less solvent. This concept can be conveniently visualised in Fig. 5, which shows the effect of temperature on the extraction for a given solvent density. As can be seen, for this bio-crude the temperature increase improves the yield of the process dramatically and reduces the solvent requirements. This improvement as temperature increases at constant solvent density is often observed in $sCO_2$ extraction of oils. In the case of the HTL bio-crude used in this work, this effect is much larger than what is found for extraction of other oils [27–29]. In addition, it was observed that the extraction of the bio-crude at 40 °C and 60 °C was characterized by sporadic clogging problems and consequent instability of both the extraction pressure and the solvent flow rate. Instead, the operation was extremely smooth at 80 °C and 120 °C at all investigated pressures.

The Vapour Phase Loading (VPL) is defined as the mass of extract obtained in a certain time interval, divided by the mass of solvent flowed in the same interval. It is one of the key process parameters determining the feasibility of the process on industrial scale, since it primarily affects the cost associated to the supercritical solvent loop. Values of VPL around 10 g/kg are generally considered minimum values for the feasibility of an industrial application [43]. In Fig. 6, the VPL is plotted against the extraction yield for the 4

different extraction temperatures. As expected, the VPL is decreasing while the extraction progresses since the oil phase inside the extractor becomes heavier and enriched in the components relatively less soluble in $sCO_2$.

The temperature effect in VPL is considerable and in line with the results presented in Fig. 4. As can be seen, the VPL ranges from values as low as 2–14 g/kg at 40 °C to values as high as 75 g/kg at 120 °C. These data compare favourably with VPL data associated to the extraction of other oils. For example, VPL values of up to 40 g/kg at solvent density of 584 kg/m$^3$ were reported for the continuous countercurrent extraction of fatty acid ethyl esters from fish oil by Riha and Brunner [44]; Gironi and Maschietti [45] reported VPL range of 13–31 g/kg when extracting fish oils ethyl esters in a batch extractor at $CO_2$ density of 500–600 kg/m$^3$; the same authors reported VPL values between 11 and 27 g/kg for continuous countercurrent deterpenation of lemon oil, with $CO_2$ density in the range 260–300 kg/m$^3$ [46].

With regard to previous data on $sCO_2$ fractionation of lignocellulosic oils, examples can be found on semicontinuous single-stage fractionation of pyrolysis oils. The published experimental campaigns however focused on operating conditions typically leading to VPL values in the range 1–10 g/kg [20,26,27,29,32,34,35]. On the other hand, the experimental results of this work clearly indicate that VPL values compatible with industrial operation can be obtained on lignocellulosic HTL oil, operating the process at relatively high temperatures (above 80 °C) and pressures (above 180 bar).

### 3.2. Water content, acid numbers and density of bio-crude and extracts

The water content of the bio-crude feed was 27 ± 1 g/kg. With regard to the extracts, the first (E1) and last (E3) extracts were measured for all extractions at solvent density 691–693 kg/m$^3$. A moderate dehydration was observed, with the water content equal to 16 ± 2 g/kg for E1 samples and 23 ± 2 g/kg for E3 samples at all temperatures.

CAN, PhAN, TAN and density of all extracts and the feed are reported in Table 2. As can be seen from the acid numbers, the bio-crude is highly acidic even when compared with high-TAN crude oils that can reach up to 5 mg KOH/g [47]. In addition, it is observed that the extraction with $sCO_2$ produces extracts exhibiting lower TAN compared to the feed. More specifically, TAN values for the first extracts are on average 74.0 mg KOH/g, i.e. 42% lower than the TAN values of the feed. This result shows that $sCO_2$ preferentially extracts non-acid components. This also explains why TAN is progressively increasing during the extraction. However, it is also apparent that in this single-stage process, acid components are also co-extracted, since TAN values are still very high when compared to fossil crudes. By contrast, CAN values of the extracts are comparable with those of the feed and, in a few cases, even higher. This indicates the presence of carboxylic acids in the feed of lower molecular weight than average molecular weight of other species, therefore exhibiting a relatively high solubility in $sCO_2$ in spite of the high polarity. On the other hand, PhAN values are consistently lower than the feed. In particular, the average PhAN of the first extract is 35 mg KOH/g, corresponding to a 59% reduction with respect to the PhAN of the feed. This result indicates that the acidity of the residue is shifting towards phenolic type as extraction progresses.

With regard to the density of the extracts, as can be seen it is moderately reduced compared to the feed. Even though the values are still too high compared to diesel fuels, they are in line with those of marine fuels, which range from 890 to 1010 kg/m$^3$ as reported in ISO 8217 2017 [48].

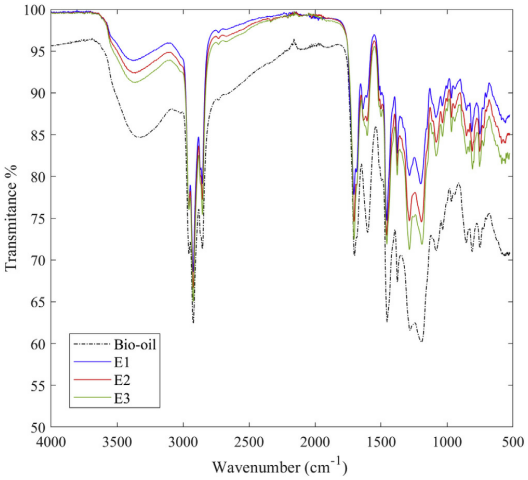


**Fig. 7.** Infrared spectra of bio-crude and the extracts from Run G (80 °C, 255 bar).

### 3.3. Chemical characterization of bio-crude and extracts

The elemental analysis of the bio-crude resulted in the following mass fractions: C 0.809 ± 0.01; H 0.086 ± 0.004; N 0.005 ± 0.0002; S 0.006 ± 0.0003. Oxygen mass fraction is estimated by difference to be 0.094 ± 0.01. These values are in line with literature for HTL bio-crudes from lignocellulosic biomass [15,17,22]. Typical data for petroleum samples are in the following ranges: C 0.83–0.87; H 0.10–0.14; N 0.001–0.02; S 0.0005–0.06; O 0.0005–0.015 [49]. From an elemental standpoint, the high oxygen content of lignocellulosic bio-crudes is clearly the parameter exhibiting the larger deviation for fossil crudes and it is therefore of interest to analyse the effect of $sCO_2$ extraction on this parameter. Oxygen mass fraction of the bio-crude and all extracts is reported in Table 2. The mass fraction of oxygen in the extracts is higher than the feed for most extract samples with mass fractions up to 0.16. In addition, the distribution of oxygen among the various extract does not show clear trends. This indicates that oxygen is widespread in the different chemical species contained in the bio-crude, as also supported by the GC–MS analysis (see Section 3.4) and it is therefore not expected that a $sCO_2$ extraction process can yield substantial differences in the oxygen content. However, as calculated by mass balances, the increased oxygen content of extracts implies that this parameter is reduced down to 0.07 in the residue. A lack of definite trends in oxygen distribution was also observed in previous works on lignocellulosic bio-crude separation applying vacuum distillation [15] or pentane liquid-liquid extraction [24]. In particular, Pedersen et al. [15], observed the absence of a clear trend in the oxygen content with increasing boiling point and that oxygen distributes throughout the entire boiling range, for a similar HTL bio-crude. From this point of view, it seems that the $sCO_2$ extraction process is in line with alternative processes, which is another indication of oxygen being widespread in the feed bio-crude and therefore the bio-crude being intrinsically difficult to be separated in terms of fractions of different oxygen content.

FTIR spectra of the bio-crude and the fractions of Run G (80 °C, 255 bar) are shown in Fig. 7. Qualitatively, Fig. 7 is representative of all experiments and therefore is discussed on the basis of literature indications [50,51]. The wide absorption band between wavenumbers 3000 and 3600 cm$^{-1}$ indicate the presence of hydroxyl groups and of hydrogen bonds. The well-defined absorptions between 2800 and 3000 cm$^{-1}$ are characteristics of C—H stretching that indi-

**Table 2**
Carboxylic acid number (CAN), total acid number (TAN), phenolic acid number (PhAN), density and elemental oxygen mass fraction of bio-crude and its $sCO_2$ fractions.

| | Acid number (mg KOH/g) | | | | |
|---|---|---|---|---|---|
| | CAN | TAN | PhAN | Density (kg/m$^3$) | Oxygen mass fraction |
| Bio-crude | 43 ± 0.9 | 129 ± 6.0 | 86 ± 6.1 | 1051 ± 0.4 | 0.10 ± 0.011 |
| Run A | | | | | |
| E1 | 34 ± 0.3 | 78 ± 0.9 | 44 ± 1.0 | 980 ± 36.0 | 0.14 ± 0.022 |
| E2 | 37 ± 0.6 | 86 ± 0.5 | 48 ± 0.8 | 998 ± 7.0 | 0.11 ± 0.028 |
| E3 | 51 ± 0.3 | 106 ± 0.7 | 56 ± 0.8 | 1002 ± 12.0 | 0.15 ± 0.024 |
| Run B | | | | | |
| E1 | 37 ± 0.2 | 74 ± 1.0 | 37 ± 1.0 | 972 ± 9.0 | 0.14 ± 0.017 |
| E2 | 40 ± 0.2 | 85 ± 0.6 | 44 ± 0.7 | 997 ± 11.0 | 0.16 ± 0.016 |
| Run C | | | | | |
| E1 | 35 ± 0.2 | 66 ± 0.5 | 32 ± 0.6 | 963 ± 8.0 | 0.16 ± 0.039 |
| E2 | 44 ± 0.3 | 94 ± 0.9 | 49 ± 1.0 | 1015 ± 6.0 | 0.15 ± 0.017 |
| E3 | 53 ± 0.4 | 114 ± 1.0 | 61 ± 1.1 | 1015 ± 5.0 | 0.11 ± 0.020 |
| Run D | | | | | |
| E1 | 38 ± 0.1 | 76 ± 0.4 | 37 ± 0.4 | 961 ± 2.0 | 0.10 ± 0.018 |
| E2 | 45 ± 0.8 | 89 ± 2.4 | 44 ± 2.5 | 986 ± 8.0 | 0.16 ± 0.026 |
| E3 | 50 ± 0.9 | 103 ± 1.1 | 54 ± 1.4 | 986 ± 0.2 | 0.10 ± 0.038 |
| Run E | | | | | |
| E1 | 50 ± 0.6 | 84 ± 0.9 | 34 ± 1.1 | 965 ± 6.0 | 0.09 ± 0.023 |
| E2 | 54 ± 0.3 | 93 ± 1.1 | 39 ± 1.1 | 984 ± 7.0 | 0.10 ± 0.004 |
| E3 | 58 ± 0.1 | 100 ± 0.6 | 42 ± 0.7 | 991 ± 4.0 | 0.12 ± 0.016 |
| Run F | | | | | |
| E1 | 32 ± 1.2 | 61 ± 0.0 | 29 ± 1.2 | 959 ± 4.0 | 0.16 ± 0.013 |
| E2 | 44 ± 0.4 | 96 ± 2.2 | 52 ± 2.2 | 989 ± 4.0 | 0.14 ± 0.009 |
| E3 | 56 ± 0.4 | 117 ± 0.5 | 62 ± 0.6 | 1014 ± 9.0 | 0.16 ± 0.020 |
| Run G | | | | | |
| E1 | 37 ± 0.4 | 73 ± 1.1 | 36 ± 1.1 | 967 ± 3.0 | 0.15 ± 0.005 |
| E2 | 48 ± 0.4 | 98 ± 1.3 | 50 ± 1.2 | 992 ± 12.0 | 0.16 ± 0.028 |
| E3 | 56 ± 1.8 | 114 ± 2.5 | 57 ± 3.1 | 1017 ± 9.0 | 0.16 ± 0.010 |
| Run H | | | | | |
| E1 | 40 ± 0.1 | 76 ± 1.1 | 36 ± 1.1 | 955 ± 4.0 | 0.08 ± 0.014 |
| E2 | 46 ± 1.0 | 87 ± 0.6 | 41 ± 1.2 | 984 ± 4.0 | 0.11 ± 0.009 |
| E3 | 50 ± 0.2 | 102 ± 3.0 | 52 ± 3.0 | 1003 ± 7.0 | 0.12 ± 0.020 |
| Run I | | | | | |
| E1 | 39 ± 0.2 | 72 ± 1.3 | 33 ± 1.3 | 968 ± 4.0 | 0.13 ± 0.012 |
| E2 | 49 ± 0.1 | 98 ± 1.0 | 48 ± 1.0 | 987 ± 2.0 | 0.12 ± 0.014 |
| E3 | 64 ± 1.0 | 120 ± 0.8 | 56 ± 1.3 | 1018 ± 6.0 | 0.15 ± 0.017 |
| Run J | | | | | |
| E1 | 47 ± 0.3 | 80 ± 0.9 | 33 ± 1.0 | 941 ± 8.0 | 0.08 ± 0.009 |
| E2 | 53 ± 0.3 | 96 ± 0.7 | 43 ± 0.8 | 1001 ± 7.0 | 0.10 ± 0.015 |
| E3 | 59 ± 0.5 | 113 ± 0.9 | 54 ± 1.0 | 1012 ± 6.0 | 0.08 ± 0.011 |

cates aliphatic structures. The absorptions at 1700 and 1600 cm$^{-1}$ are due to C=O functionalities in ketones, aldehydes, and carboxylic acids. Some peaks displaced to lower wavenumbers indicate that conjugated components are present, which is supported by the unsaturated ketones identified by GC–MS. The bands in the range of 1200–1400 cm$^{-1}$ correspond to phenolics. The spectra of Fig. 7 show that the phenolics (1200–1400 cm$^{-1}$) in the extracts are represented in lower concentrations compared to the feed and they show an increasing trend as the extraction progresses. This observation is in line with the trends of the PhAN values reported in Table 2 and previously discussed.

### 3.4. Selectivity towards specific components

Nineteen chemical components were identified by GC–MS analysis (Table 3) aimed at the lighter fraction of the bio-crude. The identified light components accounted for 5 wt% of the bio-crude feed, while they accounted for 7–9 wt% of the extracts. The identified components can be classified into the following functional classes depending on their chemical structure: 1) Cyclic aliphatic ketones ($C_7$–$C_9$), with a single unsaturation (Ketones, K); 2) Phenol and 1-ring alkylphenols with a single hydroxyl group (Phenols, P); 3) Catechols (C); 4) Fatty acids (FA); 5) Phenylethanoids (PE); 6) Phenylacetic acids (PA). Fig. 8 shows an example chromatogram of the bio-crude as it compares to 3 subsequent extracts at 183 bar and 80 °C (Run F), as well as the peaks corresponding to the identified components numbered as in Table 3.

The total extraction yield for each class of components $i$ is defined as:

$$Y_{T,i} = \frac{\sum_1^N E_k y_{ik}}{F z_i} \cdot 100$$

where $E_k$ is the mass of extract $k$, $y_{ik}$ is the mass fraction of the class $i$ in the extract $k$, $F$ is the mass of the feed, $z_i$ is the mass fraction of the class $i$ in the bio-crude. Mass fractions were estimated by the GC–MS procedure reported above (see Section 2.5.4). $Y_{T,i}$ values were found to be between 10 and 81% as it is reported in Fig. 9. The values follow the pattern of $Y_T$, which is to say it increases with increasing temperature for any given solvent-density. Ketones and 1-ring phenols were the most extracted components, with total yields up to 81% and 76%, respectively, at the maximum extraction pressure and temperature (i.e. Run J). All identified classes of components however exhibited yields higher than 50% in the

**Table 3**
Components identified by GC–MS, retention time (RT), formula, CAS number, molecular weight (MW) and functional class as defined in this work.

| # | RT | Component | Formula | CAS | MW | Class[a] |
|---|---|---|---|---|---|---|
| 1 | 9.87 | 2-Cyclopenten-1-one, 2,3-dimethyl- | $C_7H_{10}O$ | 1121-05-7 | 110.15 | K |
| 2 | 10.10 | Phenol | $C_6H_6O$ | 108-95-2 | 94.11 | P |
| 3 | 10.27 | 2-Cyclopenten-1-one, 3,4,4-trimethyl- | $C_8H_{12}O$ | 30434-65-2 | 124.18 | K |
| 4 | 10.40 | Caproic acid | $C_6H_{12}O_2$ | 142-62-1 | 116.16 | FA |
| 5 | 10.72 | 2-Cyclopenten-1-one, 2,3,4-trimethyl- | $C_8H_{12}O$ | 28790-86-5 | 124.18 | K |
| 6 | 11.02 | 2-Cyclopenten-1-one, 2,3,4,5-tetramethyl- | $C_9H_{14}O$ | – | 138.21 | K |
| 7 | 11.43 | o-Cresol | $C_7H_8O$ | 95-48-7 | 108.14 | P |
| 8 | 11.82 | p-Cresol | $C_7H_8O$ | 106-44-5 | 108.14 | P |
| 9 | 12.13 | Enanthic acid | $C_7H_{14}O_2$ | 111-14-8 | 130.19 | FA |
| 10 | 13.15 | 2,5-Xylenol | $C_8H_{10}O$ | 95-87-4 | 122.16 | P |
| 11 | 13.52 | 2,3-Xylenol | $C_8H_{10}O$ | 526-75-0 | 122.16 | P |
| 12 | 13.88 | 2,6-Xylenol | $C_8H_{10}O$ | 576-26-1 | 122.16 | P |
| 13 | 14.59 | Caprylic acid | $C_8H_{16}O_2$ | 124-07-2 | 144.21 | FA |
| 14 | 19.12 | 4-Methylcatechol | $C_7H_8O_2$ | 452-86-8 | 124.14 | C |
| 15 | 21.34 | Benzeneethanol, 2-hydroxy- | $C_8H_{10}O_2$ | 7768-28-7 | 138.16 | PE |
| 16 | 23.72 | Benzeneacetic acid, 3-hydroxy | $C_8H_8O_3$ | 621-37-4 | 152.15 | PA |
| 17 | 34.72 | Palmitic acid | $C_{16}H_{32}O_2$ | 57-10-3 | 256.42 | FA |
| 18 | 36.04 | Margaric acid | $C_{17}H_{34}O_2$ | 506-12-7 | 270.45 | FA |
| 19 | 38.30 | Stearic acid | $C_{18}H_{36}O_2$ | 57-11-4 | 284.48 | FA |

[a] 1) Cyclic aliphatic ketones ($C_7$–$C_9$), with a single unsaturation (Ketones, K); 2) Phenol and alkylphenols with a single hydroxyl group (Phenols, P); 3) Catechols (C); 4) Fatty acids (FA); 5) Phenylethanoids (PE); 6) Phenylacetic acids (PA).

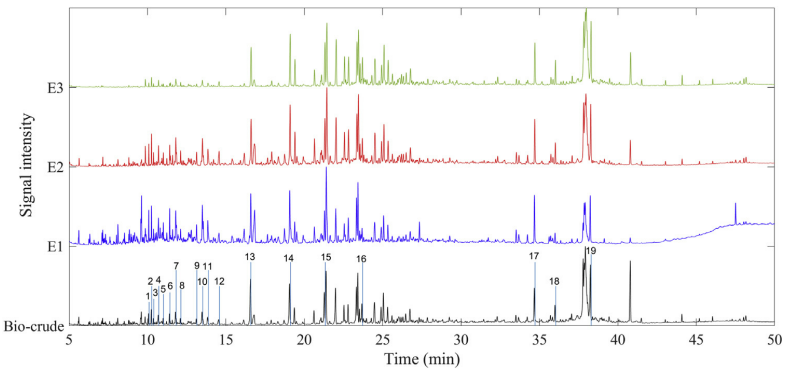


**Fig. 8.** GC–MS chromatogram of the bio-crude and the extracts of an extraction at 80 °C and 183 bar (Run F). Signals are scaled between 0 and maximum peak height for each sample.

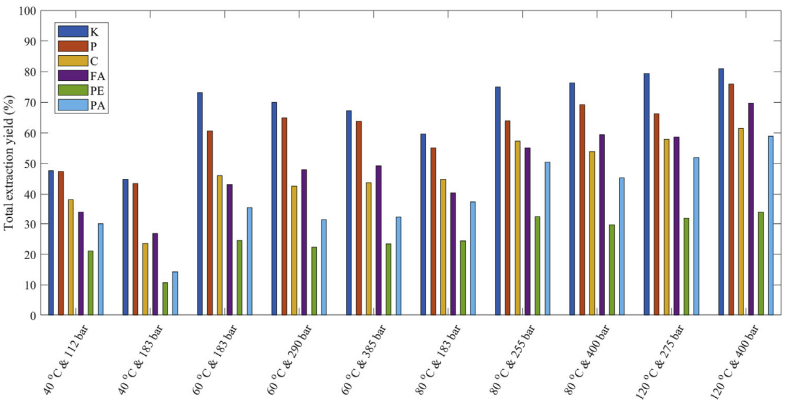


**Fig. 9.** Total extraction yields for the identified classes of components for all experimental runs. K: Cyclic aliphatic ketones (C7–C9), with a single unsaturation; P: Phenol and alkylphenols with a single hydroxyl group; C: Catechols; FA: Fatty acids; PE: Phenylethanoids; PA: Phenylacetic acids.

experiments G to J (i.e. higher temperature), with the exception of phenylethanoids (i.e. up to 34%).

In Fig. 10, the equilibrium ratios (K-values) of each class are reported for all investigated extraction conditions. Fig. 10a)–c) refer to the first, second and third extract, respectively. The K-values were calculated as:

$$K_{ik} = \frac{y_{ik}}{\frac{z_{i,k-1}+z_{ik}}{2}}$$

where: $K_{ik}$ is the K-value of class $i$ during extraction of extract $k$; $y_{ik}$ is the mass fraction of class $i$ in extract $j$ on a $CO_2$-free basis; $\frac{z_{i,k-1}+z_{ik}}{2}$ is an estimation of the average mass fraction of class $i$ inside the extractor on a $CO_2$-free basis, over the time elapsed from the collection of the extract *k-1* and the collection of the extract *k*. The mass fractions of the classes of components inside the extractor on a $CO_2$-free basis were estimated by means of the application of mass balances. They represent, as usual in $sCO_2$ extractors, a good approximation of the liquid phase mass fractions on a $CO_2$-free basis since most of the oil components inside the extractor are actually in the liquid phase.

From Fig. 10, it can be observed that ketones and 1-ring phenols are the species preferentially extracted, with K-values in the first extract in the range 2.7–4.5 for ketones and 2.1–3.3 for 1-ring phenols. Their K-values decreases during the extraction, showing that their separation is progressively more difficult as their concentration in the residue decreases. Catechol and fatty acids are also enriched in the gas-phase, even though they exhibit lower K-values (between 1.2 and 1.7 in the first extract) compared to ketones and 1-ring phenolics. It is however interesting to note that K-values above 1 for fatty acids indicate that these components, in spite of their polarity, are concentrated in the gas phase. K-values of phenylethanoids and phenylacetic acids are the lowest, with values almost consistently below 1 in the first extract, i.e. they are concentrated in the residue. However, their K-values increase during the extraction and this is particularly remarkable for phenylacetic acids, which show values above 1 in the last extraction period.

The perusal of the data shows that higher K-values are obtained for lower boiling point for all species. More specifically, the K-values decrease in order of K > P > C > PE > PA following increasing boiling points, from around 200 °C for ketones and phenolics up to 350 °C for phenylacetic acid. Fatty acids are not considered in this argument because of their wide range of boiling points (i.e. around 250 °C up to around 350 °C), although the presence of relatively low boiling point acids is consistent with the K-values higher than 1. From this standpoint, similar separation patterns are expected if comparing $sCO_2$ extraction and vacuum distillation.

The possibility of separating the identified classes of extracted components one from the other was evaluated by means of selectivity calculations. The selectivity of $sCO_2$ towards the separation of the classes i-j was calculated as:

$$s_{ij} = \frac{K_i}{K_j}$$

Selectivity values fall in the majority of cases between 1.1 and 10, which indicate that the separation of these classes of components by means of $sCO_2$ is possible, even though a multistage process is needed [52]. The pairs that are most difficult to separate are the ketones-phenols and catechol-fatty acids with selectivities always lower than 1.5 and in some cases even 1.0. As expected, ketones and phenols are the easiest to separate from the polar classes, with selectivities consistently above 2.0 in all experimental conditions, while the highest values of 5.2 and 5.0 for ketones-phenylethanoids and phenols-phenylacetic acid, respectively, are achieved at the lowest temperature (i.e. 40 °C) and with solvent density 822 kg/m$^3$.

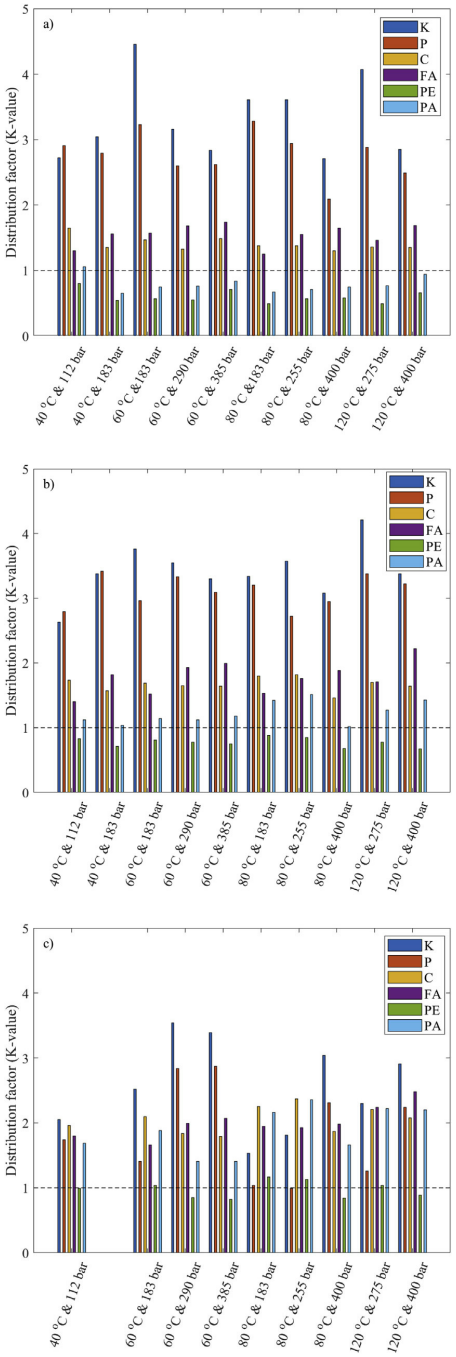


**Fig. 10.** K-values for the identified classes of components for the three extracts of each experimental run. a) Extract 1; b) Extract 2; c) Extract 3. K: Cyclic aliphatic ketones (C7–C9), with a single unsaturation; P: Phenol and alkylphenols with a single hydroxyl group; C: Catechols; FA: Fatty acids; PE: Phenylethanoids; PA: Phenylacetic acids.

## 4. Conclusion

At the operating conditions tested in this work, $sCO_2$ proved to be capable of extracting a large fraction of HTL bio-crude (between 17% and 42%). The dramatic influence of the extraction temperature on the process operability was demonstrated, with smooth operation at 80 °C and 120 °C, whereas sporadic clogging problems were encountered under operation at 40 °C and 60 °C. At the above-mentioned higher temperatures, the efficiency of the process was also much higher. In fact, increasing temperature at given solvent-density led to higher extraction yields associated to lower solvent-to-feed ratios. This is due to higher VPL values, which resulted to be in line with values typically deemed suitable for industrial applications of supercritical $CO_2$ extraction. For example, the extraction yield of 42% was obtained at 120 °C and 400 bar with a solvent-to-feed ratio as low as 13.3.

The extracts exhibited improved bulk properties compared to the feed. Density reduction to marine fuel level and up to 40% reduction of TAN suggests that $sCO_2$ extraction units can be taken into consideration in the overall valorisation of HTL bio-crudes. Oxygen content was higher than the feed in all extracts, which indicates this process not to be suitable for producing extracts that do not need hydrotreating in a fuel production perspective. The resulting reduction of oxygen in the residue, however, suggests the possibility of subjecting the lighter extracts to hydrotreating or dedicating them to production of chemicals (e.g. ketones, phenolics), while routing the heavier residue to processes focused on molecular weight reduction (e.g. cracking) or to processes aimed at the production of adsorbent bio-materials.

The experimental K-values show that both molecular weight and polarity play a role in determining the components preferentially extracted, with decreasing K-values associated to increasing boiling points. From this standpoint, the $sCO_2$ extraction process is expected to behave similarly to vacuum distillation, albeit allowing much lower operating temperatures. Targeted studies comparing vacuum distillation and $sCO_2$ extraction of HTL bio-crudes are deemed relevant as further investigation. The experimental selectivites show that $sCO_2$ can also be used as a means for downstream separation of the extracts into different classes of chemicals. In fact, selectivity values clearly indicate the feasibility of the downstream separation by means of multi-stage processes.

## Declarations of interest

None.

## Acknowledgements

The authors would like to acknowledge the valuable contribution of Linda Birkebæk Madsen, for the elemental analysis performed for this work.

This project has received funding from the European Union's Horizon 2020 research and innovation programme under grant agreement No 727531.

## Appendix A. Supplementary data

Supplementary material related to this article can be found, in the online version, at doi:https://doi.org/10.1016/j.supflu.2019.04.001.

## References

[1] D.R. Vardon, B.K. Sharma, J. Scott, G. Yu, Z. Wang, L. Schideman, Y. Zhang, T.J. Strathmann, Chemical properties of biocrude oil from the hydrothermal liquefaction of Spirulina algae, swine manure, and digested anaerobic sludge, Bioresour. Technol. 102 (2011) 8295–8303, http://dx.doi.org/10.1016/j.biortech.2011.06.041.

[2] T.H. Pedersen, I.F. Grigoras, J. Hoffmann, S.S. Toor, I.M. Daraban, C.U. Jensen, S.B. Iversen, R.B. Madsen, M. Glasius, K.R. Arturi, R.P. Nielsen, E.G. Søgaard, L.A. Rosendahl, Continuous hydrothermal co-liquefaction of aspen wood and glycerol with water phase recirculation, Appl. Energy 162 (2016) 1034–1041, http://dx.doi.org/10.1016/j.apenergy.2015.10.165.

[3] K.R. Arturi, M. Strandgaard, R.P. Nielsen, E.G. Søgaard, M. Maschietti, Hydrothermal liquefaction of lignin in near-critical water in a new batch reactor: influence of phenol and temperature, J. Supercrit. Fluids 123 (2017) 28–39, http://dx.doi.org/10.1016/j.supflu.2016.12.015.

[4] T.D.H. Nguyen, M. Maschietti, T. Belkheiri, L.E. Åmand, H. Theliander, L. Vamling, L. Olausson, S.I. Andersson, Catalytic depolymerisation and conversion of Kraft lignin into liquid products using near-critical water, J. Supercrit. Fluids 86 (2014) 67–75, http://dx.doi.org/10.1016/j.supflu.2013.11.022.

[5] T.D.H. Nguyen, M. Maschietti, L.E. Åmand, L. Vamling, L. Olausson, S.I. Andersson, H. Theliander, The effect of temperature on the catalytic conversion of Kraft lignin using near-critical water, Bioresour. Technol. 170 (2014) 196–203, http://dx.doi.org/10.1016/j.biortech.2014.06.051.

[6] Z. Zhu, L. Rosendahl, S.S. Toor, D. Yu, G. Chen, Hydrothermal liquefaction of barley straw to bio-crude oil: effects of reaction temperature and aqueous phase recirculation, Appl. Energy 137 (2015) 183–192, http://dx.doi.org/10.1016/j.apenergy.2014.10.005.

[7] B. Maddi, S. Viamajala, S. Varanasi, Comparative study of pyrolysis of algal biomass from natural lake blooms with lignocellulosic biomass, Bioresour. Technol. 102 (2011) 11018–11026, http://dx.doi.org/10.1016/j.biortech.2011.09.055.

[8] N. Doassans-Carrère, J.H. Ferrasse, O. Boutin, G. Mauviel, J. Lédé, Comparative study of biomass fast pyrolysis and direct liquefaction for bio-oils production: products yield and characterizations, Energy Fuels 28 (2014) 5103–5111, http://dx.doi.org/10.1021/ef500641c.

[9] J. Jae, R. Coolman, T.J. Mountziaris, G.W. Huber, Catalytic fast pyrolysis of lignocellulosic biomass in a process development unit with continual catalyst addition and removal, Chem. Eng. Sci. 108 (2014) 33–46, http://dx.doi.org/10.1016/j.ces.2013.12.023.

[10] T. Belkheiri, L. Vamling, T.D.H. Nguyen, M. Maschietti, L. Olausson, S.-I. Andersson, L.-E. Åmand, H. Theliander, Kraft lignin depolymerization in near-critical water: effect of changing co-solvent, Cell Chem. Technol. 48 (2014) 813–818.

[11] A.R.K. Gollakota, M. Reddy, M.D. Subramanyam, N. Kishore, A review on the upgradation techniques of pyrolysis oil, Renew. Sustain. Energy Rev. 58 (2016) 1543–1568, http://dx.doi.org/10.1016/j.rser.2015.12.180.

[12] D. Castello, T. Pedersen, L. Rosendahl, Continuous hydrothermal liquefaction of biomass: a critical review, Energies 11 (2018) 3165, http://dx.doi.org/10.3390/en11113165.

[13] H.A. Baloch, S. Nizamuddin, M.T.H. Siddiqui, S. Riaz, A.S. Jatoi, D.K. Dumbre, N.M. Mubarak, M.P. Srinivasan, G.J. Griffin, Recent advances in production and upgrading of bio-oil from biomass: a critical overview, J. Environ. Chem. Eng. 6 (2018) 5101–5118, http://dx.doi.org/10.1016/j.jece.2018.07.050.

[14] G. Haarlemmer, C. Guizani, S. Anouti, M. Déniel, A. Roubaud, S. Valin, Analysis and comparison of bio-oils obtained by hydrothermal liquefaction and fast pyrolysis of beech wood, Fuel 174 (2016) 180–188, http://dx.doi.org/10.1016/j.fuel.2016.01.082.

[15] T.H. Pedersen, C.U. Jensen, L. Sandström, L.A. Rosendahl, Full characterization of compounds obtained from fractional distillation and upgrading of a HTL biocrude, Appl. Energy 202 (2017) 408–419, http://dx.doi.org/10.1016/j.apenergy.2017.05.167.

[16] R.B. Madsen, R.Z.K. Bernberg, P. Biller, J. Becker, B.B. Iversen, M. Glasius, Hydrothermal co-liquefaction of biomasses – quantitative analysis of bio-crude and aqueous phase composition, Sustain. Energy Fuels 1 (2017) 789–805, http://dx.doi.org/10.1039/C7SE00104E.

[17] C.U. Jensen, L.A. Rosendahl, G. Olofsson, Impact of nitrogenous alkaline agent on continuous HTL of lignocellulosic biomass and biocrude upgrading, Fuel Process. Technol. 159 (2017) 376–385, http://dx.doi.org/10.1016/j.fuproc.2016.12.022.

[18] R.B. Madsen, K. Anastasakis, P. Biller, M. Glasius, Rapid determination of water, total acid number, and phenolic content in bio-crude from hydrothermal liquefaction of biomass using FT-IR, Energy Fuels 32 (2018) 7660–7669, http://dx.doi.org/10.1021/acs.energyfuels.8b01208.

[19] P. Biller, B.K. Sharma, B. Kunwar, A.B. Ross, Hydroprocessing of bio-crude from continuous hydrothermal liquefaction of microalgae, Fuel 159 (2015) 197–205, http://dx.doi.org/10.1016/j.fuel.2015.06.077.

[20] E. Pérez, C.O. Tuck, M. Poliakoff, Valorisation of lignin by depolymerisation and fractionation using supercritical fluids and conventional solvents, J. Supercrit. Fluids 133 (2018) 690–695, http://dx.doi.org/10.1016/j.supflu.2017.07.033.

[21] A.R.K. Gollakota, N. Kishore, S. Gu, A review on hydrothermal liquefaction of biomass, Renew. Sustain. Energy Rev. 81 (2018) 1378–1392, http://dx.doi.org/10.1016/j.rser.2017.05.178.

[22] J. Hoffmann, C.U. Jensen, L.A. Rosendahl, Co-processing potential of HTL bio-crude at petroleum refineries – part 1: fractional distillation and characterization, Fuel 165 (2016) 526–535, http://dx.doi.org/10.1016/j.fuel.2015.08.047.

[23] H.S. Hu, Y.L. Wu, M. De Yang, Fractionation of bio-oil produced from hydrothermal liquefaction of microalgae by liquid-liquid extraction, Biomass

Bioenergy 108 (2018) 487–500, http://dx.doi.org/10.1016/j.biombioe.2017.10.033.
[24] S. Bjelić, J. Yu, B.B. Iversen, M. Glasius, P. Biller, Detailed investigation into the asphaltene fraction of hydrothermal liquefaction derived bio-crude and hydrotreated bio-crudes, Energy Fuels 32 (2018) 3579–3587, http://dx.doi.org/10.1021/acs.energyfuels.7b04119.
[25] W. Maqbool, P. Hobson, K. Dunn, W. Doherty, Supercritical carbon dioxide separation of carboxylic scids and phenolics from bio-oil of lignocellulosic origin: understanding bio-oil compositions, compound solubilities, and their fractionation, Ind. Eng. Chem. Res. 56 (2017) 3129–3144, http://dx.doi.org/10.1021/acs.iecr.6b04111.
[26] Y.H. Chan, S. Yusup, A.T. Quitain, Y.H. Chai, Y. Uemura, S.K. Loh, Extraction of palm kernel shell derived pyrolysis oil by supercritical carbon dioxide: evaluation and modeling of phenol solubility, Biomass Bioenergy 116 (2018) 106–112, http://dx.doi.org/10.1016/j.biombioe.2018.06.009.
[27] Y. Feng, D. Meier, Supercritical carbon dioxide extraction of fast pyrolysis oil from softwood, J. Supercrit. Fluids 128 (2017) 6–17, http://dx.doi.org/10.1016/j.supflu.2017.04.010.
[28] Y.H. Chan, S. Yusup, A.T. Quitain, Y. Uemura, S.K. Loh, Fractionation of pyrolysis oil via supercritical carbon dioxide extraction: optimization study using response surface methodology (RSM), Biomass Bioenergy 107 (2017) 155–163, http://dx.doi.org/10.1016/j.biombioe.2017.10.005.
[29] Y. Feng, D. Meier, Comparison of supercritical $CO_2$, liquid $CO_2$, and solvent extraction of chemicals from a commercial slow pyrolysis liquid of beech wood, Biomass Bioenergy 85 (2016) 346–354, http://dx.doi.org/10.1016/j.biombioe.2015.12.027.
[30] T. Cheng, Y. Han, Y. Zhang, C. Xu, Molecular composition of oxygenated compounds in fast pyrolysis bio-oil and its supercritical fluid extracts, Fuel 172 (2016) 49–57, http://dx.doi.org/10.1016/j.fuel.2015.12.075.
[31] B.P. Mudraboyina, D. Fu, P.G. Jessop, Supercritical fluid rectification of lignin microwave-pyrolysis oil, Green Chem. 17 (2015) 169–172, http://dx.doi.org/10.1039/c4gc01433b.
[32] Y. Feng, D. Meier, Extraction of value-added chemicals from pyrolysis liquids with supercritical carbon dioxide, J. Anal. Appl. Pyrolysis 113 (2015) 174–185, http://dx.doi.org/10.1016/j.jaap.2014.12.009.
[33] R.N. Patel, S. Bandyopadhyay, A. Ganesh, Extraction of cardanol and phenol from bio-oils obtained through vacuum pyrolysis of biomass using supercritical fluid extraction, Energy 36 (2011) 1535–1542, http://dx.doi.org/10.1016/j.energy.2011.01.009.
[34] S. Naik, V.V. Goud, P.K. Rout, A.K. Dalai, Supercritical $CO_2$ fractionation of bio-oil produced from wheat-hemlock biomass, Bioresour. Technol. 101 (2010) 7605–7613, http://dx.doi.org/10.1016/j.biortech.2010.04.024.
[35] P.K. Rout, M.K. Naik, S.N. Naik, V.V. Goud, L.M. Das, A.K. Dalai, Supercritical $CO_2$ fractionation of bio-oil produced from mixed biomass of wheat and wood sawdust, Energy Fuels 23 (2009) 6181–6188, http://dx.doi.org/10.1021/ef900663a.
[36] C.U. Jensen, J.K. Rodriguez Guerrero, S. Karatzos, G. Olofsson, S.B. Iversen, Fundamentals of Hydrofaction™: renewable crude oil from woody biomass, Biomass Convers. Biorefinery 7 (2017) 495–509, http://dx.doi.org/10.1007/s13399-017-0248-8.
[37] C.U. Jensen, PlUS – Hydrofaction™ Platform with Integrated Upgrading Step, PhD Thesis, Aalborg University, 2018.
[38] R.P. Nielsen, R. Valsecchi, M. Strandgaard, M. Maschietti, Experimental study on fluid phase equilibria of hydroxyl-terminated perfluoropolyether oligomers and supercritical carbon dioxide, J. Supercrit. Fluids 101 (2015) 124–130, http://dx.doi.org/10.1016/j.supflu.2015.03.011.
[39] ASTM International, ASTM D664-17a, in: Standard Test Method for Acid Number of Petroleum Products by Potentiometric Titration, 2017, http://dx.doi.org/10.1520/D0664-17A.
[40] E. Christensen, J. Ferrell, M.V. Olarte, A.B. Padmaperuma, T. Lemmon, Acid Number Determination of Pyrolysis Bio-oils Using Potentiometric Titration Laboratory Analytical Procedure (LAP), Golden, CO, USA, 2016, http://dx.doi.org/10.2172/1241091.
[41] E.D. Christensen, G.M. Chupka, J. Luecke, T. Smurthwaite, T.L. Alleman, K. Iisa, J.A. Franz, D.C. Elliott, R.L. McCormick, Analysis of oxygenated compounds in hydrotreated biomass fast pyrolysis oil distillate fractions, Energy Fuels 25 (2011) 5462–5471, http://dx.doi.org/10.1021/ef201357h.
[42] E.W. Lemmon, M.O. McLinden, D.G. Friend, Thermophysical properties of fluid systems, in: P.J. Linstrom, W.G. Mallard (Eds.), NIST Chem. WebBook, NIST Stand. Ref. Database Number 69, National Institute of Standards and Technology, Gaithersburg MD, 20899, 2019, http://dx.doi.org/10.18434/T4D303.
[43] M. Maschietti, Separation of oils using supercritical carbon dioxide, in: J. Osborne (Ed.), Handb. Supercrit. Fluids, 1st ed., Nova Science Publishers, Incorporated, New York, 2014, pp. 57–78.
[44] V. Riha, G. Brunner, Separation of fish oil ethyl esters with supercritical carbon dioxide, J. Supercrit. Fluids 17 (2000) 55–64, http://dx.doi.org/10.1016/S0896-8446(99)00038-8.
[45] F. Gironi, M. Maschietti, Separation of fish oils ethyl esters by means of supercritical carbon dioxide: thermodynamic analysis and process modelling, Chem. Eng. Sci. 61 (2006) 5114–5126, http://dx.doi.org/10.1016/j.ces.2006.03.041.
[46] F. Gironi, M. Maschietti, Continuous countercurrent deterpenation of lemon essential oil by means of supercritical carbon dioxide: experimental data and process modelling, Chem. Eng. Sci. 63 (2008) 651–661, http://dx.doi.org/10.1016/j.ces.2007.10.008.
[47] J.G. Speight, Chapter 1 – naphthenic acids in petroleum, in: J.G. Speight (Ed.), High Acid Crudes, Gulf Professional Publishing, Boston, 2014, pp. 1–29, http://dx.doi.org/10.1016/B978-0-12-800630-6.00001-0.
[48] ISO 8217:2017, Petroleum Products — Fuels (Class F) — Specifications of Marine Fuels, 2017.
[49] J.G. Speight, Chemical composition, in: Chem. Technol. Pet., fifth ed., Taylor & Francis, 2014.
[50] J. Coates, Interpretation of infrared spectra, a practical approach, Encycl. Anal. Chem. (2006) 1–23, http://dx.doi.org/10.1002/9780470027318.a5606.
[51] B.H. Stuart, Infrared Spectroscopy: Fundamentals and Applications, 2004, http://dx.doi.org/10.1002/0470011149.
[52] G. Brunner, Counter-current separations, J. Supercrit. Fluids 47 (2009) 574–582, http://dx.doi.org/10.1016/j.supflu.2008.09.022.

# Supercritical carbon dioxide fractionation of bio-crude produced by hydrothermal liquefaction of pinewood

Nikolaos Montesantos[a], Thomas Helmer Pedersen[b], Rudi Pankratz Nielsen[a], Lasse Rosendahl[b], Marco Maschietti[a*]

[a] Department of Chemistry and Bioscience, Aalborg University, Niels Bohrs Vej 8A, 6700 Esbjerg, Denmark

[b] Department of Energy Technology, Aalborg University, Pontoppidanstræde 111, 9220 Aalborg Øst, Denmark

Supplementary Material: Table of K-values

Table S1: K-values of component classes for each extract K1 (E1), K2 (E2) and K3 (E3).

| | Ketones | Phenols | Catechols | Fatty acids | Phenylethanoids | Phenylacetic acids |
|---|---|---|---|---|---|---|
| | | | | **Run A** | | |
| K1 | 2.7 | 2.9 | 1.7 | 1.3 | 0.8 | 1.1 |
| K2 | 2.6 | 2.8 | 1.7 | 1.4 | 0.8 | 1.1 |
| K3 | 2.0 | 1.7 | 2.0 | 1.8 | 1.0 | 1.7 |
| | | | | **Run B** | | |
| K1 | 3.0 | 2.8 | 1.3 | 1.6 | 0.5 | 0.7 |
| K2 | 3.4 | 3.4 | 1.6 | 1.8 | 0.7 | 1.0 |
| | | | | **Run C** | | |
| K1 | 4.5 | 3.2 | 1.5 | 1.6 | 0.6 | 0.7 |
| K2 | 3.8 | 3.0 | 1.7 | 1.5 | 0.8 | 1.1 |
| K3 | 2.5 | 1.4 | 2.1 | 1.7 | 1.0 | 1.9 |

* Corresponding author: marco@bio.aau.dk (Marco Maschietti)

Table S1 continued

| | | | | | | |
|---|---|---|---|---|---|---|
| | | | **Run D** | | | |
| K1 | 3.2 | 2.6 | 1.3 | 1.7 | 0.5 | 0.8 |
| K2 | 3.5 | 3.3 | 1.6 | 1.9 | 0.8 | 1.1 |
| K3 | 3.5 | 2.8 | 1.8 | 2.0 | 0.8 | 1.4 |
| | | | **Run E** | | | |
| K1 | 2.8 | 2.6 | 1.5 | 1.7 | 0.7 | 0.8 |
| K2 | 3.3 | 3.1 | 1.6 | 2.0 | 0.7 | 1.2 |
| K3 | 3.4 | 2.9 | 1.8 | 2.1 | 0.8 | 1.4 |
| | | | **Run F** | | | |
| K1 | 3.6 | 3.3 | 1.4 | 1.2 | 0.5 | 0.7 |
| K2 | 3.3 | 3.2 | 1.8 | 1.5 | 0.9 | 1.4 |
| K3 | 1.5 | 1.0 | 2.2 | 2.0 | 1.2 | 2.2 |
| | | | **Run G** | | | |
| K1 | 3.6 | 2.9 | 1.4 | 1.6 | 0.6 | 0.7 |
| K2 | 3.6 | 2.7 | 1.8 | 1.8 | 0.9 | 1.5 |
| K3 | 1.8 | 1.0 | 2.4 | 1.9 | 1.1 | 2.4 |
| | | | **Run H** | | | |
| K1 | 2.7 | 2.1 | 1.3 | 1.7 | 0.6 | 0.8 |
| K2 | 3.1 | 2.9 | 1.5 | 1.9 | 0.7 | 1.0 |
| K3 | 3.0 | 2.3 | 1.9 | 2.0 | 0.8 | 1.7 |

Table S1 continued

| | | | | | | |
|---|---|---|---|---|---|---|
| | | | **Run I** | | | |
| K1 | 4.1 | 2.9 | 1.4 | 1.5 | 0.5 | 0.8 |
| K2 | 4.2 | 3.4 | 1.7 | 1.7 | 0.8 | 1.3 |
| K3 | 2.3 | 1.3 | 2.2 | 2.2 | 1.0 | 2.2 |
| | | | **Run J** | | | |
| K1 | 2.8 | 2.5 | 1.3 | 1.7 | 0.7 | 0.9 |
| K2 | 3.4 | 3.2 | 1.6 | 2.2 | 0.7 | 1.4 |
| K3 | 2.9 | 2.2 | 2.1 | 2.5 | 0.9 | 2.2 |

# Paper B

## High-temperature extraction of lignocellulosic bio-crude by supercritical carbon dioxide

Nikolaos Montesantos, Thomas Helmer Pedersen, Rudi Pankratz Nielsen, Lasse Rosendahl, Marco Maschietti

The manuscript has been published in

*Chemical Engineering Transactions*, Volume 79, Pages 799-804, 2019

CHEMICAL ENGINEERING TRANSACTIONS
VOL. 74, 2019
A publication of AIDIC
The Italian Association of Chemical Engineering
Online at www.cetjournal.it
Guest Editors: Sauro Pierucci, Jiří Jaromír Klemeš, Laura Piazza

**ISBN** 978-88-95608-71-6; **ISSN** 2283-9216
DOI: 10.3303/CET1974134

# High-Temperature Extraction of Lignocellulosic Bio-Crude by Supercritical Carbon Dioxide

Nikolaos Montesantos[a], Thomas H. Pedersen[b], Rudi P. Nielsen[a], Lasse A. Rosendahl[b], Marco Maschietti[a]*

[a]Department of Chemistry and Bioscience, Aalborg University, Niels Bohrs Vej 8A, 6700 Esbjerg, Denmark
[b]Department of Energy Technology, Aalborg University, Pontoppidanstræde 111, 9220 Aalborg Øst, Denmark
marco@bio.aau.dk

Supercritical carbon dioxide extraction was utilized for the fractionation of a pinewood derived hydrothermal liquefaction bio-crude. The experiments were performed at temperature 120 ºC and at pressure levels that correspond to $CO_2$ density of 500, 615 and 730 kg/m$^3$. Extraction yields of 34 to 49 % were achieved, which increased with increasing solvent density. Density was reduced for all extracts (2-10 %) while the H/C ratio increased when compared to the bio-crude. Low boiling point components such as ketones, 1-ring aromatic hydrocarbons and low molecular weight fatty acids were extracted preferentially (K-values up to 11). 1-ring phenols and benzenediols were enriched in the extracts as well (K-values 1-3). Heavy hydrocarbons and long chain fatty acids were extracted at the later stages of extraction when the lighter components were depleted.

## 1. Introduction

Bio-crudes that are produced by conversion of biomass through thermochemical processes, such as hydrothermal liquefaction (HTL) and pyrolysis, have been recognized as potential alternatives to petroleum, for the production of liquid fuels as well as commercial chemicals (Baloch et al., 2018). Especially HTL of the so-called second-generation lignocellulosic biomass, which includes non-food material (e.g. forestry, sewage, industrial residues), can be a low cost and environmentally friendly source of the above. Wood (Pedersen et al., 2016) and industrial residues, such as pulp mill excess lignin (Nguyen et al., 2014) are a few examples of second-generation lignocellulosic biomass that have successfully been converted to liquid HTL bio-crudes with promising fuel properties such as higher heating values up to 35 MJ/kg. Development of HTL has already reached demonstration scale, even though there are a few obstacles to overcome with regard to downstream fuel upgrading (Castello et al., 2018). High viscosity (e.g. 2000 mPa·s), density (e.g. over 1000 kg/m$^3$) (Haarlemmer et al., 2016) and oxygen content (e.g. 15 %) (Pedersen et al., 2017) are quality issues of HTL bio-crudes, which need to be upgraded in order to be compatible with the conventional fuel infrastructure. Catalytic hydrotreatment is the state-of-the-art upgrading process, which can bring the bio-crude to drop-in quality, with however considerable cost due to hydrogen consumption and high operating temperature (e.g. above 350 ºC) (Castello et al., 2018). In addition to the fuel perspective, HTL bio-crudes contain a large number of chemical species that range from ketones and 1-ring phenols to long-chain fatty acids and polyaromatic hydrocarbons (Pedersen et al., 2016), indicating the possibility of producing chemicals. However, the high number of components, the high boiling points of a large fraction of the bio-crude, as well as its high viscosity render the separation into fractions a complicated task. In particular, distillation needs very high temperatures even if operated under vacuum, and it is thus characterized by high operating costs. In addition, the high temperature involved may lead to uncontrolled cracking reactions resulting to equipment fouling. Conventional liquid-liquid extraction, which may have the advantage of viscosity reduction induced by the solvent dissolution in the oil, has the disadvantage of requiring the use of organic solvents, which are often petroleum-derived, that need to be regenerated by distillation (Maqbool et al., 2017).
As typical when dealing with high boiling point and viscous liquid feeds to be separated, the extraction by means of supercritical carbon dioxide ($sCO_2$) is an environmentally friendly process with the potential of

Paper Received: 19 April 2018; Revised: 9 August 2018; Accepted: 30 October 2018

Please cite this article as: Montesantos N., Pedersen T.H., Nielsen R., Rosendahl L.A., Maschietti M., 2019, High-temperature Extraction of Lignocellulosic Bio-oil by Supercritical Carbon Dioxide, Chemical Engineering Transactions, 74, 799-804 DOI:10.3303/CET1974134

competing with conventional separation processes. In the case of pyrolysis lignocellulosic oils, the possibility of producing extracts enriched in valuable components, such as phenolics, ketones and acids, was shown (Feng and Meier, 2017). In addition, Feng and Meier (2017) observed that relatively high temperatures (e.g. 80 ºC) enhances the extraction efficiency, especially when combined with high $CO_2$ density. In a previous work, carried out at Aalborg University and focused on HTL lignocellulosic bio-crude, the positive effect of the extraction temperature on the process operability and efficiency for these types of feed was highlighted. As a matter of fact, process operability and the extraction efficiency were dramatically enhanced for extraction temperatures increasing from 40 to 120 ºC (Montesantos et al., 2019). In line with these preliminary findings, the aim of this work is to investigate the potential of $sCO_2$ extraction of HTL lignocellulosic bio-crude at 120 ºC, for different pressures.

## 2. Materials and methods

### 2.1 Feed and chemicals

The bio-crude used in this work was produced by HTL of pinewood, in a pilot unit located at Aalborg University (Pedersen et al., 2016). The HTL product was demineralized and dehydrated as described by Jensen (2018). The final feed bio-crude used for the $sCO_2$ extractions was a black highly viscous liquid (Figure 1a). Carbon dioxide ($CO_2$, 99.8 %) from AGA was used for the extractions. Tetrahydrofuran (THF, 99 %), methyl ethyl ketone (MEK, 99 %) and methyl isobutyl ketone (MIBK, 99 %) from VWR were used as solvents for density measurements. For the GC-MS analysis, diethyl ether (DEE, 99 %) from VWR and pyridine (ACS grade) from Hach were used as solvents, n-heptadecane (C17, 99 %) from Acros and 4-bromophenol (99 %) from Merck as internal standards, and N,O-Bis(trimethylsilyl)trifluoroacetamide (BSTFA, 98.5 %) from Sigma Aldrich as derivatisation agent. A PerkinElmer Cystine 4G powder was used for the calibration of elemental analysis.

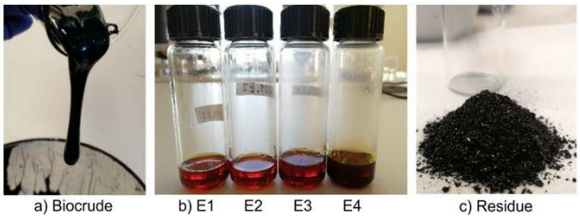


*Figure 1: a) Bio-crude, b) Extracts (yield 34 %) and c) residue. Experimental run at 120 ºC and 247 bar.*

### 2.2 Supercritical extractions

$sCO_2$ extractions were performed utilizing a supercritical extraction system described in detail by Montesantos et al. (2019). The system comprises a high pressure vessel with a basket insert (178 $cm^3$), in which a feed of approximately 30 g was charged prior to an extraction. The basket was filled up to 1/3 height with soda-lime glass beads to ensure bio-crude dispersion and an adequate contact area with the solvent. $CO_2$ was chilled to 5 ºC by a heat exchanger and fed to the bottom of the extractor by a pneumatic pump. The extraction pressure (247 to 448 bar) and the $CO_2$ flow rate (4.8 to 5.9 g/min) were maintained by manually regulating the air supply of the pump and the opening of a heated micrometering valve downstream the extractor. Before starting to flow $sCO_2$, the feed and the supercritical solvent were kept at the extraction pressure and temperature for 30 minutes under static mode. A drum-type gas meter was used to measure the $CO_2$ volumetric flow at ambient conditions, downstream a series of washing bottles comprising a cold trap (2-5 ºC). The extract was collected in the cold trap in interchangeable sampling vials. After the end of each extraction, the system was depressurized, the basket dismounted, and the residue retrieved by washing the basket and the glass beads with THF and removing the solvent by rotary vacuum evaporation.

### 2.3 Analytical characterization

The feed and extracts where characterized in terms of density, elemental composition and component identification and quantitation by gas chromatography – mass spectrometry (GC-MS), while the residue was subjected to elemental analysis (EA). Because of the high viscosity, the density of the bio-crude feed was estimated by diluting it 1:1 (w/w) in three solvents (i.e. MEK, MIBK, THF). The densities of the mixture and of the pure solvent were measured with an Anton Parr DMA 35 Ex, and the density of the bio-crude was calculated assuming a linear relation between the measured density and its mass fraction. Due to the small

quantity of the extracts, their density was measured by weighing the mass of a volume of sample displaced by a calibrated positive displacement precision pipette. EA was performed in a PerkinElmer 2400 Series II CHNS/O analyser. Carbon, hydrogen, nitrogen and sulphur were measured, whereas oxygen was calculated by difference. GC-MS analysis of bio-crude and extracts was performed by injecting 1 µl of sample in a PerkinElmer Clarus 680 GC coupled with a PerkinElmer Clarus SQ 8T MS. The analytes were separated in a PerkinElmer Elite 5 column (30 m, 0.25 mm ID, 0.1 µm). The temperature program of the GC was: 70 °C initial temperature for 1 min; 15 °C/min up to 250 °C; hold for 7 min. All identified components except the acids were quantified by means of the internal standard (IS) method, diluting the samples in DEE (15:1) spiked with a known amount of C17 (IS). The identification and quantitation of the acids were carried out by derivatizing the samples with BSTFA, using pyridine as solvent (1:1:1 (w/w)) and applying a heat treatment at 60 °C for 20 min. Pyridine contained a known amount of 4-bromophenol (IS). The derivatised samples were diluted in DEE (25:1). The identified compounds were approximately quantitated assuming proportionality between their mass fraction and the chromatographic area (Nguyen et al., 2014). All analysis (i.e. density, EA, GC-MS) were performed in triplicate.

## 3. Results and discussion

### 3.1 Extraction yields and vapour phase loading (VPL)

The operating conditions and experimental data of all extractions are reported in Table 1. The extraction temperature (T) for all runs was set to 120 ºC while pressure (P) was set to different values in order to achieve $CO_2$ densities (ρ) in the range of 500 to 730 kg/m$^3$. Pressure and temperature were maintained for the whole duration of each extraction with average standard deviations (SD) of 3 bar and 0.4 ºC, respectively. In addition, the average flow rate (Q) is reported (SD 0.8 g/min). Extractions lasted approximately 4 hours and 4-5 extracts were collected for each run (E1, E2, …, E5). The extracts appeared remarkably less viscous than the bio-crude feed while the residue was a dry solid (Figure 1b and 1c). Extraction yields at time $t$ were calculated as the ratio of the mass extracted from the beginning of the flow mode of operation $(t = 0)$ until time $t$ and the mass of the feed (F). Total extraction yields ($Y_T$) refer to the time of the last extract. They were observed to range from 34 to 49 %. The mass of the residue (RS), the cumulative solvent-to-feed ratio (S/F) and the mass balance closures (MB) are also reported in Table 1. The mass balance closure discrepancy is in line with the extracted material remaining in the dead volume of piping (estimated 6.2 ml) after the end of an extraction.

*Table 1: Operating conditions and experimental results of all extractions.*

| Run | T (°C) | P (bar) | ρ (kg/m$^3$)[a] | Q (g/min) | F (g) | E1 (g) | E2 (g) | E3 (g) | E4 (g) | E5 (g) | RS (g) | MB (%) | S/F (g/g) | $Y_T$ (%) |
|---|---|---|---|---|---|---|---|---|---|---|---|---|---|---|
| A | 120 | 247 | 500 | 6.9 | 30.8 | 2.3 | 2.1 | 3.0 | 3.0 | - | 16.6 | 87.6 | 50.9 | 33.9 |
| B | 120 | 323 | 615 | 5.8 | 30.0 | 2.7 | 2.6 | 2.5 | 4.2 | - | 13.9 | 89.9 | 42.0 | 41.9 |
| C | 120 | 448 | 730 | 4.8 | 28.0 | 2.5 | 2.4 | 2.7 | 2.7 | 3.4 | 11.6 | 90.4 | 40.6 | 48.9 |

[a] Taken from NIST

In Figure 2a, the extraction yield is plotted against S/F for all solvent densities. As expected, at the given temperature, the extraction yield for a given S/F increases with solvent density. In other words, a given extraction yield can be achieved with less solvent as solvent density increases. In Figure 2b, the Vapour Phase Loading (VPL) is plotted against the extraction yield. VPL, typically reported in g/kg, is defined as the mass extracted in a specific time interval, divided by the mass of solvent flowed through the extractor in the same interval. The figure shows an expected improvement of VPL with increasing solvent density, due to the increased solubility of the bio-crude in $sCO_2$. VPL is decreasing while the extraction proceeds since the feed remaining in the extractor becomes heavier and thus less soluble in $sCO_2$. The irregular increase shown for runs at 615 and 730 kg/m$^3$ between the first and second extract is most likely due to unsaturated solvent at the beginning of the flow mode of operation and it is a feature often seen in supercritical extractions. VPL in this work ranges from 46 g/kg for the early stages at the highest pressure to values as low as 3 g/kg at the final stages of the extractions. These results demonstrate average VPL values above 10 g/kg, which can be considered as a rule-of-thumb value for industrial application feasibility (Maschietti, 2014), at yields up to 49 %. In addition, at the high pressure and temperature values applied in this work, VPL values in line with those obtained for other types of oils (11 to 40 g/kg), for which the $sCO_2$ extraction was proved feasible (Gironi and Maschietti, 2006; Gironi and Maschietti, 2007; Riha and Brunner 2009), are found.

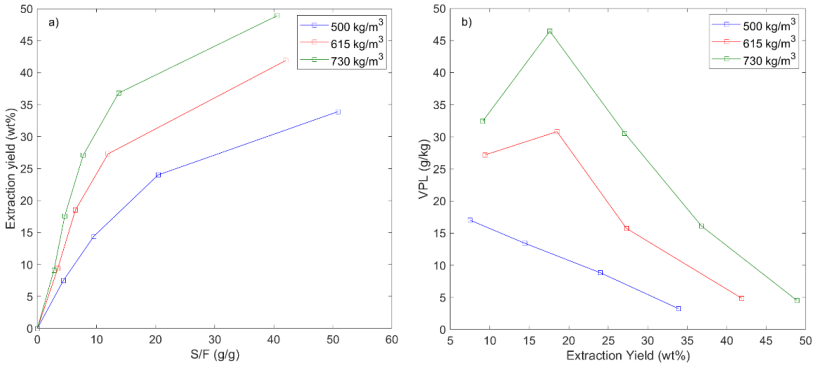


*Figure 2: a) Extraction yield vs. solvent to feed ratio (S/F) and b) vapour phase loading (VPL) vs. extraction yield for different solvent densities, at 120 ºC.*

### 3.2 Physical and chemical characterization

The density of the bio-crude was found to be 1064 kg/m$^3$ ± 15 kg/m$^3$, whereas values in the range 957 kg/m$^3$ ± 30 kg/m$^3$ to 1044 kg/m$^3$ ± 26 kg/m$^3$ were measured for the extracts. Extract density values are in line with density of marine fuels, which ranges from 890 to 1010 kg/m$^3$ as defined by ISO 8217 2017. The density of the extracts was found to increase during the extraction, which is in line with increased extraction of heavier components. The H/C ratio of the extracts was observed in the range 1.40 to 1.69, which is higher than the feed (1.21), with these values being similar to typical bitumen values (i.e. 1.5) (Speight, 2014). The residues had the lowest H/C (range 1.03 to 1.14), which is in line with the respective increase in the extracts. The O/C ratio was relatively unchanged in all extracts (range 0.08 to 0.10) compared to the bio-crude (i.e. 0.10). The standard uncertainty of H/C and O/C was 0.04 and 0.004, respectively. Similar lack of definite trends in oxygen distribution have been found in literature where lignocellulosic bio-crude was fractionated by vacuum distillation (Pedersen et al. 2017) or liquid-liquid extraction using pentane (Bjelic et al. 2018). This O/C is an order of magnitude higher than that of crude oil. However, the near absence of other heteroatoms (i.e. S, N), shown by EA, makes a 1:10 blending for refinery vacuum distillation possible. The O/C ratio in the residues of all runs was 0.12, which indicates that high boiling point oxygenated compounds remain in the residue and a robust hydrotreatment/cracking process would be needed to upgrade it for fuel purposes.

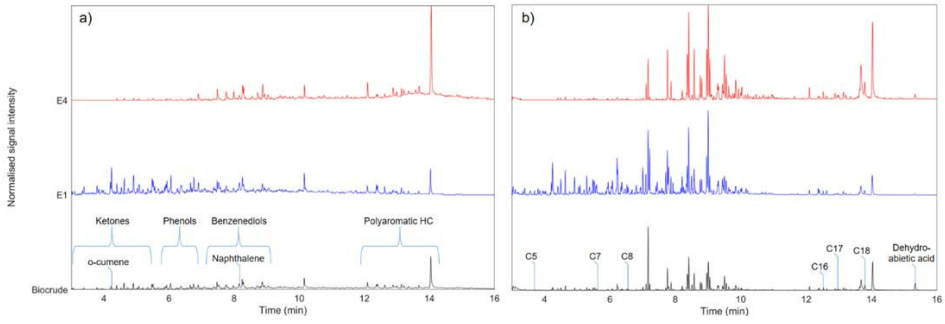


*Figure 3: Example chromatogram of extraction A (i.e. 120 ºC, 500 kg/m$^3$): a) without derivatisation, b) acid identification after derivatisation.*

Chemical species belonging to the following 8 distinct classes were identified by means of GC-MS analysis of the bio-crude and extracts: 1) cyclic aliphatic (C6-C9) saturated or monounsaturated ketones (ketones); 2) o-cumene; 3) phenol, 1-ring alkylphenols and 1-ring guaiacols (phenols); 4) benzenediols and alkylbenzenediols, with either methyl or ethyl side groups (benzenediols); 5) 2-ring and 3-ring aromatic hydrocarbons (polyaromatic HC); 6) short-chain fatty acids (C5-C8); 7) long-chain fatty acids (C16-C18); 8) dehydroabietic acid. The chromatograms of bio-crude, and extracts E1 and E4 of extraction A are shown in

Figure 3a, whereas Figure 3b shows the corresponding chromatograms of the derivatised samples that served for identifying and quantitating the acids. The boiling points of the identified extracted components varied from approximately 150 ºC for the lighter components up to higher than 400 ºC for the heavier acids, with a consistent match with increasing retention tmes.

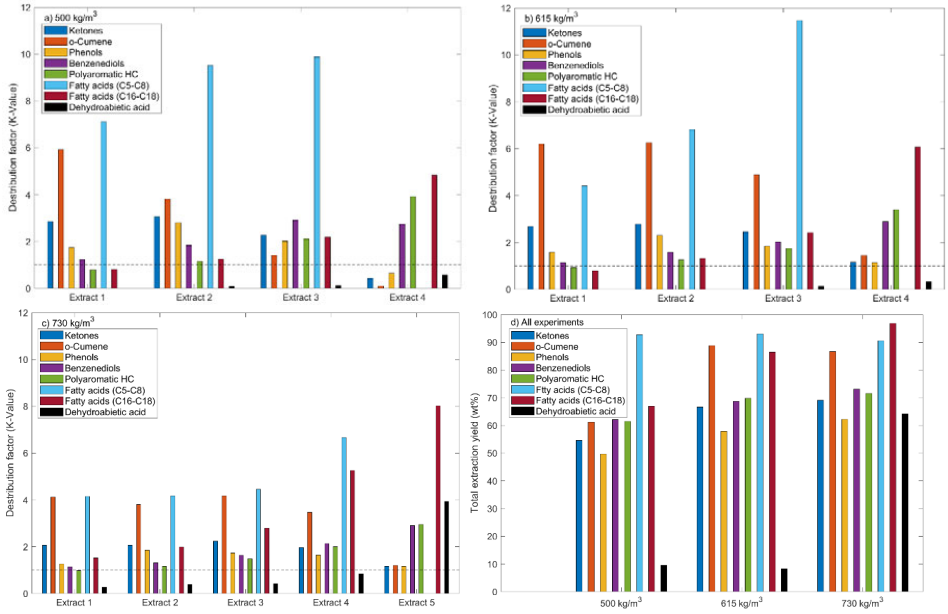


*Figure 4: a, b, c: Distribution factors of identified classes at 500, 615 and 730 kg/m$^3$ respectively; d: Total extraction yield of identified classes for all experiments.*

Figures 4a to 4c show the distribution factors (K-values) of the identified classes of components. Figure 4d shows the total extraction yield of each class. The K-values $(K_{ik})$ were calculated, in a $CO_2$-free basis, as:

$$K_{ik} = \frac{y_{ik}}{\frac{z_{i,k-1}+z_{ik}}{2}} \quad (1)$$

where $y_{ik}$ is the mass fraction of each class $i$ in an extract $k$ and $\left(\frac{z_{i,k-1}+z_{ik}}{2}\right)$ is an estimation of the average mass fraction of class $i$ in the extractor during the period of collection of the extract $k$. The total extraction yield $Y_{T,i}$ for each class $i$ was defined as:

$$Y_{T,i} = \frac{\sum_1^N E_k y_{ik}}{F z_i} \cdot 100 \quad (2)$$

where $E_k$ is the mass of extract $k$, $y_{ik}$ and $F$ were defined above, and $z_i$ is the mass fraction of the class $i$ in the feed. As can be seen from Figure 4, the lighter components (i.e ketones, o-cumene, short-chain fatty acids) are enriched in the extracts, owning the highest K-values in the initial period (up to 7) of each extraction. Phenols and benzenediols are also enriched in the first extracts, albeit with lower K-values (below 3). A noteworthy increase in the K-value for the polyaromatic hydrocarbons and the long-chain fatty acids is observed as the extraction progresses, with values close or below 1 at early extraction stages and up to 4 and 9, respectively, at the last stages. Interestingly, the K-value of dehydroabietic acid is considerably higher at 730 kg/m$^3$ compared to the lower solvent densities, leading to an extraction yieldover 60 %. This difference shows the remarkable tuneability of the $sCO_2$ extraction process by varying the solvent density. A general trend of K-values decreasing as boiling point increases was observed. The total extraction yield of the component classes follows the increase of the extraction yields, which increases with solvent density. The only exception is the fatty acids (C5-C8) that seem to be preferentially extracted in all cases and end up to yields close to 100 %. With regard to K-value ratios (i.e. selectivity between the identified classes), values

between 1.1 and 13 were found, with the majority being above 2. These selectivities indicate that multistage $sCO_2$ extraction units can separate the above-mentioned classes of chemicals in a downstream process.

## 4. Conclusion

The present work proves the feasibility of $sCO_2$ extraction of lignocellulosic HTL bio-crude at 120 ºC. Extraction yields (up to 49 %) comparable to vacuum distillation of a similar bio-crude (e.g. 52 %, Pedersen et al., 2017) .were achieved for $CO_2$ density of 730 kg/m$^3$. The extracts exhibit lower density values (956 – 1044 kg/m$^3$) compared to the feed (1064 kg/m$^3$), similar to those of marine fuels. The oxygen content of the extracts is however an order of magnitude higher than crude oil. Nevertheless, the reduced viscosity and density, as well as the enrichment of high boiling point oxygenated compounds in the residue, suggests the possibility of a milder and less problematic hydrotreatment of the extracts, compared to direct hydrotreatment of the HTL bio-crude. This, on the other hand, would require extensive cracking/hydroxydeoxygenation to be carried out on the residue. With focus to chemical composition, chemical classes such as ketones, phenols, aromatic hydrocarbons and fatty acids were identified and quantitated. These classes can be extracted with yields from 50 % up to values approaching 100 %, depending on the operating conditions. In addition, the selectivity of $sCO_2$ towards the separation of couples of classes of components shows values between 1.1 and 13, with average values around 2. This means that a downstream separation by multistage $sCO_2$ extraction is feasible, thus rendering HTL bio-crude an alternative source for the production of chemicals.

### References


Baloch H.A., Nizamuddin S., Siddiqui M.T.H., Riaz S., Jatoi A.S., Dumbre D.K., Mubarak N.M., Srinivasan M.P., Griffin G.J., 2018, Recent advances in production and upgrading of bio-oil from biomass: A critical review, Journal of Environmental Chemical Engineering, 6, 5101-5118.

Bjelic S., Yu J., Iversen B.B., Glasius M., Biller P., 2018, Detailed investigation into the asphaltene fraction of hydrothermal liquefaction derived biocrude and hydrotreated biocrudes, Energy and Fuels, 32, 3579-3587.

Castello D., Pedersen T., Rosendahl L., 2018, Continuous hydrothermal liquefaction of biomass: A critical review, Energies, 11, 3165.

Feng Y., Meier D., 2017, Supercritical carbon dioxide extraction of fast pyrolysis oil from softwood, Journal of Supercritical Fluids, 128, 6-17.

Gironi F., Maschietti M., 2007, Continuous countercurrent deterpenation of lemon essential oil by means of supercritical carbon dioxide: Experimental data and process modelling, Chemical Engineering Science, 63, 651–661.

Gironi F., Maschietti M., 2006, Separation of fish oils ethyl esters by means of supercritical carbon dioxide: Thermodynamic analysis and process modelling, Chemical Engineering Science, 61, 5114–5126.

Haarlemmer G., Guizani C., Anouti S., Déniel M., Roubaud A., Valin S., 2016, Analysis and comparison of bio-oils obtained by hydrothermal liquefaction and fast pyrolysis of beech wood, Fuel, 174, 180-188.

Jensen C.U., 2018, PIUS – Hydrofaction TM Platform with Integrated Upgrading Step, PhD Thesis, Aalborg University, Department of Energy Technology, Aalborg, Denmark.

Maqbool W., Hobson P., Dunn K., Doherty W., 2017, Supercritical carbon dioxide separation of carboxylic acids and phenolics from bio-oil of lignocellulosic origin: Understanding bio-oil compositions, compound solubilities, and their fractionation, Industrial & Engineering Chemistry Research, 56, 3129-3144.

Maschietti M.,2014, Separation of oils using supercritical carbon dioxide, Chapter in: J. Osborne (Ed.), Handbook of Supercritical Fluids, Nova Science Publishers Incorporated, New York, USA, 57-78.

Montesantos N., Pedersen T.H., Nielsen R.P., Rosendahl L., Maschietti M., 2019, Supercritical carbon dioxide fractionation of bio-crude produced by hydrothermal liquefaction of pinewood, Journal of Supercritical Fluids, Article in Press, DOI 10.1016/j.supflu.2019.04.001.

Nguyen T.D.H., Maschietti M., Belkheiri T., Åmand L.E., Theliander H., Vamling L., Olausson L., Andersson S.I., 2014, Catalytic depolymerisation and conversion of Kraft Lignin into liquid products using near-critical water, Journal of Supercritical Fluids, 86, 67-75.

Pedersen T.H., Grigoras I.F., Hoffmann J., Toor S.S., Daraban I.M. Jensen C.U., Iversen S.B., Madsen R.B., Glasius M,Arturi K.R., Nielsen R.P., Søgaard E.G., Rosendahl L.A., 2016, Continuous hydrothermal co-liquefaction of Aspen wood and glycerol with water phase recirculation, Applied Energy, 162, 1034-1041.

Pedersen T.H., Jensen C.U., Sandström L., Rosendahl L.A., 2017, Full characterization of compounds obtained from fractional distillation and upgrading of a HTL biocrude, Applied Energy, 202, 408-419.

Riha V., Bunner G., 2000, Separation of fish oil ethyl esters with supercritical carbon dioxide, Journal of Supercritical Fluids,17, 55–64.

Speight J.G., 2014, Chemical composition, Chapter in: Chemistry and Technology of Petroleum, Taylor & Francis, Boca Raton, USA, 212-236.

# Paper C

## Upgrading of nondewatered nondemetallized lignocellulosic biocrude from hydrothermal liquefaction using supercritical carbon dioxide

Nikolaos Montesantos, Rudi Pankratz Nielsen, Marco Maschietti

The manuscript has been published in

*Industrial and Engineering Chemistry Research*, Volume 59, Pages 6141-6153, 2020

I&EC research
Industrial & Engineering Chemistry Research
pubs.acs.org/IECR
Article

# Upgrading of Nondewatered Nondemetallized Lignocellulosic Biocrude from Hydrothermal Liquefaction Using Supercritical Carbon Dioxide

Nikolaos Montesantos, Rudi P. Nielsen, and Marco Maschietti*

Cite This: *Ind. Eng. Chem. Res.* 2020, 59, 6141−6153
Read Online
ACCESS | Metrics & More | Article Recommendations | Supporting Information

**ABSTRACT:** Supercritical carbon dioxide ($sCO_2$) extraction was applied on a raw biocrude, obtained by hydrothermal liquefaction of pinewood. The extractions were carried out in a semicontinuous mode, in the ranges of 80 to 150 °C and 330 to 450 bar. Extraction yields from 44 to 53 wt % were achieved. The extracts were richer in lower-molecular-weight (MW) compounds, with fatty acids and aromatic hydrocarbons concentrated up to 14 and 24 wt %, respectively. For comparable MWs, lower-polarity compounds concentrated in the extracts. Compared to the feed, the extracts exhibited a lower density (from 1030 kg/m$^3$ down to 914 kg/m$^3$), lower water content (from 5.7 wt % down to 1.3 wt %), and lower oxygen content (from 10.0 wt % down to 5.0 wt %). In addition, the metal content was drastically reduced (from 8500 mg/kg down to 170 mg/kg on average). In the context of biofuel production, the $sCO_2$ extracts are a better feed for catalytic hydrotreating.

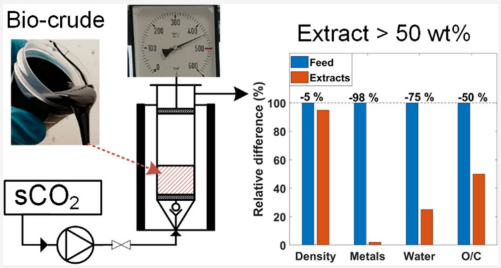




## 1. INTRODUCTION

Hydrothermal liquefaction (HTL) is a promising thermochemical process to produce liquid fuel from biomass. The process entails the depolymerization of biomass in an aqueous medium at a high temperature (e.g., 250−450 °C) and pressure (e.g., 100−350 bar).[1] One of the major advantages of HTL involves the flexibility of feedstocks that can be processed, which include both dry and wet biomasses.[2] The utilization of lignocellulosic biomass, an example of so-called second generation biomass, is particularly appealing due to lack of direct competition with food production. Wood residue and excess lignin from the paper pulp industry are examples of lignocellulosic byproducts produced in large quantities, which can be valorized to liquid fuels via HTL.[3−5]

Besides the water medium, the HTL process is typically carried out in the presence of homogeneous catalysts and pH adjusters, such as potassium carbonate ($K_2CO_3$), sodium carbonate ($Na_2CO_3$), and sodium hydroxide (NaOH).[1,6] The main products of HTL are a $CO_2$-rich gas phase (typically around 90 wt % $CO_2$),[7,8] a solid phase (i.e., char), and two liquid phases. The liquid products are an aqueous phase saturated of water-soluble organics and an oil, namely, the HTL biocrude.[1]

The HTL biocrude obtained by gravimetric separation of the products is a tight water-in-oil emulsion, with a water content in the range of 5 to 15 wt %.[9−12] Typical ash content values are reported broadly ranging from 0.01 wt % up to 5 wt %.[4,10,13] Individual values of the content of alkali and earth metals (e.g., potassium and iron) are typically not reported, except for a few cases.[3,4] In comparison to fossil crude oils, HTL biocrudes have relatively high oxygen content, typically in the range of 10 to 20 wt %.[10,12,14,15] The high oxygen content is caused by a variety of oxygenated components, such as ketones, fatty acids, and different one-ring phenols (e.g., phenol, guaiacols, and catechols). Moreover, oxygen is also expected to be contained in a complex large fraction of high boiling components, including phenolic oligomers derived from the lignin fraction.[16] The presence of a relatively large heavy fraction, essentially nonvolatile, is evident from previous works, reporting vacuum distillation of lignocellulosic HTL biocrudes. It was observed that approximately 50 wt % of the oil cannot be distilled even at very high vacuum (i.e., 1.3 mbar) at temperatures between 130 and 160 °C. The atmospheric equivalent boiling point of this heavy fraction was above 400 °C.[17,18] In the reported distillation experiments, the biocrude was dewatered prior to the process since the presence of water would reduce the distillation efficiency, resulting to unsteady boiling and creating control issues.[17] In addition to the above, HTL lignocellulosic biocrudes have a high viscosity (typically

Received: December 16, 2019
Revised: February 27, 2020
Accepted: February 27, 2020
Published: February 27, 2020





https://dx.doi.org/10.1021/acs.iecr.9b06889
*Ind. Eng. Chem. Res.* 2020, 59, 6141−6153

in the range of $10^3$ to $10^6$ cP)[19−21] and high density (typically above 1000 kg/m$^3$).[5,7,20,22]

To utilize HTL biocrudes as drop-in biofuels, the oxygen content has to be drastically reduced. The state-of-the-art method for this purpose is catalytic hydrotreating (i.e., hydrodeoxygenation, HDO).[23] However, hydrotreating of raw HTL biocrudes can lead to accelerated deactivation of the catalytic bed due to a high metal content, which originates from the alkali catalysts used in the HTL process and, to some extent, from the biomass itself.[21,24] These metals deposit on the active sites of the catalyst and promote sintering during catalyst regeneration.[25] Both of these mechanisms are irreversible. Even at low concentrations, metals can drastically reduce the lifetime of the catalyst, which needs to be replaced when the deposition of 3−4 wt % metals is reached.[26] In addition, water can reduce catalyst activity by modifying its surface or the pore structure.[25] Less water and oxygen in the HDO feed are therefore beneficial due to the lower hydrogen requirement of the process and the lower amount of water in the HDO reactor. In addition, reduced density values for the biocrude are desirable to increase the drop-in potential with different types of petroleum fuels, such as kerosene (775 to 840 kg/m$^3$),[27] diesel (820 to 845 kg/m$^3$),[28] and marine fuels (up to 991 kg/m$^3$).[29]

The application of a separation process upstream the hydrotreatment aimed at obtaining a large fraction of HTL biocrude, exhibiting favorable properties for the hydrotreating process itself (especially low water, oxygen, and metal contents), is worth analyzing. Among alternative separation processes, supercritical carbon dioxide ($sCO_2$) extraction is appealing for a number of reasons: (i) it is an environmentally friendly process, thus suitable by nature for the sustainability paradigm that should characterize biofuel production; (ii) $CO_2$ is internally generated in the HTL process; and (iii) it is a process competitive to distillation in the presence of high boiling point oils as temperatures required in distillation may be too high even at high vacuum.[30] The separation of high boiling point liquid mixtures using $sCO_2$ is at the industrial level for the fractionation of perfluoropolyether oligomers,[31] and it has been applied at the pilot or demonstration scale in a number of cases. Some representative examples include the separation of fish oil ethyl esters[32,33] or the removal of fatty acids from rice bran oil,[34] wheat germ oil,[35] and olive oil deodorizer distillate.[36]

In previous works, $sCO_2$ was reported capable of extracting a large fraction of a dewatered and demetallized lignocellulosic biocrude (extraction yields up to 49 wt %).[22,37] The procedure used for the dewatering and demetallization of the biocrude used in the mentioned previous works[22,37] is based on the dilution of the biocrude in methyl ethyl ketone followed by washing in citric acid aqueous solutions. Details on the procedure are available in the PhD thesis of Jensen.[38] The previous works[22,37] demonstrated problem-free operation above 80 °C (i.e., 80−120 °C), while the extractions were not smooth and sometimes characterized by equipment clogging at 40 and 60 °C. The only other works found on the extraction of lignocellulosic biocrudes refer to pyrolysis oils, where the extracts demonstrated a lower viscosity[39] and lower water content than the corresponding feeds.[40,41]

The aim of this work is to assess the $sCO_2$ extraction process on a raw HTL biocrude, which is to say a nondewatered nondemetallized biocrude obtained by gravimetric separation downstream the HTL reactor and without any further treatment. The specific objective of this work is therefore to assess the potential of $sCO_2$ extraction in carrying out dewatering, demetallization, and biocrude separation in a single process step, as well as to compare the characteristics of the $sCO_2$ separation on this raw biocrude with the separation reported in previous works, referring to a dewatered and demetallized biocrude.[22,37] In addition, the tested operating conditions were expanded to higher pressures (up to 450 bar) and temperatures (up to 150 °C) as the previous works[22,37] indicated a positive effect by increasing these parameters. Extraction temperatures below 80 °C were instead not considered due to the abovementioned operating problems.

## 2. MATERIALS AND METHODS

**2.1. Materials.** *2.1.1. Feed Biocrude.* The feed HTL biocrude was produced by continuous-flow hydrothermal liquefaction of pinewood at 400 °C and 300 bar using potassium carbonate as a catalyst and sodium hydroxide for pH adjustment, as previously reported in the literature.[22] Details on the effect of the operating parameters on the hydrothermal liquefaction process can be found in the work of Jensen et al.[6] As a difference compared to the previous work where $sCO_2$ was used to fractionate the biocrude obtained in this thermochemical process, in the present work, the biocrude underwent neither dewatering nor demetallization. Therefore, it is a raw biocrude simply obtained by gravimetric separation from the aqueous phase downstream of the HTL reactor. It appears as a black high-viscosity liquid (Figure 1a), even though less viscous than the biocrude of the previous work,[22] and as a stable emulsion of water in oil since no phase separation was observed during 6 months of storage.

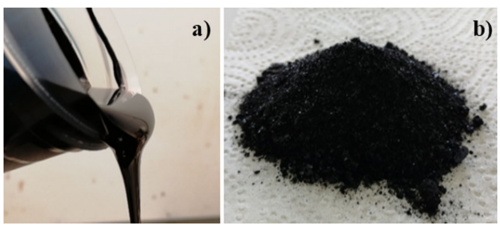


**Figure 1.** (a) HTL biocrude used in this work. (b) Example of the residue after $sCO_2$ extraction, tetrahydrofuran evaporation, and mortar grinding. The example refers to the run at 450 bar and 100 °C.

*2.1.2. Chemicals.* Carbon dioxide ($CO_2$, 99.7%) used for the supercritical extractions was purchased from Air Liquide (Denmark). Diethyl ether (DEE, 99%) from VWR and pyridine (ACS grade) from Hach were used as solvents for the GC−MS analysis, while vanillin (99.8%) and myristic acid (99%) from Sigma-Aldrich were used as internal standards. *N*,*O*-Bis(trimethylsilyl)trifluoroacetamide (BSTFA, 98.5%) from Sigma-Aldrich was used to derivatize samples. HYDRANAL titrant 2 and solvent oil from Fluka, as well as the Aquastar 1% standard from Merck were used for the Karl Fischer (KF) titrations. The elemental analyzer was calibrated with the PerkinElmer cystine 4G powder. Tetrahydrofuran (THF, 99.9%) from VWR was used as the solvent for retrieving the residue inside the $sCO_2$ extractor at the end of each extraction. Ethylene glycol (glycol, 98%) from VWR was used to prepare the aqueous solution (1:1 by mass) employed



https://dx.doi.org/10.1021/acs.iecr.9b06889
Ind. Eng. Chem. Res. 2020, 59, 6141−6153

as cooling fluid in the cold trap described in Section 2.2. Tetrabutylammonium hydroxide (TBAOH, 0.1 M) in 2-propanol/methanol from Merck and tetraethyl ammonium bromide (TEABr, 0.4 M) in ethylene glycol (Metrohm) were used as the titrant and electrode electrolyte for the total acid number (TAN) measurements. Toluene (99.5%) and 2-propanol (99.8%) from VWR were used as solvents for the TAN measurements. NIST traceable Metrohm buffers (i.e., pH 4, 7, and 9) were used for calibration of the TAN electrode. Methyl ethyl ketone (MEK, 99%) and methyl isobutyl ketone (MIBK, 99%) from VWR, as well as THF, were used as solvents to estimate the density of the biocrude. A 7 M nitric acid aqueous solution was used for acid digestion, and the PlasmaCAL multielement standard from SCP Science was used for the calibration of the ICP-OES instrument.

**2.2. Supercritical $CO_2$ Extraction.** The experimental setup was described in detail in a previous publication.[22] Therefore, only a short description of the setup and the experimental method used in this work, together with notes about modifications, is provided here. The apparatus consists of a high-pressure extraction vessel (i.e., the extractor) with a 178 $cm^3$ basket insert, where approximately 50 g of biocrude were charged prior to an extraction. The basket insert was packed with 6 mm soda-lime glass beads up to approximately 1/3 of its height. The glass beads were chosen as an inert packing material that can disperse the biocrude feed and improve its contact with the flowing $sCO_2$. A cylindrical filter (pore size, 10 $\mu$m) is used at the top of the basket to prevent entrainment of particles. An automatically controlled heating jacket maintained the extraction temperature, which, in this work, was in the range of 80 to 150 °C. The temperature indication was within ±0.5 °C of the set value in all extractions. Liquid $CO_2$ from a dip tube cylinder was subcooled by means of a heat exchanger fed with cold water (approximately 5 °C), which was provided by a thermostatic bath (Braun Frigomix U) and erogated by an immersion circulator (Julabo ED). Subsequently, the $CO_2$ was compressed by a high-pressure pneumatic pump and fed to the entry port at the bottom of the extractor. The extraction pressure and the solvent flow rate were regulated manually by the pressure of the air supply of the pump and by a micrometering valve downstream the extractor. The extraction pressures selected for this study were 330 and 450 bar. At the tested conditions, the extractions were smooth, with pressure gauge readings within ±3 bar of the set value in all runs. The micrometering valve was heated by hot air. The extract was collected in a 20 mL sampling vial inserted in a washing bottle immersed in a cold bath that was kept at approximately −10 °C by means of a refrigerating circulator (Lab Companion RW3-0525P). A subsequent gas washing bottle immersed in the cold bath was packed with 3−4 g of cotton wool and aimed at collecting any further condensate or retaining fine droplets or particles that might be entrained with the $CO_2$,to protect the downstream gas meter. The cotton wool was weighed after each extraction to account in the mass balance. The weight difference of the cotton before and after an extraction was on average 0.1 g, while there was no condensate observed in the corresponding gas washing bottle. The gas meter (Ritter TG3; max flow, 6 L/min; min flow, 0.1 L/min; accuracy, 0.5%) measured the volume of $CO_2$ flowing through it and was equipped with a thermometer for measuring the gas temperature. The $CO_2$ flow rate in this work was in the range of 3 to 4 L/min at gas meter conditions, corresponding to mass flow rates in the range of 4 to 6 g/min. After the completion of each extraction, the apparatus was depressurized and let to cool down to about 80 °C, and the basket insert was dismounted and washed with 100−150 mL of THF to retrieve the residue. Preliminary tests showed that allowing the system to cool down to ambient temperature was unfeasible since the residue solidified, incorporating the glass beads and making its own retrieval problematic even with large amounts of THF. The drawback of the recovery of the residue at 80 °C consisted in THF evaporation, together with losses of water contained in the residue, which increased the uncertainty in the mass balance of water, as discussed in Section 3. For extraction D (see Section 3.2), a small sample (approximately 1 g) of the mixture THF + residue was saved for KF analysis, prior to solvent evaporation. THF was then separated from the residue by rotary vacuum evaporation at 50 °C. The amount of THF in the mixture was estimated by subtracting the mass of the residue after evaporation from the mixture THF + residue before evaporation. After the evaporation of THF, the residue appeared as a dry solid. It was ground in a mortar to obtain a fine powder (Figure 1b) and to ensure representative sampling for analysis.

**2.3. Analytical Characterization.** *2.3.1. Elemental Analysis.* Elemental analysis (EA) was performed with a PerkinElmer 2400 Series II CHNS/O analyzer coupled with a PerkinElmer AD-6 autobalance. Carbon, hydrogen, and nitrogen were measured, while oxygen was calculated by the difference. Sulfur was in all measurements under the detection limit of the instrument and was omitted since it is not expected to be present in this type of biocrude. The instrument was calibrated by the cystine standard (single point calibration) prior to each series of measurements, which were performed at least in triplicate. The absolute relative deviation (ARD) between the measured elemental mass fractions of the standard compared to the theoretical values for C, H, and N was on average 0.4%. The relative standard deviation (RSD) on oxygen was 17% for the feed biocrude, whereas it was on average 21% for the extracts and 6.4% for the residues.

*2.3.2. Water Content.* A Metrohm 870 KF Titrino plus, coupled with a Metrohm 860 KF Thermoprep, was used for the KF water determination. The instrument was calibrated regularly with the Aquastar 1% standard, as well as controlled with the standard prior to daily measurements. The ARD between the measured mass fraction of water of the standard and its theoretical value was always below 3%. Approximately 0.1 g of biocrude, extracts, and residue (after solvent evaporation) were analyzed. A sample of approximately 0.1 g was titrated also for the residue + THF mixture sample, in the case of extraction D (see Section 3.2). In this case, however, also the pure THF used for retrieving the residue was titrated to account for water already contained in the solvent. All KF measurements were performed at least in triplicate. The RSD for the feed biocrude was 4.9%, whereas it was on average 4.8% for the extracts and 1.4% for the residues.

*2.3.3. Acid Number Measurements.* The acid number measurements were carried out by potentiometric titration on a Metrohm Titrando 888 equipped with a Metrohm Solvotrode, following a procedure based on a modification of ASTM D664 test method B, which was developed in a previous work.[22] The titration solvent was a mixture of toluene, 2-propanol, and demineralized water (100:99:0.5, by volume), instead of pure 2-propanol,[42] as this mixture proved more effective in dissolving the biocrude and its extracts of this work. Approximately 0.1 g of bio-crude, extract, or residue was


https://dx.doi.org/10.1021/acs.iecr.9b06889
Ind. Eng. Chem. Res. 2020, 59, 6141−6153

diluted in 50 mL of the titration solvent and titrated. The method allows for determination of two acid numbers: the carboxylic acid number (CAN) and the total acid number (TAN), both expressed as mg KOH/g. The difference between TAN and CAN is the acid number that corresponds to the phenolic nature of acidity (PhAN), which is an important factor in lignocellulosic biocrudes. The electrode was calibrated with three NIST traceable buffers (i.e., pH 4, 7, and 9), and the calibration always demonstrated an $R$-squared ($R^2$) of at least 0.999 between pH and the measured electrical potential. According to the method, two inflection points are observed during the titration, which correspond to CAN and TAN, respectively. All TAN measurements were performed at least in triplicate. The RSD values on TAN, CAN, and PhAN for the feed biocrude were 2.1, 1.4, and 2.9%, respectively. The average RSD values on TAN, CAN, and PhAN for the extracts were 1.6, 1.0, and 1.6%, respectively. The average RSD values on TAN, CAN, and PhAN for the residues were 1.3, 0.8, and 1.0%, respectively.

*2.3.4. Density Measurement.* The density measurements were performed following a procedure developed before.[22] The biocrude density was measured with an Anton Paar DMA 35 Ex densitometer after dilution in three solvents (THF, MIBK, and MEK), 1:1 by mass in each. Due to the small quantity of the $sCO_2$ extracts, their density was calculated by accurately measuring the mass of a volume displaced by a precision pipette (Gilson MICROMAN M1000). The mass was weighed on an analytical balance (OHAUS PA224C), and the capillary piston used for each measurement was calibrated with distilled water to calculate accurately the displaced volume. The RSD of triplicate pipetting of distilled water was always lower than 1%. Density of pure water at the laboratory ambient conditions was taken from NIST.[43] All density measurements were performed in triplicate. The RSD for the feed biocrude was 0.9%, whereas it was on average 1.4% for the extracts.

*2.3.5. Metal Content Determination by ICP-OES.* The metal content of the feed and all the extracts, together with the metal content of the residue of selected extractions, was determined by inductively coupled plasma-optical emission spectrometry (ICP-OES), utilizing a PerkinElmer Optima 8000 system. The contents of potassium (K) and sodium (Na) were measured since they were expected due to the use of $K_2CO_3$ as the catalyst and NaOH as the pH adjuster in the HTL process. Additional metals subjected to quantitation were aluminum (Al), iron (Fe), magnesium (Mg), and titanium (Ti) since they are expected to derive from wear of equipment and the natural presence in the pinewood biomass.[24] Samples were prepared by acid digestion and dilution. Approximately 0.5 g of sample was digested in an autoclave in 20 mL of 7 M aqueous nitric acid for 30 min at 120 °C and 2 bar. A blank of the nitric acid solution was digested as well for each set of samples, and nonzero concentrations were subtracted from the sample measurement to account for baseline errors. The digested samples were diluted with distilled water in a volumetric flask (class A) and filtered by filter paper (pore size, 4−12 μm). Dilution to 50 mL was performed for the biocrude and the residues, while dilution to 25 mL was applied for the extracts. In the case of visually observed turbidity of the solution, which was assumed to be due to organic particles, a second filtration was performed to acquire a transparent fluid to protect the plasma torch. To ascertain the reproducibility of the sample preparation procedure, eight samples of different masses of the feed biocrude (i.e., 0.4 to 1 g) were digested and analyzed. The extracts and residues were measured in duplicate. The standard solutions used for calibration were prepared by diluting the PlasmaCAL standard in demineralized water and measured in triplicate. The range was 0.2 to 2 mg/L for all the metals, with the exception of Fe (0.2 to 10 mg/L), K (2 to 100 mg/L), and Na (2 to 10 mg/L). The $R^2$ for all elements was always above 0.999 except for Na, which was, however, always above 0.988. The RSD of the triplicate measurements of the calibration standards was always lower than 1%, while the ARD with respect to the analyzed standard value was always between 0 and 4% for all metals except Na. In fact, Na had a higher ARD (always lower than 20%), which is assumed to be an inherent instrument inaccuracy for Na measurement. High uncertainty in Na concentration by ICP measurements has been reported in the literature for fast pyrolysis oil of woody biomass.[44]

*2.3.6. Component Identification by GC−MS.* GC−MS analysis was performed for the identification and quantitation of the GC-detectable fraction (i.e., the volatile fraction) of the biocrude feed and the extracts. In addition, GC−MS after silylation was performed to identify and quantify free fatty acids and a few phenolic components for which the ion peaks had better resolution than in the nonsilylated samples. The analysis was performed on a PerkinElmer Clarus 680 GC coupled with a PerkinElmer Clarus SQ 8T MS. For the analysis of the feed, the biocrude was extracted with DEE (biocrude to solvent ratio approximately 1:50 by mass) and the resulting DEE-rich mixture was filtered with a syringe filter (pore size, 0.45 μm). The amount of the DEE-soluble fraction of the biocrude was determined gravimetrically from the filtrate, after evaporation of the solvent overnight in a fume hood. All $sCO_2$ extracts were instead fully soluble at a 1:10 extract to DEE ratio (mass basis). GC−MS samples were prepared by mixing approximately 0.1 g of the DEE-soluble fraction of the feed or approximately 0.1 g of extract with approximately 0.7 g of a DEE solution containing a known amount of vanillin (1 wt %) as the internal standard (IS). Vanillin was selected as the IS as most of the identified components were oxygenated aromatics with some degree of similarity to vanillin, with vanillin being, however, not present in the biocrude samples and not overlapping with chromatographic peaks of species contained in the biocrude samples. With regard to the GC−MS after silylation, the feed and extract samples were silylated as follows: about 0.1 g of each sample was dried in a heating cabinet for 2 h at 120 °C, then diluted in pyridine, which contained a known amount of myristic acid (1 wt %) as the IS, and derivatized with BSTFA at 60 °C for 20 min. Myristic acid was selected as the IS as the GC−MS analysis after silylation was aimed at fatty acids, with myristic acid being, however, not present in the biocrude and not overlapping with chromatographic peaks of species contained in the biocrude samples. The mixture ratio of sample/pyridine/BSTFA was 1:1:1 in mass basis. The derivatized samples were further diluted in DEE (1:25 by mass). For all samples, 1 μL was injected in a PerkinElmer Elite-5 column (30 m, 0.25 mm ID, 0.1 μm), with the temperature ramping from 40 to 250 °C at a rate of 10 °C/min. The initial temperature was held for 3 min, while the final temperature was held for 6 min. The injector was maintained at 300 °C and the helium carrier gas at 1.0 mL/min. The mass fraction of the identified analytes i was calculated as $w_i = w_{IS} \times A_i/A_{IS}$, where $A_i$ and $A_{IS}$ are the chromatographic areas of the analyte i and the IS, respectively, whereas $w_{IS}$ is the mass


https://dx.doi.org/10.1021/acs.iecr.9b06889
Ind. Eng. Chem. Res. 2020, 59, 6141−6153

fraction of the internal standard (vanillin for pure samples and myristic acid for derivatized samples). Triplicate GC−MS measurements were performed for all samples in random consecution to account for random GC response differences.

## 3. RESULTS AND DISCUSSION

**3.1. Characterization of the Feed Biocrude.** Table 1 reports the measured bulk properties of the biocrude feed, including the DEE-soluble fraction, density, TAN, CAN, PhAN, and water and metal contents. In addition, the elemental carbon (C), hydrogen (H), nitrogen (N), and oxygen (O) mass fractions, as well as the H/C and O/C ratios, are reported on a water-free basis. As can be seen, the density of this biocrude is approximately 1030 kg/m$^3$, which is in line with values reported for HTL biocrudes from lignocellulosic biomass, reported in the range of 970 to 1140 kg/m$^3$.[5,17,20] The TAN value of 97 mg KOH/g is within the values reported in the literature, which range from 30 to 150 mg KOH/g for HTL lignocellulosic biocrudes.[5,18,45] With regard to the elemental composition, the mass fractions are also in line with typical woody HTL biocrudes (i.e., C: 0.76−0.84; H: 0.07−0.10; N: 0.002−0.030; and O: 0.05−0.15).[5,7,17,18]

**Table 1. Bulk Properties at Ambient Conditions, Elemental Composition on a Water-Free Basis, and Metal Mass Fraction of the Feed Biocrude with Standard Deviations**

| property | | metal content (mg/kg) | |
|---|---|---|---|
| DEE-soluble fraction | 0.70 ± 0.03 | Al | 40 ± 9 |
| density (kg/m$^3$) | 1030 ± 9 | Fe | 190 ± 20 |
| TAN (mg KOH/g) | 97 ± 2 | K | 3400 ± 400 |
| CAN (mg KOH/g) | 42 ± 1 | Mg | 96 ± 20 |
| PhAN (mg KOH/g) | 56 ± 2 | Na | 3800 ± 500 |
| water content (wt %) | 5.7 ± 0.4 | Ti | 40 ± 3 |
| C mass fraction | 0.80 ± 0.01 | total metals | 8500 ± 800 |
| H mass fraction | 0.08 ± 0.01 | | |
| O mass fraction | 0.10 ± 0.02 | | |
| N mass fraction | 0.017 ± 0.005 | | |
| H/C | 1.2 ± 0.1 | | |
| O/C | 0.09 ± 0.02 | | |

As can be seen in Table 1, the biocrude exhibits a water content of almost 6 wt %, which is at the lower range of typical reported values for HTL lignocellulosic biocrudes (i.e., 5−15 wt %).[4,5,7,17] In addition, the biocrude exhibits a high metal content of around 0.85 wt %, with potassium (K) and sodium (Na) constituting more than 90% of the total. The metal content is dependent on the biomass ash content, but since woody biomass has typically low ash,[46] the high metal content mostly originates from the chemicals used in the HTL process. This behavior was observed by Déniel et al.,[21] who performed HTL of blackcurrant pomace and observed ash contents in the biocrude increasing (i.e., from 0.1 to 5.3 wt %) with sodium hydroxide added, (i.e. from 0 to 9 wt %). With regard to Mg, it is known to bind with organic molecules in biomass,[47] while Al and Fe are typically introduced during the harvesting and processing of the biomass.[24] Ti is one of the less abundant metals in biomass,[47] which is assumed to be introduced by equipment wear. The presence of Mg, Al, Fe, and Ti, although in a relatively small amount (0.03 wt % in total), is confirmed in this work.

In total, 46 components were identified by GC−MS in the DEE-soluble fraction of the feed. Detailed list of the components along with retention time (RT), classification, molecular weight (MW), chemical formula, CAS registry number, and their mass fraction (wt %) in the feed biocrude is reported in the Supporting Information (Table S1). The identified components constitute 19.3 wt % feed biocrude. The unidentified components of this volatile fraction correspond to a chromatographic area that is about twice as large as the identified fraction, which means that, as a rough estimation, about 60 wt % biocrude can be assumed as volatile. The identified components were lumped into 10 categories according to their chemical functionalities: (1) saturated/mono-unsaturated cyclic aliphatic ketones (C6−C9) (ketones, K); (2) alkylbenzenes (AB); (3) phenol and alkylphenols (phenols, P); (4) guaiacol and alkylguaiacols (guaiacols, G); (5) benzenediols and acetyl derivatives of benzenediols (BD); (6) 2- and 3-ring aromatic hydrocarbons (PAH); (7) dehydroabeityl alcohol (ArAl); (8) short chain fatty acids (SFA), in the range of C2−C8; (9) long chain fatty acids (LFA), in the range of C16−C18; and (10) dehydroabietic acid (ArAcid).

The largest fraction of the identified components is constituted by PAHs, which account for 9 wt % of the biocrude. Even though such components are not often

**Table 2. Experimental Extraction Conditions and Results[a]**

| run ID | A | B | C | D | E | F | G | H |
|---|---|---|---|---|---|---|---|---|
| $T$ (°C) | 80 | 100 | 120 | 150 | 80 | 100 | 120 | 150 |
| $P$ (bar) | 330 | 330 | 330 | 330 | 450 | 450 | 450 | 450 |
| $\rho$ (kg/m$^3$)[b] | 773 | 696 | 623 | 531 | 851 | 790 | 731 | 650 |
| $Q$ (g/min) | 5.2 | 5.5 | 5.0 | 4.7 | 5.7 | 5.9 | 5.0 | 4.8 |
| $F$ (g) | 48.9 | 52.6 | 51.3 | 53.6 | 53.9 | 51.5 | 54.2 | 51.9 |
| E1 (g) | 6.6 | 5.7 | 7.7 | 5.4 | 5.3 | 8.4 | 6.9 | 6.6 |
| E2 (g) | 6.1 | 5.9 | 5.3 | 6.9 | 5.3 | 5.8 | 6.4 | 7.6 |
| E3 (g) | 8.9 | 6.0 | 5.6 | 5.0 | 5.3 | 5.5 | 6.9 | 6.2 |
| E4 (g) | | 6.2 | 5.0 | 7.5 | 8.1 | 7.2 | 7.8 | 7.3 |
| $R$ (g) | 23.1 | 24.4 | 22.8 | 23.8 | 23.9 | 21.0 | 22.2 | 18.0 |
| $L$ (%) | 8.2 | 6.5 | 9.4 | 9.0 | 9.4 | 7.0 | 8.5 | 12.0 |
| $S/F$ (g/g) | 30.2 | 36.5 | 36.3 | 31.6 | 32.4 | 36.7 | 33.3 | 30.0 |
| $Y_T$ (%) | 44.1 | 45.1 | 46.0 | 46.3 | 47.3 | 52.4 | 51.5 | 53.4 |

[a]Temperature ($T$), pressure ($P$), $CO_2$ density ($\rho$), average $CO_2$ mass flow rate ($Q$), mass of feed ($F$), mass of extract samples (E1, E2, E3, E4), mass of residue ($R$), losses ($L$), solvent-to-feed ratio ($S/F$), and total yield ($Y_T$). [b]Taken from NIST.[43]



https://dx.doi.org/10.1021/acs.iecr.9b06889
Ind. Eng. Chem. Res. 2020, 59, 6141−6153

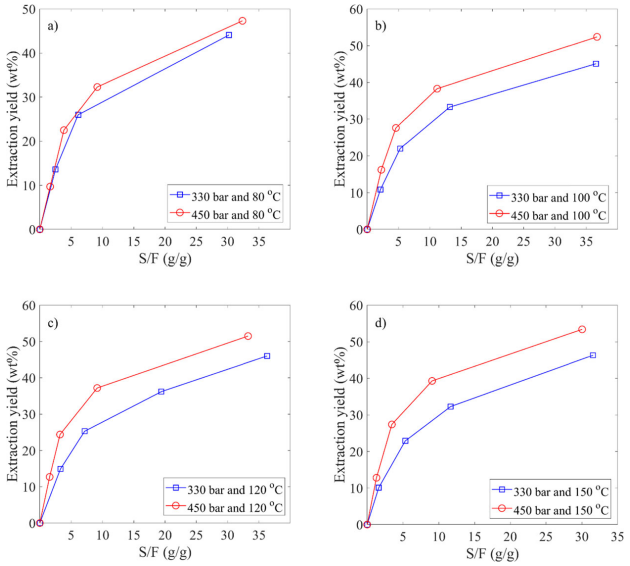


**Figure 2.** Pressure effect on the extraction yield vs solvent-to-feed ratio ($S/F$) at (a) 80 °C, (b) 100 °C, (c) 120 °C, and (d) 150 °C.

reported, some have been reported by Pedersen et al.[18] in the distillation residue of woody HTL biocrude. Retene has been reported in the HTL biocrude of softwood lignin.[48] Retene and phenanthrenes are possibly the degradation products of dehydroabietic acid in the biomass since they are typically found as products of its thermal degradation (e.g., wood smoke).[49,50]

Single-ring aromatic hydrocarbons (alkylbenzenes, AB) are also found, albeit in a lower amount (1 wt %). Aliphatic hydrocarbons are not observed. Fatty acids (SFA + LFA) are the second most abundant group, accounting for almost 4 wt % oil, with the LFA being largely predominant (3.75 wt %). Fatty acids are typically one of the most abundant classes in biocrudes,[51] although their mass fractions are not often reported. Dehydroabietic acid and dehydroabeityl alcohol are also observed in remarkable amounts, 1.8 and 0.4 wt %, respectively. Abietane skeleton diterpenoids are major structures of conifers such as pine,[50] and dehydroabietic acid is therefore expected to be present in the pine biomass of the biocrude used in this work. The presence of dehydroabietic acid in the biocrude suggests that it remains unconverted, to some extent, during the HTL process. Ketones are always present in lignocellulosic biocrudes. However, even though they are numerous, they are in a low amount, summing up to 0.5 wt % oil. Single-ring phenolics (alkylphenols, catechols, and other types of benzenediols, and guaiacol) account altogether for 2.6% biocrude. Alkylphenols, catechols, and guaiacols are typically observed in HTL of softwood lignin,[3,14,48] with the ratio of catechols to guaiacols increasing with the HTL reaction temperature.[14,48] Their presence and the low guaiacol/catechol ratio are therefore qualitatively in line with the high-temperature hydrothermal decomposition of the lignin contained in the original biomass of this work.

**3.2. Extraction Conditions and Yields.** The experimental conditions and mass balances for each supercritical extraction are reported in Table 2. Four different extraction temperatures (i.e., 80, 100, 120, and 150 °C) were tested at two pressures (i.e., 330 and 450 bar). The lower pressure (330 bar) was chosen to be within the typical pressure range of the HTL process,[19] therefore allowing the investigation of the $sCO_2$ extraction at pressure levels comparable to the HTL reactor, as higher pressures in the downstream separation would be less favorable for process economics. The higher pressure (450 bar) was selected on the basis of previous works,[22,37] which showed promising results in terms of attainment of high extraction yields. The duration of the extractions was between 5.3 and 6.4 h. Table 2 also reports the density of pure $CO_2$ at the operating conditions of the extraction ($\rho$), the average solvent mass flow rate ($Q$), the mass of feed biocrude charged in the extractor at the beginning of an experiment ($F$), the mass of the four extracts collected in each extraction (E1, E2, E3, and E4), with the exception of run A where only three extracts were collected. Run A was the extraction with the lowest yield, and the third sampling vial (i.e,. E3) was maintained for a longer period to avoid ending up with E4 sample mass inadequate for analysis. The mass balance discrepancy (losses, $L$) of each run is also reported, together with the total solvent-to-feed ratio (i.e., at the end of the run) and the total extraction yield. The total extraction yield is defined as the ratio of the total mass of the collected extracts to the mass of the feed. It is therefore determined gravimetrically. Data from Table 2 were also used to calculate the vapor phase loading (VPL) as the extractions progress. VPL is defined as the ratio of the mass of extract in a given time interval over the mass of solvent flowed in the same interval. VPL values were also used to evaluate the reproducibility of the extraction procedure. In this regard, six repetitions of run H were carried out, and the RSD values on VPLs were found to be 7.1% for extract 1 (E1), 11.6% for


https://dx.doi.org/10.1021/acs.iecr.9b06889
Ind. Eng. Chem. Res. 2020, 59, 6141−6153

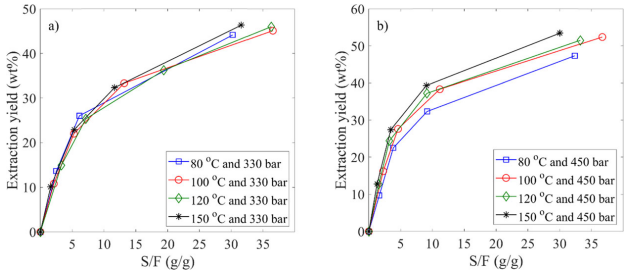


**Figure 3.** Temperature effect on the extraction yield vs solvent-to-feed ratio ($S/F$) at (a) 330 bar and (b) 450 bar.

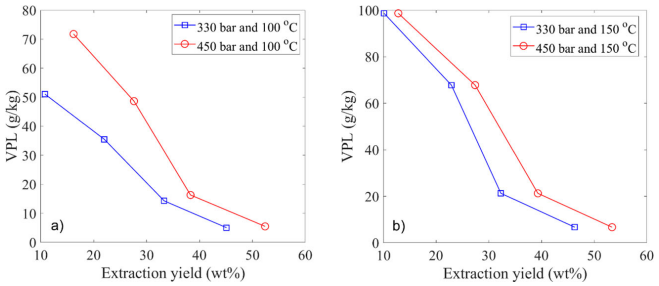


**Figure 4.** Pressure effect on the vapor phase loading (VPL) vs extraction yield at (a) 100 °C and (b) 150 °C.

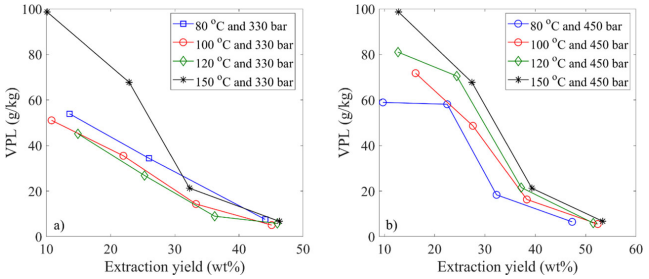


**Figure 5.** Temperature effect on the vapor phase loading (VPL) vs extraction yield at (a) 330 bar and (b) 450 bar.

extract 2 (E2), 14.0% for extract 3 (E3), and 11.3% for extract 4 (E4).

In Table 2, it can be seen that the highest extraction yield of 53.4% is not achieved at the highest solvent density but, in fact, at the highest temperature and in combination with high pressure. This observation highlights the importance of high temperatures for $sCO_2$ separation of biocrudes, and it is in line with previous works,[22,37] where extraction yields up to 48.9% have been achieved at 448 bar and 120 °C, while low efficiency and bad operability were observed below 80 °C. Importantly, not only was run H characterized by the highest yield but also by the lowest $S/F$ (i.e., 30 g/g). These results indicate that operating conditions of the downstream $sCO_2$ separation at pressures higher than the pressure of the HTL reactor should not be discarded a priori in the design of the process.

In Figure 2, the extraction yield is plotted versus the solvent-to-feed ratio at four different temperatures and two pressures. In all cases, the effect of pressure is beneficial for the extraction efficiency, showing higher extraction yields at given $S/F$ values. This is a general feature in $sCO_2$ separation processes since higher pressures at given temperatures lead to higher solvent density and increased solvent power. The perusal of Figure 2 also shows that the increase in process efficiency with pressure at given temperature is more pronounced at higher temperatures. This is due to the isothermal variation of the solvent density, which is monotonically increasing with temperature, ranging from 78 to 119 kg/m$^3$ as temperature increases from 80 to 150 °C. The increase of the yield for given $S/F$ as pressure increases at constant temperature, which is to say the increased extract-to-solvent ratio ($E/S$) with pressure, is typically observed in $sCO_2$ extraction processes. The primary reason is the increase in solubility of extractable species in the supercritical solvent. However, it is recognized that the extraction yield is affected by both the solubility of extractable species and by mass transfer parameters.[52]



https://dx.doi.org/10.1021/acs.iecr.9b06889
Ind. Eng. Chem. Res. 2020, 59, 6141−6153

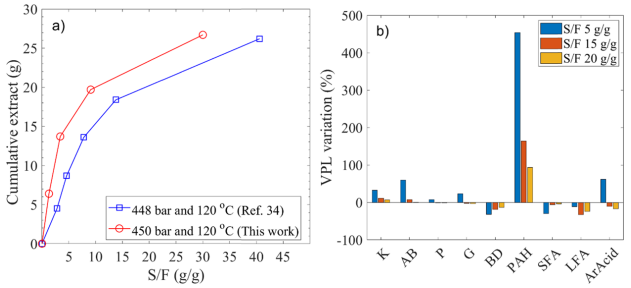


**Figure 6.** (a) Cumulative extract mass (normalized to 50 g of feed) vs $S/F$ for extraction of dewatered biocrude (2.7 wt % water)[37] and the biocrude of this work (5.7 wt % water). (b) Vapor phase loading (VPL) variation of chemical classes between dewatered biocrude[37] and the biocrude studied in this work. Ketones (K); alkylbenzenes (AB); phenols (P); guaiacols (G); benzenediols (BD); 2- and 3-ring aromatic hydrocarbons (PAH); short chain fatty acids (SFA), in the range of C2−C8; long chain fatty acids (LFA), in the range C16−C18; and dehydroabietic acid (ArAcid).

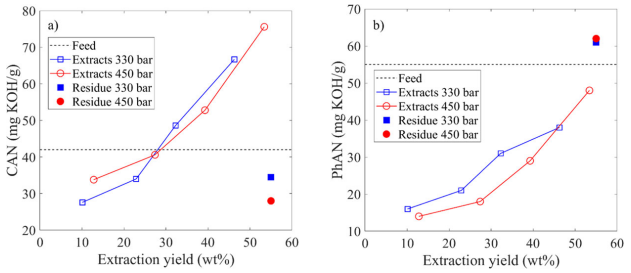


**Figure 7.** Effect of pressure on (a) CAN vs extraction yield and (b) PhAN vs extraction yield at 150 °C.

To visualize this combined effect, Figure 3 shows the extraction yield against $S/F$ at the two studied pressures (i.e., 330 and 450 bar). At 330 bar, it is observed that, even though the increase of temperature decreases the solvent density, the extraction yields are comparable for all temperatures. This could indicate that the solubility of the biocrude at this pressure reduces with temperature, but the mass transfer parameters improve enough to counteract the reducing solubility. Contrary to the behavior at 330 bar, at 450 bar, the extraction yield slightly increases with temperature. This could be either due to a crossover pressure between 330 and 450 bar that results to solubility increasing with temperature or due to mass transfer improvements, prevailing to the solubility decrease with temperature. Phase equilibrium measurements of the solubility of this type of biocrude in $sCO_2$ are not available in the literature, and they would be needed to prove the abovementioned hypotheses.

In theory, the slope of the curves in Figure 2 and Figure 3 ($dE/dS$) indicates the vapor phase loading (VPL), that is, the instantaneous value of the mass of components extracted per unit mass of solvent. The collection of a number of extracts per each run allowed to estimate average VPL values ($\Delta E/\Delta S$) as the extraction proceeds. Results are presented for the extractions at 100 °C (Figure 4a) and 150 °C (Figure 4b) and at 330 (Figure 5a) and 450 bar (Figure 5b). Similar trends as shown in Figure 4 are observed at all temperatures being studied.

As usual, VPL values decrease during the extraction, as the unextracted biocrude remaining inside the extractor becomes progressively heavier. As can be seen from Figure 4, higher pressure at given temperature leads to higher VPL values, which resulted to the highest extraction yield with the least solvent used in run H. On the other hand, the effect of temperature is more complex, as can be seen in Figure 5. Figure 5b shows that higher temperatures affect positively the VPL at 450 bar, especially in the early stages of the extraction, whereas at 330 bar (Figure 5a), this effect is only observed at the highest temperature (i.e., 150 °C) and for extraction yields below approximately 30 wt %.

An interesting observation arises when the results of this work at 120 °C and 450 bar are compared with an extraction run carried out at basically the same conditions (120 °C and 448 bar) on a dewatered biocrude (water content, 2.7%), presented in a previous work.[37] In Figure 6a, the cumulative extract is plotted against $S/F$ for a normalized feed mass (i.e., 50 g). It can be seen that the extraction is more efficient for the nondewatered biocrude of this work. The results of this work show an increase in extract in the range of 3 to 6 g, for given $S/F$ values ranging from 1.3 to 30. The difference in the water content for 50 g of the two biocrudes is 1.5 g. Considering that the variation of the extract mass is 2 to 4 times higher than the water content in the feed, it is apparent that the increase in the extract cannot be entirely attributed to the extraction of water itself. Therefore, the presence of water actually enhances the extraction of other molecules contained in the biocrude feed.

This enhancement can be discussed in further detail with the aid of Figure 6b, where the variation of VPL, in the two abovementioned experiments, is shown for specific chemical


https://dx.doi.org/10.1021/acs.iecr.9b06889
Ind. Eng. Chem. Res. 2020, 59, 6141−6153

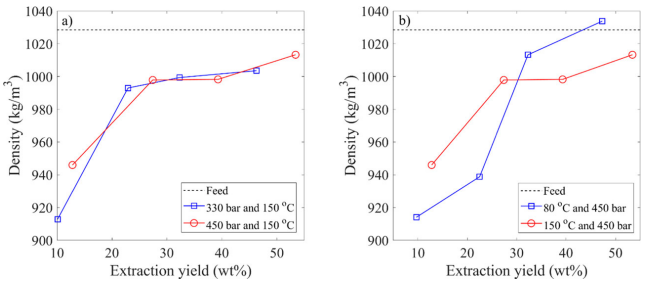


**Figure 8.** Density vs extraction yield at (a) constant temperature (150 °C) and (b) constant pressure (450 bar).

classes at different $S/F$ ratios. In Figure 6b, 9 out of 10 classes defined in this work are represented since no aromatic alcohols were reported in the previous work. The major observation from Figure 6b is that the higher water content enhances dramatically the VPL of the nonpolar hydrocarbons (i.e., AB and PAH). In addition, components of low polarity (e.g., K, P, and G) are extracted more efficiently. The more polar components (i.e., BD, SFA, and LFA) have, in general, higher VPL for the biocrude with the lower initial water content. In all cases, the benefit of the presence of water is reduced, while the extraction progresses, which is in line with the slope in the curves of Figure 6a, and suggests that this effect becomes less pronounced as the unextracted residue becomes drier. The above indicates that the application of $sCO_2$ extraction on the nondewatered biocrude leads to both increased VPL and selectivity with respect to polar and apolar components.

**3.3. Bulk Properties and Elemental Composition.** The values of CAN and PhAN for the extracts increase with the extraction yields ($E/F$) at all conditions. As an example, the CAN and PhAN values of the extractions at 150 °C are plotted versus the extraction yield and shown in Figure 7.

CAN values of the first extracts range from 28 to 41 mg KOH/g, which are values always lower than the CAN value of the feed (42 mg KOH/g). This observation indicates that fatty acids are not preferentially extracted at the beginning of the batch separation process. As the extraction proceeds, the CAN value of the extracts increases, with values ranging from 34 to 41 mg KOH/g for E2, 49 to 53 mg KOH/g for E3, and 67 to 76 for E4 mg KOH/g. The trend of the CAN indicates that fatty acids are progressively more extracted as the extraction proceeds. CAN of the residues ranges from 28 to 35 mg KOH/g, which means that, in most of the cases, the residue is partially depleted of carboxylic acids. When CAN values in this work are compared to those of previous work on a dewatered biocrude,[22] it is observed that in the early stages of the extraction ($S/F$ up to 5 g/g), the literature CAN values are higher (i.e., 37−47 mg KOH/g) than those of this work (at similar conditions, 80−120 °C and 255−400 bar). This further indicates that, at the beginning of the separation process, the fatty acids are less extracted in the presence of higher water content.

On the other hand, PhAN values of the extracts are always lower than the value of the feed (55 mg KOH/g). In this case, the values range from 14 to 16 mg KOH/g for E1, 18 to 21 mg KOH/g for E2, 29 to 31 mg KOH/g for E3, and 38 to 48 mg KOH/g for E4. Consistently, the PhAN value of the residue is higher than the feed, resulting to be in the range of 61 to 62 mg KOH/g. Overall, the reduced CAN and increased PhAN in the residue indicates that its type of acidity is shifted toward phenolic nature. The highest value of CAN was observed for extract E4 at 450 bar and 150 °C (i.e., 76 mg KOH/g), while the lowest PhAN was observed for extract E1 for the same extraction (i.e., 14 mg KOH/g). A high CAN and low PhAN are advantageous for hydrotreating since HDO of fatty acids is easier than opening aromatic rings.[53,54] In addition, the increased PhAN indicates that high-molecular-weight phenolic components remain in the residue. This fraction is expected to be resistant to HDO as it was similarly shown for the residue of *n*-pentane extraction of lignocellulosic biocrude.[55]

The density of the extracts was found in the range of 914 to 1034 kg/m$^3$, increasing with the extraction progression. Most of the $sCO_2$ extracts exhibit a moderate reduction compared to the feed, with the maximum being a 10% reduction for early extracts (i.e, E1 and E2). The later extracts show a density comparable to the feed, with only the final extracts (i.e., E4) at 80 °C and 300 bar and 100 °C and 450 bar, exhibiting a density slightly higher than the feed (see example in Figure 8b). The extraction conditions show negligible influence on the density of the extracts. As in the case of acidity, also in the case of density, the trends were similar at all experimental conditions. Figure 8a shows an example referred to the extractions at 150 °C, whereas Figure 8b shows two cases at 450 bar.

The water content of the extracts was measured for the experimental runs B, E, D, and H and resulted to be in the range of 1.3 to 1.8 wt %, with no clear trend with the extraction pressure and temperature. Importantly, the values are consistently and remarkably lower than the water content of the feed (i.e., 5.7 wt %). The water content of the residues of the same extractions was measured after evaporation of the solvent used for their recovery. The obtained values were in the range of 0.9 to 1.6 wt %. The fact that the water content was observed to decrease both in the residue and in the extract clearly indicates that it was not possible to recover all the water from the system due to lack of complete recovery in the cold trap and/or water losses during the recovery of the residue at the end of the extraction. The mass balances indicate that approximately 50% of the water originally in the feed was not retrieved in the extracts and in the residue. For extraction D, the water content of the residue was measured by means of direct KF titration of a sample of THF solution, that is, before the solvent evaporation. The value was 1.2 wt %, while the corresponding value after solvent evaporation was 0.9 wt %. This means that about 2% of the water in the feed was lost during the vacuum evaporation, which is not significant with regard to the total water losses. Interestingly, the earlier


https://dx.doi.org/10.1021/acs.iecr.9b06889
Ind. Eng. Chem. Res. 2020, 59, 6141−6153

extracts (i.e., E1 and E2) exhibited spontaneous separation of water, with water droplets collecting at the bottom of the storage vials. This was not observed for the later extracts (i.e., E3 and E4). This freely separated water was determined for extractions at 150 °C, and it was 0.4 and 0.6 g for extractions H and D, respectively, which correspond to 13 and 20% of the original water in the feed. Even though it was not possible to close the mass balances on water, the results clearly indicate that $sCO_2$ process coextracts water from the HTL biocrude, induces the separation of water from the extracts, and allows reducing the water content in the residue as well.

The carbon mass fraction in the extracts was in the range of 0.80 to 0.81, which are values close to the values of the feed (i.e., 0.80) and the residue (0.78−0.79). The hydrogen content (on a water-free basis) is slightly increased in the extracts (0.09−0.11), with respect to the feed (i.e., 0.08) and the residues (range of 0.07−0.08). The oxygen mass fraction of the extracts (on a water-free basis) for all extractions was lower than that of the feed, ranging from 0.05 to 0.07 (vs 0.10 in the feed). In line with this, the mass fraction of oxygen of the residues increased, ranging from 0.13 to 0.15. The oxygen mass fraction of the extractions performed at 150 °C is plotted in Figure 9 as a function of the extraction yield. Similar trends are observed in all extractions.

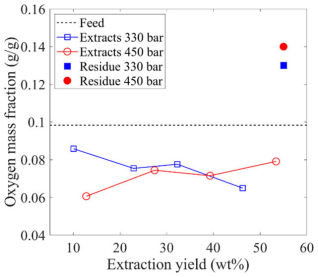


**Figure 9.** Oxygen content on a water-free basis vs extraction yield for extractions at 150 °C.

**3.4. Metal Content of Biocrude Extracts and Residues.** The metal content of extracts and residues was measured for extraction B, D, G, and H. In all cases, the extracts were found almost completely devoid of metals. The metal content was reduced from 95 to 99%, compared to the feed value. The analysis of the residues confirmed that the metals are concentrated in the unextracted phase. The trends were very similar in all runs. As an example, the results obtained with the extraction at 330 bar and 150 °C are reported in Figure 10.

As can be seen in Figure 10, potassium and sodium, which constitute more than 90% of the metal content of the feed, are reduced from 3400 and 3800 mg/kg down to values ranging from 30 to 40 mg/kg and 70 to 100 mg/kg, respectively. Aluminum, iron, and titanium are reduced in the extracts down to values below 10 mg/kg in all extracts. Interestingly, magnesium remains unchanged, which suggests that it may be in organometallic components[24] that can be solubilized by $sCO_2$. In all cases, the total metal content was found to be drastically reduced from 8500 mg/kg down to an average value of 170 mg/kg.

The small amount of metals in the extracts indicates that either they can be entrained together with fine water droplets where they are dissolved in or they are present, albeit in a very small amount, as organometallic components that are soluble in $sCO_2$. The 10 $\mu$m filter at the top of the basket insert is expected to act as a factor, limiting the entrainment of water droplets.

**3.5. Chemical Composition by GC−MS.** Figure 11a shows the total ion chromatograms (normalized with respect to the highest peaks) of the nonderivatized samples of the feed biocrude and the extracts obtained at 330 bar and 150 °C. Figure 11a shows the corresponding chromatograms for the derivatized (silylated) samples. The trends shown in Figure 11 are qualitatively representative of all extractions carried out in this work. It is noted that some classes of components exhibit overlapping retention time (RT) ranges, which does not allow assuming that all components in a certain RT range are expected to belong to a specific class. As can be seen in Figure 11a, the concentration of lower retention time components (up to 17 min) is increased in the first extract, while it decreases in subsequent extracts. This indicates that these components are preferentially extracted at the beginning of the process and depleted in the unextracted oil. The peak areas of higher retention time components (21−25 min) increase over time, which is particularly visible by the increasing difference between the largest peak of the chromatograms (retene at 23.8 min) and the IS (vanillin at 15.1 min). This indicates that they are not preferentially extracted in the early stages of the extraction but are substantially extracted as their concentration in the residue increases. A similar trend is observed in the derivatized sample (Figure 11b), with light components (RT up to 15 min) extracted preferentially in the early stages while

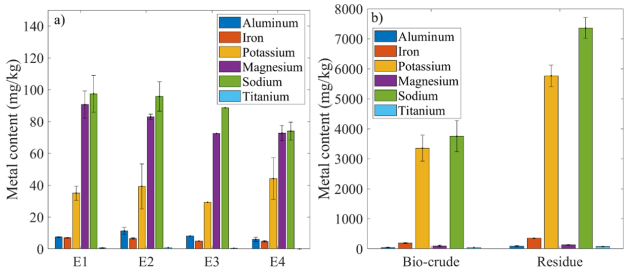


**Figure 10.** Metal distribution between biocrude, extracts (i.e. E1, ..., E4), and residue for the extraction at 330 bar and 150 °C. Error bars represent the standard deviation of at least duplicate measurements.



https://dx.doi.org/10.1021/acs.iecr.9b06889
Ind. Eng. Chem. Res. 2020, 59, 6141−6153

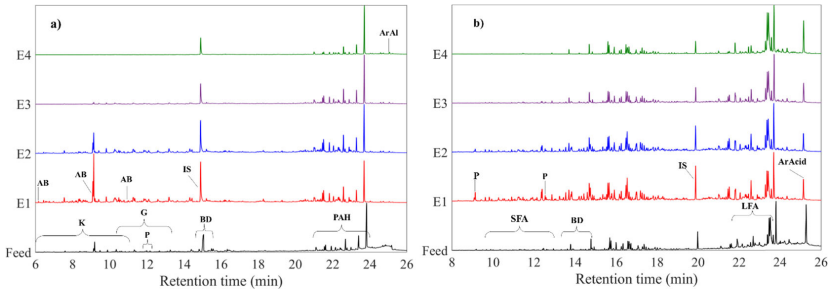


**Figure 11.** Chromatograms of feed biocrude and extracts E1−E4 of the extraction at 330 bar and 150 °C. (a) Nonderivatized samples. (b) Derivatized (silylated) samples. Ketones (K); alkylbenzenes (AB); phenols (P); guaiacols (G); benzenediols (BD); 2- and 3-ring aromatic hydrocarbons (PAH); aromatic alcohol (ArAl); short chain fatty acids (SFA), in the range of C2−C8; long chain fatty acids (LFA), in the range of C16−C18; and dehydroabietic acid (ArAcid).

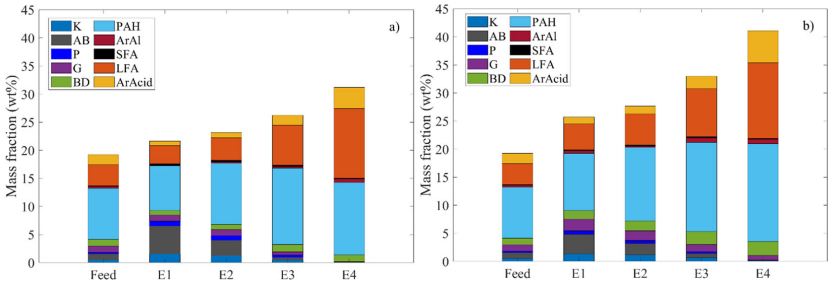


**Figure 12.** Mass fractions on a water-free basis of the feed and $sCO_2$ extracts for the experimental runs at (a) 330 bar and 150 °C and (b) 450 bar and 150 °C. Ketones (K); alkylbenzenes (AB); phenols (P); guaiacols (G); benzenediols (BD); 2- and 3-ring aromatic hydrocarbons (PAH); aromatic alcohol (ArAl); short chain fatty acids (SFA), in the range of C2−C8; Long chain fatty acids (LFA), in the range of C16−C18; and dehydroabietic acid (ArAcid).

gradually depleted. In this case, the heavy acids (i.e., LFA and ArAcid, RT above 21 min) are progressively extracted in relatively higher amounts as the extraction proceeds.

Figure 12 shows the progress of the mass fractions of the identified classes of components with the extraction time with reference to the extractions at 150 °C, which are taken as a representative example of all extractions. The total identified components in the $sCO_2$ extracts are in the range of 27 to 40 wt%, which are higher values compared to the feed (19 wt %). This observation, together with the reduction in density (see Section 3.3), indicates that the extract has lower average molecular weight than the feed. A lower average molecular weight is expected to reduce coking during catalytic hydrotreatment, thus prolonging the lifecycle of the catalyst.[25]

Ketones, alkylbenzenes, phenols, guaiacols, and short chain fatty acids are decreasing monotonically with extraction progression, while benzenediols, polyaromatic hydrocarbons, long chain fatty acids, and the aromatic acid increase. The aromatic alcohol does not show any specific trend mostly being unchanged between the extracts. In further detail, the mass fractions of the abovementioned species in the extracts were found in the ranges of ketones (0.06−1.9 wt %), alkylbenzenes (0.05−6.6 wt %), phenols (0.03−0.9 wt %), guaiacols (0.04−2.5 wt %), benzenediols (0.8−3.6 wt %), polyaromatic hydrocarbons (8−23 wt %), dehydroabeityl alcohol (0.1−1.4 wt %), short chain fatty acids (0.09−0.3 wt %), long chain fatty acids (3−14 wt %), and dehydroabietic acid (0.8−6 wt %).

Overall, the GC−MS analysis shows that the trend of the separation is mainly determined by molecular weight, with the lighter components preferentially extracted in the early stages of the extraction. The polarity plays, however, an important role as well, as can be observed by different behaviors between guaiacols, preferentially extracted in the early stages, and benzenediols, which are more polar and are extracted at later stages even though having a slightly lower molecular weight.

## 4. CONCLUSIONS

This work proves that $sCO_2$ extraction is an effective process for the separation of raw (i.e., nondewatered and nondemetallized) HTL lignocellulosic biocrude. The process is capable of extracting a large fraction of the biocrude (yields of extract up to 53 wt %) with relatively low solvent-to-feed ratios (i.e., 30 to 37 g/g) compared to typical values for $sCO_2$ extractions. The extracts showed favorable properties toward downstream catalytic hydrotreatment. More specifically, they were drastically demetallized (from 8500 mg/kg down to 170 mg/kg on average), substantially dewatered (from 6 wt % down to 1.3−1.8 wt %), and exhibited a lower oxygen content (from 30 to 50% reduction on a water-free basis) and lower average molecular weight, and their acidity was shifted toward carboxylic nature, with a reduction of the phenolic acidity. Interestingly, not only is the $sCO_2$ process capable of simultaneous demetallization, dewatering, and upgrading of the biocrude but also the process efficiency was improved,


https://dx.doi.org/10.1021/acs.iecr.9b06889
Ind. Eng. Chem. Res. 2020, 59, 6141−6153

compared to $sCO_2$ extractions at similar conditions on a dewatered biocrude. Overall, these properties are expected to lead to longer catalyst life, lower hydrogen requirements, and less coking. Experimental studies on hydrotreatment of $sCO_2$ extracts are needed to confirm the expectations and to provide data allowing to evaluate if the advantages that can be obtained in the hydrotreatment step prevail on the reduced yield of hydrotreatment feed with respect to the initial biomass.

## ■ ASSOCIATED CONTENT

### Supporting Information

The Supporting Information is available free of charge at https://pubs.acs.org/doi/10.1021/acs.iecr.9b06889.

List of GC−MS identified components (Table S1) (PDF)

## ■ AUTHOR INFORMATION


### Corresponding Author

**Marco Maschietti** − *Department of Chemistry and Bioscience, Aalborg University 6700 Esbjerg, Denmark;* orcid.org/0000-0002-3120-7560; Email: marco@bio.aau.dk

### Authors

**Nikolaos Montesantos** − *Department of Chemistry and Bioscience, Aalborg University 6700 Esbjerg, Denmark;* orcid.org/0000-0002-4022-6050

**Rudi P. Nielsen** − *Department of Chemistry and Bioscience, Aalborg University 6700 Esbjerg, Denmark;* orcid.org/0000-0001-8820-1445

Complete contact information is available at: https://pubs.acs.org/10.1021/acs.iecr.9b06889


### Notes

The authors declare no competing financial interest.

## ■ ACKNOWLEDGMENTS

The authors would like to acknowledge the valuable contribution of Linda Birkebæk Madsen, for performing the elemental analysis for this work.

## ■ REFERENCES


(1) Castello, D.; Pedersen, T.; Rosendahl, L. Continuous Hydrothermal Liquefaction of Biomass: A Critical Review. *Energies* **2018**, *11*, 3165.

(2) Kim, J. Y.; Lee, H. W.; Lee, S. M.; Jae, J.; Park, Y. K. Overview of the Recent Advances in Lignocellulose Liquefaction for Producing Biofuels, Bio-Based Materials and Chemicals. *Bioresour. Technol.* **2019**, *279*, 373−384.

(3) Nguyen, T. D. H.; Maschietti, M.; Belkheiri, T.; Åmand, L. E.; Theliander, H.; Vamling, L.; Olausson, L.; Andersson, S. I. Catalytic Depolymerisation and Conversion of Kraft Lignin into Liquid Products Using Near-Critical Water. *J. Supercrit. Fluids* **2014**, *86*, 67−75.

(4) Pedersen, T. H.; Grigoras, I. F.; Hoffmann, J.; Toor, S. S.; Daraban, I. M.; Jensen, C. U.; Iversen, S. B.; Madsen, R. B.; Glasius, M.; Arturi, K. R.; et al. Continuous Hydrothermal Co-Liquefaction of Aspen Wood and Glycerol with Water Phase Recirculation. *Appl. Energy* **2016**, *162*, 1034−1041.

(5) Jarvis, J. M.; Billing, J. M.; Hallen, R. T.; Schmidt, A. J.; Schaub, T. M. Hydrothermal Liquefaction Biocrude Compositions Compared to Petroleum Crude and Shale Oil. *Energy Fuels* **2017**, *31*, 2896−2906.

(6) Jensen, C. U.; Rodriguez Guerrero, J. K.; Karatzos, S.; Olofsson, G.; Iversen, S. B. Fundamentals of Hydrofaction™: Renewable Crude Oil from Woody Biomass. *Biomass Convers. Biorefin.* **2017**, *7*, 495−509.

(7) Jensen, C. U.; Rosendahl, L. A.; Olofsson, G. Impact of Nitrogenous Alkaline Agent on Continuous HTL of Lignocellulosic Biomass and Biocrude Upgrading. *Fuel Process. Technol.* **2017**, *159*, 376−385.

(8) Cao, L.; Zhang, C.; Chen, H.; Tsang, D. C. W.; Luo, G.; Zhang, S.; Chen, J. Hydrothermal Liquefaction of Agricultural and Forestry Wastes: State-of-the-Art Review and Future Prospects. *Bioresour. Technol.* **2017**, *245*, 1184−1193.

(9) Ong, B. H. Y.; Walmsley, T. G.; Atkins, M. J.; Walmsley, M. R. W. Hydrothermal Liquefaction of Radiata Pine with Kraft Black Liquor for Integrated Biofuel Production. *J. Cleaner Prod.* **2018**, *199*, 737−750.

(10) Jarvis, J. M.; Albrecht, K. O.; Billing, J. M.; Schmidt, A. J.; Hallen, R. T.; Schaub, T. M. Assessment of Hydrotreatment for Hydrothermal Liquefaction Biocrudes from Sewage Sludge, Microalgae, and Pine Feedstocks. *Energy Fuels* **2018**, *32*, 8483−8493.

(11) Belkheiri, T.; Andersson, S. I.; Mattsson, C.; Olausson, L.; Theliander, H.; Vamling, L. Hydrothermal Liquefaction of Kraft Lignin in Sub-Critical Water: The Influence of the Sodium and Potassium Fraction. *Biomass Convers. Biorefin.* **2018**, *8*, 585−595.

(12) Anastasakis, K.; Biller, P.; Madsen, R.; Glasius, M.; Johannsen, I. Continuous Hydrothermal Liquefaction of Biomass in a Novel Pilot Plant with Heat Recovery and Hydraulic Oscillation. *Energies* **2018**, *11*, 1−23.

(13) Sintamarean, I. M.; Grigoras, I. F.; Jensen, C. U.; Toor, S. S.; Pedersen, T. H.; Rosendahl, L. A. Two-Stage Alkaline Hydrothermal Liquefaction of Wood to Biocrude in a Continuous Bench-Scale System. *Biomass Convers. Biorefin.* **2017**, *7*, 425−435.

(14) Arturi, K. R.; Strandgaard, M.; Nielsen, R. P.; Søgaard, E. G.; Maschietti, M. Hydrothermal Liquefaction of Lignin in Near-Critical Water in a New Batch Reactor: Influence of Phenol and Temperature. *J. Supercrit. Fluids* **2017**, *123*, 28−39.

(15) Nguyen Lyckeskog, H.; Mattsson, C.; Åmand, L. E.; Olausson, L.; Andersson, S. I.; Vamling, L.; Theliander, H. Storage Stability of Bio-Oils Derived from the Catalytic Conversion of Softwood Kraft Lignin in Subcritical Water. *Energy Fuels* **2016**, *30*, 3097−3106.

(16) Lyckeskog, H. N.; Mattsson, C.; Olausson, L.; Andersson, S. I.; Vamling, L.; Theliander, H. Thermal Stability of Low and High Mw Fractions of Bio-Oil Derived from Lignin Conversion in Subcritical Water. *Biomass Convers. Biorefin.* **2017**, *7*, 401−414.

(17) Hoffmann, J.; Jensen, C. U.; Rosendahl, L. A. Co-Processing Potential of HTL Bio-Crude at Petroleum Refineries − Part 1: Fractional Distillation and Characterization. *Fuel* **2016**, *165*, 526−535.

(18) Pedersen, T. H.; Jensen, C. U.; Sandström, L.; Rosendahl, L. A. Full Characterization of Compounds Obtained from Fractional Distillation and Upgrading of a HTL Biocrude. *Appl. Energy* **2017**, *202*, 408−419.

(19) Ramirez, J. A.; Brown, R. J.; Rainey, T. J. A Review of Hydrothermal Liquefaction Bio-Crude Properties and Prospects for Upgrading to Transportation Fuels. *Energies* **2015**, *8*, 6765−6794.

(20) Haarlemmer, G.; Guizani, C.; Anouti, S.; Déniel, M.; Roubaud, A.; Valin, S. Analysis and Comparison of Bio-Oils Obtained by Hydrothermal Liquefaction and Fast Pyrolysis of Beech Wood. *Fuel* **2016**, *174*, 180−188.

(21) Déniel, M.; Haarlemmer, G.; Roubaud, A.; Weiss-Hortala, E.; Fages, J. Optimisation of Bio-Oil Production by Hydrothermal Liquefaction of Agro-Industrial Residues: Blackcurrant Pomace (Ribes Nigrum L.) as an Example. *Biomass Bioenergy* **2016**, *95*, 273−285.

(22) Montesantos, N.; Pedersen, T. H.; Nielsen, R. P.; Rosendahl, L.; Maschietti, M. Supercritical Carbon Dioxide Fractionation of Bio-Crude Produced by Hydrothermal Liquefaction of Pinewood. *J. Supercrit. Fluids* **2019**, *149*, 97−109.

(23) Elliott, D. C. Historical Developments in Hydroprocessing Bio-Oils. *Energy Fuels* **2007**, *21*, 1792−1815.

(24) Leijenhorst, E. J.; Wolters, W.; Van De Beld, L.; Prins, W. Inorganic Element Transfer from Biomass to Fast Pyrolysis Oil: Review and Experiments. *Fuel Process. Technol.* **2016**, *149*, 96−111.
(25) Furimsky, E.; Massoth, F. E. Deactivation of Hydroprocessing Catalysts. *Catal. Today* **1999**, *52*, 381−495.
(26) Eijsbouts, S.; Battiston, A. A.; van Leerdam, G. C. Life Cycle of Hydroprocessing Catalysts and Total Catalyst Management. *Catal. Today* **2008**, *130*, 361−373.
(27) ASTM International. ASTM D1655-19a, *Standard Specification for Aviation Turbine Fuels*; ASTM International: West Conshohocken, PA 2019.
(28) European Committee for Standardization. EN590:2013+A1 *Automotive Fuels -Diesel -Requirements and Test Methods*; European Committee for Standardization: 2017.
(29) ISO 8217:2017, *Petroleum Products — Fuels (Class F) — Specifications of Marine Fuels*. 2017.
(30) Brunner, G. Counter-Current Separations. *J. Supercrit. Fluids* **2009**, *47*, 574−582.
(31) Nielsen, R. P.; Valsecchi, R.; Strandgaard, M.; Maschietti, M. Experimental Study on Fluid Phase Equilibria of Hydroxyl-Terminated Perfluoropolyether Oligomers and Supercritical Carbon Dioxide. *J. Supercrit. Fluids* **2015**, *101*, 124−130.
(32) Riha, V.; Brunner, G. Separation of Fish Oil Ethyl Esters with Supercritical Carbon Dioxide. *J. Supercrit. Fluids* **2000**, *17*, 55−64.
(33) Gironi, F.; Maschietti, M. Separation of Fish Oils Ethyl Esters by Means of Supercritical Carbon Dioxide: Thermodynamic Analysis and Process Modelling. *Chem. Eng. Sci.* **2006**, *61*, 5114−5126.
(34) Dunford, N. T.; Teel, J. A.; King, J. W. A Continuous Countercurrent Supercritical Fluid Deacidification Process for Phytosterol Ester Fortification in Rice Bran Oil. *Food Res. Int.* **2003**, *36*, 175−181.
(35) Eisenmenger, M.; Dunford, N. T.; Eller, F.; Taylor, S.; Martinez, J. Pilot-Scale Supercritical Carbon Dioxide Extraction and Fractionation of Wheat Germ Oil. *J. Am. Oil Chem. Soc.* **2006**, *83*, 863−868.
(36) Vázquez, L.; Torres, C. F.; Fornari, T.; Señoráns, F. J.; Reglero, G. Recovery of Squalene from Vegetable Oil Sources Using Countercurrent Supercritical Carbon Dioxide Extraction. *J. Supercrit. Fluids* **2007**, *40*, 59−66.
(37) Montesantos, N.; Pedersen, T. H.; Nielsen, R. P.; Rosendahl, L. A.; Maschietti, M. High-Temperature Extraction of Lignocellulosic Bio-Crude by Supercritical Carbon Dioxide. *Chem. Eng. Trans.* **2019**, *74*, 799−804.
(38) Jensen, C. U. *PIUS − Hydrofaction™ Platform with Integrated Upgrading Step*; PhD Thesis, Aalborg University, 2018.
(39) Patel, R. N.; Bandyopadhyay, S.; Ganesh, A. Extraction of Cardanol and Phenol from Bio-Oils Obtained through Vacuum Pyrolysis of Biomass Using Supercritical Fluid Extraction. *Energy* **2011**, *36*, 1535−1542.
(40) Feng, Y.; Meier, D. Supercritical Carbon Dioxide Extraction of Fast Pyrolysis Oil from Softwood. *J. Supercrit. Fluids* **2017**, *128*, 6−17.
(41) Feng, Y.; Meier, D. Extraction of Value-Added Chemicals from Pyrolysis Liquids with Supercritical Carbon Dioxide. *J. Anal. Appl. Pyrolysis* **2015**, *113*, 174−185.
(42) ASTM International. ASTM D664-17a, *Standard Test Method for Acid Number of Petroleum Products by Potentiometric Titration*; ASTM International: West Conshohocken, PA, 2017.
(43) Lemmon, E. W.; McLinden, M. O.; Friend, D. G. Thermophysical Properties of Fluid Systems. In *NIST Chemistry WebBook, NIST Standard Reference Database Number 69*; Linstrom, P. J., Mallard, W. G., Eds.; National Institute of Standards and Technology: Gaithersburg MD, 2011, 20899.
(44) Oasmaa, A.; Van De Beld, B.; Saari, P.; Elliott, D. C.; Solantausta, Y. Norms, Standards, and Legislation for Fast Pyrolysis Bio-Oils from Lignocellulosic Biomass. *Energy Fuels* **2015**, *29*, 2471−2484.
(45) Madsen, R. B.; Bernberg, R. Z. K.; Biller, P.; Becker, J.; Iversen, B. B.; Glasius, M. Hydrothermal Co-Liquefaction of Biomasses − Quantitative Analysis of Bio-Crude and Aqueous Phase Composition. *Sustain. Energy Fuels* **2017**, *1*, 789−805.
(46) Rowell, R.; Pettersen, R.; Tshabalala, M. Cell Wall Chemistry. In *Handbook of Wood Chemistry and Wood Composites*, Second *Edition*; Rowell, R. M., Ed.; CRC Press; 2012; pp 33−72, .
(47) Vassilev, S. V.; Baxter, D.; Andersen, L. K.; Vassileva, C. G.; Morgan, T. J. An Overview of the Organic and Inorganic Phase Composition of Biomass. *Fuel* **2012**, *94*, 1−33.
(48) Nguyen, T. D. H.; Maschietti, M.; Åmand, L. E.; Vamling, L.; Olausson, L.; Andersson, S. I.; Theliander, H. The Effect of Temperature on the Catalytic Conversion of Kraft Lignin Using Near-Critical Water. *Bioresour. Technol.* **2014**, *170*, 196−203.
(49) Standley, L. J.; Simoneit, B. R. T. Resin Diterpenoids as Tracers for Biomass Combustion Aerosols. *J. Atmos. Chem.* **1994**, *18*, 1−15.
(50) Carpy, A.; Marchand-Geneste, N. Molecular Characterization of Retene Derivatives Obtained by Thermal Treatment of Abietane Skeleton Diterpenoids. *J. Mol. Struct. THEOCHEM* **2003**, *635*, 45−53.
(51) Madsen, R. B.; Zhang, H.; Biller, P.; Goldstein, A. H.; Glasius, M. Characterizing Semivolatile Organic Compounds of Biocrude from Hydrothermal Liquefaction of Biomass. *Energy Fuels* **2017**, *31*, 4122−4134.
(52) McHugh, M. A.; Krukonis, V. J. Phase Diagrams for Supercritical Fluid−Solute Mixtures. In *Supercritical Fluid Extraction*; Brenner, H., Ed.; Elsevier, 1994; pp 27−84.
(53) Kokayeff, P.; Zink, S.; Roxas, P. Hydrotreating in Petroleum Processing. In *Handbook of Petroleum Processing*; Treese, S. A., Pujadó, P. R., Jones, D. S. J., Eds.; Springer International Publishing, 1995; pp 363−434.
(54) Mortensen, P. M.; Grunwaldt, J. D.; Jensen, P. A.; Knudsen, K. G.; Jensen, A. D. A Review of Catalytic Upgrading of Bio-Oil to Engine Fuels. *Appl. Catal. A Gen.* **2011**, *407*, 1−19.
(55) Bjelić, S.; Yu, J.; Iversen, B. B.; Glasius, M.; Biller, P. Detailed Investigation into the Asphaltene Fraction of Hydrothermal Liquefaction Derived Bio-Crude and Hydrotreated Bio-Crudes. *Energy Fuels* **2018**, *32*, 3579−3587.


https://dx.doi.org/10.1021/acs.iecr.9b06889
*Ind. Eng. Chem. Res.* 2020, 59, 6141−6153

# Upgrading of non-dewatered non-demetalized lignocellulosic bio-crude from hydrothermal liquefaction using supercritical carbon dioxide

Supporting information

Nikolaos Montesantos, Rudi P. Nielsen, Marco Maschietti*

Department of Chemistry and Bioscience, Aalborg University, Niels Bohrs Vej 8A, 6700, Esbjerg, Denmark

* E-mail: marco@bio.aau.dk

**Table S1**. Components identified by GC-MS with their retention time (RT), classification, molecular weight (MW), chemical formula, CAS registry number and their mass fraction (wt%) in the feed bio-crude. Components with a Match Factor above 800 or above 700 while reported in HTL lignocellulosic bio-crudes two or more times, are considered exactly identified (denoted with ✓). In all other cases, the components were identified as chemical class and formula, reporting the isomer with the highest Match Factor (denoted with ○). The RSD of triplicate analysis for the reported mass fractions ranges from 0.5 % to 21 %, being 10 % on average, with respect to the reported values.

| # | RT | Class | Component | | MW | Formula | CAS | $wt\%_{feed}$ |
|---|---|---|---|---|---|---|---|---|
| 1 | 5.61 | K | Cyclopentanone, 2-methyl- | ✓ | 98 | $C_6H_{10}O$ | 1120-72-5 | 0.04 |
| 2 | 6.17 | AB | p-Xylene | ✓ | 106 | $C_8H_{10}$ | 95-47-6 | 0.02 |
| 3 | 6.49 | K | Cyclopentanone, 2,5-dimethyl | ✓ | 96 | $C_6H_8O$ | 1120-73-6 | 0.04 |
| 4 | 7.48 | K | Cyclopentanone, 2,4,4-trimethyl- | ✓ | 126 | $C_8H_{14}O$ | 4694-12-6 | 0.02 |
| 5 | 8.37 | K | Cyclohexanone, 2-ethyl- | ○ | 126 | $C_8H_{14}O$ | 4423-94-3 | 0.07 |
| 6 | 9.12 | AB | p-Cymene | ✓ | 134 | $C_{10}H_{14}$ | 535-77-3 | 0.28 |
| 7 | 9.18 | AB | o-Cymene | ✓ | 134 | $C_{10}H_{14}$ | 527-84-4 | 0.67 |

| | | | | | | | | |
|---|---|---|---|---|---|---|---|---|
| 8 | 9.45 | K | 2-Cyclopenten-1-one, 2,3-dimethyl- | ✓ | 110 | $C_7H_{10}O$ | 1121-05-7 | 0.14 |
| 9 | 9.85 | K | 2-Cyclopenten-1-one, 2,3,4-trimethyl- | ✓ | 124 | $C_7H_8O$ | 106-44-5 | 0.16 |
| 10 | 10.33 | G | Guaiacol | ✓ | 124 | $C_7H_8O_2$ | 90-05-1 | 0.25 |
| 11 | 10.81 | K | 2-Cyclopenten-1-one, 2,3,4,5-tetramethyl- | ✓ | 138 | $C_9H_{14}O$ | 54458-61-6 | 0.05 |
| 12 | 11.38 | AB | Benzene, pentyl- | ○ | 148 | $C_{11}H_{16}$ | 538-68-1 | 0.07 |
| 13 | 11.54 | AB | Benzene, (1-methylbutyl)- | ○ | 148 | $C_{11}H_{16}$ | 2719-52-0 | 0.01 |
| 14 | 11.98 | G | Creosol | ○ | 138 | $C_8H_{10}O_2$ | 93-51-6 | 0.17 |
| 15 | 12.14 | P | Phenol, 2,3,6-trimethyl- | ○ | 136 | $C_9H_{12}O$ | 2416-94-6 | 0.13 |
| 16 | 12.50 | P | Phenol, 3-ethyl-5-methyl- | ○ | 136 | $C_9H_{12}O$ | 698-71-5 | 0.03 |
| 17 | 13.25 | G | 4-Ethylguaiacol | ✓ | 152 | $C_9H_{12}O_2$ | 2785-89-9 | 0.21 |
| 18 | 14.82 | BD | 1,3-Benzenediol, 4-ethyl | ✓ | 138 | $C_8H_{10}O_2$ | 2896-60-8 | 0.31 |
| 19 | 15.09 | BD | 1,3-Benzenediol, 2,5-dimethyl- | ✓ | 138 | $C_8H_{10}O_3$ | 488-87-9 | 0.04 |
| 20 | 15.26 | PAH | Naphthalene, 1,4-dimethyl- | ○ | 156 | $C_{12}H_{12}$ | 571-58-4 | 0.12 |
| 21 | 15.44 | BD | 1,4-Benzenediol, 2,3,5-trimethyl- | ✓ | 152 | $C_9H_{12}O_2$ | 700-13-0 | 0.40 |
| 22 | 15.54 | BD | Resorcinol, 2-acetyl- | ○ | 152 | $C_8H_8O_3$ | 699-83-2 | 0.47 |
| 23 | 21.07 | PAH | Anthracene, 2-methyl- | ○ | 192 | $C_{15}H_{12}$ | 613-12-7 | 0.33 |
| 24 | 21.54 | PAH | 18-Norabieta-8,11,13-triene | ✓ | 256 | $C_{19}H_{28}$ | | 0.26 |
| 25 | 21.59 | PAH | Heptamethyl-3-phenyl-1,4-cyclohexadiene | ○ | 254 | $C_{19}H_{26}$ | | 0.40 |
| 26 | 21.90 | PAH | 18-Norabieta-8,11,13-triene | ○ | 256 | $C_{19}H_{28}$ | | 0.37 |
| 27 | 22.13 | PAH | 10,18-Bisnorabieta-8,11,13-triene | ✓ | 242 | $C_{18}H_{26}$ | 32624-67-2 | 0.36 |
| 28 | 22.66 | PAH | 10,18-Bisnorabieta-5,7,9(10),11,13-pentaene | ✓ | 238 | $C_{18}H_{22}$ | 6566-19-4 | 0.92 |
| 29 | 23.37 | PAH | Anthracene, 9-butyl-1,2,3,4-tetrahydro- | ○ | 238 | $C_{18}H_{22}$ | | 1.15 |

| | | | | | | | | |
|---|---|---|---|---|---|---|---|---|
| 30 | 23.79 | PAH | Retene | ✓ | 234 | $C_{18}H_{18}$ | 483-65-8 | 5.14 |
| 31 | 25.14 | ArAl | Dehydroabeityl alcohol | ○ | 286 | $C_{20}H_{30}O$ | 3772-55-2 | 0.36 |
| Components identified after derivatization | | | | | | | | |
| 32 | 9.68 | P | Phenol | ✓ | 94 | $C_6H_6O$ | 108-95-2 | 0.03 |
| 33 | 10.00 | SFA | Hexanoic Acid | ✓ | 116 | $C_6H_{12}O_2$ | 142-62-1 | 0.02 |
| 34 | 10.11 | SFA | Glycolic acid | ○ | 76 | $C_2H_4O_3$ | 79-14-1 | 0.006 |
| 35 | 11.53 | SFA | Heptanoic acid | ✓ | 130 | $C_7H_{14}O_2$ | 111-14-8 | 0.03 |
| 36 | 12.42 | P | 2,3-Xylenol | ✓ | 122 | $C_8H_{10}O$ | 526-75-0 | 0.06 |
| 37 | 12.62 | P | 3,5-Xylenol | ✓ | 122 | $C_8H_{10}O$ | 108-68-9 | 0.03 |
| 38 | 12.95 | SFA | Octanoic acid | ✓<br>○ | 144 | $C_8H_{16}O_2$ | 124-07-2 | 0.05 |
| 39 | 13.78 | BD | Catechol | ✓ | 110 | $C_6H_6O_2$ | 120-80-9 | 0.20 |
| 40 | 14.77 | BD | 4-Methylcatechol | ✓ | 124 | $C_7H_8O_2$ | 452-86-8 | 0.26 |
| 41 | 21.88 | LFA | Palmitic acid | ✓ | 256 | $C_{16}H_{32}O_2$ | 57-10-3 | 0.44 |
| 42 | 22.54 | LFA | Margaric acid | ✓ | 270 | $C_{17}H_{34}O_2$ | 506-12-7 | 0.21 |
| 43 | 23.46 | LFA | 9-Octadecenoic acid, (E)- | ✓ | 282 | $C_{18}H_{34}O_2$ | 112-79-8 | 1.09 |
| 44 | 23.52 | LFA | 11-Octadecenoic acid, (E)-, | ✓ | 282 | $C_{18}H_{34}O_2$ | 693-72-1 | 1.71 |
| 45 | 23.66 | LFA | Stearic Acid | ✓ | 284 | $C_{18}H_{36}O_2$ | 57-11-4 | 0.30 |
| 46 | 25.26 | ArAcid | Dehydroabietic acid | ✓ | 300 | $C_{20}H_{28}O_2$ | 1740-19-8 | 1.83 |

# Paper D

## Supercritical carbon dioxide extraction of lignocellulosic bio-oils: The potential of fuel upgrading and chemical recovery

Nikolaos Montesantos, Marco Maschietti

The manuscript has been published in

*Energies,* Volume 13, Pages 1600, 2020

energies

MDPI

*Review*

# Supercritical Carbon Dioxide Extraction of Lignocellulosic Bio-Oils: The Potential of Fuel Upgrading and Chemical Recovery

**Nikolaos Montesantos and Marco Maschietti ***

Department of Chemistry and Bioscience, Aalborg University, Niels Bohrs Vej 8A, 6700 Esbjerg, Denmark; nmo@bio.aau.dk

* Correspondence: marco@bio.aau.dk

Received: 31 January 2020; Accepted: 30 March 2020; Published: 1 April 2020


**Abstract:** Bio-oils derived from the thermochemical processing of lignocellulosic biomass are recognized as a promising platform for sustainable biofuels and chemicals. While significant advances have been achieved with regard to the production of bio-oils by hydrothermal liquefaction and pyrolysis, the need for improving their physicochemical properties (fuel upgrading) or for recovering valuable chemicals is currently shifting the research focus towards downstream separation and chemical upgrading. The separation of lignocellulosic bio-oils using supercritical carbon dioxide ($sCO_2$) as a solvent is a promising environmentally benign process that can play a key role in the design of innovative processes for their valorization. In the last decade, fundamental research has provided knowledge on supercritical extraction of bio-oils. This review provides an update on the progress of the research in $sCO_2$ separation of lignocellulosic bio-oils, together with a critical interpretation of the observed effects of the extraction conditions on the process yields and the quality of the obtained products. The review also covers high-pressure phase equilibria data reported in the literature for systems comprising $sCO_2$ and key bio-oil components, which are fundamental for process design. The perspective of the supercritical process for the fractionation of lignocellulosic bio-oils is discussed and the knowledge gaps for future research are highlighted.

**Keywords:** lignocellulosic; bio-oil; biocrude; upgrading; supercritical extraction; supercritical $CO_2$; hydrotreatment; biorefinery; pyrolysis; hydrothermal liquefaction

## 1. Introduction

The contemporary society is heavily dependent on fossil fuels, both for energy and for the production of chemicals and materials. Indicatively, in 2017, about $10^8$ barrels/day of crude oil, $10^{10}$ $m^3$/day of natural gas, and 22 Mt/day of coal were consumed worldwide [1,2]. The volumetric figures for crude oil and natural gas correspond to approximately 11 Mt/day and 12 Mt/day, respectively. The $CO_2$ emissions related to the consumption of fossil fuels amounted to 96 Mt/day in 2017. In addition, the use of crude oil, natural gas, and coal is predicted to increase by 20%, 32%, and 10% by 2050 [1]. These figures clearly show that the development of efficient technological pathways for substantially increasing the production share of energy, chemicals, and materials from biomass, in partial substitution of fossil fuels, is a key aspect for reducing net $CO_2$ emissions and paving the way for a sustainable society based on renewable resources.

Biomass can be classified into first and second generation. First generation biomass is considered edible biomass, which can be extensively cultivated expressly for energy production [3]. Related technological examples are the production of bioethanol from corn and sugar cane and the production of biodiesel from soybean [4]. Second generation biomass is non-edible biomass, characterized by

lignocellulosic structure and typically available in the form of waste or by-products from forestry, agriculture, municipal waste management, and the pulp and paper industry [3]. Not being in direct competition with food production, with respect to land and water utilization, the development of process pathways for exploiting second generation biomass is particularly appealing. Low-value utilization of residual lignocellulosic biomass as a source of heating by direct combustion is widespread, both in households (e.g., wood pellets) and in industrial plants where it is produced (e.g., lignin from pulp and paper industry). On the other hand, higher value-added utilizations (i.e., production of liquid fuels and chemicals) are still extremely limited. An indicative example is that lignocellulosic biofuels from forestry and agricultural residues (i.e., bio-oils) account for only 3% of worldwide biofuel production [5].

In line with the above, a huge research effort has been made in the last few decades, aimed at advancing the technologies for the conversion of lignocellulosic feedstocks into liquid fuels and chemicals. Thermochemical processes have shown promising results, as in the case of pyrolysis and hydrothermal liquefaction (HTL). The main product of these processes is a lignocellulosic crude bio-oil, along with gas and biochar as side-products [6]. In the majority of scientific literature, the lignocellulosic oil produced by means of pyrolysis is named bio-oil, whereas the lignocellulosic oil produced by means of HTL is named biocrude (or bio-crude). The same approach is followed in this review. However, in this work, the term bio-oil is also used when pyrolysis and HTL oils are discussed jointly.

With regard to fuel production, crude bio-oils require both physical and chemical upgrading steps in order to be inserted into the current technological chain (e.g., blending with specific petroleum fuels). The utilization of typical refinery processes developed for fossil fuels is challenging, owing to the marked difference between bio-oils and petroleum. More specifically, from a chemical standpoint, lignocellulosic bio-oils (LC bio-oils) suffer from high average molecular weights (MWs), high oxygen and water content, as well as high acidity. From a physical standpoint, they suffer from high density and viscosity [7,8]. The production of specific chemicals is also challenging, as LC bio-oils are complex mixtures of a large number of compounds that show diverse molecular weight and polarity. The diversity in polarity is a marked difference compared with fossil crudes, which makes existing separation and chemical processes developed for fossil crudes not straightforwardly applicable to LC bio-oils. On the one hand, the development of thermochemical conversion processes of lignocellulosic biomass has been the focus in previous years; on the other hand, it is expected that the research focus in the coming years will shift towards the development of separation processes to be applied downstream of the thermochemical conversion unit. Such processes aim to produce either upgraded fuel fractions or specific value-added chemicals.

Among separation processes available in the chemical industry for the fractionation of oils, distillation and liquid–liquid extraction (LLE) are particularly relevant and widespread. However, in the case of LC bio-oils, the high molecular weight leads to very high distillation temperatures or very high vacuum requirements. For example, distillate fractions not exceeding 50 wt%–60 wt% of the bio-oil are reported for pressures as low as 0.1 mbar [9–12]. In addition, temperatures above 100 °C during distillation promote side-reactions (e.g., polymerization) [8,13]. Another factor negatively affecting the distillation of bio-oils is their water content. It was reported to reduce the efficiency of the separation and to lead to unsteady boiling and process control difficulties [9]. In addition, the water content is one of the main factors reducing the viscosity of bio-oils [8]. This implies that, in the lower stages of a continuous-flow distillation column, the bio-oil flowing downwards is expected to be extremely viscous, leading to operational problems. With regard to LLE, the process requires large quantities of organic solvents, the majority of which are produced from petroleum (e.g., dichloromethane, n-pentane) [14,15], thus spoiling one of the selling points of renewable fuels by using petroleum-based materials for bio-oil processing. In addition, organic solvents are often noxious and their recovery downstream of the extraction requires an additional process step (e.g., solvent evaporation).

An alternative for the separation of oils is represented by the extraction using supercritical carbon dioxide ($sCO_2$) as a solvent. In the supercritical region (i.e., above 73.8 bar and 31 °C), carbon

dioxide behaves as a liquid solvent, exhibiting liquid-like densities and good solvent power towards apolar and moderately polar compounds. In addition, $sCO_2$ has favorable transport properties (e.g., high diffusivity, low viscosity), which make it an efficient solvent. Downstream of the separation unit, carbon dioxide can be easily recovered by, for example, partial decompression, and recycled. From a solvent perspective, $CO_2$ is environmentally benign, safe (non-flammable), low-cost, and readily available. It is considered a particularly valid alternative for the separation of oils with high boiling temperatures (i.e., low volatility) [16]. For example, it finds industrial application for the fractionation of low volatility liquid mixtures, as in the case of hydroxyl-terminated perfluoropolyether oligomers [17]. The supercritical process is expected to have operational advantages as the dissolution of $sCO_2$ in the liquid phase causes oil expansion and a drop in viscosity, which facilitate the flow of the oil in continuous countercurrent equipment. As an example, these mechanisms are exploited in enhanced oil recovery processes based on $CO_2$ injection, which are particularly effective with respect to heavy oils and tar sands [18].

For the reasons stated above, research papers reporting the use of $sCO_2$ for separating LC bio-oils have appeared in the literature in the last decade. The main objectives of this review paper are as follows: (i) to provide an update on the progress of the research on $sCO_2$ separation of LC bio-oils; (ii) to provide an update on the progress of the research on high-pressure phase equilibria of systems comprising $sCO_2$ and bio-oil components; and (iii) to highlight knowledge gaps inspiring future research work in this area. The review paper is structured as follows. Section 2 describes the properties of LC bio-oils, also in relation to the starting biomass and the thermochemical conversion process, and highlights the issues encountered in the downstream upgrading aimed at fuel and chemicals production. Section 3 provides basic features of $sCO_2$ extraction processes and reviews in detail the literature providing experimental data on $sCO_2$ extraction of LC bio-oils. Section 4 analyzes available experimental data of phase equilibrium of carbon dioxide at supercritical conditions and key components of LC bio-oils and provides data correlations and interpretation based on the Chrastil model. Section 5 summarizes the authors' view with regard to the integration of this technology in the downstream upgrading of LC bio-oils and highlights research and technology gaps.

## 2. Lignocellulosic Bio-Oils

### 2.1. Lignocellulosic Feedstocks

Second generation lignocellulosic biomass is abundant in the form of agricultural, forestry, and municipal residues, as well as industrial byproducts such as lignin from the pulp and paper industry. In 2017, the agriculture sector was estimated to be able to generate from 11 to 47 Mt/day of lignocellulosic residues, whereas forestry residues were estimated to be 2.1 Mt/day [19]. Their quantitative potential as raw materials alternative to fossil fuels is thus significant. However, when considering the inherent difficulties in collecting a sparse resource and conveying it to conversion plants, together with the yields of transformation into valuable products, it is probable that only a fraction of fossil-based fuels and chemicals can realistically be substituted by LC counterparts. The potential contribution of municipal sewage sludge is rather small (e.g., approximately 25 kt/day of dry biomass in the European Union (EU) in 2010 [20]), even though it is worth considering it in the context of an overall effort aimed at raw material shift from fossil fuels to renewables. With regard to industrial lignocellulosic residues, Kraft lignin from the pulp and paper industry and lignin-rich residues from bio-ethanol plants (i.e., residual enzymatic lignin) are currently made available in small quantities, with an estimated 0.19 Mt/day [21] and 0.74–2.2 kt/day [22], respectively. In spite of the small quantities currently available, lignin is attractive owing to the peculiar chemical structure, which is composed of aromatic moieties. In addition, lignin is available with reproducible quality as a by-product of industrial systems that are either well-established (Kraft process) or under development (lignocellulosic to ethanol). These aspects make lignin an interesting by-product for the production of fuel additives, as well as bulk and fine aromatic chemicals [23,24]. Another interesting industrial example is represented by

residues of the palm industry, such as palm kernel shells. In 2006, Malaysia produced approximately 0.14 Mt/day of lignocellulosic residues associated to palm oil production, which can be an attractive feedstock for the production of bio-oils [25].

Lignocellulose consists in its majority of three natural macromolecules (i.e., cellulose, hemicellulose, and lignin), as well as a small weight percent of ash (i.e., inorganics). The ratio between these macromolecules varies widely from biomass to biomass and is one of the parameters affecting the composition of bio-oils. Key examples of these feedstocks that were studied in the literature, with respect to their conversion to bio-oils, are reported in Table 1, with typical ranges of mass fraction for cellulose, hemicellulose, lignin, and ash.

**Table 1.** Lignocellulosic biomass and distribution of cellulose, hemicellulose, lignin, and ash (wt%) on a water-free basis [26].

| Residual Biomass Type | Forestry | | Agricultural | | Industrial | Municipal |
|---|---|---|---|---|---|---|
| | Poplar | Pine | Sugarcane Bagasse | Wheat Straw | Kraft Lignin | Sewage Sludge [1] |
| Cellulose | 41–49 | 38–50 | 34–42 | 29 –52 | 0–1 | - |
| Hemicellulose | 17–33 | 18–30 | 19–43 | 11–39 | 0–1 | - |
| Lignin | 18–32 | 23–28 | 19–21 | 8–30 | 90 | - |
| Ash | 0–2 | 0–6 | 2–12 | 1–14 | 1–2 | 26–55 |

[1] Organic content is reported as total volatile matter in the range of 40 wt%–74 wt%.

Besides the composition in terms of cellulose, hemicellulose, and lignin, the overall elemental composition is another basic parameter that affects the properties of the bio-oil that can be obtained by LC biomass. Table 2 reports the oxygen content, the H/C and O/C ratios, and the higher heating value (HHV) for specific LC feedstocks that were studied in the context of bio-oil production. Elemental data and HHV are given on a water-free basis. HHV is calculated as reported in the literature [27], when the experimental data were not provided.

**Table 2.** Examples of lignocellulosic biomass, studied for bio-oil production, and their properties. Elemental composition, ash, and higher heating value (HHV) are reported on a water-free basis. Water content is also reported when available.

| Biomass Type | Industrial Residue | Softwood | Hardwood | Energy Crops | Agricultural Residues |
|---|---|---|---|---|---|
| | Kraft Lignin | Pine Bark | Beech | Wheat Stalk | Sugarcane Bagasse |
| Water (wt%) | 32.6 | NA | 8.7 | 10.5 | NA |
| Oxygen (wt%) | 26 | 42.13 | 44.5 | 47.9 | 52.5 |
| H/C | 1.04 | 1.38 | 1.38 | 1.53 | 2.00 |
| O/C | 0.31 | 0.64 | 0.69 | 0.79 | 1.00 |
| Ash | 0.8 | 1.07 | 0.8 | NA | NA |
| HHV (MJ/kg) | 27.67 | 20.2[1] | 19.2[1] | 17.8[1] | 16.4[1] |
| Reference | [28] | [29] | [30] | [31] | [32] |

[1] Calculated; NA: not reported.

As can be seen, the elemental composition of woody biomass is rather constant for pine (softwood) and beech (hardwood). Lignin is the biomass with the lowest oxygen content, which results in the highest HHV. The crop residues have the highest oxygen content, and thus the lowest HHVs.

### *2.2. Lignocellulosic Bio-Oils*

Bio-oils are defined here as the organic-rich liquid product of the thermochemical conversion of biomass. The two most prominent conversion processes are pyrolysis and hydrothermal liquefaction (Table 3). Pyrolysis employs high temperature to thermally break the macromolecules constituting the biomass in an oxygen-free environment. Drying of the biomass is required prior to pyrolysis. Depending on the residence time, the process is denoted as fast (i.e., a few seconds) or slow (i.e., hours to days). Microwaves can be used as an alternative heating source [8]. HTL can handle both dry

and wet biomass, whose macromolecular constituents are broken down by a complex set of reactions in subcritical or supercritical water environment, with or without assisting chemicals (e.g., catalysts, pH regulators, co-solvents) [33].

**Table 3.** Thermochemical conversion methods for bio-oil production [8,33]. HTL, hydrothermal liquefaction.

| Process | Pretreatment | Temperature | Pressure | Bio-Oil Yield |
|---|---|---|---|---|
| Pyrolysis | Drying, size reduction | 500–600 °C | Atmospheric | up to 75 wt% |
| HTL | Size reduction | 250–450 °C | 100–350 bar | up to 75 wt% |

Pyrolysis has reached industrial production level, with several plants around the world [8]. Licensed pyrolysis technologies (e.g., BTG-BTL, Ensyn, VTT) are being used in plants that produce bio-oil mostly from forestry residues. Characteristic examples are the Empyro plant (Twence – Empyro) in the Netherlands with production of approximately 65 t/day [34] and the Côte-Nord plant (Ensyn) in Canada with a capacity of approximately 130 t/day [35]. The HTL technology is utilized in several pilot plants around the globe [33] and one demonstration plant is under construction in Norway by Steeper energy and Silva Green Fuel with a production capacity of approximately 4 t/day [36].

LC bio-oils produced by pyrolysis and HTL are typically viscous dark liquids (Figure 1), composed to a large extent of oxygenated organic components. These oils are tight water-in-oil emulsions with water mass fractions typically in the range of 20 wt% to 30 wt% for pyrolysis oils [37], while lower values are observed for HTL biocrudes (4 wt%–15 wt%) [38–42]. Owing to the polarity induced by oxygen to many chemical constituents, raw bio-oils are not fully miscible with hydrocarbon solvents. They are, however, miscible with oxygen-containing organic solvents such as acetone and tetrahydrofuran [40,43]. In some cases, inorganics (i.e., ash) are present in bio-oils. They can either originate from the biomass or be introduced during processing [44]. Some quantitative information concerning physical and chemical properties of bio-oils is available in the literature and is reviewed in the following.

(**a**) (**b**)

**Figure 1.** Example of lignocellulosic bio-oil from pinewood. (**a**) hydrothermal liquefaction (HTL); (**b**) pyrolysis.

Density values for LC bio-oils are typically higher than 1000 kg/m$^3$, with small variations depending on the source of biomass. For example, values between 970 kg/m$^3$ and 1100 kg/m$^3$ are typical for HTL biocrudes [9,45,46]. Somewhat higher values are typically reported for pyrolysis oils, namely between 1100 kg/m$^3$ and 1200 kg/m$^3$ [47]. Density values are thus higher than petroleum and petroleum liquid products, which typically range from 800 kg/m$^3$ for light crude oils up to 1000 kg/m$^3$ for heavy oils and bitumens [48].

Kinematic viscosity values for LC pyrolysis oils are reported in a broad range, from 7 to 53 cSt at 40 °C [37,49]. The variation is strongly connected to the water content of the bio-oil (i.e., 17 wt%–48 wt%), with viscosity markedly decreasing with the water content. In another work, the kinematic viscosity is reported to be 28 cSt at 60 °C [50]. With regard to LC biocrudes (obtained by means of HTL), dynamic viscosity values are reported in a much broader range, namely from 1700 cP to $4{\cdot}10^6$ cP [30,51,52]. The higher values correspond to semisolids and result from the drying of the biocrude. Another work reports the kinematic viscosity of a dehydrated HTL biocrude being 12 cSt at 40 °C [9]. The major difference in viscosity between pyrolysis and HTL oils is, at least in large part, owing to the difference in the water content. As reported data typically refer to different water contents, caution is required in drawing conclusions related to the quality of the bio-oil on the basis of viscosity.

With regard to bulk chemical properties, the most important characteristic of LC bio-oils is the high oxygen content (O), which can widely range from as low as 10 wt% to as high as 50 wt%. In Table 4, a few examples are reported. As can be seen, oxygen ranges from 19 wt% to 40 wt%. In all cases, the oxygen of the bio-oil is lower than that of the biomass, which also translates into a higher HHV and a lower O/C ratio. Nevertheless, the oxygen values are at least one order of magnitude higher than the typical values for crude oils, where they lie in the range 0.05 wt% to 1.5 wt% [53]. Therefore, deoxygenation of LC bio-oil is a requirement in the perspective of fuel production.

**Table 4.** Properties of HTL bio-oils for different biomass feedstocks. Oxygen (O), H/C, O/C, ash, and higher heating value (HHV) on a water-free basis.

| Biomass Type | Industrial Residue | | Softwood | Hardwood | | Energy Crop | Agricultural Residue | |
|---|---|---|---|---|---|---|---|---|
| | Kraft Lignin | Palm Shell | Pine Bark | Beech | Eucalyptus | Wheat Stalk | Wheat Straw | Sugarcane Bagasse |
| Process | HTL | Pyrolysis | HTL | HTL | Pyrolysis | HTL | Pyrolysis | HTL |
| Oxygen (wt%) | 21 | 33 | 28.3 | 27.3 | 23.9 | 18.8 | 40.0 | 36.3 |
| H/C | 1.11 | 1.74 | 1.2 | 1.19 | 1.08 | 1.29 | 1.35 | 1.64 |
| O/C | 0.23 | 0.43 | 0.33 | 0.30 | 0.26 | 0.20 | 0.56 | 0.49 |
| HHV (MJ/kg) | 31.7 | 27 | 27.4[1] | 28.3[1] | 29.2 | 32.4[1] | 21.9 | 24.8[1] |
| Reference | [28] | [54] | [29] | [30] | [55] | [31] | [56] | [32] |

[1] Calculated as reported in the literature [27].

The inorganic content of bio-oils, cumulatively reported as ash, is the result of both the presence of metals in the original biomass and their introduction during processing. Examples of metals found in bio-oils are sodium (Na), potassium (K), and iron (Fe) [44,57,58]. Pyrolysis oils typically have a low ash content (e.g., 0.01 wt%–0.2 wt%) [47,59], as most of the metals are not contained in volatile compounds, and thus do not transfer in the gas stream. In addition, entrained particles in the gas stream are retained by filters. The small amounts of ash reported in pyrolysis oils are typically associated to volatile organometallic components [44]. On the other hand, HTL biocrudes are typically obtained by processes where catalysts (e.g., potassium carbonate [57]) and pH regulators (e.g., sodium hydroxide [60]) are utilized. These chemicals dissolve in the water droplets emulsified in the biocrude, resulting in high ash contents. For example, when an alkali catalyst is used, the ash content of the biocrude can be as high as 5 wt% [45]. With regard to the biomass feedstock, Anastasakis et al. [41] performed non-catalytic HTL of miscanthus and spirulina, which contained 2.7 wt% and 6.5 wt% of ash, respectively, and the biocrudes ended up on average with 2.8 wt% and 6.6 wt% ash, respectively. It is important to note that even metal content values as low as 0.5 wt% can be detrimental for the downstream catalytic upgrading (e.g., hydrotreating). Therefore, the metal content of bio-oils must be substantially reduced if the oil is to be hydrotreated [57].

Another relevant characteristic of LC bio-oils is the acidity. The total acid number (TAN) of LC bio-oils is reported in the range of 9 to 200 mg KOH/g [30,59–64], depending on the bio-oil and on the measurement method. TAN is a representation of the acidity of the liquid mixture and is a cumulative

effect of carboxylic acids and phenolic components that are present in the LC bio-oils. Considering these two partial acid numbers, namely the carboxylic acid number (CAN) and phenolic acid number (PhAN), the determination of the latter is not always achieved, when methods developed for petroleum are used. In some cases, the reported (cumulative) TAN values are essentially CAN. A modification of ASTM D664 [65] was reported by Christensen et al. [63], which successfully determines both acid numbers in pyrolysis oils. Montesantos et al. [64] measured the TAN of a LC biocrude from HTL, using a method inspired by this modification, and reported a CAN value of 43 mg KOH/g and TAN of 129 mg KOH/g. On the other hand, most of the literature for HTL biocrudes reports values of TAN up to 67 mg KOH/g [30,61,66]. This suggests that, at least in some cases, CAN values are those actually reported. Therefore, the methodology for the determination of TAN for bio-oils is one of the properties that requires standardization to ensure meaningful comparisons between different works. In this respect, Oasmaa et al. [27] published an interesting review of properties and analytical methods for the case of LC pyrolysis oils.

With regard to the detailed chemical structure of LC bio-oils, they are complex mixtures consisting of an overwhelming number of chemical components. Ketones, phenols, organic acids, and aromatic hydrocarbons are commonly found in the volatile fraction [7,67] of LC bio-oils. Other components such as aldehydes, esters, furans, and sugars are reported in the volatile fraction of pyrolysis oils [67]. The nonvolatile fraction of bio-oils contains mainly oligomers with several carbon and oxygen atoms (e.g., 15–29 carbon and 8–10 oxygen atoms [68]). This heavy fraction includes both phenolic and carbonyl functional groups [68,69], but little is known in detail. The average molecular weight of bio-oils is typically in the range of 300 to 1000 g/mol [70–72], with individual components with molecular weight ranging from less than 100 g/mol to several thousand g/mol [15,68,73].

More information is available for the volatile fraction, which is typically studied by gas-chromatography coupled with mass spectrometry (GC-MS). A discussion on this fraction is reported in the following. In most cases, the relative amounts of components of the volatile fraction are simply reported in terms of chromatographic peak area ratios. When internal standards are used, the mass fraction of identified components rarely accounts for more than 50 wt% of the bio-oil. The highest values are typically associated with pyrolysis oils, owing to several low molecular weight components (e.g., acetol, acetic acid, and glycoladehyde) that each constitute up to 10 wt% of the oil. In addition, levoglucosan is typically found in woody pyrolysis oils at high mass fractions (e.g., 10 wt%) [43,54,74–78]. On the other hand, single components at such a high concentration are not observed in the volatile fraction of HTL biocrudes, which is characterized by total mass fractions of identified components in a lower range (e.g., 10 wt%–30 wt%) [28,40,64,76,79,80]. However, chemical classes like polyaromatic hydrocarbons (e.g., retene) [57] and long chain fatty acids (e.g., hexadecanoic acid) [64] were found to constitute up to 9 wt% and 4 wt% [58] of HTL biocrudes, respectively. Such components are often not reported in the characterization of HTL biocrudes, even though they seemingly are a considerable part of it.

Table 5 reports the main chemical classes observed in the volatile fraction of LC bio-oils, together with typical ranges of molecular weight and number of carbon atoms (carbon number). In addition, an example is provided in which two pinewood bio-oils, produced by fast pyrolysis and HTL, are directly compared. The chemical classes include components with a wide range of molecular weights (i.e., 60 g/mol to above 300 g/mol) and volatilities, with boiling points ranging from around 100 °C (as normal boiling points) to values by far exceeding 300 °C (as atmospheric equivalent temperature, AET). The presence of these components in LC bio-oils results in high oxygen content, polarity, and acidity.

**Table 5.** Typical chemical classes identified by gas-chromatography coupled with mass spectrometry (GC-MS) in bio-oils with examples of mass fractions in pyrolysis oils and HTL biocrudes from pinewood and examples of specific components [10,43,57,58,76,81–84]. MW, molecular weight.

| Chemical Class | Pyrolysis [43] | HTL [58] | MW | Carbon Number | Examples |
|---|---|---|---|---|---|
| Ketones | Up to 8 wt% | Up to 0.5 wt% | 74–124 | C3–C10 | Hydroxyacetone<br>Cyclopenten-1-one, 2-<br>Cyclopentanone, 2,5-dimethyl |
| Phenols | Up to 0.1 wt% | Up to 0.3 wt% | 94–122 | C6–C8 | Phenol<br>o-Cresol<br>4-Ethylphenol |
| Guaiacols | Up to 0.5 wt% | Up to 0.6 wt% | 124–178 | C7–C10 | Guaiacol<br>Eugenol<br>Creosol |
| Benzenediols | - | Up to 1.7 wt% | 110–124 | C6–C8 | Catechol<br>4-Ethylcatechol |
| Short chain fatty acids[1] | Up to 5 wt% | Up to 0.2 wt% | 60–144 | C2–C8 | Acetic acid<br>Octanoic acid |
| Long chain fatty acids | - | Up to 3.8 wt% | 172–284 | C10–C19 | Decanoic acid<br>Octadecanoic acid |
| Aromatic acids | - | Up to 1.8 wt% | 152–300 | C8–C20 | Dehydroabietic acid<br>Benzeneacetic acid, 3-hydroxy |
| Furans | Up to 0.5 wt% | - | 84–132 | C4–C8 | Furfural<br>Furanone, 2(5H)- |
| Aldehydes | Up to 8 wt% | - | 60–152 | C2–C8 | Glycolaldehyde<br>Benzaldehyde, 3-hydroxy-4-methyl- |
| Esters | - | - | 130–296 | C6–C19 | Benzoic acid, 4-methoxy-, methyl ester<br>Furoic acid methylester |
| Sugars | Up to 10 wt% | - | 132–144 | C5–C6 | Levoglucosan<br>2,3-Anhydro-d-galactosan |
| Benzenes | - | Up to 1 wt% | 92–134 | C7–C10 | o-Cymene<br>Toluene |
| Polyaromatic hydrocarbons | - | Up to 9 wt% | 128–234 | C10–C18 | Naphthalene<br>Retene |

[1] For simplicity, small carboxylic acids (i.e., acetic, propanoic) are included in this class.

As different lignocellulosic biomasses own different fractions of cellulose, hemicellulose, and lignin, it follows that some component types will be favored during thermochemical conversion. More specifically, a larger fraction of lignin increases the fraction of phenolic components such as phenol, alkylphenols, guaiacols, and benzenediols [85]. For example, the mass fraction of phenolic components (relative to the total mass fraction of GC-MS identified components) reported by Belkheiri et al. [40] for an HTL biocrude from Kraft lignin was 97%, whereas the analogous ratio (in terms of peak areas) observed by Pedersen et al. [57] for an HTL biocrude from aspen wood was only 27%. Other chemical classes like ketones, furans, and acids are abundant in bio-oils that originate from biomass with a high content of cellulose and hemicellulose [86]. For example, the peak area fraction of ketones reported by Pedersen et al. [57] was 21% for a biocrude originating from biomass with 67% of cellulose and hemicellulose. The analogous quantity reported by Chan et al. [87] was 21% in a biocrude originating from biomass with 50% of cellulose and hemicellulose.

Another important aspect of LC bio-oils is the stability under storage. Kosinkova et al. [46] reported an increase in density of about 5% for an HTL biocrude under ambient conditions upon 25 weeks of storage. The increase reached 30% when the biocrude was stored at 43 °C for the same duration. The density increase was connected to the increase of the average molecular weight, which in turn resulted from polymerization reactions of certain lignin-derived phenolic components. Nguyen et al. [79] observed composition changes in a lignin-derived HTL biocrude (lignin oil), which can be attributed to instability of the biocrude. Specifically, alkylphenols, benzenediols, and phenolic dimers

decreased over time, while the average molecular weight of the oil increased after two years under ambient conditions. The increase in MW was observed by means of gel permeation chromatography (GPC), and was in line with the decrease of the GC-MS identified fraction of components from 15 wt%, for the fresh biocrude, to 11 wt% after long-term storage. Interestingly, a diethyl ether extracted fraction (corresponding to 66 wt% of the biocrude) was very stable, with the identified GC-MS fraction exhibiting only a 1% reduction in two years at ambient conditions. An important observation of this work is that the presence of inorganic solids in the lignin oil catalyzes the polymerization reactions, resulting in a higher aging rate. Elliott et al. [37] reported an increase of the kinematic viscosity of a fast pyrolysis oil between 60% and 70% during an aging test at 80 °C for 24 h. This viscosity difference, together with the reported increase of the average molecular weight, is indicative of the relatively low stability of pyrolysis oil. A similar increase of viscosity was observed after 12 months at 21 °C. Storage at 5 °C and −17 °C resulted in smaller increases of viscosity, equal to 19% and 7%, respectively [37].

### 2.3. Valorization

#### 2.3.1. Fuel Upgrading

Hydrotreating (HT) is the most prominent process for removing heteroatoms. It is a catalytic process adopted from the mature oil industry, where it is typically performed at temperatures of 90–390 °C and pressures of 15–170 bar. HT aims to remove heteroatoms like sulfur, nitrogen, oxygen, and hydrogenate C = C bonds (hydrogenation, HYD). The main expenditure is the consumption of hydrogen ($H_2$), with typical refinery values in the range of 10 to 850 $Nm^3$ of $H_2$ per $m^3$ of feed. The variation in the process conditions depends on the feedstock composition as well as on the objective of HT. Higher heteroatom contents usually require more severe conditions. Typically, fixed bed reactors are used, with the most common catalysts being cobalt-molybdenum (CoMo) and nickel molybdenum (NiMo) [88].

With regard to bio-oils, HT was studied at laboratory scale, with the main objective being the hydrodeoxygenation (HDO) of the liquid feed [89,90]. Reaction temperatures and pressures are reported in the range of 150 to 400 °C and 40 to 140 bar, with most typical values being 300–400 °C and 100 bar [39,89–91]. The most commonly used catalysts are commercially available CoMo and NiMo on $Al_2O_3$ support, although several other catalysts were also studied [92]. The economics of the process is mainly affected by the high $H_2$ partial pressures required. In particular, the large oxygen fraction of bio-oils requires $H_2$ to feed ratios in the range of 300 to 600 $Nm^3/m^3$ [9,89,93], which are similar to the ratios required for the sulfur-rich heavy fractions of crude oil refineries (e.g., residual oil) [88].

One of the issues of HT is the formation of coke, which leads to gradual deactivation of the catalyst. Typically, high molecular weight and high boiling point components accelerate deactivation because of deposition on the catalyst active sites [94]. Bjelic et al. [15] investigated the chemistry of a wood-derived HTL biocrude, as well as the chemistry of the extract and the residue obtained from the hydrotreated biocrude by means of liquid–liquid extraction using n-pentane (C5). The presence of HT resistant species in the residue was observed and the recommendation of separating the C5-insoluble fraction from the biocrude prior to HT was formulated. The metal content of some bio-oils (mainly HTL biocrudes) is also expected to pose problems to HT, because of rapid deactivation of the catalyst. Metal deposition is irreversible; it substantially reduces the catalytic activity and increases the pressure drop in the HT reactor [88,94]. When metals are deposited on the catalyst bed, regeneration (e.g., to remove coke) can sinter the catalyst surface, resulting in area loss [94]. These factors make necessary the demetallization of bio-oils prior to HT.

In spite of the abovementioned problems, research on HT of bio-oils has shown promising results indicating that, using optimal catalysts and conditions for hydrotreating, fuel grade oils can be achieved. Jensen et al. [90] performed HT experiments on HTL lignocellulosic biocrude on a commercial $NiMo/Al_2O_3$ catalyst. This parametric study highlighted the importance of high temperature and high $H_2$ partial pressure for achieving high-levels of HDO. The maximum HDO level attained in this work

corresponded to a reduction of oxygen from 5.3 wt% (feed biocrude) down to 0.1 wt% (hydrotreated oil), with operating conditions of 350 °C, 97 bar, and an $H_2$ to biocrude ratio of 500 $Nm^3/m^3$. The same authors performed GCxGC-MS on HTL biocrude and its HT product, and qualitatively reported (i.e., based on peak area ratios) an increase of alkanes and cycloalkanes from about 10%–15% to more than 50%. Another important observation of this work regards the total acid number, which was reduced to zero after hydrotreating. These results prove the feasibility of HT of LC bio-oils at laboratory scale. Nevertheless, further work is needed on a larger scale to verify the process operability and economics, especially with respect to catalyst deactivation rates and fouling. The physical upgrading (separation) of LC bio-oils upstream of the HT unit may be a key factor to improve the HT operability on commercial catalysts on an industrial scale.

#### 2.3.2. Production of Green Chemicals

Another perspective of valorization of LC bio-oils is the production of green chemicals. Pyrolysis oils contain some chemicals at relatively high mass fractions. Among them are acetic acid (up to 9 wt%) and acetol (up 8 wt%) [84]. Acetol is used as intermediate to produce polyols and acrolein [95], and acetic acid is an important chemical with a production exceeding 33 kt/day. Other chemicals with high mass fractions are glycolaldehyde (up to 6 wt%) and levoglucosan (up to 9 wt%) [68]. Even though it has no industrial application at this moment, levoglucosan has been identified as a potential building block for the chemical synthesis of high value-added pharmaceutical products [96–99]. Phenol is one of the most studied chemicals in LC bio-oils owing to its huge global demand, which has reached 27 kt/day in 2015 [100]. Phenol and its derivatives (e.g., guaiacol) can be used to produce resins and adhesives, as well as in the pharmaceuticals, food, or perfumery industries. Phenol mass fractions in LC bio-oils typically range from 0.1 wt% to 2 wt% [101], with values up to 5 wt% reported in the literature for pyrolysis oils from high-lignin content bio-mass [54]. High-value specialty chemicals are also found in LC bio-oils, albeit in low mass fractions. For example, vanillin, which is produced in majority by petroleum-derived guaiacol (approximately 85% of world production) [102], can be found in pyrolysis oils between 0.1 wt% and 1 wt% [43,54,84,101,103]. The production of vanillin in 2018 reached 100 t/day [104].

Recently, the antioxidant activity of bio-oil fractions has been studied for both pyrolysis and HTL oils derived by different biomasses [105–108]. Phenolic dimers and oligomers are suggested as the active antioxidant components, as monomers exhibited small to no antioxidant activity. The phenolic fractions were compared with commercial stabilizing agents (i.e., butylated hydroxytoluene, BHT) and showed identical or even better antioxidant activity in bio-diesel and bio-lubricants [106,107].

## 3. $sCO_2$ Separation of Bio-Oils

### *3.1. $sCO_2$ Basics*

Carbon dioxide exists in a supercritical state at conditions that exceed 73.8 bar and 31 °C. The pressure–temperature (P–T) phase diagram of pure $CO_2$, plotted from experimental data available in the literature [109–111], is shown in Figure 2. Even though $CO_2$ is a low-density vapor at standard conditions (i.e., 0 °C and 1 bar), in the supercritical region, it can exhibit liquid-like densities while keeping relatively high diffusivities and low viscosities [112]. The presence of high-density regions, at pressures not exceedingly high, allow $sCO_2$ to exhibit solvent power comparable to liquid solvents in pressure ranges where separation processes are feasible.

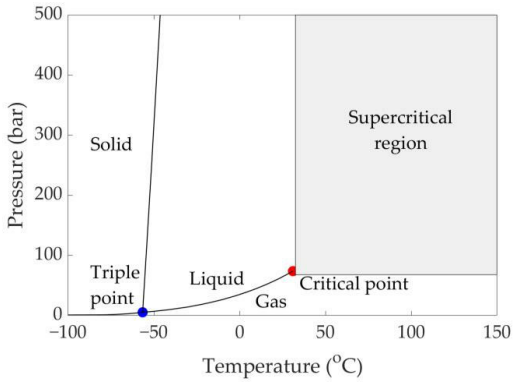


**Figure 2.** $CO_2$ phase diagram. Data taken from the literature [109–111].

The density of $CO_2$ at the critical point is approximately 468 kg/m$^3$, while its viscosity is approximately 0.03 cP [109]. Within the supercritical region, the density varies widely depending on pressure and temperature. For example, for temperatures and pressures in the range of 35 to 150 °C and 75 to 400 bar, respectively, it varies between 105 kg/m$^3$ and 973 kg/m$^3$. Even at the highest densities, $sCO_2$ exhibits viscosities remarkably lower than those of typical liquid solvents, such as hexane (i.e., approximately four times lower). In addition, in a broad area of the supercritical region, the density of $sCO_2$ can be varied remarkably with relatively small variations of pressure and temperature. This aspect provides a high tunability of the solvent characteristics, namely solvent power and selectivity, on the basis of two degrees of freedom (i.e., pressure and temperature). This is a distinct advantage over conventional liquid solvents, where a single parameter (i.e., temperature) can be varied to alter the properties of the solvent.

Another interesting property of $CO_2$ is that, even though it has zero dipole moment [113], it has a large quadrupole moment, which makes it a good solvent for both apolar and low polarity compounds [114]. In addition, $sCO_2$ is non-toxic, not flammable, and widely available at low cost. Its use in renewable chemical production is likely to be neutral with respect to $CO_2$ emissions into the atmosphere, as $CO_2$ does not need to be produced on purpose, contrary to most petroleum-derived organic solvents. Moreover, it may even be speculated that a spread in utilization of $sCO_2$ in industrial applications has the potential of a slight reduction of $CO_2$ emissions, as its storages will increase in the growth period of the $sCO_2$ technology. Furthermore, underground $CO_2$ storage facilities might be utilized in combination with units employing $sCO_2$ as a solvent for renewable production processes, thus taking advantage of the in situ presence of high-pressure $CO_2$ and developing negative $CO_2$-emission processes.

Typical process unit configurations include semi-continuous (i.e., batch) extraction, which can be performed either in a single stage extractor or a multi-stage column, and countercurrent continuous extraction [16,112,113,115]. In semi-continuous single-stage extractions (Figure 3a), the feed material is charged in a high-pressure extractor vessel and $sCO_2$ is continuously delivered to the bottom of the extractor. The $CO_2$-rich stream exits the vessel from the top and is expanded in a separator in order to release the extracted matter by reduction of the solubility, while the solute-free solvent is recompressed and recirculated. Alternatively, membranes or adsorbents can be used to separate the solutes from the $sCO_2$ without depressurization. Such an example is the use of activated carbon in the supercritical decaffeination of coffee beans [116]. In the case of multi-stage semi-continuous operation (Figure 3b), a reflux loop is added, where part of the extract is refluxed at the top of the column. In this mode of operation, the feed is contacted with the ascending $CO_2$-rich phase in a multiple-stage manner to achieve a better separation, compared with the single-stage operation [117]. The unextracted material (i.e., raffinate) remains in the vessel until the end of the batch extraction.

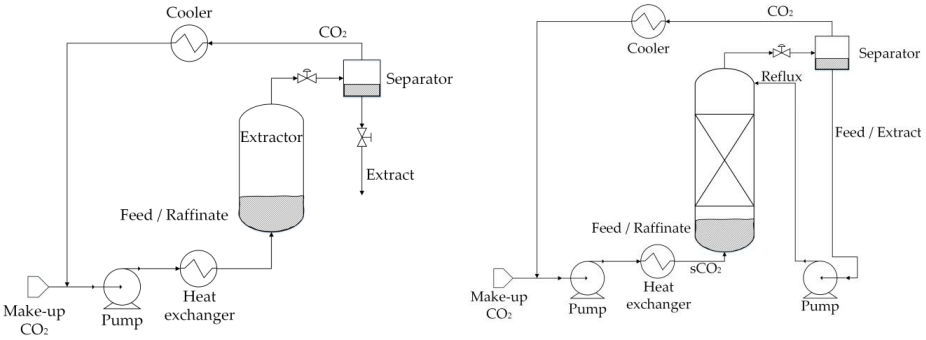


**Figure 3.** Flow diagram of semi-continuous extraction processes. (**a**) Single stage; (**b**) multi-stage.

The continuous countercurrent operation involves continuous flow of the feed from an entry point at the top or at an intermediate point of an extraction column, while the $sCO_2$ flows continuously from the bottom. Depending on the feed entry point, the extract is either continuously collected (Figure 4a) or partly recompressed and refluxed at the top of the column (Figure 4b). In both cases, the raffinate exits from the bottom. Another mode of operation for the reflux process is the use of a temperature gradient in the top section of the column (the enrichment section), which serves to induce a drop in solubility, producing an internal reflux. This mode of operation can be exploited in some $sCO_2$-oil systems, depending on the P–T region, and is based on retrograde condensation phenomena [16,118].

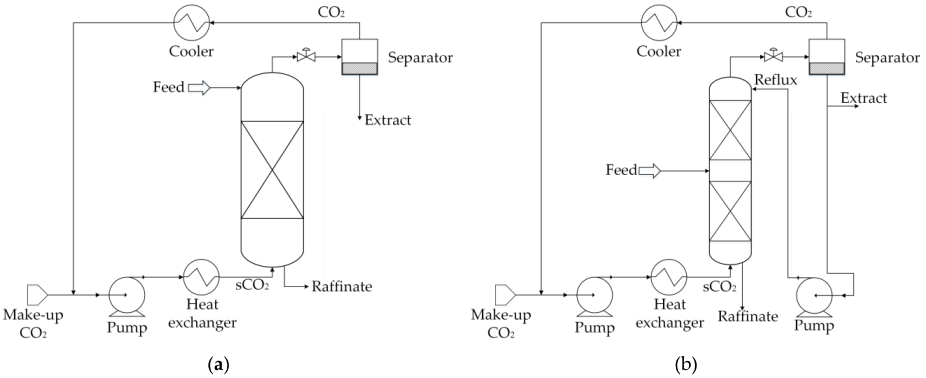


**Figure 4.** Flow diagram of continuous countercurrent extraction process. (**a**) Without reflux; (**b**) with reflux.

A few industrial applications have been established to exploit the advantages of $sCO_2$ as a solvent, which are mostly extractions from solid matter. Examples are coffee and tea decaffeination and the extraction of essential oils from plant feedstocks [113]. Such extractions from solid material are typically performed as batch semi-continuous operations by intermittently charging batches of the solid (e.g., coffee beans) and removing part of the spent materials from the bottom of the system without depressurizing (i.e., without shut down), while adding fresh material from the top [113]. A niche industrial application of $sCO_2$ on liquid feeds is the fractionation of perfluoropolyethers, aimed at narrowing the molecular weight distribution of polymer fractions used as lubricants [17]. In addition, separation of many other oils proved feasible using $sCO_2$ as a solvent. Such cases are the deterpenation of citrus oils [117,119], separation of fish oil ethyl esters [118,120,121], extraction of

squalene from vegetable oils [16], and purification of frying oil [122,123]. These research works show the potential of continuous countercurrent systems for oily feeds. Literature studies on $sCO_2$ extraction applications of crude oil mainly suggest the use of $sCO_2$ for fractionation of heavy oils and bitumens, aimed at recovering a lighter extract, separating it from a heavy asphaltenic residue. The extracts show lower molecular weight, boiling point, and viscosity, thus being more easily conveyed to other refinery units, while the residue can be used for electricity production [124,125].

### *3.2. $sCO_2$ Extraction of Lignocelulosic Bio-Oils*

The majority of the literature studies on $sCO_2$ separation of LC bio-oils refer to pyrolysis oils, with only a few cases referring to HTL biocrudes. Table 6 summarizes these works and their main aspects, regarding the nature of the biomass feedstock, the thermochemical conversion process producing the bio-oil, the system size, and the year of publication. All data so far are limited to laboratory-scale $sCO_2$ extraction systems and the semi-continuous single-stage mode of operation, with the exception of Mudraboyina et al. [126], where the extractor was coupled with a rectification column with a temperature gradient, allowing an internal reflux operation. The data selection was delimited to literature referring to extraction of LC bio-oils obtained by phase separation (e.g., gravity settling) of the reaction products of the thermochemical process. In particular, this means that extraction of LC bio-oil species dissolved or dispersed in water or in organic solvents is not considered relevant in this context.

**Table 6.** Experimental studies of semi-continuous $sCO_2$ fractionation of bio-oils.

| Feedstock | Thermochemical Process | Extractor Volume ($cm^3$) | Year | Ref. |
|---|---|---|---|---|
| Pine | HTL | 178 | 2020 | [58] |
| Pine | HTL | 178 | 2019 | [127] |
| Pine | HTL | 178 | 2019 | [64] |
| Palm kernel shell | Slow pyrolysis | 50 | 2018 | [128] |
| Pine | Fast pyrolysis | 640 | 2017 | [43] |
| Palm kernel shell | Slow pyrolysis | 50 | 2017 | [129] |
| Beech | Slow pyrolysis | 640 | 2016 | [130] |
| Red pine | Fast pyrolysis | 25 | 2016 | [131] |
| Kraft lignin | Microwave pyrolysis | 160[1] | 2015 | [126] |
| Beech | Slow pyrolysis and fast pyrolysis | 600 | 2015 | [84] |
| Sugarcane bagasse and cashew shells | Pyrolysis | - | 2011 | [132] |
| Wheat-hemlock | Fast pyrolysis | - | 2010 | [103] |
| Wheat-sawdust | Fast pyrolysis | - | 2009 | [133] |

[1] The extractor was coupled with a rectification column.

A generalized laboratory scale system is shown in Figure 5, which represents all literature studies except for Mudraboyina et al. [126], where the extractor was coupled with a rectification column. Such a typical system utilizes a $CO_2$ cylinder for supplying the solvent. $CO_2$ is subcooled via a heat exchanger and pumped as liquid to pressurize the vessel. $CO_2$ can be supplied to the system by different types of positive displacement pumps such as pneumatic [64], syringe [126], and diaphragm [43]. In some cases, the pumped $CO_2$ is preheated before entering the extractor [43,84,126,128–130]. The extraction vessel may contain an insert that can be dismounted for easy charging of the feed and retrieving the residue [64,127].

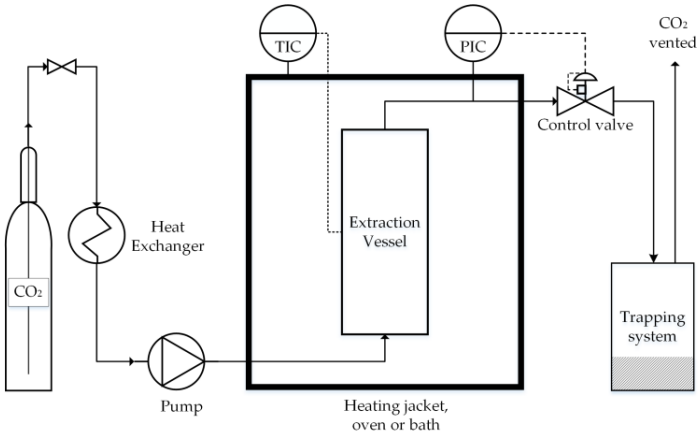


**Figure 5.** Generalized semi-continuous $sCO_2$ extraction system.

An inert packing material can be used to provide feed dispersion, thus increasing the contact area of $CO_2$ and the feed. For this purpose, glass beads [64,103,127,128,133] can be used, or a porous media (e.g., silica, activated carbon) [43,84,130,131] on which the bio-oil can be adsorbed prior to the $sCO_2$ extraction. In the latter case, some authors reported the introduction of effects that render the interpretation of the extraction results more complex. More specifically, Feng and Meier [43] reported different extraction yields between activated carbon and silica at the same extraction conditions, with the former achieving lower extraction yield than the latter at most extraction conditions, whereas the effect was inverted at 300 bar and 80 °C. However, the difference in these results is not adequate to provide a clear understanding of the effect of the two adsorbents. The potential of using experimental data that combine extraction and adsorption effects is limited in the perspective of scaling up the process to large-scale production, as the adsorbent use would raise issues for continuous operation. Exceptions would be presented only for batch separations aimed at extracting small quantities of high-value compounds, where solid–liquid interactions can be advantageously exploited.

With regard to practical aspects, the use of a non-return valve [64] at the bottom of the extraction vessel is advantageous in order to avoid back-flow of liquid feed and fouling of the upstream pipeline. This is particularly important for foulant residues that cannot be dissolved by pure $sCO_2$ and are difficult to dissolve with most solvents, as is the case for LC bio-oils. The extraction vessel can be heated by a heating jacket [64], an oven [128], or a bath [126], in order to maintain a constant extraction temperature. An automatic or manual valve can be used downstream the extractor to control the flow rate of $CO_2$. Downstream of the valve, the expanded fluid releases the components that are dissolved in $sCO_2$, which are collected in a trapping system while $CO_2$ gas is vented. This type of system is adequate for research purposes, although a potential industrial application would require separation of $CO_2$ from the extracts and a solvent recycle loop.

The trapping system should be considered carefully and ensure adequate collection of the extracts. In this regard, it is particularly important to (i) ensure a low temperature to allow maximum condensation of the extracts dissolved in the $CO_2$-rich phase (the gas phase); (ii) limit entrainment of liquid droplets and solid particles in the $CO_2$ gas stream exiting the expansion valve; and (iii) ensure a smooth flow of viscous extracts downstream of the expansion valve until the collection container. Such a trapping system can consist of a series of elements (e.g., washing bottles) that serve to capture the condensed extract, followed by additional elements such as adsorbents (e.g., activated carbon) or absorbents (e.g., water) to reduce entrainment of fine droplets. The trap can be at ambient or freezing temperature. The latter can greatly improve the condensation as well as reduce evaporation of the collected condensed extracts exposed to $CO_2$ flow during long extractions. This can be essential for

pyrolysis oils that contain a large mass fraction of relatively low-boiling organic components (e.g., acetic acid) and water. The latest work of Feng and Meier [43] highlights this important detail, where the authors used several traps at ambient conditions, including cotton wool, activated carbon, and water, while reporting mass balance discrepancies at the range of 6 wt% to 14 wt%. The same range of losses was encountered during the extraction of HTL lignocellulosic bio-oil, albeit using a cold (approximately 5) trapping system, but no adsorbent [64,127]. Another consideration is the viscosity of the extract, which increases as the extraction progresses. This may lead to the requirement of heating the tube downstream of the expansion valve in order to improve the flow towards the trap.

### *3.3. Experimental Conditions, Extraction Yields, and Vapor Phase Loadings*

Table 7 reports the operating parameters (i.e., extraction pressure (P) and temperature (T), initial mass of the feed (F), $CO_2$ mass flow rate, and solvent-to-feed ratio (S/F)) and the outcome of the experiments of $sCO_2$ extraction of LC bio-oils that were found in the literature. The outcome is reported in terms of total extraction yield (Y) and vapor phase loading (VPL). Y is the ratio of the total mass of extract to the mass of the feed. VPL is defined as the mass of extract retrieved for a given mass of $sCO_2$ that flowed in the extraction vessel (i.e., the solute loaded in the solvent). It is typically expressed as g of extract per kg of $sCO_2$ in a specific time interval. In addition, the density of pure $sCO_2$ is reported, taken from the NIST database [109].

**Table 7.** Experimental conditions and technical data of experiments of $sCO_2$ extraction of lignocellulosic bio-oils found in the literature. Pressure (P), temperature (T), $CO_2$ density, feed mass (F), $CO_2$ mass flow rate, solvent-to-feed ratio (S/F), total extraction yield (Y), and vapor phase loading (VPL) are reported.

| P (bar) | T (°C) | $CO_2$ Density (kg/m$^3$) | F (g) | $CO_2$ Flow (g/min) | S/F (g/g) | Y (wt%) | VPL (g/kg) | Ref. |
|---|---|---|---|---|---|---|---|---|
| 330–450 | 80–150 | 531–851 | 49–54 | 4.7–5.9 | 30.0–36.7 | 44.1–53.4 | 5.9–99.7 | [58] |
| 247–448 | 120 | 500–730 | 28.0–30.8 | 4.8–6.9 | 40.6–50.9 | 33.9–48.9 | 2.7–46.5 | [127] |
| 112–400 | 40–120 | 548–882 | 40.9–51.1 | 3.2–7.0 | 12.8–85.5 | 17.1–41.8 | 13.1–36.5 | [64] |
| 300–400 | 50–70 | 788–923 | 1.8–2.4 | 3.1–3.8 | 78.7–116.3 | 4.7–12.0 | 0.4–1.0 | [128] |
| 100–300 | 60–80 | 221–830 | 100[1] | 8.3 [1] | 30 [1] | 0.1–14.3 | 0.03–4.8 | [43] |
| 150–400 | 33–66 | 691–961 | 2.5 | 1.1–8.3 | 26.6–199.0 | 4.2–30.4 | 0.9–2.2 | [129] |
| 200 | 60 | 723 | 40–80 | 8.3 | 37.5–75.0 | 23.4–40.9 | 3.1–10.9 | [130] |
| 100–300 | 50 | 384–870 | 1.0 | 0.4–0.9 | 56.3 | 71.1 [2] | 30.6 [3] | [131] |
| 80–100 | 35 (45–95) [4] | 490–700 | 2–5 | 2–10 | 40–100 | 11–31 | 2.2–5.1 | [126] |
| 150–250 | 60 | 603–786 | 80 | 10 | 45 | 7.3–41.4 | 1.6–11.5 | [84] |
| 120–300 | 50 | 510–870 | 100 | 11.7–20 | 21–36 | 9–15 | 4.2–4.3 | [132] |
| 100–300 | 40 | 628–910 | 50 | 40 | 288 | 46 | 0.7–2.16 | [103] |
| 250–300 | 45 | 857–890 | 50 | 30 | 288 | 45 | 0.7–2.8 | [133] |

[1] Normalized data are provided only; [2] achieved with the use of co-solvent (i.e., methanol); [3] average value; [4] rectification column temperatures in parentheses.

The temperature in the literature studies was in the range of 40 to 120 °C. The pressure was largely varied between 80 bar and 448 bar, with the aim of a wide range of solvent density (i.e., 221 to 961 kg/m$^3$). However, only the studies of Chan et al. [128] and Montesantos et al. [58,64,127] explored pressures higher than 300 bar. $CO_2$ flowrates used in these studies ranged from values much lower than 1 g/min up to 40 g/min, which, in some cases, resulted in very low extraction yields or very high solvent-to-feed ratios. Depending on the applied conditions, extraction yield values in the range 0.1 wt% to 48.9 wt% are reported using pure $sCO_2$. Cheng et al. [131] achieved up to 71 wt% extraction yield with the use of up to 25 vol% of methanol as a co-solvent.

Regarding the effect of the extraction conditions, some important conclusions can be drawn. The increase of pressure at constant temperature is consistently reported as beneficial for extraction yields and vapor phase loadings. This is straightforwardly explained by the increase of the solvent power (i.e., increased solubility of bio-oil components in $sCO_2$). The effect of temperature increase at constant pressure is more complex, as it leads to improved mass transfer, but it can also lead to reduced solubility. Feng and Meier [43], on pyrolysis oils, and Montesantos et al. [58,64], on HTL biocrudes,

observed that a temperature increase at constant pressure generally increases Y and VPL, especially at high pressures (e.g., 300–400 bar). This indicates that, even though the increase of temperature is often associated with reduced solvent power, because of the decrease of solvent density, the enhanced mass transfer parameters improve the extraction rate and can improve Y and VPL of the process. In addition, Montesantos et al. [64] reported operational problems (i.e., sporadic clogging of the system) with HTL bio-oils at low temperatures. These problems were severe at 40 °C and moderate at 60 °C, while smooth operation was achieved at 80 °C and above.

### *3.4. Physical and Chemical Properties of $sCO_2$ Extracts*

$sCO_2$ extracts exhibit lower viscosity and density compared with the bio-oil feed. Patel et al. [132] reported the kinematic viscosity of sugarcane bagasse pyrolysis oil $sCO_2$ extracts and compared it with previously published viscosities of similar non-fractionated LC bio-oils [50]. The extracts, which accounted for only 9 wt%–15 wt% of the feed, exhibited a lower viscosity (i.e., approximately 18 cSt) than the crude bio-oil (approximately 28 cSt). It is important to note that, in an aging test of 60 days, the extracted oil showed greater stability with regard to viscosity, with an increase of only 4 cSt compared with approximately 22 cSt for the non-fractionated LC bio-oil.

Wang et al. [134] performed extraction of a corn stalk pyrolysis oil by a sequence of pressurization–depressurization steps (intermittent extraction), and reported that the density of the bio-oil (i.e., 1150 kg/m$^3$) was reduced down to 952–980 kg/m$^3$ for the extracts. Montesantos et al. [64] reported a reduction from 1051 kg/m$^3$ down to 941–1017 kg/m$^3$ for the extracts of HTL bio-oil from pinewood. Although the density reduction is moderate, from a fuel perspective, the $sCO_2$ extracts exhibit densities in line with residual marine fuels, which are typically in the range of 920 to 1010 kg/m$^3$ [135].

In the work of Montesantos et al. [64], TAN reductions from 129 mg KOH/g down to 61 to 120 mg KOH/g are reported for the $sCO_2$ extracts, with the TAN values increasing with the extraction progression (i.e., over time). Carboxylic acids were sequentially extracted, with short chain fatty acids extracted at the earlier stages and long chain fatty acids at later stages of the extraction. In addition, the acidity of $sCO_2$ residue shifted from carboxylic to phenolic nature, as the fatty acids were extracted preferentially with respect to more polar and heavier phenolic components.

Regarding water content, Feng and Meier [84] reported a reduction in both the extract and the residues for two fast pyrolysis oils. Even though this result clearly indicates the operational difficulties in collecting the extracted water in the trap, and thus the difficulties in closing the water mass balances, it also indicates that water is co-extracted. Therefore, $sCO_2$ extraction can be used as a means for dewatering the LC bio-oil while fractionating it. In the work of Feng and Meier [84], the water content of the two feeds was 19 wt% and 43 wt%; for the extract, it ranged from 10 wt% to 13 wt% and 14 wt% to 19 wt%; and for the residues, it ranged from 6 wt% to 8 wt% and 10 wt% to 13 wt%, respectively. Reduction of water in the $sCO_2$ extract of a HTL biocrude was observed by Montesantos et al. [58] as well, where the extracts were dewatered up to 77%, with respect to the initial water content.

Regarding metal content, in a recent work, Montesantos et al. [58] focused on the effect of $sCO_2$ extraction on the removal of metals from HTL biocrude. The authors reported 95%–98% removal of metals (i.e., metal content reduced from 8500 mg/kg to lower than 200 mg/kg), which represents a significant improvement of the quality of the extracts, with respect to the feed biocrude, in light of the downstream hydrotreating. With regard to the elemental composition, the difference between $sCO_2$ extracts and their respective feeds can be seen in Figure 6, where the H/C atomic ratio and the oxygen mass fractions on a water-free basis are compared. In the case of extracts, values corresponding to extractions at different pressure and temperature conditions on the same feed were averaged.

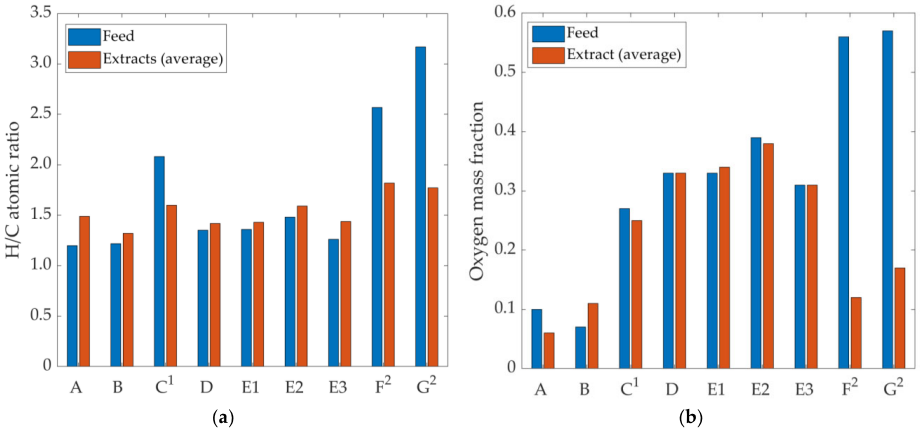


**Figure 6.** (**a**) H/C atomic ratio and (**b**) oxygen mass fraction of bio-oils (feed) and their $sCO_2$ extracts on a water-free basis. A: Montesantos et al. [58]; B: Montesantos et al. [64]; C: Chan et al. [129]; D: Feng and Meier [130]; E1–E3: Feng and Meier [84]; F: Naik et al. [103]; G: Rout et al. [133]. E1–E3 correspond to different feeds. [1] It was assumed that the data were reported on a water-free basis (unspecified by the authors); [2] it was assumed that the data were reported including water (unspecified by the authors).

In most cases, the H/C ratio and oxygen mass fraction are not affected, or are moderately affected, by the extraction. In particular, the absence of significant variation of the oxygen content indicates that oxygen is widespread in many classes of molecules of different polarity and molecular weight, making it difficult to have a selective process in this regard. For an HTL biocrude, Montesantos et al. [58] reported a partial deoxygenation (i.e., oxygen mass fraction 0.10 down to 0.05–0.07). The oxygen reduction can be explained in terms of the increased VPL of alkylbenzenes and polyaromatic hydrocarbons, especially in the first extracts, in the presence of water in the biocrude (extraction of nondewatered bio-oil). The data from Naik et al. [103] and Rout et al. [133] appear to be strong outliers. In these works, a fast pyrolysis oil with an extremely high oxygen content is reported, which is higher than the oxygen content of the biomass feedstock. In addition, the majority of GC-MS identified components are oxygenated organic molecules, with a lower oxygen content than the oxygen reported by elemental analysis. All things considered, the data from Naik et al. [103] and Rout et al. [133] seem to show some inconsistencies.

### *3.5. Chemical Composition $sCO_2$ Extracts*

The components identified in the volatile fraction of $sCO_2$ extracts of LC bio-oils can be generally grouped into the following chemical classes: (1) ketones; (2) phenols; (3) guaiacols; (4) benzenediols; (5) aldehydes; (6) esters; (7) furans; (8) syringols; (9) short chain fatty acids (SFAs); (10) long chain fatty acids (LFAs); (11) aromatic acids (ArAcid); (12) single-ring aromatic hydrocarbons (benzenes); and (13) polyaromatic hydrocarbons (PAHs). These classes, with indication of the key components reported in the literature, are presented in Table 8.

**Table 8.** Typical chemical classes and key components observed in $sCO_2$ extracts [43,58,64,84,103,126,129,130,132,133].

| Number | Class | MW Range | Key Components | Carbon Number |
|---|---|---|---|---|
| 1 | Ketones | 74–124 | Acetol | 3 |
| | | | Acetylacetone | 5 |
| | | | 2-pentanone | 5 |
| | | | Propan-2-one. 1-acetyloxy- | 5 |
| | | | 2-Cyclopenten-1-one, 2,3-dimethyl- | 7 |
| 2 | Phenols | 94–122 | Phenol | 6 |
| | | | o-cresol | 7 |
| | | | m-cresol | 7 |
| | | | p-cresol | 7 |
| | | | 2,5-Dimethylphenol (p-xylenol) | 8 |
| 3 | Guaiacols | 124–178 | Guaiacol | 7 |
| | | | 4-methyl guaiacol | 8 |
| | | | 4-ethyl guaiacol | 8 |
| | | | 4-propyl guaiacol | 8 |
| | | | Eugenol | 10 |
| | | | Isoeugenol | 10 |
| | | | Creosol | 8 |
| | | | Vanillin | 8 |
| 4 | Benzenediols | 110–124 | 1,2-Benzenediol | 6 |
| 5 | Aldehydes | 60–152 | Glycolaldehyde | 2 |
| 6 | Esters | 130–296 | Pentanoic acid. 4-oxo-. methylester | 6 |
| 7 | Furans | 84–126 | Furfural | 5 |
| | | | 5-Hydroxymethylfurfural | 6 |
| 8 | Syringols | 154 | Syringol | 8 |
| 9 | Short chain fatty acids | 60–144 | Acetic acid | 2 |
| | | | Propionic acid | 3 |
| | | | Hexanoic acid | 6 |
| 10 | Long chain fatty acids | 256–284 | n-Hexadecanoic acid | 16 |
| | | | n-Octadecanoic acid | 18 |
| 11 | Aromatic acids | 136 | Benzeneacetic acid, 3-hydroxy | 8 |
| 12 | Benzenes | 120 | o-Cumene | 10 |
| 13 | Polyaromatic hydrocarbons | 128 | Naphthalene | 10 |

Most of these classes include low molecular weight components. Some chemical classes comprise components characterized by a narrow molecular weight range, whereas fatty acids [64] and esters [84], observed in HTL and pyrolysis oil extracts, respectively, are characterized by a wide range of molecular weight (see Table 5). The boiling point distribution in the extracts is in a wide range as well, from as low as 117 °C for acetic acid, reaching up to 400 °C for the high molecular weight fatty acids.

Most components are typically in low amounts in the $sCO_2$ extracts (below 1 wt%) of both oils, with a few exceptions. In extracts of pyrolysis oils, short chain carboxylic acids, acetol, and glycolaldehyde are observed in large amounts; in some cases, as high as 20 wt% [43,84,130]. In addition, guaiacol, furfural, and syringol are reported with noteworthy mass fractions (1 wt%–5 wt%) in extracts of LC bio-oils of both pyrolysis and HTL. As a result of the concentration of these components, the $sCO_2$ extracts exhibit a larger volatile fraction, with the fraction of the oil that can be identified by GC-MS being larger than the feed (e.g., up to 70 wt% [84]). On the other hand, levoglucosan (a sugar) present in pyrolysis oils (see Section 2.2.) is not extracted and remains entirely in the residue.

In an attempt of highlighting trends and providing some quantitative indication, values of distribution factors (K-values) were calculated from the available data reported in the literature. The calculated K-values are reported in Figure 7. using a box plot, covering the range of P, T, and composition corresponding to the experimental conditions. It should be noted that, as compositional information mostly refers to the lighter fraction of the bio-oil, most of the identified components are extracted preferentially, thus with K-values higher than 1.

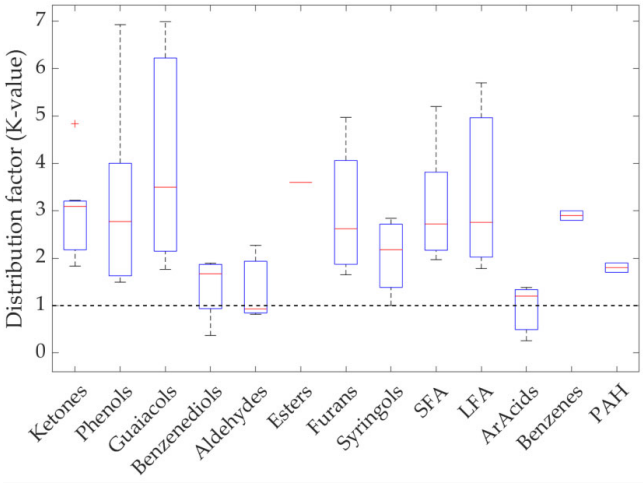


**Figure 7.** Distribution factors (K-values) of component classes identified in the literature. K-values correspond to the pressure, temperature, and compositional ranges reported in the literature. The boxes include the 50% distributed around the average, the red line is the median value, the whiskers are the extreme values (over 75% and under 25%), and the "+" denotes values considered outliers [58,64,84,126,127,129,130]. SFA, short chain fatty acid; LFA, long chain fatty acid; PAH, polyaromatic hydrocarbon.

As can be seen, guaiacols are among the most preferentially extracted components, with the highest median K-value (close to 4). Among other hydroxybenzenes, phenols, syringol, and benzenediols show descending K-values in the range of 2.8 down to 1.8. This is in line with the solubility predictions performed by Maqbool et al. [101], which show that guaiacols have the highest solubility in $sCO_2$, followed by phenols and benzenediols. The lower K-values of benzenediols are connected with their higher polarity, owing to the presence of two hydroxyl groups. They were, however, observed to be extracted with yields up to 60 wt%, after the preferentially extracted components (e.g., guaiacols) were depleted in the feed [64]. Low molecular weight ketones and furans (see Table 8) are other classes of components preferentially extracted, with K-values close to 3. The extracted components of these classes show similar molecular weight and polarity. Glycolaldehyde is the only aldehyde found in a considerable amount in pyrolysis oils (up to 8 wt%), and has one of the lowest MWs of the reported components [43]. For this component, the available literature data do not allow calculating K-values, although it was reported by Feng and Meier [43] to be remarkably concentrated up to 16 wt%. Esters are typically not detected in the feeds, but low molecular weight esters (i.e., 100–130) were reported in a single case in the $sCO_2$ extracts (up to 1.6 wt%), indicating high expected K-values [84].

With regard to the acids, most literature works report acetic and propionic acids, which are found in pyrolysis oil feed at high concentrations. Their K-values are typically above 2–3, which is in line with their low molecular weight. Montesantos et al. [58,64,127] identified several fatty acids ranging between C5 and C18, as well as two aromatic acids. As an example, Figure 8 shows the K-values of said acids in terms of extraction progression (extraction time increasing from left to right). All reported extractions were at 120 °C, but with different pressures (and thus different solvent densities). As can be

seen, the short chain fatty acids (i.e., C5–C8, SFA) maintain high K-values for the whole duration of the extraction, which is in line with their relatively low MW. On the contrary, the long chain fatty acids (i.e., C6–C18, LFA) and the aromatic acids (i.e., dehydroabietic acid, ArAcid) initially exhibit K-values lower than 1 and, at the latest stages, they are extracted with K-values up to 8 and 4, respectively. This figure highlights the possibility of sequential extraction and fractionation of different acids on the basis of their molecular weight. From a theoretical standpoint, it also highlights the high dependency of K-values on the composition of the mixture, which reflects the strong thermodynamic non-ideality of the system $sCO_2$ + bio-oil.

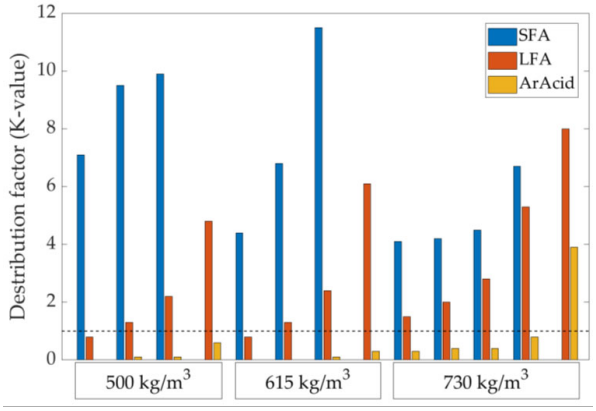


**Figure 8.** Variation of K-values with extraction progression (left to right) of different types of acids: short chain fatty acids (SFAs); long chain fatty acids (LFAs); aromatic acids (ArAcid). Extraction temperature: 120 °C. Three different solvent densities [127].

Finally, the only cases reporting the extraction of aromatic hydrocarbons are the works of Montesantos et al. [58,127] on an HTL biocrude. In these works, alkylbenzenes (e.g., o-cymene) exhibited the highest K-values (up to 6) and were extracted with yields up to 90 wt%. Polyaromatic hydrocarbons were the largest fraction of the extract (up to 23 wt%) and included some of the highest molecular weight components (e.g., retene). They exhibited increasing K-values with extraction progression, as the lower MW components were depleted from the feed, achieving extraction yields up to 83 wt%. The possibility of extracting these components is in line with the known capability of $sCO_2$ of extracting hydrocarbons, even at a very high molecular weight.

## 4. High Pressure Solubility Data and Modelling

The process design of $sCO_2$ extraction and downstream separation of LC bio-oils requires the development of suitable thermodynamic models (e.g., based on cubic equations of state) in order to estimate the K-values of the different species to be separated, for a given pressure, temperature, and overall composition of the system. In turn, the development of such models for complex mixtures as LC bio-oils requires strategies of lumping bio-oil components into classes, defining thermodynamic properties (e.g., critical properties and acentric factors) for each class of components, as well as collecting experimental data of high-pressure phase equilibrium of $sCO_2$ and selected class-representative components. Experimental data are used for model validation and model tuning by estimation of optimal values of binary interaction parameters. This procedure is analogous to what has been developed for decades for petroleum reservoir fluids, also in relation to $sCO_2$ injection studies [136]. However, crude LC bio-oils (i.e., prior to hydrotreating) are drastically different from fossil crude oils, with a large amount of oxygen and polar components spread in the entire molecular weight range, which leads to notes of complexity in the definition of optimal lumping strategies.

In addition, literature data on high-pressure phase equilibria for $sCO_2$ and key components of LC bio-oils are very scarce. The fact that a large fraction of LC bio-oils is not fully characterized adds to this complexity.

The available solubility data of key components of LC bio-oils in the $sCO_2$-rich phase are correlated with the semi-empirical density-based model of Chrastil [137]. This procedure proved satisfactory for systems composed of $sCO_2$ and bio-oil components by Maqbool et al. [101] and, in this work, it is substantially extended to a larger number of components and chemical classes. The equation suggested by Chrastil takes the following form:

$$S = \rho^k \exp\left(\frac{a}{T} + b\right) \quad (1)$$

where:

*S*: solubility of the solute in the $sCO_2$-rich phase (grams of solute per liters of pure solvent at the P, T conditions of interest);
$\rho$: density of the pure solvent (g/L) at the P, T conditions of interest;
k: association number (i.e., number of $CO_2$ molecules associated with one solute molecule);
a: constant connected to the enthalpy of solvation and vaporization;
T: temperature (K);
b: constant connected to the molecular weights of the solvent and the solute.

The basic assumption of the Chrastil model is that a molecule of the solute is associated with a fixed number (k) of solvent molecules at a given temperature. The correlation proved successful for many components dissolved in $sCO_2$ corresponding to or having a similar structure to species found in LC bio-oils (e.g., phenol, naphthalene, octadecenoic acid [101,137]). In addition, it proved successful in a wide range of pressures and temperatures, provided that the solubility of the solute is not too high (typically solubility *S* not above 200 g/L) [137]. Considering that the VPLs of LC bio-oils, in the range of operating conditions of interest (see Section 3), are typically below 100 g/kg, the Chrastil model is expected to be a valid tool for correlation and data analysis.

*Binary Phase Equilibrium Data of LC Bio-Oil Components and $sCO_2$*

Table 9 reports a summary of the binary phase equilibrium data available in the literature, with reference to relevant components of LC bio-oils and $sCO_2$. For each publication, the component is specified, together with the pressure and temperature range of the measurements, as well as the corresponding density of pure $sCO_2$. The method of measurement is reported as analytical or synthetic, corresponding to the classification introduced by Dohrn and Brunner [138]. In short, the analytical method indicates that sampling and consequent analysis of the phases were performed, whereas in the synthetic method, bubble or dew point pressures are determined at given temperatures and overall compositions. With regard to the type of data, the symbol VLE indicates that both the solubility of the bio-oil components in the $sCO_2$-rich phase and the solubility of $CO_2$ in the liquid phase are reported. When "solubility" is indicated, the solubility of the bio-oil component in the $sCO_2$-rich phase is the only type of data reported. The complete solubility data can be found in the Supporting Information (Table S1). Table S1 collects all numerical data that are reported by the listed publications at supercritical $sCO_2$ conditions.

**Table 9.** Chemical components studied and experimental conditions of measured phase equilibrium data with $sCO_2$ in the literature. Temperature range (T), pressure range (P), $sCO_2$ density range (ρ), type of measurement (method), and type of data (data) are reported.

| Component | T (°C) | P (bar) | ρ (kg/m$^3$) [1] | Method | Data | Ref. |
|---|---|---|---|---|---|---|
| Cyclohexanone | 160–180 | 90–220 | 115–332 | Analytical | VLE | [139] |
| 5-Hydroxymethylfurfural | 41–70 | 97–196 | 390–823 | Synthetic | Solubility | [140] |
| Heptanoic acid | 40–60 | 85–200 | 212–840 | Analytical | Solubility | [141] |
| Hexadecanoic acid | 40 | 80–248 | 278–878 | Analytical | Solubility | [142] |
| | 35–55 | 138–414 | 610–977 | Analytical | Solubility | [143] |
| | 35 | 99–230 | 709–888 | Analytical | Solubility | [144] |
| | 35–55 | 128–226 | 560–885 | Analytical | Solubility | [145] |
| | 40–45 | 101–233 | 512–864 | Synthetic | Solubility | [146] |
| | 64–78 | 105–260 | 643–759 | Synthetic | VLE | [147] |
| Cumene | 40–120 | 76–183 | 131–376 | Analytical | VLE | [148] |
| | 70 | 87–116 | 197–324 | Analytical | VLE | [149] |
| | 50 | 80–88 | 220–270 | Analytical | VLE | [150] |
| Naphthalene | 35–65 | 81–287 | 208–903 | Analytical | Solubility | [151] |
| | 121–162 | 77–166 | 120–313 | Analytical | VLE | [152] |
| Benzeneacetic acid | 35–45 | 90–200 | 381–852 | Analytical | Solubility | [153] |
| Benzoic acid | 35–70 | 101–364 | 252–958 | Analytical | Solubility | [154] |
| | 45–65 | 120–280 | 384–878 | Analytical | Solubility | [155] |
| Phenol | 60–90 | 100–350 | 203–863 | Analytical | Solubility | [156] |
| | 36–60 | 79–249 | 334–897 | Analytical | Solubility | [157] |
| | 100 | 107–301 | 207–663 | Analytical | VLE | [158] |
| Catechol | 60–90 | 100–350 | 203–863 | Analytical | Solubility | [156] |
| | 35–65 | 122–405 | 396–974 | Analytical | Solubility | [159] |
| Vanillin | 40–80 | 80–277 | 160–895 | Analytical | Solubility | [160] |
| | 35–45 | 83–195 | 466–857 | Analytical | Solubility | [153] |
| | 68–136 | 216–1341 | 561–1115 | Synthetic | VLE | [161] |
| Guaiacol | 50–120 | 80–200 | 128–784 | Analytical | VLE | [162] |
| o-Cresol | 100 | 104–263 | 199–610 | Analytical | VLE | [158] |
| | 50–200 | 99–300 | 121–848 | Analytical | VLE | [163] |
| m-Cresol | 35–55 | 80–240 | 204–895 | Analytical | VLE | [164] |
| | 100 | 102–300 | 194–662 | Analytical | VLE | [158] |
| p-Cresol | 50–200 | 100–348 | 123–898 | Analytical | VLE | [163] |
| | 80–150 | 80–200 | 113–594 | Analytical | VLE | [162] |
| | 100 | 103–302 | 196–663 | Analytical | VLE | [158] |

[1] Taken from NIST [109].

The components reported in Table 9 are chosen to represent the chemical classes indicated in Table 8, taking into account the availability of phase equilibrium data in the literature. All data retrieved in the literature were included in the analysis, with the exception of a few data sets concerning hexadecanoic acid and naphthalene. With regard to the former, six works were selected owing to the fact they show consistent data at the same P and T conditions, besides being based on high purity solutes and sound methodology. With regard to naphthalene, several literature sources exist. In this case, the work of McHugh and Paulaitis [151] was selected as their data are often used as reference by other works. In addition, the data reported by Yanagiuchi et al. [152] were chosen because they report data at high temperatures, as opposed to the typical range of 35–80 °C for all other published works.

Solubility data of LC bio-oil components in the $sCO_2$-rich phase were correlated using the linearized form of the Chrastil equation:

$$\ln(S) = k ln(\rho) + \left(\frac{a}{T} + b\right) \quad (2)$$

Equation (2) was thus used for performing a multiple linear regression analysis of the experimental data reported in Table 9, referring to the $sCO_2$-rich phase. The density of pure $CO_2$ is taken from the NIST webbook, whose data are based on the Span–Wagner equation of state [109]. The set of optimal values for the parameters k, a, and b is reported for each component in Table 10, together with the regression statistics.

**Table 10.** Chrastil solubility constants (k, a, b) for the binary systems of bio-oil components and $sCO_2$, statistical properties of the regression ($R^2$, ARD), and number of experimental data regressed (N).

| | Regressed Parameter | | | Goodness of Fit | | |
|---|---|---|---|---|---|---|
| **Component** | **k** | **a (K)** | **b** | **$R^2$** | **ARD %** | **N** |
| Cyclohexanone | 2.0216 | −3425.3 | 0.45405 | 0.984 | 2.0 | 10 |
| 5-Hydroxymethylfurfural | 4.0412 | −3263.6 | −15.267 | 0.973 | 9.0 | 19 |
| Heptanoic acid | 6.0527 | −3806.1 | −23.733 | 0.987 | 8.1 | 15 |
| Hexadecanoic acid | 7.5664 | −9042.3 | −20.706 | 0.950 | 19.0 | 62 |
| Cumene | 2.5852 | −3481.6 | −2.1835 | 0.963 | 9.3 | 41 |
| Naphthalene | 3.7852 | −4080.9 | −8.1975 | 0.940 | 14.7 | 63 |
| Benzeneacetic acid | 6.1072 | −10177 | −5.2314 | 0.986 | 4.9 | 24 |
| Benzoic acid | 5.2174 | −5860.4 | −14.636 | 0.986 | 13.4 | 53 |
| Phenol | 3.0544 | −3081.4 | 6.9331 | 0.729 | 10.8 | 73 |
| Catechol | 3.7457 | −3716.1 | −12.417 | 0.977 | 18.2 | 62 |
| Vanillin | 4.0675 | −4210.7 | −11.707 | 0.948 | 18.4 | 74 |
| Guaiacol | 4.0447 | −2597.8 | −14.042 | 0.965 | 21.0 | 13 |
| o-Cresol | 3.4937 | −3026.3 | −9.2413 | 0.867 | 13.1 | 16 |
| m-Cresol | 3.8196 | −2950.5 | −12.383 | 0.98 | 18.0 | 23 |
| p-Cresol | 3.2734 | −3441.3 | −7.5747 | 0.924 | 15.7 | 30 |

For most data, the linearity is good, with $R^2$ values above 0.92. Exceptions are the values for phenol and o-cresol. For the latter, it is because of several solubility values being above 100–200 g/L. In this case, the density of the mixture starts departing from the solvent density and the model becomes less accurate [137]. In all cases, the average relative deviation between the calculated and experimental values is between 2% and 21%. The association value k is generally in line with available literature values [101,137,140,143]. It is observed that phenolics have values between 3 and 4, which is in line with the values reported by Maqbool et al. [101], even though the datasets are substantially expanded in this work. Cumene (1-ring aromatic hydrocarbon) exhibits one of the lowest k (i.e., 2.6), while naphthalene exhibits a higher value (i.e., 3.8), which is in line with its higher molecular size. Fatty acids have higher values, increasing with the molecular size as well.

Experimental solubilities of LC bio-oil components in the $sCO_2$-rich phase, expressed as grams of solute per kg of solvent, are plotted in Figure 9 as a function of the $sCO_2$ density for different temperatures. In the same figure, isotherms predicted by the Chrastil model are shown (continuous lines) for the corresponding values of temperature and solvent density. When more than one data source for the same experimental temperature exists, the one with the largest solvent density range was plotted.

In Figure 9, the effect of density and temperature can be appreciated. It is noted that increasing the solvent density at a given temperature corresponds to increasing pressures. As expected, the solubility increases with the solvent density for all isotherms. In addition, in all cases, higher temperatures at constant density conditions (i.e., increasing pressure) result in higher solubilities.

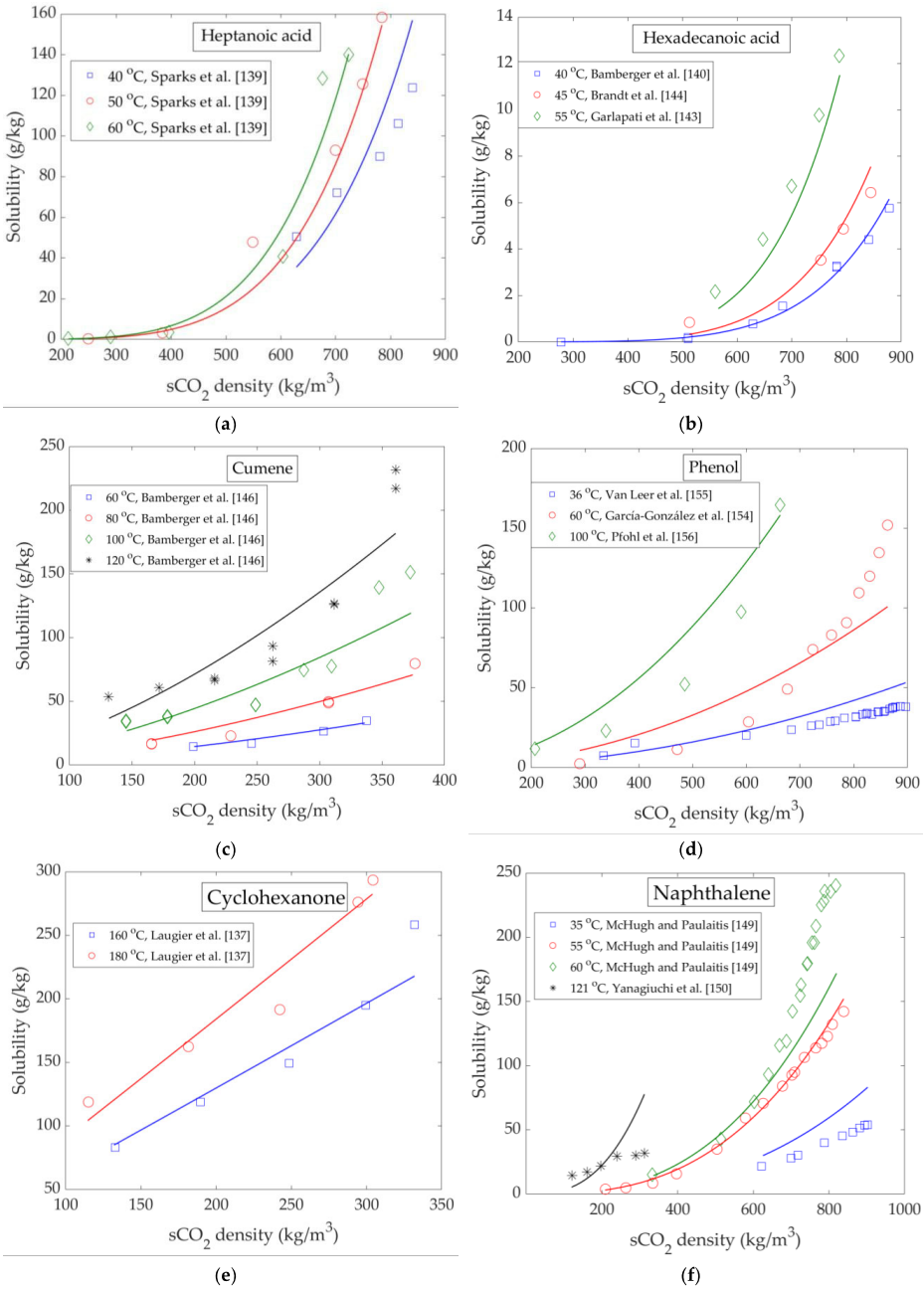


**Figure 9.** *Cont.*

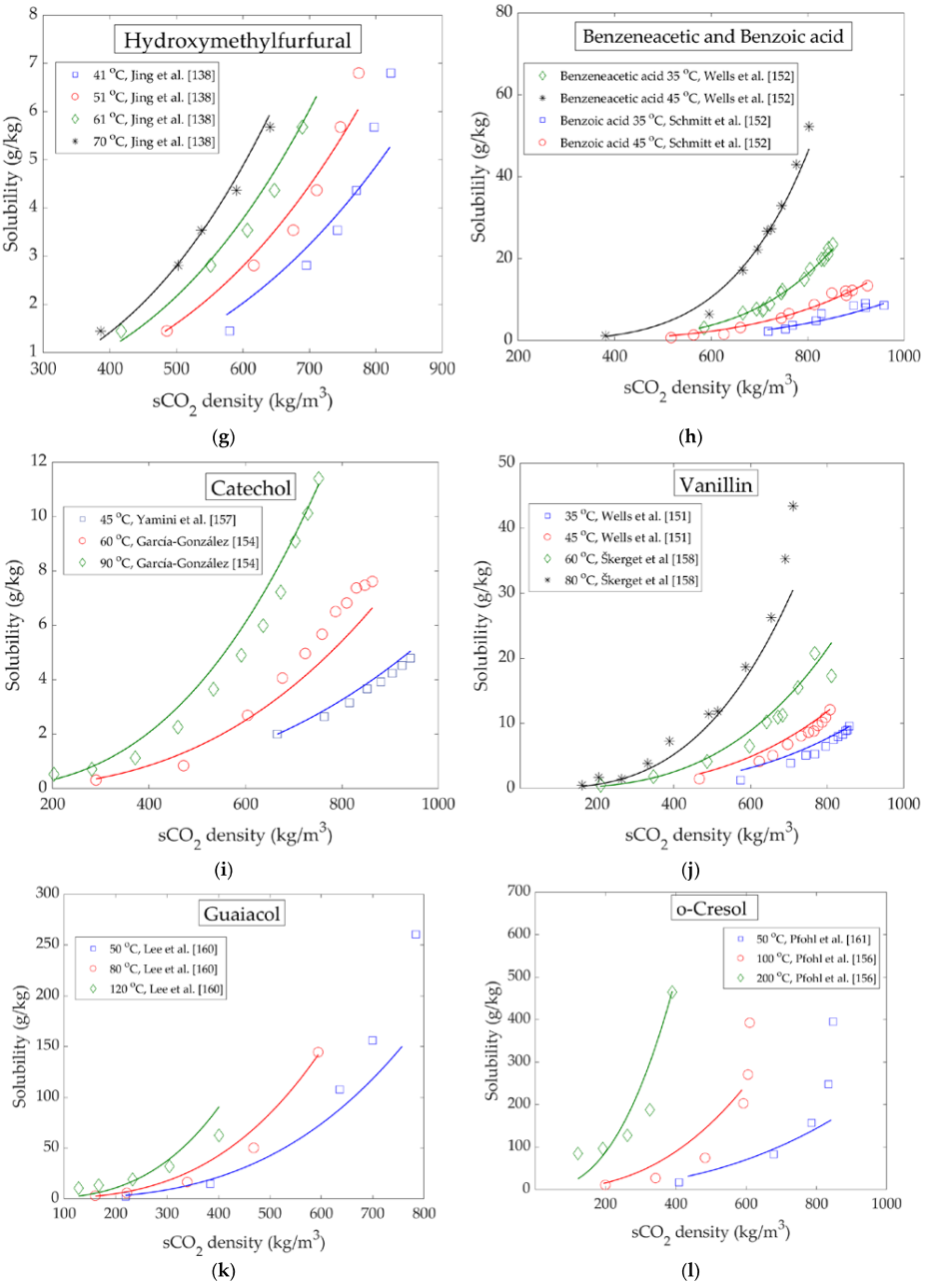


**Figure 9.** *Cont.*

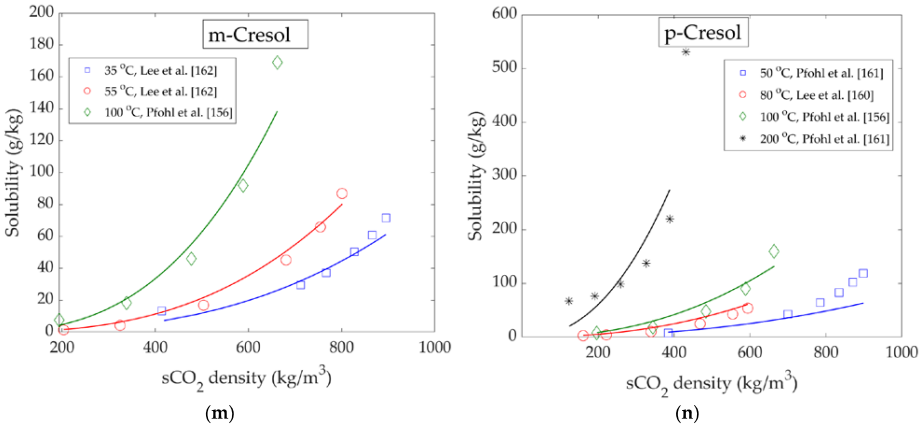


**Figure 9.** Solubility isotherms vs. $sCO_2$ density for all components studied. Markers indicate experimental data, while continuous lines are obtained with the Chrastil model. (**a**) Heptanoic acid; (**b**) Hexadecanoic acid; (**c**) Cumene; (**d**) Phenol; (**e**) Cyclohexanone; (**f**) Naphthalene; (**g**) Hydroxymethylfurfural; (**h**) Benzeneacetic and benzoic acid; (**i**) Catechol; (**j**) Vanillin; (**k**) Guaiacol; (**l**) o-Cresol; (**m**) m-Cresol; (**n**) p-Cresol.

These trends are in line with VPL values of $sCO_2$ extraction of LC bio-oils discussed in Section 3.3. A good example of the effect of temperature is vanillin, whose solubility at 80 °C increases considerably with the increasing solvent density, while at the lower temperatures, the increase is much less significant.

The solubility of $sCO_2$ in the liquid phase is provided only in a few cases. The available data show that $sCO_2$ exhibits high solubility in liquid hydrocarbons. For example, the solubility of $sCO_2$ in cumene ranges from 165 to 586 g/kg at 120 °C [148]. At the same temperature, naphthalene can dissolve 100–303 g/kg of $CO_2$ for pressure ranging from approximately 80 to 160 bar [152] $CO_2$. For the system $sCO_2$ + cyclohexanone, at the relatively high temperatures reported (i.e., 160 °C and 180 °C), $CO_2$ solubilities range from 146 to 555 g/kg [139]. A relatively large amount of $CO_2$ is dissolved in hexadecanoic acid as well, with the range being from 244 to 415 g/kg [147]. The solubility of $CO_2$ in phenolic components follows the trend cresols and guaiacol > phenol > vanillin [158–164]. In all cases, however, values above 380 g/kg were reported at the higher pressures (200–300 bar), with the exception of vanillin, where such high values were only reached at extremely high pressures (i.e., 762–1357 bar) [161]. In general, the data show that a large amount of $sCO_2$ can be dissolved in this type of liquid components. This is a favorable property for the separation of LC bio-oils in countercurrent equipment, as the dissolution of the supercritical solvent in the liquid causes the viscosity to drop, thus improving process operability.

## 5. Conclusions and Perspectives

The current work reviews the state-of-the-art on $sCO_2$ extraction of second-generation lignocellulosic bio-oils, produced by pyrolysis or hydrothermal liquefaction. $sCO_2$ extraction is deemed a promising physical separation process that can be integrated in the downstream of the thermochemical conversion unit with the aim of valorizing the raw bio-oils. Two main application areas are envisaged: (1) high yield extraction of HTL biocrudes for drop in bio-fuel production; (2) extraction of specific chemicals from pyrolysis oils.

In the case of HTL biocrudes, the application of $sCO_2$ allows extraction yields above 50%, with the production of extracts with favorable properties towards hydrotreatment. Namely, extracts have lower water content, lower average molecular weight, lower density, viscosity, and acidity, with the acidity nature shifted towards carboxylic instead of phenolic. In addition, the metal content of

$sCO_2$ extracts is drastically reduced, from the very high values of HTL biocrudes (e.g., 8500 mg/kg) to values below 200 mg/kg, as metals are left in the residue of the $sCO_2$ extraction processes [58]. These properties are expected to lead to a lower deactivation rate of the hydrotreatment catalyst and reduced coking and fouling, overall leading to better process operability and economics. Moreover, the hydrotreatment products are expected to be shifted towards lighter hydrocarbon fractions, which are more valuable. On the other hand, the oxygen content of the extracts is comparable to that of the feed, or only moderately decreased, which means that significantly lower hydrogen requirements (per unit hydrotreatment feed) are not expected. However, this aspect is comparable to the experimental findings of vacuum distillation of HTL bio-oils, which also reported oxygen to be widespread in the whole range of distilled fractions. In this context, experimental works focusing on the comparison of hydrotreating of raw HTL biocrudes versus $sCO_2$ extracts is an important knowledge gap. Future research work is needed in this area.

In the case of pyrolysis oils, $sCO_2$ can be used for the recovery of fractions rich in short chain organic acids, such as acetic and propionic acids, short chain fatty acids, acetol, and furfural, owing to their relative abundance in this type of oil. The recovery of fractions rich in 1-ring lignin-derived phenolics (phenols and guaiacols) and their separation from benzenediols and long chain fatty acids is also deemed feasible on the basis of K-value analysis. High value chemicals like vanillin can also be recovered and made available for downstream purification. On the other hand, the $sCO_2$ residue of pyrolysis oil is concentrated in sugars and might have the potential to be fed to other biorefinery processes such as anaerobic digestion. In the case of pyrolysis oils, the use of $sCO_2$ for the downstream separation of the extracted components into several classes is a topic requiring further research in order to provide basic process schemes that can be evaluated in terms of process economics.

For both types of oils, the knowledge of the heavy fraction is scarce. Further studies addressing this aspect would be needed, in order to envisage possible utilizations of the residue, other than burning it for heat recovery. For example, it may have similarities with biochar and hydrochar, and can provide the base material for the production of adsorbents [165]. Phenolic oligomers from bio-oils were suggested as potential fuel antioxidants [105,107,108]. As $sCO_2$ extracts preferentially phenolic monomers, the residue is expected to be enriched in these components. The possibility of recovering this fraction using $sCO_2$, as pure solvent or with the use of small quantities of modifiers (e.g., ethanol, propanol), is another area of research to be developed.

As the natural competitor of $sCO_2$ extraction on LC bio-oils is vacuum distillation, experimental works aimed at comparing the two processes would be relevant to assess the advantages and drawbacks of the two processes in terms of yields and selectivity, as well as energy requirements for continuous countercurrent processing at a large scale.

**Supplementary Materials:** The following are available online at http://www.mdpi.com/1996-1073/13/7/1600/s1, Literature solubility of bio-oil components in $sCO_2$, Table S1.

**Author Contributions:** Conceptualization, N.M. and M.M.; methodology, N.M. and M.M.; writing—original draft preparation, N.M.; writing—review and editing, N.M. and M.M; Data Curation N.M.; Formal Analysis: N.M. and M.M.; Investigation: N.M. and M.M.; Visualization: N.M.; supervision, M.M. All authors have read and agreed to the published version of the manuscript.

**Funding:** This research received no external funding.

**Conflicts of Interest:** The authors declare no conflict of interest.

## References

1. International Energy Outlook 2019. Available online: https://www.eia.gov/outlooks/ieo/ (accessed on 17 December 2019).
2. IEA. World Energy Statistics 2019. IEA: Paris, France, 2019. Available online: https://www.iea.org/reports/world-energy-statistics-2019 (accessed on 1 September 2019).

3. Kosinkova, J.; Doshi, A.; Maire, J.; Ristovski, Z.; Brown, R.; Rainey, T.J. Measuring the regional availability of biomass for biofuels and the potential for microalgae. *Renew. Sustain. Energy Rev.* **2015**, *49*, 1271–1285. [CrossRef]
4. US Environmental Protection Agency. *Biofuels and the Environment: Second Triennial Report to Congress*; US Environmental Protection Agency: Washington, DC, USA, 2018.
5. IEA Renewables 2019. Available online: https://www.iea.org/reports/renewables-2019 (accessed on 17 December 2019).
6. Baloch, H.A.; Nizamuddin, S.; Siddiqui, M.T.H.; Riaz, S.; Jatoi, A.S.; Dumbre, D.K.; Mubarak, N.M.; Srinivasan, M.P.; Griffin, G.J. Recent advances in production and upgrading of bio-oil from biomass: A critical overview. *J. Environ. Chem. Eng.* **2018**, *6*, 5101–5118. [CrossRef]
7. Ramirez, J.A.; Brown, R.J.; Rainey, T.J. A review of hydrothermal liquefaction bio-crude properties and prospects for upgrading to transportation fuels. *Energies* **2015**, *8*, 6765–6794. [CrossRef]
8. Bridgwater, A.V. Review of fast pyrolysis of biomass and product upgrading. *Biomass Bioenergy* **2012**, *38*, 68–94. [CrossRef]
9. Hoffmann, J.; Jensen, C.U.; Rosendahl, L.A. Co-processing potential of HTL bio-crude at petroleum refineries-Part 1: Fractional distillation and characterization. *Fuel* **2016**, *165*, 526–535. [CrossRef]
10. Pedersen, T.H.; Jensen, C.U.; Sandström, L.; Rosendahl, L.A. Full characterization of compounds obtained from fractional distillation and upgrading of a HTL biocrude. *Appl. Energy* **2017**, *202*, 408–419. [CrossRef]
11. Elkasabi, Y.; Mullen, C.A.; Boateng, A.A. Distillation and isolation of commodity chemicals from bio-oil made by tail-gas reactive pyrolysis. *ACS Sustain. Chem. Eng.* **2014**, *2*, 2042–2052. [CrossRef]
12. Capunitan, J.A.; Capareda, S.C. Characterization and separation of corn stover bio-oil by fractional distillation. *Fuel* **2013**, *112*, 60–73. [CrossRef]
13. Taghipour, A.; Ramirez, J.A.; Brown, R.J.; Rainey, T.J. A review of fractional distillation to improve hydrothermal liquefaction biocrude characteristics; future outlook and prospects. *Renew. Sustain. Energy Rev.* **2019**, *115*, 109355. [CrossRef]
14. Hu, H.S.; Wu, Y.L.; Yang, M.D. Fractionation of bio-oil produced from hydrothermal liquefaction of microalgae by liquid-liquid extraction. *Biomass Bioenergy* **2018**, *108*, 487–500. [CrossRef]
15. Bjelić, S.; Yu, J.; Iversen, B.B.; Glasius, M.; Biller, P. Detailed investigation into the asphaltene fraction of hydrothermal liquefaction derived bio-crude and hydrotreated bio-crudes. *Energy and Fuels* **2018**, *32*, 3579–3587. [CrossRef]
16. Brunner, G. Counter-current separations. *J. Supercrit. Fluids* **2009**, *47*, 574–582. [CrossRef]
17. Nielsen, R.P.; Valsecchi, R.; Strandgaard, M.; Maschietti, M. Experimental study on fluid phase equilibria of hydroxyl-terminated perfluoropolyether oligomers and supercritical carbon dioxide. *J. Supercrit. Fluids* **2015**, *101*, 124–130. [CrossRef]
18. Speight, J.G. Nonthermal methods of recovery. In *Enhanced Recovery Methods for Heavy Oil and Tar Sands*; Elsevier: Austin, TX, USA, 2009; pp. 185–220. ISBN 9780127999883.
19. Kummamuru, B. *Global Bioenergy Statistics*; World Bioenergy Association: Stockholm, Sweden, 2017.
20. Mateo-Sagasta, J.; Raschid-Sally, L.; Thebo, A. Global Wastewater and Sludge Production, Treatment and Use. In *Wastewater: Economic Asset in an Urbanizing World*; Drechsel, P., Qadir, M., Wichelns, D., Eds.; Springer: Dordrecht, The Netherlands, 2015; pp. 15–38. ISBN 978-94-017-9545-6.
21. Lignin Products Global Market Size, Sales Data 2017-2022 & Applications in Animal Feed Industry. Available online: https://www.orbisresearch.com/contacts/request-sample/218258 (accessed on 13 May 2019).
22. Tian, X.; Fang, Z.; Smith, R.L.; Wu, Z.; Liu, M. Properties, chemical characteristics and application of lignin and its derivatives. In *Production of Biofuels and Chemicals from Lignin*; Fang, Z., Smith, R.L., Jr., Eds.; Springer: Singapore, 2016; pp. 3–33. ISBN 978-981-10-1965-4.
23. Zakzeski, J.; Bruijnincx, P.C.A.; Jongerius, A.L.; Weckhuysen, B.M. The catalytic valorization of lignin for the production of renewable chemicals. *Chem. Rev.* **2010**, *110*, 3552–3599. [CrossRef]
24. Miliotti, E.; Dell'Orco, S.; Lotti, G.; Rizzo, A.M.; Rosi, L.; Chiaramonti, D. Lignocellulosic ethanol biorefinery: Valorization of lignin-rich stream through hydrothermal liquefaction. *Energies* **2019**, *12*, 723. [CrossRef]
25. Sumathi, S.; Chai, S.P.; Mohamed, A.R. Utilization of oil palm as a source of renewable energy in Malaysia. *Renew. Sustain. Energy Rev.* **2008**, *12*, 2404–2421. [CrossRef]
26. ECN.TNO Phyllis2, Database for Biomass and Waste. Available online: https://phyllis.nl/ (accessed on 18 November 2019).

27. Oasmaa, A.; Van De Beld, B.; Saari, P.; Elliott, D.C.; Solantausta, Y. Norms, standards, and legislation for fast pyrolysis bio-oils from lignocellulosic biomass. *Energy Fuels* **2015**, *29*, 2471–2484. [CrossRef]
28. Nguyen, T.D.H.; Maschietti, M.; Åmand, L.E.; Vamling, L.; Olausson, L.; Andersson, S.I.; Theliander, H. The effect of temperature on the catalytic conversion of Kraft lignin using near-critical water. *Bioresour. Technol.* **2014**, *170*, 196–203. [CrossRef]
29. Feng, S.; Yuan, Z.; Leitch, M.; Xu, C.C. Hydrothermal liquefaction of barks into bio-crude - Effects of species and ash content/composition. *Fuel* **2014**, *116*, 214–220. [CrossRef]
30. Haarlemmer, G.; Guizani, C.; Anouti, S.; Déniel, M.; Roubaud, A.; Valin, S. Analysis and comparison of bio-oils obtained by hydrothermal liquefaction and fast pyrolysis of beech wood. *Fuel* **2016**, *174*, 180–188. [CrossRef]
31. Chen, Y.; Cao, X.; Zhu, S.; Tian, F.; Xu, Y.; Zhu, C.; Dong, L. Synergistic hydrothermal liquefaction of wheat stalk with homogeneous and heterogeneous catalyst at low temperature. *Bioresour. Technol.* **2019**, *278*, 92–98. [CrossRef]
32. Baloch, H.A.; Nizamuddin, S.; Siddiqui, M.T.H.; Mubarak, N.M.; Dumbre, D.K.; Srinivasan, M.P.; Griffin, G.J. Sub-supercritical liquefaction of sugarcane bagasse for production of bio-oil and char: Effect of two solvents. *J. Environ. Chem. Eng.* **2018**, *6*, 6589–6601. [CrossRef]
33. Castello, D.; Pedersen, T.; Rosendahl, L. Continuous hydrothermal liquefaction of biomass: A critical review. *Energies* **2018**, *11*, 3165. [CrossRef]
34. BTG-BTL Empyro Project. Available online: https://www.btg-btl.com/en/company/projects/empyro (accessed on 22 October 2019).
35. Ensyn Côte-Nord. Available online: http://www.ensyn.com/quebec.html (accessed on 22 October 2019).
36. Silva Green Fuel. Available online: https://www.statkraft.com/about-statkraft/Projects/norway/value-creation-tofte/silva-green-fuel/ (accessed on 22 October 2019).
37. Elliott, D.C.; Oasmaa, A.; Meier, D.; Preto, F.; Bridgwater, A.V. Results of the IEA round robin on viscosity and aging of fast pyrolysis bio-oils: Long-Term tests and repeatability. *Energy Fuels* **2012**, *26*, 7362–7366. [CrossRef]
38. Ong, B.H.Y.; Walmsley, T.G.; Atkins, M.J.; Walmsley, M.R.W. Hydrothermal liquefaction of Radiata Pine with Kraft black liquor for integrated biofuel production. *J. Clean. Prod.* **2018**, *199*, 737–750. [CrossRef]
39. Jarvis, J.M.; Albrecht, K.O.; Billing, J.M.; Schmidt, A.J.; Hallen, R.T.; Schaub, T.M. Assessment of hydrotreatment for hydrothermal liquefaction biocrudes from sewage sludge, microalgae, and pine feedstocks. *Energy Fuels* **2018**, *32*, 8483–8493. [CrossRef]
40. Belkheiri, T.; Andersson, S.I.; Mattsson, C.; Olausson, L.; Theliander, H.; Vamling, L. Hydrothermal liquefaction of kraft lignin in sub-critical water: the influence of the sodium and potassium fraction. *Biomass Convers. Biorefinery* **2018**, *8*, 585–595. [CrossRef]
41. Anastasakis, K.; Biller, P.; Madsen, R.B.; Glasius, M.; Johannsen, I. Continuous hydrothermal liquefaction of biomass in a novel pilot plant with heat recovery and hydraulic oscillation. *Energies* **2018**, *11*, 2695. [CrossRef]
42. Gollakota, A.R.K.; Kishore, N.; Gu, S. A review on hydrothermal liquefaction of biomass. *Renew. Sustain. Energy Rev.* **2018**, *81*, 1378–1392. [CrossRef]
43. Feng, Y.; Meier, D. Supercritical carbon dioxide extraction of fast pyrolysis oil from softwood. *J. Supercrit. Fluids* **2017**, *128*, 6–17. [CrossRef]
44. Leijenhorst, E.J.; Wolters, W.; Van De Beld, L.; Prins, W. Inorganic element transfer from biomass to fast pyrolysis oil: Review and experiments. *Fuel Process. Technol.* **2016**, *149*, 96–111. [CrossRef]
45. Sintamarean, I.M.; Grigoras, I.F.; Jensen, C.U.; Toor, S.S.; Pedersen, T.H.; Rosendahl, L.A. Two-stage alkaline hydrothermal liquefaction of wood to biocrude in a continuous bench-scale system. *Biomass Convers. Biorefinery* **2017**, *7*, 425–435. [CrossRef]
46. Kosinkova, J.; Ramirez, J.A.; Ristovski, Z.D.; Brown, R.; Rainey, T.J. Physical and chemical stability of bagasse biocrude from liquefaction stored in real conditions. *Energy Fuels* **2016**, *30*, 10499–10504. [CrossRef]
47. Elliott, D.C.; Meier, D.; Oasmaa, A.; Van De Beld, B.; Bridgwater, A.V.; Marklund, M. Results of the international energy agency round robin on fast pyrolysis bio-oil production. *Energy Fuels* **2017**, *31*, 5111–5119. [CrossRef]
48. Speight, J.G. Petroleum Analysis. In *The Chemistry and Technology of Petroleum*; CRC Press: Boca Raton, FL, USA, 2006; pp. 274–314. ISBN 9780429118494.

49. Fahmi, R.; Bridgwater, A.V.; Donnison, I.; Yates, N.; Jones, J.M. The effect of lignin and inorganic species in biomass on pyrolysis oil yields, quality and stability. *Fuel* **2008**, *87*, 1230–1240. [CrossRef]
50. Das, P.; Ganesh, A.; Wangikar, P. Influence of pretreatment for deashing of sugarcane bagasse on pyrolysis products. *Biomass Bioenergy* **2004**, *27*, 445–457. [CrossRef]
51. Minowa, T.; Kondo, T.; Sudirjo, S.T. Thermochemical liquefaction of Indonesian biomass residues. *Biomass Bioenergy* **1998**, *14*, 517–524. [CrossRef]
52. Déniel, M.; Haarlemmer, G.; Roubaud, A.; Weiss-Hortala, E.; Fages, J. Optimisation of bio-oil production by hydrothermal liquefaction of agro-industrial residues: Blackcurrant pomace (Ribes nigrum L.) as an example. *Biomass Bioenergy* **2016**, *95*, 273–285. [CrossRef]
53. Speight, J.G. Chemical Composition. In *The Chemistry and Technology of Petroleum*; Chemical Industries; CRC Press: Boca Raton, FL, USA, 2014; ISBN 9781439873892.
54. Ghorbannezhad, P.; Kool, F.; Rudi, H.; Ceylan, S. Sustainable production of value-added products from fast pyrolysis of palm shell residue in tandem micro-reactor and pilot plant. *Renew. Energy* **2020**, *145*, 663–670. [CrossRef]
55. Gómez-Monedero, B.; Bimbela, F.; Arauzo, J.; Faria, J.; Ruiz, M.P. Pyrolysis of red eucalyptus, camelina straw, and wheat straw in an ablative reactor. *Energy Fuels* **2015**, *29*, 1766–1775. [CrossRef]
56. Hernando, H.; Jiménez-Sánchez, S.; Fermoso, J.; Pizarro, P.; Coronado, J.M.; Serrano, D.P. Assessing biomass catalytic pyrolysis in terms of deoxygenation pathways and energy yields for the efficient production of advanced biofuels. *Catal. Sci. Technol.* **2016**, *6*, 2829–2843. [CrossRef]
57. Pedersen, T.H.; Grigoras, I.F.; Hoffmann, J.; Toor, S.S.; Daraban, I.M.; Jensen, C.U.; Iversen, S.B.; Madsen, R.B.; Glasius, M.; Arturi, K.R.; et al. Continuous hydrothermal co-liquefaction of aspen wood and glycerol with water phase recirculation. *Appl. Energy* **2016**, *162*, 1034–1041. [CrossRef]
58. Montesantos, N.; Nielsen, R.P.; Maschietti, M. Upgrading of nondewatered nondemetallized lignocellulosic biocrude from hydrothermal liquefaction using supercritical carbon dioxide. *Ind. Eng. Chem. Res.* **2020**, accepted. [CrossRef]
59. Elliott, D.C.; Oasmaa, A.; Preto, F.; Meier, D.; Bridgwater, A.V. Results of the IEA round robin on viscosity and stability of fast pyrolysis bio-oils. *Energy Fuels* **2012**, *26*, 3769–3776. [CrossRef]
60. Jensen, C.U.; Rodriguez Guerrero, J.K.; Karatzos, S.; Olofsson, G.; Iversen, S.B. Fundamentals of Hydrofaction$^{TM}$: Renewable crude oil from woody biomass. *Biomass Convers. Biorefinery* **2017**, *7*, 495–509. [CrossRef]
61. Jarvis, J.M.; Billing, J.M.; Hallen, R.T.; Schmidt, A.J.; Schaub, T.M. Hydrothermal liquefaction biocrude compositions compared to petroleum crude and shale oil. *Energy Fuels* **2017**, *31*, 2896–2906. [CrossRef]
62. Madsen, R.B.; Bernberg, R.Z.K.; Biller, P.; Becker, J.; Iversen, B.B.; Glasius, M. Hydrothermal co-liquefaction of biomasses-quantitative analysis of bio-crude and aqueous phase composition. *Sustain. Energy Fuels* **2017**, *1*, 789–805. [CrossRef]
63. Christensen, E.D.; Chupka, G.M.; Luecke, J.; Smurthwaite, T.; Alleman, T.L.; Iisa, K.; Franz, J.A.; Elliott, D.C.; McCormick, R.L. Analysis of oxygenated compounds in hydrotreated biomass fast pyrolysis oil distillate fractions. *Energy Fuels* **2011**, *25*, 5462–5471. [CrossRef]
64. Montesantos, N.; Pedersen, T.H.; Nielsen, R.P.; Rosendahl, L.; Maschietti, M. Supercritical carbon dioxide fractionation of bio-crude produced by hydrothermal liquefaction of pinewood. *J. Supercrit. Fluids* **2019**, *149*, 97–109. [CrossRef]
65. ASTM International. ASTM D664-17a. *Standard Test Method for Acid Number of Petroleum Products by Potentiometric Titration*; ASTM: West Conshohocken, PA, USA, 2017.
66. Jensen, C.U.; Rosendahl, L.A.; Olofsson, G. Impact of nitrogenous alkaline agent on continuous HTL of lignocellulosic biomass and biocrude upgrading. *Fuel Process. Technol.* **2017**, *159*, 376–385. [CrossRef]
67. Jacobson, K.; Maheria, K.C.; Kumar Dalai, A. Bio-oil valorization: A review. *Renew. Sustain. Energy Rev.* **2013**, *23*, 91–106. [CrossRef]
68. Stankovikj, F.; McDonald, A.G.; Helms, G.L.; Garcia-Perez, M. Quantification of bio-oil functional groups and evidences of the presence of pyrolytic humins. *Energy Fuels* **2016**, *30*, 6505–6524. [CrossRef]
69. Madsen, R.B.; Anastasakis, K.; Biller, P.; Glasius, M. Rapid determination of water, total acid number, and phenolic content in bio-crude from hydrothermal liquefaction of biomass using FT-IR. *Energy Fuels* **2018**, *32*, 7660–7669. [CrossRef]

70. Harman-Ware, A.E.; Ferrell, J.R. Methods and challenges in the determination of molecular weight metrics of bio-oils. *Energy Fuels* **2018**, *32*, 8905–8920. [CrossRef]
71. Hwang, H.; Lee, J.H.; Choi, I.G.; Choi, J.W. Comprehensive characterization of hydrothermal liquefaction products obtained from woody biomass under various alkali catalyst concentrations. *Environ. Technol. (United Kingdom)* **2019**, *40*, 1657–1667. [CrossRef]
72. Belkheiri, T.; Vamling, L.; Nguyen, T.D.H.; Maschietti, M.; Olausson, L.; Andersson, S.-I.; Åmand, L.-E.; Theliander, H. Kraft lignin depolymerization in near-critical water: effect of changing co-solvent. *Cell Chem. Technol.* **2014**, *48*, 813–818.
73. Lyckeskog, H.N.; Mattsson, C.; Olausson, L.; Andersson, S.I.; Vamling, L.; Theliander, H. Thermal stability of low and high Mw fractions of bio-oil derived from lignin conversion in subcritical water. *Biomass Convers. Biorefinery* **2017**, *7*, 401–414. [CrossRef]
74. Conrad, S.; Blajin, C.; Schulzke, T.; Deerberg, G. Comparison of fast pyrolysis bio-oils from straw and miscanthus. *Environ. Prog. Sustain. Energy* **2019**, *38*, e13287. [CrossRef]
75. Yildiz, G.; Ronsse, F.; Venderbosch, R.; van Duren, R.; Kersten, S.R.A.; Prins, W. Effect of biomass ash in catalytic fast pyrolysis of pine wood. *Appl. Catal. B Environ.* **2015**, *168–169*, 203–211. [CrossRef]
76. Doassans-Carrère, N.; Ferrasse, J.H.; Boutin, O.; Mauviel, G.; Lédé, J. Comparative study of biomass fast pyrolysis and direct liquefaction for bio-oils production: Products yield and characterizations. *Energy Fuels* **2014**, *28*, 5103–5111. [CrossRef]
77. Azargohar, R.; Jacobson, K.L.; Powell, E.E.; Dalai, A.K. Evaluation of properties of fast pyrolysis products obtained, from Canadian waste biomass. *J. Anal. Appl. Pyrolysis* **2013**, *104*, 330–340. [CrossRef]
78. Undri, A.; Abou-Zaid, M.; Briens, C.; Berruti, F.; Rosi, L.; Bartoli, M.; Frediani, M.; Frediani, P. A simple procedure for chromatographic analysis of bio-oils from pyrolysis. *J. Anal. Appl. Pyrolysis* **2015**, *114*, 208–221. [CrossRef]
79. Nguyen Lyckeskog, H.; Mattsson, C.; Åmand, L.E.; Olausson, L.; Andersson, S.I.; Vamling, L.; Theliander, H. Storage stability of bio-oils derived from the catalytic conversion of softwood Kraft lignin in subcritical water. *Energy Fuels* **2016**, *30*, 3097–3106. [CrossRef]
80. Nguyen, T.D.H.; Maschietti, M.; Belkheiri, T.; Åmand, L.E.; Theliander, H.; Vamling, L.; Olausson, L.; Andersson, S.I. Catalytic depolymerisation and conversion of Kraft lignin into liquid products using near-critical water. *J. Supercrit. Fluids* **2014**, *86*, 67–75. [CrossRef]
81. Maddi, B.; Viamajala, S.; Varanasi, S. Comparative study of pyrolysis of algal biomass from natural lake blooms with lignocellulosic biomass. *Bioresour. Technol.* **2011**, *102*, 11018–11026. [CrossRef]
82. Aqsha, A.; Tijani, M.M.; Moghtaderi, B.; Mahinpey, N. Catalytic pyrolysis of straw biomasses (wheat, flax, oat and barley) and the comparison of their product yields. *J. Anal. Appl. Pyrolysis* **2017**, *125*, 201–208. [CrossRef]
83. Zhu, Z.; Rosendahl, L.; Toor, S.S.; Yu, D.; Chen, G. Hydrothermal liquefaction of barley straw to bio-crude oil: Effects of reaction temperature and aqueous phase recirculation. *Appl. Energy* **2015**, *137*, 183–192. [CrossRef]
84. Feng, Y.; Meier, D. Extraction of value-added chemicals from pyrolysis liquids with supercritical carbon dioxide. *J. Anal. Appl. Pyrolysis* **2015**, *113*, 174–185. [CrossRef]
85. Li, C.; Zhao, X.; Wang, A.; Huber, G.W.; Zhang, T. Catalytic transformation of lignin for the production of chemicals and fuels. *Chem. Rev.* **2015**, *115*, 11559–11624. [CrossRef]
86. Nanda, S.; Mohammad, J.; Reddy, S.N.; Kozinski, J.A.; Dalai, A.K. Pathways of lignocellulosic biomass conversion to renewable fuels. *Biomass Convers. Biorefinery* **2014**, *4*, 157–191. [CrossRef]
87. Chan, Y.H.; Quitain, A.T.; Yusup, S.; Uemura, Y.; Sasaki, M.; Kida, T. Liquefaction of palm kernel shell in sub- and supercritical water for bio-oil production. *J. Energy Inst.* **2018**, *91*, 721–732. [CrossRef]
88. Kokayeff, P.; Zink, S.; Roxas, P. Hydrotreating in petroleum processing. In *Handbook of Petroleum Processing*; Treese, S.A., Pujadó, P.R., Jones, D.S.J., Eds.; Springer International Publishing: Berlin/Heidelberg, Germany, 1995; pp. 363–434. ISBN 978-3-319-14529-7.
89. Castello, D.; Haider, M.S.; Rosendahl, L.A. Catalytic upgrading of hydrothermal liquefaction biocrudes: Different challenges for different feedstocks. *Renew. Energy* **2019**, *141*, 420–430. [CrossRef]
90. Jensen, C.U.; Hoffmann, J.; Rosendahl, L.A. Co-processing potential of HTL bio-crude at petroleum refineries. Part 2: A parametric hydrotreating study. *Fuel* **2016**, *165*, 536–543. [CrossRef]
91. Gollakota, A.R.K.; Reddy, M.; Subramanyam, M.D.; Kishore, N. A review on the upgradation techniques of pyrolysis oil. *Renew. Sustain. Energy Rev.* **2016**, *58*, 1543–1568. [CrossRef]

92. Hoffmann, J.; Pedersen, T.H.; Rosendahl, L.A. Near-critical and supercritical water and their applications for biorefineries. In *Biofuels and Biorefineries*; Fang, Z., Xu, C., Eds.; Biofuels and Biorefineries; Springer: Dordrecht, The Netherlands, 2014; Volume 2, pp. 373–400. ISBN 978-94-017-8922-6.
93. Han, Y.; Gholizadeh, M.; Tran, C.-C.; Kaliaguine, S.; Li, C.-Z.; Olarte, M.; Garcia-Perez, M. Hydrotreatment of pyrolysis bio-oil: A review. *Fuel Process. Technol.* **2019**, *195*, 106140. [CrossRef]
94. Furimsky, E.; Massoth, F.E. Deactivation of hydroprocessing catalysts. *Catal. Today* **1999**, *52*, 381–495. [CrossRef]
95. Mohamad, M.H.; Awang, R.; Yunus, W.Z.W. A Review of acetol: Application and production. *Am. J. Appl. Sci.* **2011**, *8*, 1135–1139. [CrossRef]
96. Chen, L.; Zhao, J.; Pradhan, S.; Brinson, B.E.; Scuseria, G.E.; Zhang, Z.C.; Wong, M.S. Ring-locking enables selective anhydrosugar synthesis from carbohydrate pyrolysis. *Green Chem.* **2016**, *18*, 5438–5447. [CrossRef]
97. Rover, M.R.; Aui, A.; Wright, M.M.; Smith, R.G.; Brown, R.C. Production and purification of crystallized levoglucosan from pyrolysis of lignocellulosic biomass. *Green Chem.* **2019**, *21*, 5980–5989. [CrossRef]
98. Werpy, T.; Petersen, G. *Top Value Added Chemicals from Biomass: Volume I-Results of Screening for Potential Candidates from Sugars and Synthesis Gas*; National Renewable Energy Laboratory (NREL): Golden, CO, USA, 2004.
99. Longley, C.J.; Fung, D.P.C. Potential Applications and Markets for Biomass-Derived Levoglucosan. In *Advances in Thermochemical Biomass Conversion*; Springer: Dordrecht, The Netherlands, 1993; pp. 1484–1494. ISBN 978-94-011-1336-6.
100. What's New in Phenol Production? Available online: https://www.acs.org/content/acs/en/pressroom/cutting-edge-chemistry/what-s-new-in-phenol-production-.html (accessed on 12 August 2019).
101. Maqbool, W.; Hobson, P.; Dunn, K.; Doherty, W. Supercritical carbon dioxide separation of carboxylic scids and phenolics from bio-oil of lignocellulosic origin: Understanding bio-oil compositions, compound solubilities, and their fractionation. *Ind. Eng. Chem. Res.* **2017**, *56*, 3129–3144. [CrossRef]
102. Fiege, H.; Voges, H.-W.; Hamamoto, T.; Umemura, S.; Iwata, T.; Miki, H.; Fujita, Y.; Buysch, H.-J.; Garbe, D.; Paulus, W. Phenol Derivatives. In *Ullmann's Encyclopedia of Industrial Chemistry*; Wiley-VCH Verlag GmbH & Co. KGaA: Weinheim, Germany, 2012; Volume 26, pp. 552–553.
103. Naik, S.; Goud, V.V.; Rout, P.K.; Dalai, A.K. Supercritical $CO_2$ fractionation of bio-oil produced from wheat-hemlock biomass. *Bioresour. Technol.* **2010**, *101*, 7605–7613. [CrossRef] [PubMed]
104. Vanilla and Vanillin Market: Global Industry Trends, Share, Size, Growth, Opportunity and Forecast 2019-2024. Available online: https://www.researchandmarkets.com/research/n4fxw5/global_vanilla?w=12 (accessed on 28 October 2019).
105. Wu, X.F.; Zhou, Q.; Li, M.F.; Li, S.X.; Bian, J.; Peng, F. Conversion of poplar into bio-oil via subcritical hydrothermal liquefaction: Structure and antioxidant capacity. *Bioresour. Technol.* **2018**, *270*, 216–222. [CrossRef] [PubMed]
106. Larson, R.A.; Sharma, B.K.; Marley, K.A.; Kunwar, B.; Murali, D.; Scott, J. Potential antioxidants for biodiesel from a softwood lignin pyrolyzate. *Ind. Crops Prod.* **2017**, *109*, 476–482. [CrossRef]
107. Chandrasekaran, S.R.; Murali, D.; Marley, K.A.; Larson, R.A.; Doll, K.M.; Moser, B.R.; Scott, J.; Sharma, B.K. Antioxidants from slow pyrolysis bio-oil of birch wood: Application for biodiesel and biobased lubricants. *ACS Sustain. Chem. Eng.* **2016**, *4*, 1414–1421. [CrossRef]
108. Qazi, S.S.; Li, D.; Briens, C.; Berruti, F.; Abou-Zaid, M.M. Antioxidant activity of the lignins derived from fluidized-bed fast pyrolysis. *Molecules* **2017**, *22*, 372. [CrossRef] [PubMed]
109. Lemmon, E.W.; McLinden, M.O.; Friend, D.G. Thermophysical Properties of Fluid Systems. In *NIST Chemistry WebBook, NIST Standard Reference Database Number 69*; Linstrom, P.J., Mallard, W.G., Eds.; National Institute of Standards and Technology: Gaithersburg, MD, USA, 1998.
110. Michels, A.; Blaisse, B.; Hoogschagen, J. The melting line of carbon dioxide up to 2800 atmospheres. *Physica* **1942**, *9*, 565–573. [CrossRef]
111. Dortmund Data Bank. Available online: http://www.ddbst.com/en/EED/PCP/VAP_C1050.php (accessed on 29 October 2019).
112. Brunner, G. Supercritical fluids: Technology and application to food processing. *J. Food Eng.* **2005**, *67*, 21–33. [CrossRef]
113. McHugh, M.A.; Krukonis, V.J. *Supercritical Fluid Extraction*, 2nd ed.; Brenner, H., Ed.; Butterworth-Heinemann series in chemical engineering; Elsevier: Amsterdam, The Netherlands, 1994; ISBN 9780080518176.

114. Gupta, R.B.; Shim, J.-J. *Solubility in Supercritical Carbon Dioxide*; Gupta, R.B., Shim, J.-J., Eds.; CRC Press: Boca Raton, FL, USA, 2006; ISBN 9780429122088.
115. Reverchon, E.; De Marco, I. Supercritical fluid extraction and fractionation of natural matter. *J. Supercrit. Fluids* **2006**, *38*, 146–166. [CrossRef]
116. McHugh, M.A.; Krukonis, V.J. Processing Pharmaceuticals, Natural Products, Specialty Chemicals, and Waste Streams. In *Supercritical Fluid Extraction*; Butterworth-Heinemann: Oxford, UK, 1994; pp. 293–310. ISBN 9780080518176.
117. Gironi, F.; Maschietti, M. Supercritical carbon dioxide fractionation of lemon oil by means of a batch process with an external reflux. *J. Supercrit. Fluids* **2005**, *35*, 227–234. [CrossRef]
118. Maschietti, M.; Pedacchia, A. Supercritical carbon dioxide separation of fish oil ethyl esters by means of a continuous countercurrent process with an internal reflux. *J. Supercrit. Fluids* **2014**, *86*, 76–84. [CrossRef]
119. Gironi, F.; Maschietti, M. Continuous countercurrent deterpenation of lemon essential oil by means of supercritical carbon dioxide: Experimental data and process modelling. *Chem. Eng. Sci.* **2008**, *63*, 651–661. [CrossRef]
120. Gironi, F.; Maschietti, M. Separation of fish oils ethyl esters by means of supercritical carbon dioxide: Thermodynamic analysis and process modelling. *Chem. Eng. Sci.* **2006**, *61*, 5114–5126. [CrossRef]
121. Riha, V.; Brunner, G. Separation of fish oil ethyl esters with supercritical carbon dioxide. *J. Supercrit. Fluids* **2000**, *17*, 55–64. [CrossRef]
122. Osséo, L.S.; Caputo, G.; Gracia, I.; Reverchon, E. Continuous fractionation of used frying oil by supercritical $CO_2$. *JAOCS J. Am. Oil Chem. Soc.* **2004**, *81*, 879–885. [CrossRef]
123. Kim, S.K.; Han, J.Y.; Hong, S.A.; Lee, Y.W.; Kim, J. Supercritical $CO_2$-purification of waste cooking oil for high-yield diesel-like hydrocarbons via catalytic hydrodeoxygenation. *Fuel* **2013**, *111*, 510–518. [CrossRef]
124. Meyer, T. Extracting and upgrading heavy hydrocarbons using supercritical carbon dioxide 2011. UK Patent GB 2471862 A, 19 January 2011.
125. Subramanian, A.; Floyd, R. Residuum oil supercritical extraction process 2011. US Patent 2011/0094937 A1, 28 April 2011.
126. Mudraboyina, B.P.; Fu, D.; Jessop, P.G. Supercritical fluid rectification of lignin microwave-pyrolysis oil. *Green Chem.* **2015**, *17*, 169–172. [CrossRef]
127. Montesantos, N.; Pedersen, T.H.; Nielsen, R.P.; Rosendahl, L.A.; Maschietti, M. High-temperature extraction of lignocellulosic bio-crude by supercritical carbon dioxide. *Chem. Eng. Trans.* **2019**, *74*, 799–804.
128. Chan, Y.H.; Yusup, S.; Quitain, A.T.; Chai, Y.H.; Uemura, Y.; Loh, S.K. Extraction of palm kernel shell derived pyrolysis oil by supercritical carbon dioxide: Evaluation and modeling of phenol solubility. *Biomass Bioenergy* **2018**, *116*, 106–112. [CrossRef]
129. Chan, Y.H.; Yusup, S.; Quitain, A.T.; Uemura, Y.; Loh, S.K. Fractionation of pyrolysis oil via supercritical carbon dioxide extraction: Optimization study using response surface methodology (RSM). *Biomass Bioenergy* **2017**, *107*, 155–163. [CrossRef]
130. Feng, Y.; Meier, D. Comparison of supercritical $CO_2$, liquid $CO_2$, and solvent extraction of chemicals from a commercial slow pyrolysis liquid of beech wood. *Biomass Bioenergy* **2016**, *85*, 346–354. [CrossRef]
131. Cheng, T.; Han, Y.; Zhang, Y.; Xu, C. Molecular composition of oxygenated compounds in fast pyrolysis bio-oil and its supercritical fluid extracts. *Fuel* **2016**, *172*, 49–57. [CrossRef]
132. Patel, R.N.; Bandyopadhyay, S.; Ganesh, A. Extraction of cardanol and phenol from bio-oils obtained through vacuum pyrolysis of biomass using supercritical fluid extraction. *Energy* **2011**, *36*, 1535–1542. [CrossRef]
133. Rout, P.K.; Naik, M.K.; Naik, S.N.; Goud, V.V.; Das, L.M.; Dalai, A.K. Supercritical $CO_2$ fractionation of bio-oil produced from mixed biomass of wheat and wood sawdust. *Energy Fuels* **2009**, *23*, 6181–6188. [CrossRef]
134. Wang, J.; Cui, H.; Wei, S.; Zhuo, S.; Wang, L.; Li, Z.; Yi, W. Separation of biomass pyrolysis oil by supercritical $CO_2$ extraction. *Smart Grid Renew. Energy* **2010**, *01*, 98–107. [CrossRef]
135. ISO 8217:2017. *Petroleum Products-Fuels (class F)-Specifications of Marine Fuels*; ISO: Geneva, Switzerland, 2017.
136. Pedersen, K.S.; Christensen, P.L.; Shaikh, J.A. *Phase Behavior of Petroleum Reservoir Fluids*, 2nd ed.; CRC Press: Boca Raton, FL, USA, 2014; ISBN 9780429110306.
137. Chrastil, J. Solubility of solids and liquids in supercritical gases. *J. Phys. Chem.* **1982**, *86*, 3016–3021. [CrossRef]
138. Dohrn, R.; Brunner, G. High-pressure fluid-phase equilibria: Experimental methods and systems investigated (1988–1993). *Fluid Phase Equilib.* **1995**, *106*, 213–282. [CrossRef]

139. Laugier, S.; Richon, D. High-pressure vapor-liquid equilibria of two binary systems: Carbon dioxide + cyclohexanol and carbon dioxide + cyclohexanone. *J. Chem. Eng. Data* **1997**, *42*, 155–159. [CrossRef]
140. Jing, Y.; Hou, Y.; Wu, W.; Liu, W.; Zhang, B. Solubility of 5-Hydroxymethylfurfural in supercritical carbon dioxide with and without ethanol as cosolvent at (314.1 to 343.2) K. *J. Chem. Eng. Data* **2011**, *56*, 298–302. [CrossRef]
141. Sparks, D.L.; Hernandez, R.; Estévez, L.A.; Holmes, W.E.; French, W.T. Solubility of small-chain fatty acids in supercritical carbon dioxide. *AIChE Annu. Meet. Conf. Proc.* **2008**, *55*, 4922–4927.
142. Bamberger, T.; Erickson, J.C.; Cooney, C.L.; Kumar, S.K. Measurement and model prediction of solubilities of pure fatty acids, pure triglycerides, and mixtures of triglycerides in supercritical carbon dioxide. *J. Chem. Eng. Data* **1988**, *33*, 327–333. [CrossRef]
143. Maheshwari, P.; Nikolov, Z.L.; White, T.M.; Hartel, R. Solubility of fatty acids in supercritical carbon dioxide. *J. Am. Oil Chem. Soc.* **1992**, *69*, 1069–1076. [CrossRef]
144. Iwai, Y.; Fukuda, T.; Koga, Y.; Arai, Y. Solubilities of myristic acid, palmitic acid, and cetyl alcohol in supercritical carbon dioxide at 35 °C. *J. Chem. Eng. Data* **1991**, *36*, 430–432. [CrossRef]
145. Garlapati, C.; Madras, G. Solubilities of palmitic and stearic fatty acids in supercritical carbon dioxide. *J. Chem. Thermodyn.* **2010**, *42*, 193–197. [CrossRef]
146. Brandt, L.; Elizalde-Solis, O.; Galicia-Luna, L.A.; Gmehling, J. Solubility and density measurements of palmitic acid in supercritical carbon dioxide + alcohol mixtures. *Fluid Phase Equilib.* **2010**, *289*, 72–79. [CrossRef]
147. Schwarz, C.E.; Knoetze, J.H. Phase equilibrium measurements of long chain acids in supercritical carbon dioxide. *J. Supercrit. Fluids* **2012**, *66*, 36–48. [CrossRef]
148. Bamberger, A.; Schmelzer, J.; Walther, D.; Maurer, G. High-pressure vapour-liquid equilibria in binary mixtures of carbon dioxide and benzene compounds: experimental data for mixtures with ethylbenzene, isopropylbenzene, 1,2,4-trimethylbenzene, 1,3,5-trimethylbenzene, ethenylbenzene and isopropenylbenzene, and their correlation with the generalized Bender and Skjold-Jorgensen's group contribution equation of state. *Fluid Phase Equilib.* **1994**, *97*, 167–189. [CrossRef]
149. Jennings, D.W.; Schucker, R.C. Comparison of high-pressure vapor-liquid equilibria of mixtures of $CO_2$ or propane with nonane and C9 alkylbenzenes. *J. Chem. Eng. Data* **1996**, *41*, 831–838. [CrossRef]
150. Phiong, H.S.; Lucien, F.P. Volumetric expansion and vapour-liquid equilibria of α-methylstyrene and cumene with carbon dioxide at elevated pressure. *J. Supercrit. Fluids* **2003**, *25*, 99–107. [CrossRef]
151. McHugh, M.; Paulaitls, M.E. Solid solubilities of naphthalene and biphenyl in supercritical carbon dioxide. *J. Chem. Eng. Data* **1980**, *25*, 326–329. [CrossRef]
152. Yanagiuchi, M.; Ueda, T.; Matsubara, K.; Inomata, H.; Arai, K.; Saito, S. Fundamental investigation on supercritical extraction of coal-derived aromatic compounds. *J. Supercrit. Fluids* **1991**, *4*, 145–151. [CrossRef]
153. Wells, P.A.; Chaplin, R.P.; Foster, N.R. Solubility of phenylacetic acid and vanillan in supercritical carbon dioxide. *J. Supercrit. Fluids* **1990**, *3*, 8–14. [CrossRef]
154. Schmitt, W.J.; Reid, R.C. Solubility of monofunctional organic solids in chemically diverse supercritical fluids. *J. Chem. Eng. Data* **1986**, *31*, 204–212. [CrossRef]
155. Kurnlk, R.T.; Holla, S.J.; Reid, R.C. Solubility of solids in supercritical carbon dioxide and ethylene. *J. Chem. Eng. Data* **1981**, *26*, 47–51. [CrossRef]
156. García-González, J.; Molina, M.J.; Rodríguez, F.; Mirada, F. Solubilities of phenol and pyrocatechol in supercritical carbon dioxide. *J. Chem. Eng. Data* **2001**, *46*, 918–921. [CrossRef]
157. Van Leer, R.A.; Paulaitis, M.E. Solubilities of phenol and chlorinated phenols in supercritical carbon dioxide. *J. Chem. Eng. Data* **1980**, *25*, 257–259. [CrossRef]
158. Pfohl, O.; Brunner, G. Two-and three-phase equilibria in systems containing benzene derivatives, carbon dioxide, and water at 373.15 K and 10–30 MPa. *Fluid Phase Equilibria* **1997**, *141*, 179–206. [CrossRef]
159. Yamini, Y.; Fat'Hi, M.R.; Alizadeh, N.; Shamsipur, M. Solubility of dihydroxybenzene isomers in supercritical carbon dioxide. *Fluid Phase Equilibria* **1998**, *152*, 299–305. [CrossRef]
160. Škerget, M.; Čretnik, L.; Knez, Ž.; Škrinjar, M. Influence of the aromatic ring substituents on phase equilibria of vanillins in binary systems with $CO_2$. *Fluid Phase Equilibria* **2005**, *231*, 11–19. [CrossRef]
161. Liu, J.; Kim, Y.; McHugh, M.A. Phase behavior of the vanillin-$CO_2$ system at high pressures. *J. Supercrit. Fluids* **2006**, *39*, 201–205. [CrossRef]

162. Lee, M.J.; Kou, C.F.; Cheng, J.W.; Lin, H.M. Vapor-liquid equilibria for binary mixtures of carbon dioxide with 1,2-dimethoxybenzene, 2-methoxyphenol, or p-cresol at elevated pressures. *Fluid Phase Equilibria* **1999**, *162*, 211–224. [CrossRef]
163. Pfohl, O.; Pagel, A.; Brunner, G. Phase equilibria in systems containing o-cresol, p-cresol, carbon dioxide, and ethanol at 323.15-473.15 K and 10-35 MPa. *Fluid Phase Equilibria* **1999**, *157*, 53–79. [CrossRef]
164. Lee, R.J.; Chao, K.C. Extraction of 1-methylnaphthalene and m-cresol with supercritical carbon dioxide and ethane. *Fluid Phase Equilibria* **1988**, *43*, 329–340. [CrossRef]
165. Kambo, H.S.; Dutta, A. A comparative review of biochar and hydrochar in terms of production, physico-chemical properties and applications. *Renew. Sustain. Energy Rev.* **2015**, *45*, 359–378. [CrossRef]


energies

MDPI

*Supplementary information*

# Supercritical Carbon Dioxide Extraction of Lignocellulosic Bio-Oils: The Potential of Fuel Upgrading and Chemical Recovery

**Nikolaos Montesantos [1] and Marco Maschietti [1,*]**

[1] Department of Chemistry and Bioscience, Aalborg University, Niels Bohrs Vej 8A, 6700 Esbjerg, Denmark; nmo@bio.aau.dk

[*] Correspondence: marco@bio.aau.dk

Received: 31 January 2020; Accepted: 30 March 2020; Published: date

**Table S1.** Solubility data of bio-oil components at different temperature and pressure conditions.

| **Cyclohexanone** | | | | | | | Ref. |
|---|---|---|---|---|---|---|---|
| P (bar) @ 160 °C | 96 | 131 | 165 | 194 | 213 | | [139] |
| Solubility (g/kg) | 83.0 | 118.8 | 149.4 | 195.0 | 258.2 | | |
| P (bar) @ 180 °C | 89 | 135 | 175 | 209 | 215 | | |
| Solubility (g/kg) | 118.8 | 162.4 | 191.5 | 276.0 | 293.4 | | |
| **5-Hydroxymethylfurfural** | | | | | | | Ref. |
| P (bar) @ 41 °C | 97 | 116 | 133 | 148 | 166 | 187 | [140] |
| Solubility (g/kg) | 1.4 | 2.8 | 3.5 | 4.4 | 5.7 | 6.8 | |
| P (bar) @ 51 °C | 110 | 128 | 144 | 158 | 177 | 196 | |
| Solubility (g/kg) | 1.4 | 2.8 | 3.5 | 4.4 | 5.7 | 6.8 | |
| P (bar) @ 61 °C | 119 | 140 | 153 | 166 | 184 | | |
| Solubility (g/kg) | 1.4 | 2.8 | 3.5 | 4.4 | 5.7 | | |
| P (bar) @ 70 °C | 127 | 149 | 153 | 166 | 184 | | |
| Solubility (g/kg) | 1.4 | 2.8 | 3.5 | 4.4 | 5.7 | | |
| **Heptanoic Acid** | | | | | | | Ref. |
| P (bar) @ 40 °C | 100 | 115 | 150 | 175 | 200 | | [141] |
| Solubility (g/kg) | 50.6 | 72.1 | 89.9 | 106.2 | 123.8 | | |
| P (bar) @ 50 °C | 85 | 100 | 115 | 150 | 175 | 200 | |
| Solubility (g/kg) | 0.3 | 3.2 | 47.8 | 93.0 | 125.6 | 158.4 | |
| P (bar) @ 60 °C | 85 | 100 | 115 | 150 | 175 | 200 | |
| Solubility (g/kg) | 0.5 | 1.2 | 3.5 | 40.9 | 128.3 | 140.1 | |
| **Hexadecanoic Acid** | | | | | | | Ref. |
| P (bar) @ 35 °C | 99 | 127 | 157 | 186 | 206 | 230 | [142] |

| | | | | | | | | | | |
|---|---|---|---|---|---|---|---|---|---|---|
| Solubility (g/kg) | 0.9 | 1.9 | 2.3 | 2.6 | 2.8 | 2.9 | | | | |
| P (bar) @ 35 °C | 129 | 148 | 168 | 197 | 227 | | | | | [143] |
| Solubility (g/kg) | 1.5 | 1.8 | 2.1 | 2.3 | 2.6 | | | | | |
| P (bar) @ 45 °C | 129 | 148 | 168 | 197 | 227 | | | | | |
| Solubility (g/kg) | 2.2 | 3.2 | 4.1 | 5.0 | 6.1 | | | | | |
| P (bar) @ 55 °C | 129 | 148 | 168 | 197 | 227 | | | | | |
| Solubility (g/kg) | 2.2 | 4.4 | 6.7 | 9.8 | 12.3 | | | | | |
| P (bar) @ 35 °C | 138 | 275 | 414 | | | | | | | [144] |
| Solubility (g/kg) | 1.9 | 3.2 | 3.6 | | | | | | | |
| P (bar) @ 45 °C | 138 | 275 | 414 | | | | | | | |
| Solubility (g/kg) | 5.2 | 23 | 23 | | | | | | | |
| P (bar) @ 55 °C | 138 | 275 | 414 | | | | | | | |
| Solubility (g/kg) | 4.0 | 47 | 76 | | | | | | | |
| P (bar) @ 40 °C | 80 | 91 | 91 | 100 | 110 | 151 | 151 | 201 | 248 | [145] |
| Solubility (g/kg) | 0.003 | 0.14 | 0.20 | 0.8 | 1.6 | 3.2 | 3.3 | 4.4 | 5.8 | |
| P (bar) @ 40 °C | 121 | 129 | 146 | 155 | 171 | 202 | 229 | | | [146] |
| Solubility (g/kg) | 2.1 | 2.3 | 2.9 | 3.3 | 3.7 | 4.6 | 5.2 | | | |
| P (bar) @ 45 °C | 101 | 156 | 184 | 234 | | | | | | |
| Solubility (g/kg) | 0.8 | 3.5 | 4.9 | 6.4 | | | | | | |
| P (bar) @ 64 – 65 °C | 214 | 218 | 219 | 221 | 228 | 248 | | | | [147] |
| Solubility (g/kg) | 14.4 | 14.2 | 15.9 | 17.7 | 19.3 | 22.4 | | | | |
| P (bar) @ 70 – 72 °C | 224 | 225 | 229 | 230 | 236 | 255 | | | | |
| Solubility (g/kg) | 14.2 | 14.4 | 15.9 | 17.7 | 19.3 | 22.4 | | | | |
| P (bar) @ 78 °C | 232 | 234 | 235 | 249 | | | | | | |
| Solubility (g/kg) | 14.4 | 14.2 | 15.9 | 19.3 | | | | | | |
| | | | | | **Cumene** | | | | | Ref. |
| P (bar) @ 40 °C | 76 | 76 | 81 | 81 | | | | | | [148] |
| Solubility (g/kg) | 7.6 | 7.6 | 12.2 | 14.3 | | | | | | |
| P (bar) @ 50 °C | 80 | 85 | 88 | | | | | | | [149] |
| Solubility (g/kg) | 14.6 | 19.2 | 22.3 | | | | | | | |
| P (bar) @ 70 °C | 87 | 106 | 116 | | | | | | | [150] |

| | | | | | | | | | | | | | |
|---|---|---|---|---|---|---|---|---|---|---|---|---|---|
| Solubility (g/kg) | 19.2 | 34.5 | 58.9 | | | | | | | | | | |
| **Naphthalene** | | | | | | | | | | | | | Ref. |
| P (bar) @ 35 °C | 86 | 97 | 105 | 131 | 167 | 197 | 220 | 239 | 252 | | | | [151] |
| Solubility (g/kg) | 21.5 | 27.9 | 30.4 | 40.0 | 45.4 | 48.2 | 51.5 | 53.6 | 54 | | | | |
| P (bar) @ 55 °C | 81 | 91 | 101 | 108 | 120 | 132 | 142 | 159 | 169 | 173 | 187 | 208 | |
| Solubility (g/kg) | 3.8 | 4.9 | 8.5 | 15.7 | 35.0 | 59.2 | 70.7 | 84.0 | 92.6 | 94.8 | 106.4 | 113.8 | |
| P (bar) @ 55 °C | 221 | 235 | 248 | 284 | | | | | | | | | |
| Solubility (g/kg) | 117.4 | 122.8 | 132.2 | 142.1 | | | | | | | | | |
| P (bar) @ 60 °C | 107 | 132 | 151 | 162 | 173 | 181 | 190 | 201 | 203 | 214 | 215 | 224 | |
| Solubility (g/kg) | 15.1 | 42.9 | 71.8 | 93.0 | 115.6 | 119.1 | 142.2 | 154.5 | 162.8 | 179.0 | 179.6 | 195.9 | |
| P (bar) @ 60 °C | 229 | 233 | 245 | 252 | 254 | 270 | 288 | | | | | | |
| Solubility (g/kg) | 195.9 | 208.7 | 225.0 | 227.9 | 235.9 | 235.4 | 240.4 | | | | | | |
| P (bar) @ 65 °C | 150 | 169 | 183 | 190 | 210 | 222 | 229 | | | | | | |
| Solubility (g/kg) | 67.5 | 102.3 | 118.9 | 133.3 | 167.0 | 186.8 | 199.9 | | | | | | |
| P (bar) @ 121 °C | 77 | 97 | 115 | 134 | 155 | 164 | | | | | | | [152] |
| Solubility (g/kg) | 14.4 | 17.3 | 22.1 | 29.4 | 30.0 | 31.9 | | | | | | | |
| P (bar) @ 162 °C | 83 | 102 | 119 | 136 | 150 | 166 | | | | | | | |
| Solubility (g/kg) | 29.7 | 27.5 | 30.8 | 31.1 | 49.6 | 51.5 | | | | | | | |
| **Benzeneacetic Acid** | | | | | | | | | | | | | Ref. |
| P (bar) @ 35 °C | 84 | 91 | 96 | 99 | 99 | 103 | 111 | 112 | 135 | 143 | 161 | 167 | [153] |
| Solubility (g/kg) | 3.1 | 6.8 | 7.7 | 6.6 | 7.7 | 8.9 | 11.7 | 12.3 | 15.0 | 17.4 | 19.8 | 19.8 | |
| P (bar) @ 35 °C | 174 | 175 | 184 | | | | | | | | | | |
| Solubility (g/kg) | 21.0 | 22.5 | 23.4 | | | | | | | | | | |
| P (bar) @ 45 °C | 93 | 109 | 122 | 131 | 138 | 142 | 152 | 171 | 191 | | | | |
| Solubility (g/kg) | 1.2 | 6,5 | 17.1 | 22.2 | 26.7 | 27.3 | 33.0 | 43.0 | 52.2 | | | | |
| **Benzoic Acid** | | | | | | | | | | | | | Ref. |
| P (bar) @ 35 °C | 101 | 113 | 120 | 151 | 160 | 240 | 280 | 282 | 364 | | | | [154] |
| Solubility (g/kg) | 2.2 | 2.9 | 3.8 | 4.8 | 6.5 | 8.6 | 9.1 | 8.1 | 8.7 | | | | |
| P (bar) @ 45 °C | 101 | 105 | 113 | 120 | 151 | 160 | 200 | 240 | 280 | 282 | 303 | 363 | |
| Solubility (g/kg) | 0.7 | 1.4 | 1.6 | 3.2 | 5.5 | 6.6 | 8.8 | 11.6 | 12.1 | 11.0 | 12.2 | 13.4 | |
| P (bar) @ 55 °C | 101 | 105 | 111 | 120 | 126 | 151 | 160 | 200 | 240 | 281 | 303 | 363 | |
| Solubility (g/kg) | 0.4 | 0.6 | 0.8 | 1.4 | 2.1 | 5.4 | 6.3 | 10.6 | 14.2 | 15.6 | 17.5 | 19.6 | |

| | | | | | | | | | | | | | | |
|---|---|---|---|---|---|---|---|---|---|---|---|---|---|---|
| P (bar) @ 70 °C | 101 | 111 | 126 | 151 | 201 | 281 | 364 | | | | | | | |
| Solubility (g/kg) | 0.3 | 0.6 | 1.5 | 4.3 | 13.8 | 24.6 | 34.7 | | | | | | | |
| P (bar) @ 45 °C | 120 | 160 | 200 | 240 | 280 | | | | | | | | | [155] |
| Solubility (g/kg) | 3.2 | 6.5 | 8.8 | 11.6 | 12.1 | | | | | | | | | |
| P (bar) @ 55 °C | 120 | 160 | 200 | 240 | 280 | | | | | | | | | |
| Solubility (g/kg) | 1.4 | 6.3 | 10.6 | 14.2 | 20.1 | | | | | | | | | |
| P (bar) @ 65 °C | 120 | 160 | 200 | 240 | 280 | | | | | | | | | |
| Solubility (g/kg) | 0.9 | 4.8 | 11.3 | 19.1 | 26.8 | | | | | | | | | |
| | | | | | **Phenol** | | | | | | | | | Ref. |
| P (bar) @ 60 °C | 100 | 125 | 150 | 175 | 200 | 225 | 250 | 275 | 300 | 325 | 350 | | | [156] |
| Solubility (g/kg) | 2.4 | 11.4 | 28.6 | 49.1 | 74.0 | 83.1 | 90.8 | 109.5 | 119.9 | 134.6 | 151.9 | | | |
| P (bar) @ 75 °C | 100 | 125 | 150 | 175 | 200 | 225 | 250 | 275 | 300 | 325 | 350 | | | |
| Solubility (g/kg) | 3.9 | 7.4 | 15.6 | 34.2 | 57.9 | 74.5 | 82.2 | 111.9 | 124.0 | 139.6 | 158.4 | | | |
| P (bar) @ 90 °C | 100 | 125 | 150 | 175 | 200 | 225 | 250 | 275 | 300 | 325 | 350 | | | |
| Solubility (g/kg) | 4.4 | 6.9 | 15.9 | 24.3 | 41.4 | 58.0 | 79.2 | 104.4 | 130.1 | 152.3 | 175.5 | | | |
| P (bar) @ 36 °C | 79 | 81 | 87 | 97 | 106 | 111 | 119 | 124 | 133 | 146 | 147 | 156 | | [157] |
| Solubility (g/kg) | 7.4 | 15.5 | 20.3 | 23.8 | 26.2 | 27.0 | 28.8 | 29.3 | 31.2 | 31.6 | 31.8 | 33.4 | | |
| P (bar) @ 36 °C | 162 | 163 | 172 | 183 | 183 | 194 | 196 | 208 | 214 | 216 | 222 | 234 | 249 | |
| Solubility (g/kg) | 33.7 | 34.3 | 33.4 | 35.1 | 34.7 | 35.0 | 35.4 | 36.8 | 37.5 | 37.6 | 38.2 | 38.4 | 38.0 | |
| P (bar) @ 60 °C | 114 | 127 | 146 | 146 | 153 | 160 | 168 | 178 | 183 | 187 | 193 | 204 | | |
| Solubility (g/kg) | 13.8 | 26.0 | 38.9 | 39.2 | 37.8 | 45.8 | 46.1 | 58.6 | 60.1 | 63.3 | 65.2 | 64.9 | | |
| P (bar) @ 60 °C | 211 | 222 | 233 | 242 | | | | | | | | | | |
| Solubility (g/kg) | 79.7 | 74.8 | 90.8 | 94.6 | | | | | | | | | | |
| P (bar) @ 100 °C | 107 | 152 | 202 | 251 | 301 | | | | | | | | | [158] |
| Solubility (g/kg) | 11.9 | 23.0 | 52.2 | 97.7 | 164.5 | | | | | | | | | |
| | | | | | **Catechol** | | | | | | | | | Ref. |
| P (bar) @ 60 °C | 100 | 125 | 150 | 175 | 200 | 225 | 250 | 275 | 300 | 325 | 350 | | | [156] |
| Solubility (g/kg) | 0.3 | 0.8 | 2.7 | 4.1 | 5.0 | 5.7 | 6.5 | 6.8 | 7.4 | 7.5 | 7.6 | | | |
| P (bar) @ 60 °C | 100 | 125 | 150 | 175 | 200 | 225 | 250 | 275 | 300 | 325 | 350 | | | |
| Solubility (g/kg) | 0.4 | 0.9 | 1.4 | 2.6 | 3.8 | 4.8 | 5.9 | 6.7 | 7.7 | 8.7 | 9.6 | | | |
| P (bar) @ 60 °C | 100 | 125 | 150 | 175 | 200 | 225 | 250 | 275 | 300 | 325 | 350 | | | |

| | | | | | | | | | | | | | |
|---|---|---|---|---|---|---|---|---|---|---|---|---|---|
| Solubility (g/kg) | 0.5 | 0.7 | 1.1 | 2.3 | 3.7 | 4.9 | 6.0 | 7.2 | 9.1 | 10.1 | 11.4 | | |
| P (bar) @ 35 °C | 122 | 162 | 203 | 243 | 284 | 324 | 365 | 405 | | | | | [159] |
| Solubility (g/kg) | 1.7 | 2.4 | 2.5 | 2.7 | 2.9 | 3.0 | 3.3 | 3.3 | | | | | |
| P (bar) @ 45 °C | 122 | 162 | 203 | 243 | 284 | 324 | 365 | 405 | | | | | |
| Solubility (g/kg) | 2.0 | 2.6 | 3.1 | 3.7 | 3.9 | 4.2 | 4.5 | 4.8 | | | | | |
| P (bar) @ 55 °C | 122 | 162 | 203 | 243 | 284 | 324 | 365 | 405 | | | | | |
| Solubility (g/kg) | 1.9 | 3.2 | 4.1 | 4.7 | 5.5 | 6.0 | 6.2 | 6.4 | | | | | |
| P (bar) @ 65 °C | 122 | 162 | 203 | 243 | 284 | 324 | 365 | 405 | | | | | |
| Solubility (g/kg) | 1.6 | 3.9 | 5.4 | 6.4 | 7.4 | 8.1 | 9.0 | 9.8 | | | | | |
| **Vanillin** | | | | | | | | | | | | | Ref. |
| P (bar) @ 40 °C | 87 | 117 | 149 | 174 | 187 | 198 | 205 | 227 | 235 | 259 | 273 | | [160] |
| Solubility (g/kg) | 1.0 | 4.3 | 9.6 | 11.6 | 12.1 | 12.6 | 12.9 | 13.4 | 13.4 | 12.9 | 13.2 | | |
| P (bar) @ 60 °C | 84 | 109 | 127 | 148 | 162 | 173 | 178 | 200 | 233 | 277 | | | |
| Solubility (g/kg) | 0.5 | 1.8 | 4.1 | 6.5 | 10.3 | 10.9 | 11.3 | 15.5 | 20.7 | 17.3 | | | |
| P (bar) @ 80 °C | 80 | 95 | 112 | 128 | 141 | 166 | 173 | 197 | 230 | 254 | 268 | | |
| Solubility (g/kg) | 0.5 | 1.7 | 1.5 | 3.8 | 7.3 | 11.4 | 11.8 | 18.7 | 26.2 | 35.3 | 43.4 | | |
| P (bar) @ 35 °C | 83 | 98 | 110 | 120 | 136 | 151 | 161 | 172 | 180 | 185 | 190 | | [153] |
| Solubility (g/kg) | 1.3 | 3.9 | 5.1 | 5.3 | 6.5 | 7.5 | 8.0 | 8.3 | 8.9 | 9.0 | 9.6 | | |
| P (bar) @ 45 °C | 98 | 113 | 120 | 131 | 145 | 155 | 163 | 170 | 178 | 185 | 195 | | |
| Solubility (g/kg) | 1.5 | 4.2 | 5.1 | 6.8 | 8.1 | 8.6 | 8.8 | 9.7 | 10.2 | 10.9 | 12.1 | | |
| Solubility (g/kg) | 10.3 | | | 52.3 | | | | 96.3 | | | 147.1 | | [161] |
| T (°C) | 83 | 105 | 71 | 94 | 119 | 136 | 88 | 103 | 123 | 95 | 107 | 122 | |
| P (bar) | 216 | 249 | 414 | 391 | 385 | 389 | 664 | 592 | 528 | 807 | 711 | 658 | |
| Solubility (g/kg) | 318.3 | | | | | | | | | | | | |
| T (°C) | 74 | 79 | 94 | 102 | | | | | | | | | |
| P (bar) | 1341 | 1238 | 999 | 919 | | | | | | | | | |
| **Guaiacol** | | | | | | | | | | | | | Ref. |
| P (bar) @ 50 °C | 80 | 100 | 130 | 150 | 180 | | | | | | | | [162] |
| Solubility (g/kg) | 2.4 | 14.9 | 107.6 | 156.0 | 260.5 | | | | | | | | |
| P (bar) @ 80 °C | 80 | 100 | 130 | 160 | 200 | | | | | | | | |
| Solubility (g/kg) | 3.2 | 5.9 | 16.6 | 50.2 | 144.5 | | | | | | | | |
| P (bar) @ 120 °C | 80 | 100 | 130 | 160 | 200 | | | | | | | | |
| Solubility (g/kg) | 10.7 | 13.3 | 19.2 | 32.0 | 62.5 | | | | | | | | |
| **o-Cresol** | | | | | | | | | | | | | Ref. |

| | | | | | | | |
|---|---|---|---|---|---|---|---|
| P (bar) @ 50 °C | 102 | 142 | 201 | 250 | 268 | | [163] |
| Solubility (g/kg) | 17.5 | 82.9 | 156.7 | 248.1 | 395.1 [1] | | |
| P (bar) @ 200 °C | 99 | 152 | 202 | 250 | 300 | | |
| Solubility (g/kg) | 84.9 | 96.8 | 127.4 | 187.6 | 464.6 [1] | | |
| P (bar) @ 100 °C | 104 | 153 | 201 | 252 | 260 | 263 | [158] |
| Solubility (g/kg) | 11.0 | 27.1 | 74.7 | 203.0 | 270.6 | 392.5 [1] | |
| **m-Cresol** | | | | | | | Ref. |
| P (bar) @ 35 °C | 80 | 100 | 120 | 160 | 200 | 240 | [164] |
| Solubility (g/kg) | 13.3 | 29.5 | 37.2 | 50.3 | 60.9 | 71.5 | |
| P (bar) @ 45 °C | 80 | 100 | 120 | 160 | 200 | 240 | |
| Solubility (g/kg) | 1.8 | 14.4 | 30.4 | 50.5 | 66.1 | 80.5 | |
| P (bar) @ 55 °C | 80 | 100 | 120 | 160 | 200 | 240 | |
| Solubility (g/kg) | 1.4 | 4.2 | 16.9 | 45.2 | 65.9 | 86.9 | |
| P (bar) @ 100 °C | 102 | 152 | 199 | 250 | 300 | | [158] |
| Solubility (g/kg) | 7.6 | 18.2 | 45.9 | 92.0 | 169.1 | | |
| **p-Cresol** | | | | | | | Ref. |
| P (bar) @ 50 °C | 100 | 150 | 200 | 250 | 301 | 348 | [163] |
| Solubility (g/kg) | 7.6 | 42.6 | 64.1 | 82.9 | 102.3 | 118.8 | |
| P (bar) @ 200 °C | 101 | 151 | 200 | 250 | 299 | 336 | |
| Solubility (g/kg) | 66.8 | 76.5 | 98.8 | 137.2 | 219.7 | 530.5 [1] | |
| P (bar) @ 80 °C | 80 | 100 | 130 | 160 | 185 | 200 | [162] |
| Solubility (g/kg) | 2.6 | 4.1 | 10.0 | 24.7 | 42.6 | 53.8 | |
| P (bar) @ 120 °C | 80 | 100 | 130 | 160 | 200 | | |
| Solubility (g/kg) | 8.5 | 10.4 | 14.7 | 22.9 | 41.5 | | |
| P (bar) @ 150 °C | 80 | 100 | 130 | 160 | 200 | | |
| Solubility (g/kg) | 20.1 | 21.7 | 27.1 | 35.6 | 49.6 | | |
| P (bar) @ 100 °C | 103 | 154 | 202 | 251 | 302 | | [158] |
| Solubility (g/kg) | 7.8 | 18.5 | 47.5 | 89.8 | 159.7 | | |

[1] One phase was detected

ISSN (online): 2446-1636
ISBN (online): 978-87-7210-670-0 AALBORG UNIVERSITY PRESS